Insights into the aetiology and epidemiology of an emerging protistan disease of amphibians

Submitted by

Vanessa Smilansky

to the University of Exeter as a thesis for the degree of

Doctor of Philosophy in Biological Sciences

[*September, 2020*]

I certify that all material in this thesis which is not my own work has been identified and that no material has previously been submitted and approved for the award of a degree by this or any other University.

(Signature) Vanessa Smilansky……

“Amphibians are dying out like crazy, and frogs and salamanders may be largely extinct by the end of the twenty-first century. Imagine an animal that begins its life in the water, but ends it on land - already, that's pretty weird. But, also, a lot of them are incredibly tiny and look wildly improbable. They have funny little toes, they stretch their throats into weird bubble shapes when they croak, and some of them are poisonous to the touch. I think kids from the twenty-second century might mythologize amphibians the way kids today mythologize dinosaurs.”

- Annalee Newitz

Table of Contents

Appendix

Acknowledgements

Thanks to the EU Research and Innovation Programme Horizon 2020 (Grant No. H2020-MSCA-ITN-2015-675752) for funding support, and thanks to the SINGEK network for providing a broad spectrum of training opportunities. Thanks to my supervisor Tom Richards for his support through ups and downs of the project, and his encouragement of international collaborations, which strengthened both the project and my own professional growth. For their support as both friends and colleagues, thanks to current and former members of the Richards Lab: David Milner, Guy Leonard, Vicky Attah, Estelle Kilias, Eli Alacid, Fiona Savory, Ben Jenkins, Mark Morrison, Yumei Dai, Adam Monier, Raquel Rodriguez, and Jeremy Wideman. Thanks to David Milner for advisement and assistance in the steel-top jungle, as well as the actual jungle. Thanks to Guy Leonard for his bioinformatics brilliance: without it, many aspects of the project would not have been possible. Thanks to Estelle Kilias and Leandro Junges for help running the DADA2 pipeline in Chapter 5. Thanks to Mark Morrison for technical assistance in the LSI lab. Thanks to Aurélie Chambouvet for advisement and providing Perkinsea samples. Thanks to Milosh Jirků and Julius Lukeš for access to laboratory facilities at the Institute of Parasitology, CAS, Czech Republic. Thanks to Milosh Jirků for his indispensable assistance collecting and processing tadpoles for the experimental infections in Chapter 2 and for the Panama survey in Chapter 4. Thanks to Brian Gratwicke and the staff at the Smithsonian Tropical Research Institute (STRI) for permits and approvals of fieldwork and access to laboratory facilities in Panama. Thanks to Roberto Ibañez and the staff at the Gamboa Amphibian Research and Conservation Center for providing amphibian expertise and technical assistance with lab work. Thanks to Eyda Gomez and staff at the STRI Naos Marine and Molecular Laboratories for technical assistance with molecular lab work. Thanks to Andy Nicholls for providing *Hyla arborea* samples. Thanks to Matt Atkinson and Anna Savage for access to facilities at the University of Central Florida, and for assisting with the tadpole cannibalism experiment in Chapter 2. And thanks to Elizabeth Harper for pointing me in their direction. Thanks to Zehra Kahveci and Jari Iannucci for help with fluorescence microscopy for cell viability tests in Chapter 2. Thanks to Konrad Paszkiewicz, Karen Moore, and staff at the Exeter Sequencing Service for help with many sequencing aspects of the project. Finally, thanks to the friendly orange campus cat for providing my weekly cat fix.

Abstract

Severe Perkinsea infection (SPI) is an emerging disease that has been linked to mass die-offs of tapdoles across a broad geographic range in the USA. The exact relationship between Perkinsea infection and SPI disease remains undefined and untested. It is not known if certain co-factors (e.g. co-infection with other pathogens, exposure to pollution, host microbiome composition) contribute to disease progression, or if differences in host susceptibility affect the distribution of Perkinsea infection and SPI disease. We have yet to determine if the two known lineages of amphibian Perkinsea (i.e. a putatively pathogenic lineage and a putatively non-pathogenic lineage) are distinct strains, or if they are genetic variants of the same strain. Finally, we must continue to explore the extent of the parasite's geographic range, particularly in regions with high amphibian diversity and/or a large number of threatened species. This thesis aims to elucidate some of the unknown aetiological and epidemiological aspects of Perkinsea infection and SPI disease in amphibians. These aims were addressed with a variety of experimental approaches. We investigated the aetiology and transmission of SPI disease by experimentally infecting healthy tadpoles with Perkinsea parasites, and by feeding tissue from putatively infected tadpoles to healthy tadpoles. We developed a field-compatible duplex qPCR assay for the rapid detection of the two lineages of amphibian Perkinsea, to be used as an epidemiological tool for monitoring amphibian health. We used phylogenetic analysis to investigate Perkinsea infection in captive tadpoles from the UK and wild tadpoles from Panama, a global centre of amphibian diversity and a biosphere greatly affected by amphibian decline. We used amplicon-based metagenomics to compare the intestinal eukaryotic microbiomes of healthy and Perkinsea-infected tadpoles. Our experimental infections did not result in a pathogenic interaction in our sample, and we did not detect ribosomal activity in the parasites. The results for the cannibalism feeding experiment were obscured by a pre-existing cryptic infection in our sample. Our results suggest that Perkisnea pathogenicity is limited, or is only manifest under specific ecological circumstances. Our optimization efforts confirmed that our novel duplex qPCR assay is specific, efficient, and sensitive in most conditions, thereby supporting its application as a tool for amphibian health surveys, and means to improve understanding of the dynamics of Perkinsea infection and SPI disease. We found molecular evidence of Perkinsea infection in a wide host range in Panama, and

in the UK aquaculture samples, thereby expanding amphibian Perkinsea's known biogeographical range and providing a broader base for risk assessment with a view to conservation. The results of our microbiome comparison did not reveal any major compositional differences in the intestinal eukaryotic microbiomes between healthy and Perkinsea-infected tadpoles; however, more specific taxonomic ranks need to be investigated before conclusions can be made. The outcomes of these experiments offer novel insights into under-studied aetiological and epidemiological aspects of this emerging protistan disease of amphibians. These insights can potentially improve amphibian management strageies to help mitigate the impact of Perkinsea infection and SPI disease, and possibly prevent disease outbreaks.

List of Tables and Figures

Chapter 1: Introduction

Chapter 2. Experimental infection of ranid tadpoles with putatively pathogenic amphibian Perkinsea

Chapter 3. Development of a novel duplex qPCR assay to detect multiple clades of Perkinsea in amphibian tissues

Chapter 4. Phylogenetic analysis of amphibian disease associated Perkinsea expands the identified geographic and host range of infections

Chapter 5: Discussion

List of Acronynms and Abbreviations

ASV	Amplicon sequence variant	126
Cq	Quantitation cycle	74
DMEM/F-12	Dulbecco's Modified Eagle Medium/Nutrient Mixture F-12	45
LoD	Limit of detection	74
MCP	Major capsid protein	101
ML	Maximum likelihood	98
MS-222	Tricaine methane-sulfonate	45
MSA	Multiple sequence alignment	98
NAG01	Novel Alveolate Group 1	28
NAG01a-c	Novel Alveolate Group 1 Clades A-C	28
NTC	No template control	74
PCR	Polymerase chain reaction	34
PI	Propidium iodide	48
PPC	Pathogenic Perkinsea Clade	28
qPCR	Quantitative polymerase chain reaction	35
RT-PCR	Reverse transcriptase polymerase chain reaction	35
SAR	Stramenopiles, Alveolata, Rhizaria	127
SPI	Severe Perkinsea infection	27
SNP	Single nucleotide polymorphism	36
Ta	Annealing temperature	74
UMI	Universal molecular identifier	123

Chapter 1. Introduction

Information in this chapter went toward the following publications:

Chambouvet A, Smilansky V, Jirků M, Isidoro-Ayza M, Itoı¨z S, Derelle E, et al. (2020) Diverse alveolate infections of tadpoles, a new threat to frogs? *PLoS Pathog* 16(2): e1008107

1.1. AMPHIBIAN OVERVIEW: DIVERSITY, LIFE HISTORY, AND SIGNIFICANCE

The class Amphibia comprises ~6,700 species of frogs and toads (order Anura), ~700 species of salamanders and newts (order Caudata), and ~200 species of caecilians (order Gymnophiona) (Jetz & Pyron 2018). Amphibians are broadly distributed across the globe, with the greatest diversity occurring in the tropics (Figure 1.1.). Anurans inhabit every continent except Antarctica, including some species with ranges in the Arctic Circle such as the wood frog *Lithobates sylvaticus* and Siberian salamander *Salamandrella keyserlingii* (Martof & Humphries 1959, Borkin et al. 1984). With over 1,100 species, Brazil is the global centre of anuran diversity (Guerra et al. 2020). Caudates can be found in North America, Europe, Asia, and the Amazon Basin, although their ranges tend to be restricted to the Holarctic realm. The greatest caudate diversity occurs in the Appalachian Mountains in the eastern USA.

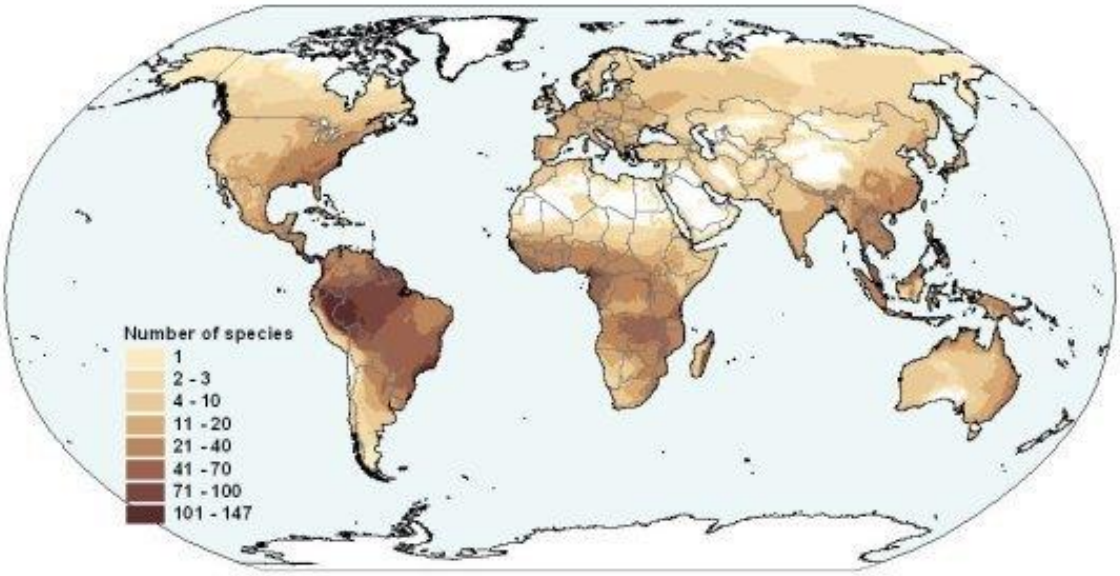

Figure 1.1. Global diversity of known amphibians (IUCN 2008).

Amphibians have a wide variety of morphologies that are specialized for their diverse habitats and lifestyles. Caecilians are a group of limbless, fossorial animals found in wet, tropical regions of South and Central America, Africa, and Southeast Asia. They are adapted to burrowing and feature heavily ossified skulls, dermally embedded calcite scales, and visualization limited to dark-light perception (Crump 2009). Anurans inhabit the broadest diversity of ecosystems. In adults, the different demands of their terrestrial, arboreal, and aquatic lifestyles correspond to variation in

their limb length, webbing of feet, and smoothness of skin (Crump 2009). Adult caudates can be fully aquatic, whilst others take to the water intermittently or spend their time entirely on land or underground (Crump 2009). They typically have elongated, 'lizard-like' bodies with smooth skin, and those that subsist in the water are equipped with gills and finned tails (Crump 2009).

Despite their morphological diversity, all amphibians share the unique characteristic of permeable skin (Crump 2009), which is used to exchange gases with their surroundings (Feder & Burggren 1985). It supplements their pulmonary respiration and that which occurs via the lining of their mouths. This enables them to remain submerged for extended periods, such as those that occur during predator evasion and hibernation (Feder & Burggren 1985). Lungless amphibians rely entirely on cutaneous and oral respiration, including the plethodontid salamanders (Feder & Burggren 1985), and one species each of frog and caecilian (*Barbourula kalimantanensis* and *Microcaecilia iwokramae*, respectively) (Bickford et al. 2008, Wake & Donnelly 2010). Permeable skin predisposes amphibians to infiltration by infectious pathogens and environmental contaminants (which makes them effective ecological indicators) (Kiesecker et al. 2004). Glycoprotein-rich secretions from mucous glands keep their skin moist and can promote growth and maintenance of healthy microbiota (Austin 2000), which helps to compensate their vulnerability. The mucous layer also contains components of the innate and adaptive immune systems, including lysozymes, antimicrobial peptides, and mucosal antibodies (Rollins-Smith & Woodhams 2012).

Another defining feature of anurans and caudates is their metamorphic process. They typically lay their eggs in jellylike masses or strings from which larvae hatch and develop into either terrestrial or aquatic adults. Like their permeable skin, their embryonic development enables them to serve as ecological indicators of water quality because they are fully exposed to aquatic stressors. Their shell-less eggs are especially vulnerable to the effects of UV-B radiation, which has potential for population-level impact as it has been shown to impede hatching success (Blaustein et al. 1994, Kiesecker & Blaustein 1995). Such impacts can be mitigated by early stage survival, since amphibian populations are regulated by larval-stage density dependence (Vonesh & De La Cruz 2002). Larvae survival is undermined by the fact that their immune systems do not fully develop until after metamorphosis (Rollins-

Smith 1998). In their larval stage, amphibians are dependent on innate immunity (i.e. a rapid and nonspecific response to foreign bodies by phagocytic macrophages) (Pasquier et al. 1989). Innate immunity lacks the robustness and specificity of adaptive immunity (e.g. lymphocyte response) (Pasquier et al. 1989). Therefore, larvae have increased susceptibility to infection and disease, particularly those with non-bacterial aetiologies (Andino et al. 2012, Chambouvet et al. 2016, 2020). Furthermore, it has been found that amphibian larvae have lower diversity of skin-associated microbiota than their adult counterparts (Kueneman et al. 2014). Skin microbiota can confer disease resistance by indirectly promoting host immune responses and by directly competing with foreign invaders (Woodhams et al. 2016). Reduced diversity of skin microbiota in larvae is negatively correlated to later-life resistance to parasites (Knutie et al. 2017).

Amphibians play significant ecological roles as both predators and prey. The early and late life stages tend to occupy different niches in the food web: eggs and larvae are typically preyed upon by invertebrates, whereas adults are consumed by a wide variety of higher-level predators, including fish, birds, reptiles, and mammals. Occasionally, predation of amphibians serves as an intermediate step by which parasites are transmitted to their definitive host (i.e. the hosts in which they mature and reproduce, often vertebrates), such as that which occurs during the typical trematode life cycle.

As adults, amphibians are generalist predators of invertebrates. They help regulate insect populations, including those of mosquitos, which are carriers of human pathogens, including *Plasmodium falciparum* (the agent of malaria) and the West Nile virus (WNV). Indeed, malaria and WNV epidemics have been correlated to amphibian declines (Kiesecker 2004). Some species also engage in anurophagy, including the invasive American bullfrog *Lithobates catesbeianus*, which has been linked to declines of native frogs (Lawler et al. 1999). Tadpoles are voracious consumers of algae and detritus, and the structure of the periphyton community has been shown to be dependent on their grazing (Dickman 1968, Kupferberg 1997).

In addition to their ecological significance, amphibians have anthropocentric value as food, pets, fishing bait, and sources of medicine. Frog legs are avidly consumed in many countries, including China, France, Belgium, Luxembourg, the US,

and those in Southeast Asia. Indonesia is the world's largest exporter of frog legs: over 5,000 tonnes are shipped annually around the world. Amphibians are also transported internationally as pets (e.g. poison dart frogs) and fishing bait (e.g. tiger salamander larvae), and are often extracted from their native habitats to support these trades. Medicinal applications of amphibians have focused on their skin secretions, which have antimicrobial and analgesic properties (Clarke 1997, Rollins-Smith & Woodhams 2012). Digestion-inhibiting substances secreted by the embryos of gastric-brooding frogs (*Rheobatrachus* spp.) were once considered for peptic ulcer treatment, but the frogs went extinct before it could be developed (Chivian 2013). Amphibian commerce poses a conservation problem because it can lead to their overexploitation, and facilitate the spread of invasive species and infectious disease (Collins & Storfer 2003, Picco & Collins 2008, Gratwicke et al. 2010).

1.2. GLOBAL AMPHIBIAN DECLINE

There is a consensus among scientists that the earth is experiencing a mass extinction as a result of climate change and the burgeoning human population (Thomas et al. 2004, Wake & Vredenburg 2008). Recognized as the most threatened of the vertebrate taxa, amphibians are at the forefront of this extinction (Wake & Vredenburg 2008). According to the latest global assessment, nearly one-third (32.4%) of known species are classified as threatened or extinct, whilst at least 42% of all species are declining in population (Stuart et al. 2004). Not surprisingly, the highest concentrations of threatened species occur in areas of great diversity and specialization, including Central and South America, and Southeast Asia (Figures 1.1 & 1.2). Although a large proportion of caudates are listed as threatened or extinct (49.8%), the average amphibian threat level is mainly driven by the species-rich anurans, of which 31.6% are red-listed (IUCN 2008). These figures have likely shifted since the time they were last updated, highlighting the need for a new and improved amphibian assessment incorporating current taxonomy, newly described species, and changes to species' status.

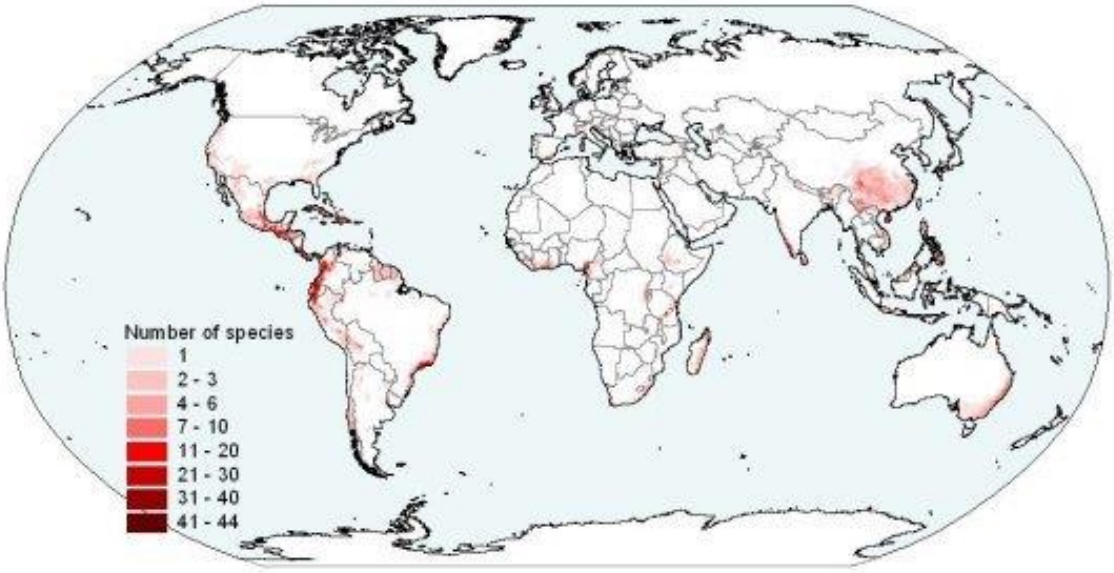

Figure 1.2. Global distribution of threatened amphibians (IUCN 2008).

The dominant factor in the declines of most threatened taxa is habitat degradation, and amphibians are no exception (Figure 1.3). Degradation can occur as complete loss (e.g. wetland conversion due to urbanization), alteration (e.g. livestock grazing), or fragmentation (a secondary effect of conversion). It is most extensive in regions of high human population growth, including biodiversity hotspots, such as the Amazon Basin, Eastern Arc, and Indonesia (Gallant et al. 2007). Amphibians are especially vulnerable because of their narrow habitat tolerances and relatively low vagilities, which impedes their ability to relocate. For species with aquatic larvae, fragmentation is particularly problematic because they are often forced to migrate between habitat remnants in order to breed (Becker et al. 2007). As populations become increasingly fragmented, they suffer from a loss of genetic diversity that can lead to reduced fitness and localized extinctions, even among species with larger dispersal abilities (Reed & Frankham 2003, Dixo et al. 2009). Dixo et al. (2009) found that genetic diversity among populations of *Rhinella ornata* (a species with aquatic larvae) was positively related to the size of forest fragments in the Atlanatic Coastal Forest in Brazil.

Other major factors contributing to the global amphibian decline are invasive species, fires, pollution, and disease (Figure 1.3). Invasive species can reduce populations of native amphibians through predation, resource competition, introduction of pathogens, and hybridization (Lawler et al. 1999, Kiesecker et al. 2001,

Kats & Ferrer 2003, Collins & Storfer 2003). Their dissemination is linked to anthropogenic expansion and is often intentional, as in the case of fish stocking (Kats & Ferrer 2003). It can be further accelerated by the direct and indirect effects of climate change, including warmer water temperatures, altered streamflow patterns, flooding, and expansion of fish-culture facilities and reservoirs (Rahel & Olden 2008). Climate change is also associated with an increase in the frequency and intensity of wildfires. This phenomenon can impact populations through direct mortality, increased water temperature, and UV-B exposure (resulting from reduced shade), and post-fire runoff; however, the effects are dependent on species' ecological niches and life history traits, and are not necessarily negative (Pilliod et al. 2003). Species that breed in cold streams (e.g. *Ascaphus* spp.) or on land (e.g. plethodontid salamanders) tend to be more susceptible to wildfire than species that breed in ponds (e.g. *Anaxyrus* spp.), as the former are often longer-lived with delayed maturity and lower fecundity (Hossack & Pilliod 2011). Environmental pollutants (e.g. agrochemicals, industrial chemicals, acid rain) can reduce populations by causing direct mortality, increasing susceptibility to disease, and impeding larval development and the ability to avoid predation (Carey & Bryant 1995, Kiesecker 2002, Rohr et al. 2008). Atrazine, one of the most commonly used herbicides in the world, has been shown to induce gonadal abnormalities and hermaphroditism in male frogs (Hayes et al. 2002), which has clear repercussions for reproductive success. Whilst the impact of infectious disease tends to be less evident than some of the aforementioned factors, it is still recognized as a significant contributor to amphibian decline (Collins & Storfer 2003). Non-infectious diseases, such as neoplasia (abnormal tissue growth with potential for malignancy), can also contribute; however, the focus here is on infectious diseases because they are directly related to the thesis.

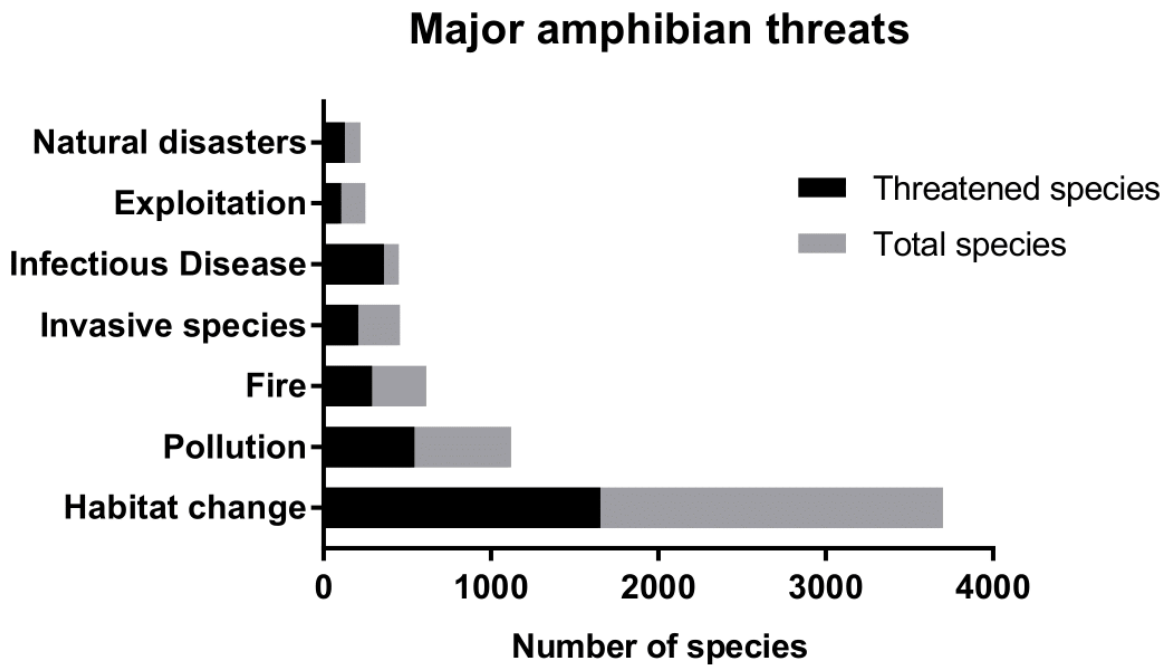

Figure 1.3. Seven major threats to amphibians, and the total and threatened numbers of species that are affected by each. Adapted from Chanson et al. (2008).

1.3. INFECTIOUS DISEASES OF AMPHIBIANS

Infectious diseases of amphibians are linked to a broad diversity of pathogens with varying levels of infectivity, virulence, and potential to cause population decline. Infectious disease affects a larger proportion (80%) of threatened species compared to the other major threats (Figure 1.3). Some of the most well-studied diseases have aetiologies that are bacterial (e.g. red-leg syndrome, flavobacteriosis, chlamydiosis), viral (e.g. ranavirosis), or mycotic (e.g. chytridiomycosis, saprolegniasis) (Densmore & Green 2007). Protistans (e.g. 'amoebae', ciliates, 'flagellates', sporozoans) and metazoans (e.g. myxozoans, trematodes) are also known to parasitize amphibians (Densmore & Green 2007). Co-infections with multiple pathogens are not unusual (Landsberg et al. 2013, Whitfield et al. 2013, Chambouvet et al. 2016, Warne et al. 2016), and there is potential for their synergism to compound clinical manifestations. Co-infections by ranavirus (agent of ranavirosis) and *Batrachochytrium dendrobatidis* (agent of chytridiomycosis) have been detected in anurans in Costa Rica and the Tropical Andes, raising concerns that their synergy might increase host morbidity and mortality (Whitfield et al. 2013, Warne et al. 2016).

Alterations in environmental conditions (e.g. temperature, moisture) or pollutant concentrations sometimes correlate with increased disease prevalence and severity (Carey et al. 1999, Daszak et al. 1999, Collins & Storfer 2003, Stuart et al. 2004). Contamination by water-borne agrochemicals has been linked to an increase in trematode infections and limb deformities in ranids in the USA (Kiesecker 2002, Rohr et al. 2008). Excessive ultraviolet radiation is associated with the proliferation of parasites in the environment, thereby increasing the odds of host exposure. For example, increased UV-B exposure was linked to an outbreak of the oomycete *Saprolegnia ferax* (the agent of saprolegniasis) that resulted in the mass mortality of anuran embryos in Oregon, USA (Kiesecker & Blaustein 1995). It has been proposed that environmental stress increases hosts' susceptibility to infection, either by directly inhibiting immune cell function or by increasing stress hormone levels (Carey et al. 1999). This susceptibility could be augmented by natural, stress-inducing events such as metamorphosis, intensive breeding, and food deprivation (Rollins-Smith et al. 2011).

At the extreme end of the pathological spectrum are ranaviruses, a group of double-stranded DNA viruses in the family Iridoviridae, and amphibian chytrid fungi (*Batrachochytrium* spp.). Ranaviruses are known to infect amphibians, reptiles, and teleost fishes. The first ranaviruses were isolated from northern leopard frogs (*Lithobates pipiens*, formerly *Rana pipiens*) in 1965, including frog virus 3 (FV3) (Granoff et al. 1965), which is now the most well-studied member of Iridoviridae. Ranavirus-associated mass mortality events (MMEs) have been reported since at least the early 1990s and have been observed in Europe, Asia, and the Americas, particularly Canada and the USA (Gray et al. 2009). Ranavirus is thought to be the second most common infectious agent of amphibians worldwide (Daszak et al. 1999), and is especially damaging to larval anurans and early metamorphs (Hoverman et al. 2010). Although it can infect systemically, the virus exhibits a tropism for the tissues of the liver, kidneys, spleen, and intestines, where it causes cellular necrosis, haemorraghing, and eventually organ failure (Gray et al. 2009, Miller et al. 2011). Transmission can occur indirectly from exposure to pathogens in the environment, or directly through ingestion of infected tissue or skin-to-skin contact (Gray et al. 2009, Miller et al. 2011). The genomes of *Ambystoma tigrinum* virus (ATV), an agent of

ranavirosis in salamanders, and the FV3 virus were sequenced in 2003 and 2004, respectively (Jancovich et al. 2003, Tan et al. 2004).

Chytridiomycosis has the distinction of being “the most devastating disease on record to impact vertebrate biodiversity” (Skerratt et al. 2007). It has been linked to declines in at least 501 amphibian species worldwide (approximately 6.5% of total described species) since the late 1970s (Scheele et al. 2019). Its unparalleled destruction has motivated a broad range of research in phylogeny, ecology, and epidemiology, including the discovery of a second chytrid pathogen, *B. salamandrivorans* (*Bsal*), in 2013 (Martel et al. 2013). *Bsal* has been implicated in the decline of numerous species of European salamanders, and poses a substantial global risk to urodeles, particularly those in the eastern USA (Richgels et al. 2016). The following paragraphs summarize the early stages of the chytridiomycosis investigation, thereby providing a comparison for the current state of research related to amphibian Perkinsea.

In 1993, researchers in Queensland, Australia began to investigate the decline of 14 species of stream-dwelling frogs, endemic to the montane rain forests of eastern Australia (Laurance et al. 1996). During the preceding 15 years, these species had experienced sharp declines (more than 90%) and even disappearances from their mountain habitats (Laurance et al. 1996). Habitat degradation was/is the prevailing contributor to amphibian decline; however, many of the affected sites appeared pristine (Stuart et al. 2004). Further investigation refuted the possible contributions of pollutants, UV-B radiation, feral predators, and climate change (Stuart et al. 2004). The researchers theorized that the cause of the die-offs was an infectious disease of unknown aetiology (Laurance et al. 1996). Due to its extreme virulence, they proposed that the disease had been introduced to the Australian rain forests where it was now wreaking havoc on naïve host populations (Laurance et al. 1996). Furthermore, it was likely being disseminated by anthropogenic intercontinental movement of amphibians; indeed, frogs appeared to be dying of the same of the disease in Central America.

A team of investigators from Australia and Central America determined that the etiologic agent was a chytridiomycete fungus using a combination of pathology, microbiology, electron microscopy, and DNA sequencing (Berger et al. 1998). Their discovery was published in the Proceedings of the National Academy of Science in

1998, marking the first formal report of chytridiomycosis. They had confirmed that the disease could be transmitted by exposure to environmental contaminants, which was later expanded to include direct cutaneous contact (Rowley & Alford 2007). The fungus was classified as a new genus and species, *Batrachochytrium dendrobatidis* (*Bd*); the specific epithet being a reference to the genus of South American poison dart frogs from which it had been isolated into pure culture (Longcore et al. 1999, Pessier et al. 1999). A survey of archived *Xenopus laevis* specimens by Weldon et al. (2004) indicated that *Bd* originated in Africa, where it persisted sub-clinically in *X. laevis* frogs, and was likely disseminated by the international trade of *X. laevis* for use in human pregnancy tests in the early 20th century. However, a more recent analysis of the genomes of 234 *Bd* isolates from around the world led to the discovery of a hyperdiverse lineage (*Bd*ASIA-1) native to the Korean Peninsula that shares more genetic diversity with the global population of *Bd* than any other known lineage (O'Hanlon et al. 2018). Consequently, *Bd*ASIA-1 is now believed to be the ancestral population of *Bd*, and might have been spread by anthropogenic activity during the Korean War (O'Hanlon et al. 2018).

The mechanism by which *Bd* causes death was identified 10 years after its taxonomic classification. *Bd* causes hyperkeratosis (i.e. the thickening of the stratum corneum), which inhibits cutaneous electrolyte transport, leading to osmotic imbalance and eventually asystolic cardiac arrest (Voyles et al. 2009). Further studies have indicated that *Bd*'s pathogenicity is accelerated by lower environmental temperatures as well as its direct inhibition of the host lymphocyte-mediated response (Rollins-Smith et al. 2011, Fites et al. 2013). Variation in the hosts' ability to resist the immunosuppressive tactics of *Bd* has been linked to interspecific differential expression of genes associated with skin integrity and inflammatory responses (Ellison et al. 2015).

In addition to climate change and habitat disruption, genome evolution has been found to play an important role in *Bd*'s pathogenicity. Sun et al. (2011) used phylogenomic analyses to hypothesize that *Bd* had acquired two families of virulence effector genes from oomycetes and bacteria: a "crinkler protein" gene family involved in infection of keratinized tissue, and a family encoding serine peptidases, respectively. Genomic comparison of *Bd* to its closest known relative, the non-pathogenic chytrid *Homolaphlyctis polyrhiza,* revealed that its transition to

pathogenicity was likely facilitated by the lineage-specific expansions of three protease gene families (Joneson et al. 2011). Indeed, these expansions predated the emergence of chytridiomycosis as a contributor to amphibian decline.

1.4. TADPOLE MORTALITIES ASSOCIATED WITH PATHOGENIC PERKINSEA

Around the same time that chytridiomycosis was first being characterized in Australia and Central America, researchers in the USA were beginning to investigate an emerging disease linked to mass die-offs of tadpoles. The die-offs had occurred in multiple locations in the Northeast and seemed to be affecting the larvae of true frogs (family Ranidae). Moribund tadpoles appeared lethargic and bloated, with some exhibiting extensive haemorrhaging of the skin and enlargement and yellowing of the liver. In some locations, populations were experiencing very high mortalities up to 95% (Green et al. 2002), rousing conservation concerns.

The first documented MMEs occurred in New Hampshire in 1999 (Green et al. 2003). Researchers discovered that the tissues of diseased tadpoles, particularly the liver tissue, had been permeated by hundreds of thousands of small, spherical organisms (Green et al. 2003). Similar organisms (about 6 µm in diameter) were harvested from the livers of tadpoles that had perished during a MME in Georgia in 2006 (Davis et al. 2007). A combination of amplicon sequencing of small subunit (SSU) ribosomal DNA (rDNA) and phylogenetic analysis linked these organisms to the class Perkinsea, a group of alveolate protists traditionally thought to be marine and known to parasitize dinoflagellates and molluscs (Perkins 1988, Goggin et al. 1989, Davis et al. 2007, Chambouvet et al. 2008). Since 1999, MMEs associated with severe Perkinsea infection (SPI; Isidoro-Ayza et al. 2017) have been reported in seven other states across a broad geographic range: Florida, Mississippi, Virginia, Maryland, New York, Minnesota, and Alaska (Green et al. 2002, Davis et al. 2007, Landsberg et al. 2013, Isidoro-Ayza et al. 2017). Based on this distribution, it is highly likely that SPI-associated MMEs have also been occurring throughout Canada.

Most of these mortality events have occurred in tadpoles of the *Lithobates* genus, including *L. sylvaticus* (wood frog), *L. pipiens* (northern leopard frog) *L. sphenocephalus* (southern leopard frog), *L. catesbeianus* (American bullfrog), *L. clamitans* (green frog), *L. septrionalis* (mink frog), and *L. sevosus* (Mississippi gopher

frog) (Green et al. 2003, Davis et al. 2007, Landsberg et al. 2013, Isidoro-Ayza et al. 2017). *Lithobates sevosus* is of particular conservation concern, as the only known remaining population consists of about 100 individuals at a single site which is continuously declining (Ritcher et al. 2003, Cook 2009). MMEs have also occurred in larval hylids (family Hylidae), including *Pseudacris crucifer* (spring peeper) and *Acris gryllus* (southern cricket frog) (Isidoro-Ayza et al. 2017). There is some evidence that Perkinsea microbes occasionally infect adult frogs (Green et al. 2003, Jones et al. 2012, Karwacki et al. 2018); however, all known SPI-associated MMEs have been restricted to tadpoles (Isidoro-Ayza et al. 2017).

Recent phylogenetic analysis of SSU rDNA classified these potential tadpole pathogens as a distinctive clade within a broad monophyletic group known as Novel Alveolate Group 01 (NAG01; Chambouvet et al. 2015). This broad group includes three other clades (Clades A, B, and C; i.e. NAG01a-c) known to infect tadpoles in Africa, Europe, and South America without causing identifiable gross or tissue-level symptoms of disease (Chambouvet et al. 2015) (Table 1.1). This absence of pathology suggests that pathogenicity is restricted to the clade in North America, which has been designated Pathogenic Perkinsea Clade (PPC; Isidoro-Ayza et al. 2017) (Table 1.1). Many of the NAG01a-c samples were collected from early development phases or museum samples; therefore, it is difficult to exclude NAG01a-c pathologies as they might have gone undetected in these samples.

PPC initially comprised representatives from a single mass mortality event in Georgia (Davis et al. 2007). It was later expanded to include all known SPI-associated MMEs in the USA (Isidoro-Ayza et al. 2017). Only 2.5% (2/81) of healthy tadpoles surveyed in US localities with current or historical SPI outbreaks were found to harbour subclinical PPC infections similar to the NAG01 infections observed by Chambouvet et al. (2015; Isidoro-Ayza et al. 2017), providing further evidence that Perkinsea pathogenicity is primarily a North American phenomenon. NAG01 sequences have also been identified in planktonic freshwater samples from the UK, France, French Guiana, and Upstate New York, USA (Richards et al. 2005, Lefèvre et al. 2007, 2008, Chambouvet et al. 2015). These sequences were found to be closely related to NAG01 sequences derived from subclinically infected tadpoles, suggesting that the parasite also exists in a free-living phase and/or in association with other (planktonic) hosts (Chambouvet et al. 2015).

Table 1.1. Clades within the Novel Alveolate Group 1 (NAG01) that are known infectious agents of amphibians. Clade D (PPC) has been linked to Severe Perkinsea Infection (SPI) disease in tadpoles in North America; however, without fulfilment of Koch's postulates, the exact relationship between PPC and SPI disease remains unknown.

NAG01 Clade	Affiliated region	Associated with morbidity	Reference
Clade A	Africa, Europe, South America	No	Chambouvet et al. (2015)
Clade B	Africa, Europe, South America	No	Chambouvet et al. (2015)
Clade C	Europe, South America	No	Chambouvet et al. (2015)
Clade D (PPC)	North America	Yes	Isidoro-Ayza et al. (2017)

1.4.1. Overview of Alveolata

Perkinsea are a parasitic lineage within the eukaryotic superphylum Alveolata. Alveolata are a monophyletic group of primarily single-celled eukaryotes that are characterized by the presence of lipid-encased fluid sacs beneath their cell membranes (i.e. alveoli). They include three main phyla: Ciliophora (~4,500 known species; Fossiner & Hawksworth 2009), Dinoflagellata (~3,000 known species; Gómez 2012), and Apicomplexa (~4,500 known species; Levine 1988) (Figure 1.4). Ciliates are predators of other microorganisms and are characterized by short, dense, hair-like structures (i.e. cilia) covering the outside of their cell walls, which are used for mobility and catching prey. Dinoflagellates can be parasites, free-living predators, photoautotrophs, and mixotrophs (Taylor 1987, Stoecker 1999). They are characterized by dual flagella, and novel cytoskeletal and nuclear features (e.g. permanently condensed chromosomes) (Taylor 1987, Taylor et al. 2008). Apicomplexans are obligate endosymbionts characterized by a collection of cytoskeletal structures and organelles at the anterior end of the cell called the 'apical complex', which is used to facilitate infection of host cells (Lim & McFadden 2010, del Campo et al. 2019).

Phylogenetic analyses of multiple protein genes show that apicomplexans and dinoflagellates are more closely related to each other than either are to ciliates (Fast et al. 2002, Leander & Keeling 2004). Together they comprise the alveolate subgroup Myzozoa ("sucking life"), along with three other phyla: Colpodellida (free-living, predatory flagellates), Chromerida (e.g. photosynthetic symbionts of coral), and

Perkinsozoa (Calvalier-Smith & Chao 2004). Perkinsozoa (includes class Perkinsea) are intracellular parasites of mollusks (*Perkinsus* spp.) (Levine 1978), dinoflagellates (*Parvilucifera* spp.) (Norén et al. 1999), and (putatively) amphibians (the unnamed parasites which are the focus of this thesis) (Davis et al. 2007, Chambouvet et al. 2015).

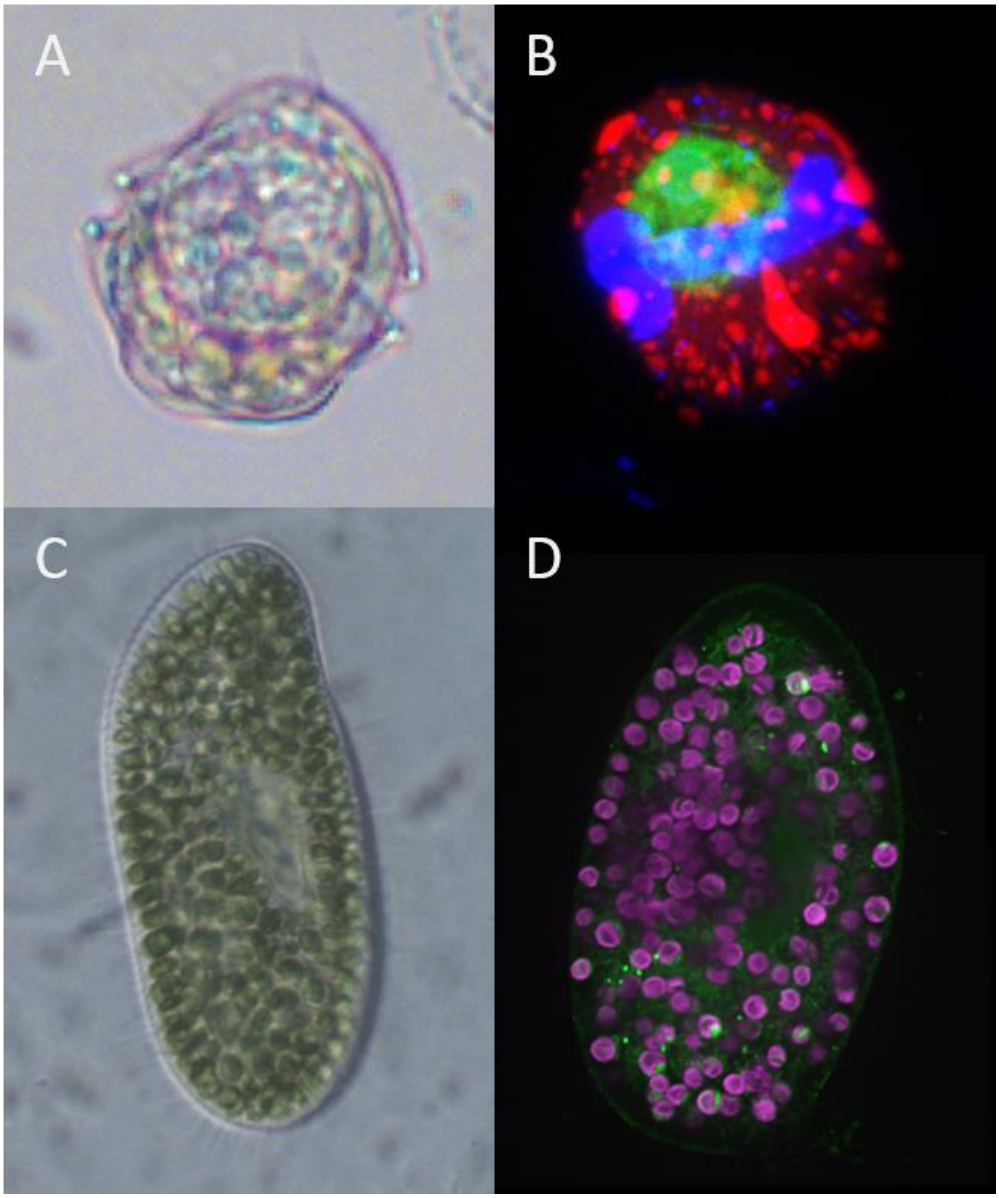

Figure 1.4. Bright field images (A & C) and fluorescence images (B & D) depicting the three major Alveolata phyla: Ciliophora, Dinoflagellata, and Apicomplexa.
A. *Alexandrium minutum* (Dinoflagellata) infected by *Parvilucifera sinerae* (Apicomplexa) (Credit: E. Alacid)
B. *Alexandrium minutum* (red) infected by *P. sinerae* (green) (Alacid et al. 2015)

C. *Paramecium bursaria* (Ciliophora) and algal symbionts (Credit: B. Jenkins)
D. *Paramecium bursaria* showing host lysosomes (green) and algal chlorophyll autofluorescence (purple) (Credit: B. Jenkins)

1.4.2. Parasite diversity, parasitic strategies, and the putative life cycle of amphibian Perkinsea

Parasitism can be defined as a symbiotic relationship between two organisms that is beneficial to one (the parasite) and costly to the other (the host). The parasite lives on or inside the host for all or a portion of its life, exploiting the host for nutrients and/or a means of reproduction. It is an extremely successful mode of life, as evidenced by the sheer number of parasite species in existence, and by the number of times that it has evolved in unrelated lineages (Blaxter et al. 1998, Westwood et al. 2010, Blouin & Lane 2012, Poulin & Randhawa 2015, Weinstein and Kuris 2016). Nearly every living organism is subject to exploitation by parasites; in fact, humans are host to nearly 300 species of parasitic worm and over 70 species of protozoa (Cox 2002). In metazoans, it has evolved independently at least 223 times across 15 phyla (primarily Arthropoda), and can be found in about 40% of species (400,000 – 800,000 species) (Weinstein and Kuris 2016). Parasitic plants have evolved independently at least 12 times, and comprise about 4,500 (1%) flowering species (Westwood et al. 2010). All viruses are obligate intracellular parasites because they cannot reproduce without the assistance of host cell metabolic machinery. Parasitism is found in many protists (notably the aforementioned Apicomplexa), fungi (including Microsporidia), and prokaryotes (including many agents of human disease). There is currently no (credible) means of estimating the number of species in these groups because they are vastly understudied. Furthermore, the concepts typically used to define species (e.g. biological and morphological species concepts) are obfuscated by frequent asexual reproduction and complex life cycles in these groups (de Meeûs et al. 1998, Kunz 2002).

Each independent transition to parasitism faces the same selective pressures, including invasion of and survival on or within the host, sustainable use of host resources, and transmission to new hosts (Poulin & Randhawa 2015). These uniform pressures have pushed unrelated lineages along the same evolutionary path, leading

to a convergence of six general parasitic strategies: parasitoidism, parasitic castration, directly transmission, trophically transmission, vector-transmission, and micropredation (Poulin & Randhawa 2015). Parasitoids (i.e. endoptergyote insects, such as parasitoid wasps) and parasitic castrators (e.g. barnacle parasites of crustaceans) are both highly virulent parasites, and their body size can be within several magnitudes of their host; the primary difference is that parasitoidism usually ends with the host's death, whilst parasitic castration terminates the host's reproduction (Kuris 1974, Poulin & Randhawa 2015). They occur at low frequencies in host populations, which ensures that their extreme virulence does not inadvertently impede their own survival by reducing host availability. Among directly transmitted parasites, the ratio of parasite to host size can vary dramatically (e.g. head lice vs. a cold virus); however, they (almost) invariably feature intensity-dependent virulence and an aggregated distribution among host populations (i.e. a small number of hosts harbour the majority of the parasite population) (Poulin 2013, Poulin & Randhawa 2015). Trophically and vector-transmitted parasites are similar in that both use an (often behaviourally manipulated) intermediate host to reach their definitive hosts; the former use the definitive host's prey as their intermediate host, and the latter exploit micropredators (e.g. blood-sucking dipteran insects). The parasite to host size ratio is variable in trophically-transmitted parasites, whilst vector-transmitted parasites are usually many orders of magnitude smaller than their hosts (Poulin & Randhawa 2015). An example of a trophically transmitted parasite is the apicomplexan *Toxoplasma gondii*, which is ingested by an intermediate rodent host that is in turn preyed upon by the parasite's definitive feline host (Berdoy et al. 2000). An example of a vector-transmitted parasite is the apicomplexan *Plasmodium falciparum*, which is transmitted between its intermediate human hosts by anopheline mosquitoes (Day et al. 1998).

The specific parasitic strategy of amphibian Perkinsea is currently unknown. We can speculate that it shares the same strategy of direct transmission implemented by other Perkinsea species (e.g. *Perkinsus* spp.) (Perkins 1966, 1988). Microscopic observations of clinical samples have revealed multiple cell types (i.e. hypnospore-like and trophozoite-like) with morphologies similar to those of *Perkinsus* spp. (e.g. *P. marinus*, *P. olseni*) (Perkins 1966, 1988, Green et al. 2003, Davis et al. 2007, Cook 2009, Landsberg et al. 2013, Isidoro-Ayza et al. 2017, 2018). Based on these observations, we can speculate that the life cycle of amphibian Perkinsea is direct and

obligate, and comprises four stages: hypnospores (prezoosporangia), zoosporangia, zoospores, and trophozoites (Villalba et al. 2004) (Figure 1.5). The zoospores are the likely agents of infection, whilst the trophozoites are the primary agents of disease (Villalba et al. 2004). Inside the host, trophozoites replicate by schizogony (i.e. multiple fission) (Villalba et al. 2004), forming aggregates of burgeoning meronts that disseminate throughout the host liver (preferentially), kidney, spleen, and pancreas (Isidoro-Ayza et al. 2017, 2018). As the infection intensifies, the host begins to show symptoms of SPI disease. The parasites are released into the environment in the form of thick-walled hypnospores (Villalba et al. 2004). During this free-living phase, the hypnospores proliferate into zoosporangia, eventually forming tubular outgrowths that release myriad biflagellated anisokont zoospores (Villalba et al. 2004). This proliferation is presumably triggered when the parasite senses proximity of a host. The zoospores likely invade new hosts through oral mucosa, gills, or gut tissue, where they develop locally into trophozoites, which are disseminated systemically within leukocytes through blood vessels and lymphatics (Isidoro-Ayza et al. 2018).

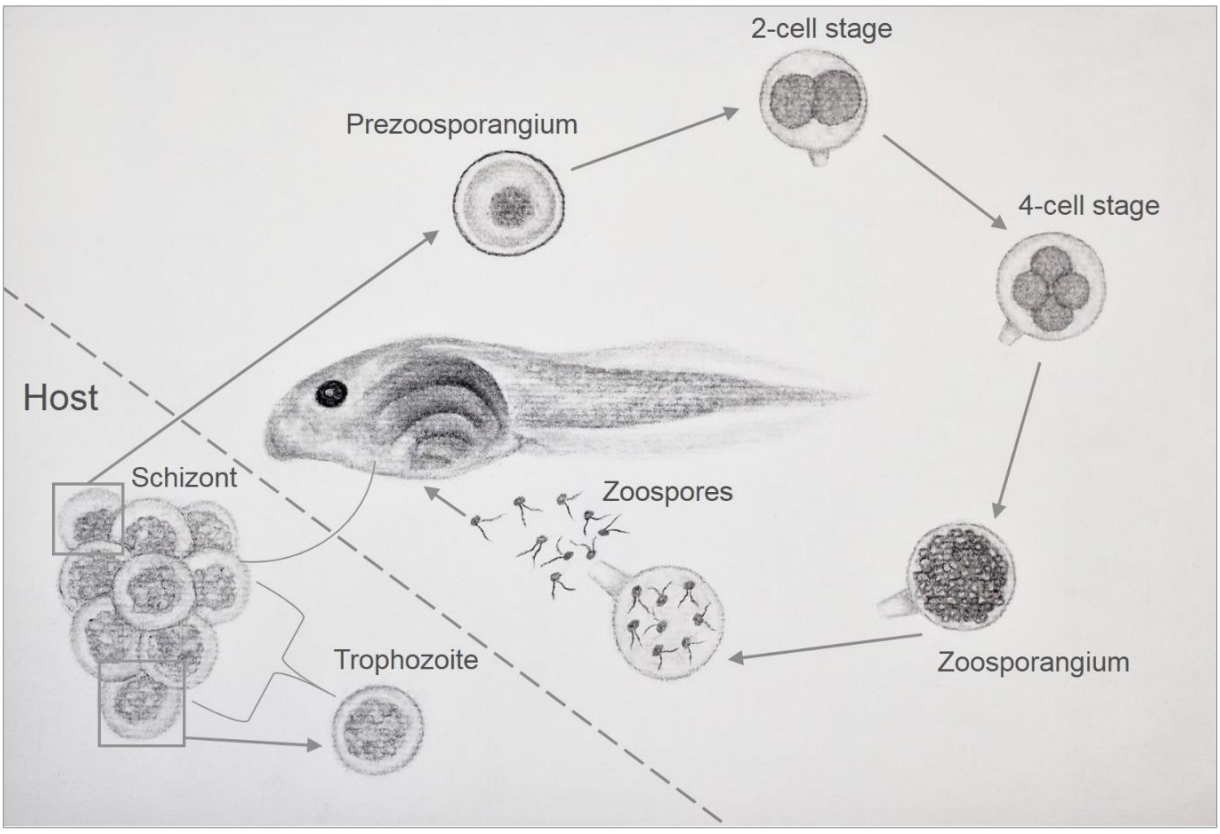

Figure 1.5. Putative life cycle of amphibian Perkinsea based on my own microscopic observation of cells resembling prezoosporangia and trophozoites, harvested from

‘clinical’ samples, as well as speculation based on my own review of Perkinosis in molluscs by Villalba et al. (2004).

1.5. THE USE OF MOLECULAR METHODS IN INFECTIOUS DISEASE RESEARCH

Beginning in the 1930s, several previously distinct scientific disciplines joined forces to lay the foundations of modern-day molecular biology. Numerous biologists, chemists, and physicists worked together to tease apart the dynamics between genes and proteins. Their breakthroughs included the discovery that genes are comprised of DNA (Avery et al. 1944, Hershey & Chase 1952), the discovery of the double helical structure of DNA (Watson & Crick 1953), the discovery of an intermediary molecule between DNA and proteins (i.e. messenger RNA) (Jacob & Monod 1961), and the revelation of the genetic code: an arrangement of triplet bases (codons) that determine amino acid sequence and ultimately protein structure (Nirenberg & Matthaei 1961, Gardner et al. 1962, Wahba et al. 1963, Nirenberg et al. 1965). The following decades saw further development and refinement of molecular biology techniques, including molecular cloning, polymerase chain reaction (PCR), gel electrophoresis, microarrays, and next-generation sequencing. These techniques have greatly increased the rapidity, sensitivity, and specificity of DNA and RNA detection and characterization, and have provided increasingly large amounts of sequence data, which has driven a convergence with the field of bioinformatics. The techniques have been readily adopted by researchers of infectious disease.

Before the molecular revolution, infectious disease research was dependent on symptom identification and histopathological observation. Undoubtedly, this led to many misdiagnoses, as many diseases share the same symptoms and even look similar under a microscope. In 1884, a set of postulates (for controlled infection experiments) were designed as a means to establish the relationship between infection and disease causation (Koch 1884a), and were successfully applied to the bacterial diseases anthrax, cholera, and tuberculosis. However, strict adherence to the postulates has proven more of a hindrance than help with respect to many diseases because they are inevitably invalidated by microorganisms that cannot be grown in pure culture, such as viruses, or carried by asymptomatic hosts, such as numerous gut bacteria capable of commensal-to-pathogen transition. In light of these

shortcomings, the postulates have been adopted as guidelines for establishing disease causality, and are not strictly necessary to reach a conclusion. In more recent times, infectious disease research has relied on advancements in the ability to detect and manipulate nucleic acids in order to identify pathogens and further elucidate the host-pathogen relationship (Fredricks & Relman 1996).

Advances in molecular biology have revolutionized the field of wildlife epidemiology. Genetics and genomics can be used to identify pathogens, map routes of transmission, elucidate the mechanisms underlying disease susceptibility (Blanchong et al. 2016), and determine the origin of disease outbreaks (e.g. the aforementioned use of genomes from 234 *Bd* isolates to trace the origin of the global chytriodiomycosis outbreak to the Korea Peninsula; O'Hanlon et al. 2018). PCR, quantitative PCR (qPCR), and reverse transcriptase PCR (RT-PCR) have been widely applied as means of detection and quantification (of pathogen load) for many wildlife pathogens, including bacteria (e.g. *Mycobacterium bovis*, an agent of tuberculosis-like disease in mammals; Roug et al. 2014), fungi (e.g. *Bd*; Retallick et al. 2006), protists (e.g. *Plasmodium* spp.; Knowles et al. 2011), and both DNA and RNA viruses, such as ranavirus (Galli et al. 2006) and rabies (Black et al. 2002), respectively. In 2018, a qPCR assay was developed for PPC (i.e. the putatively pathogenic clade of amphibian Perkinsea), which was used to compare pathogen loads in different host tissues, species, locations, and seasons (Karwacki et al. 2018). The power of PCR is vastly increased by multiplexing, which allows for the simultaneous detection (and quantification) of multiple pathogens (e.g. Picco et al. 2007). PCR approaches that target conserved genes (e.g. the 16S small subunit (SSU) rRNA gene in bacteria, the 18S SSU rRNA gene in protozoa, and the ITS rRNA region in fungi) can be applied to clinical samples in which the specific agent of disease is unsuspected. These approaches rely on comparisons to sequences in a reference database to infer pathogen identities.

Molecular methods can provide insights into routes of wildlife disease transmission. For example, genetic methods that measure host relatedness (e.g. microsatellite genotyping) can reveal how kin-structure affects disease transmission. These revelations are especially important for directly transmitted diseases, such as chronic wasting disease, which has been linked to spread within family groups of white-tailed deer (*Odocoileus virginianus*) (Grear et al. 2010). Alternatively, pathogen

genetic data can provide the same insights on familial transmission, as revealed among groups of sleepy lizards (*Tiliqua rugosa*) sharing the same *Salmonella enterica* genotypes (Bull et al. 2012). Furthermore, analysis of spatial genetic structure of host populations can discern their migration patterns, and therefore help predict the spread of disease and identify high risk populations. These predictions are enhanced when the impact of landscape features is considered (i.e. landscape genetics). For example, rivers were found to act as barriers to gene flow among raccoon (*Procyon lotor*) populations in Ontario, which was linked to restricted transmission of rabies (Cullingham et al. 2009). Phylogeographic patterns can also reveal how host dispersal affects the evolution of pathogens, as evidenced by the highly diverse spatial genetic structure of feline immunodeficiency virus (FIV) isolates derived from long ranging mountain lions (*Puma concolor*) compared to the localized spatial genetic structure of FIV isolates derived from shorter ranging bobcats (*Lynx rufus*) (Lee et al. 2014).

Attributes of both host and pathogen influence host susceptibility to disease in terms of resistance (i.e. the host ability to prevent infection after pathogen exposure) and tolerance (i.e. the host ability to minimize disease severity once infected by the pathogen). Genetic diversity in hosts has been associated with increased host resistance and tolerance, particularly in the major histocompatibility complex (MHC), a family of immunity response genes responsible for recognizing foreign pathogens. For example, Hedrick et al. (2001) found that inbred Gila topminnows (*Poeciliopsis occidentalis*) that were homozygous for a particular MHC gene exhibited higher infection intensities (and lower survival) when exposed to an exotic fluke (*Gyrodactylus turnbulli*), in comparison to the heterozygous, outbred group. Host resistance has also been linked to (non-MHC) genes encoding cytokines, molecules used to signal between immune cells and regulate immune responses. For example, Turner et al. (2011) found that genetic variation (i.e. single nucleotide polymorphisms; SNPs) at specific interleukin loci was associated with either increased or decreased resistance to infection by multiple pathogens in a population of field voles (*Microtus agrestis*). Alternatively, genetic variation in the pathogens themselves can affect their infectivity and virulence. For example, experimental infections of two frog species (*L. pipiens* and *L. sylvaticus*) with three genetically distinct ranavirus strains revealed strain-specific mortality in *L. pipiens* (but not in *L. sylvaticus*) (Echaubard et al. 2014). The

same experiments also revealed that mortality rates were affected by host genotype and temperature (Echaubard et al. 2014).

The rise of molecular methods in wildlife disease research has enhanced our understanding of host-pathogen dynamics. As these methods continue to progress, particularly the omics approaches, the amount of data available for host and pathogen genomes and transcriptomes will greatly increase, as will metagenomic data from a variety of environmental and veterinary samples. This will pave the way for more in depth investigations of the mechanisms by which pathogens evade host immune responses, and allow us to potentially identify therapeutic targets for the treatment of disease. It will also increase our capacity to identify novel pathogens. Furthermore, the developing field of landscape epidemiology will provide a better understanding of how landscape complexity influences the spatial distribution and spread of disease (Blanchong et al. 2016). In light of these developments, the future of wildlife disease research will depend on collaborations from a variety of disciplines, including ecology, epidemiology, and bioinformatics. These collaborations will lead to better-informed wildlife management strategies that will more effectively mitigate the impacts of disease and protect biodiversity.

1.6. THESIS AIMS

SPI is an emerging disease of amphibians that is (negatively) impacting an already imperilled animal group. Surveys dating back to 1999 show that is it the third most common infectious disease of amphibians in North America (Isidoro-Ayza et al. 2017). Since the first report of a "*Perkinsus*-like agent" in tadpole livers during die-offs in New Hampshire, USA (Green et al. 2003), phylogenetic analysis has confirmed that these organisms are part of Perkinsea (Davis et al. 2007). Further phylogenetic analyses identified two distinct lineages of amphibian Perkinsea: one that is associated with cryptic infections in Africa, Europe, and South America (Chambouvet et al. 2015), and one that is associated with SPI disease and mortality in North America (Isidoro-Ayza et al. 2017). The pathology of SPI disease has been described in detail by Isidoro-Ayza et al. (2018).

Despite these advances, there are many aspects of amphibian Perkinsea and SPI disease that are still unknown. We have yet to successfully grow the parasite in

culture or in the presence of an amphibian host. Doing so would allow us to confirm our speculations about its life cycle (i.e. that it is similar to those of *Perkinsus* spp.) (Figure 1.5). Actively growing cells in culture could provide (suitable) material for use in experimental infections, as Koch's postulates have yet to be fulfilled for SPI disease. The field has not yet established that amphibian Perkinsea directly leads to SPI disease, nor have we confirmed if certain co-factors (e.g. environmental stress, pollution, co-infection) contribute to disease progression. Although Perkinsea infection and SPI disease are known to be distributed across a broad range of amphibians (Chambouvet et al. 2015, Isidoro-Ayza et al. 2017), we do not know if differences in host susceptibility shape this distribution. We have yet to determine if the two lineages of amphibian Perkinsea are distinct strains, or if they are the same strain with multiple copies of the 18S SSU rRNA gene encoded on the same genome. Finally, we must continue to explore the extent of the parasite's geographic range, particularly in regions with high amphibian diversity and/or a large number of threatened species.

This thesis aims to shed light on some of the unknown aetiological and epidemiological aspects of amphibian Perkinsea. Collectively, this work seeks to further understand the role of this protist group in the ecology of amphibians, whilst providing tools for future research.

- The first aim is to elucidate the relationship between Perkinsea infection and SPI disease in amphibians, and to investigate cannibalism as a potential route of transmission. This aim is addressed by the Chapter 2 objectives: experimental infection of *Rana dalmatina* tadpoles with Perkinsea cells in accordance wth Koch's postulates, and a feeding experiment in which *Lithobates sphenocephalus* tadpoles were fed liver tissue from other *L. sphenocephalus* tadpoles that had been experimentally exposed to Perkinsea cells.

- The second aim is to develop a method to rapidly and simultaneously detect the two clades of amphibian Perkinsea (i.e. PPC and NAG01a-c), which can be used to assess the prevalence of one or both of these clades (possibly as a product of co-infection), and therefore provide improved understanding of

infection dynamics. This aim is addressed by the Chapter 3 objective: the development of a novel duplex qPCR assay for the rapid and simultaenous detection of multiple Perkinsea clades in amphibian tissues.

- The third aim is to further explore the geographic and host ranges of amphibian Perkinsea, and the co-association of the two clades, which can help provide insights into the origins of the clades, as well as possible differences in host susceptibility. This aim is addressed by the Chapter 4 objective: investigation of amphibian Perkinsea infection in captive tadpoles from the UK and wild tadpoles from Panama (a global centre of amphibian diversity) using phylogenetic analyses.

- The fourth aim is to assess gut microbiome composition as a potential co-factor for Perkinsea infection in amphibians. This aim is addressed in the Discussion, which describes a study comparing the intestinal eukaryotic microbiomes of healthy and Perkinsea-infected tadpoles using amplicon-based metagenomics. This study was intended to be a separate data chapter, but could not be brought to completion due to experimental complexities.

Chapter 2. Experimental infection of ranid tadpoles with putatively pathogenic amphibian Perkinsea

ABSTRACT

Alveolates in the class Perkinsea have been found to infect amphibians across a broad taxonomic and geographic range. Phylogenetic analysis of a subsection of the nuclear SSU rRNA gene has indicated that there are two distinct lineages of Perkinsea associated with amphibians: a putatively non-pathogenic lineage linked to infections of tadpoles in Africa, Europe, and South America (with no identifiable signs of pathology), and a putatively pathogenic lineage linked to disease and mass mortality of tadpoles in North America. However, the exact relationship between amphibian Perkinsea infection and disease remains unclear, particularly in the absence of the fulfilment of Koch's postulates. We examined this aetiology by experimentally infecting ranid tadpoles with the putatively pathogenic lineage of Perkinsea using direct injections and tank exposures, and by feeding tadpoles infected (liver) tissue. *Rana dalmatina* tadpoles were either directly injected with Perkinsea cells or retained in tanks containing varying cell densities. We investigated cannibalism as a possible transmission route by feeding *Lithobates sphenocephalus* tadpoles liver tissue from other *L. sphenocephalus* tadpoles that had been experimentally exposed to Perkinsea cells (in tanks). We monitored the tadpoles for approximately six weeks and five weeks, respectively. During this time, none exhibited disease symptoms. Tissue samples were molecularly screened for Perkinsea. Our results for the experimental infections of *R. dalmatina* indicate that our transmission was successful (as indicated by detection of Perkinsea DNA); however, the parasites did not demonstrate symptoms of a pathogenic interaction, nor could we identify RNA gene transcription indicating ribosomal activity. The results for the cannibalism feeding experiment were obscured by a pre-existing cryptic infection among our experimental tadpoles, which was revealed by posthumous molecular screening. Nonetheless, other data suggest: an incompatibility between host and parasite, the contribution of co-factors to the development of disease, and/or a reduced infectivity of the parasite life stage used for inoculation, implying that pathogenicity is either limited for this lineage or is only manifest under specific ecological circumstances.

2.1. INTRODUCTION

Over the last few decades, declines in amphibian populations have accelerated dramatically (Stuart et al. 2004, Wake & Vredenburg 2008). Major contributors to amphibian decline include habitat destruction, pollution, invasive species, and infectious disease (Chanson et al. 2008). The unique life history and skin permeability of amphibians increases their susceptibility to certain infections. Larval anurans (tadpoles) are especially vulnerable because they rely solely on a rapid but nonspecific innate immune response, as opposed to adult frogs which also have a fully developed adaptive immune system (Pasquier et al. 1989, Chambouvet et al. 2020). Since the late 1990s, tadpole mortalities across a broad taxonomic and geographic range in North America have been linked to alveolate protists in the class Perkinsea (Green et al. 2002, Green et al. 2003, Davis et al. 2007, Landsberg et al. 2013, Isidoro-Ayza et al. 2017), but no formal experimental assessment has been published to prove the relationship between infection and disease. Macroscopic and histological examination of tissues from severely infected tadpoles reveals extensive haemorrhaging of the skin and enlargement and yellowing of the liver, as well as the invasion of the liver (preferentially), kidney, spleen, and pancreas by a large number of Perkinsea cells (Isidoro-Ayza et al. 2017, 2018). Collectively, these symptoms have been used to describe Severe Perkinsea Infection (SPI) associated disease (Isidoro-Ayza et al. 2017).

SPI disease is linked to a specific lineage of Perkinsea, designated Pathogenic Perkinsea Clade (PPC; Isidoro-Ayza et al. 2017) (Table 1.1), which is part of a broad monophylogenetic group of alveolates known as Novel Alveolate Group 01 (NAG01; Chambouvet et al. 2015). Another NAG01 lineage comprising three clades (Clades A-C) is associated with putatively asymptomatic tadpole infections in Africa, Europe, and South America (Chambouvet et al. 2015) (Table 1.1). The absence of morbidity in tadpoles infected by NAG01 Clades A-C (NAG01a-c) suggests that pathogenicity might be restricted to PPC. PPC sequences have been recovered from moribund tadpoles from all known SPI-associated mortality events in the USA (Davis et al. 2007, Isidoro-Ayza et al. 2017), whereas they have only been recovered from 2.5% (2/81) of apparently normal tadpoles surveyed (in localities with current or historical SPI outbreaks) (Isidoro-Ayza et al. 2017). These findings suggest that PPC is indeed a

disease-causing pathogen; however, neither the presence of PPC sequences nor the presence of SPI disease symptoms (which are also associated with infections by other pathogens, such as ranavirus) are sufficient evidence to conclude that PPC causes disease. Formally, disease causation can be established by applying Koch's postulates to controlled infection experiments (e.g. Longcore et al. 1999, Dungan et al. 2007, Lorch et al. 2011).

Koch's postulates were established by German physician and microbiologist Robert Koch in 1884 after he used them to identify the cause of tuberculosis (Koch 1884a). They include four criteria: 1) The microbe must be present in every case of the disease, but not in the absence of disease. 2) The microbe must be isolated from a diseased host and grown in pure culture. 3) The cultured microbe should induce the same disease when inoculated into healthy host. 4) The microbe should be reisolated from the experimentally inoculated host, and should be identical to the original. The first postulate has been (indirectly) upheld by USA-based surveys that recovered PPC sequences from all symptomatic tadpoles and only 2.5% (2/81) of asymptomatic tadpoles (Isidoro-Ayza et al. 2017); although, this low level of association with asymptomatic tadpoles could be a product of sampling organisms at an early stage of infection. The remaining postulates, I am to address in this study.

Koch's postulates have limitations with regard to certain microbes. For example, commensal microbes that only become pathogenic under certain conditions (e.g. *Vibrio cholerae*) prevent the fulfillment of the first postulate, a limitation that was recogizned by Koch himself (Koch 1884b). Microbes that cannot be grown in pure culture, such as viruses, prevent the fulfillment of the second postulate (Rivers 1937). Because of their limitations, the postulates are not always a feasible means of establishing disease causation. Nevertheless, they have served as guidelines which have illuminated numerous human and wildlife disease pathologies (Koch 1884a, Fredericks & Relman 1996, Longcore et al. 1999, Dungan et al. 2007, Lorch et al. 2011). The postulates have been satisfied for both *Batrachochytrium dendobatidis* and *B. salmandrivorans*, the agents of chytriodiomycosis in frogs and salamanders, respectively (Longcore et al. 1999, Davidson et al. 2003, Martel et al. 2013). When the postulates are satisified, it is in essence proven that the disease in question manifests as a direct result of host-pathogen interactions, as opposed to the synergistic effects of co-infections and/or environmental conditions (i.e. the pathogen

is likely a primary pathogen as opposed to an opportunistic pathogen). This confirmation is useful for informing disease management, as it indicates a greater need to prevent transmission rather than mitigate the selective forces that might increase pathogenicity. In other words, the disease would likely be managed more effectively with a focus on strategies that directly prevent movement of the disease (e.g. avoiding translocation of animals, controlling host populations through culling or reproductive control, vaccination) (Wobeser 2002, Gortázar et al. 2014), instead of attempting to identify and treat co-factors contributing to disease (by comprising host immunity).

For this study, we applied Koch's postulate tests to SPI disease by experimentally infecting *Rana dalmatina* tadpoles with Perkinsea cells isolated from *Lithobates sylvaticus* tadpoles. We were unable to acquire live *L. sylvaticus* tadpoles for our experimental infections due to the geographical incongruence between the range of *L. sylvaticus* and the location of our experiments; however, *Rana* is closely related to *Lithobates*. Indeed, the two genera were both classified as *Rana* until Frost et al. (2006) established the distinction between North American and European species. It is therefore conceivable, based on taxonomic association, that *R. dalmatina* is susceptible to infection by PPC, and that the infection has potential to cause disease.

Although the pathogenesis of SPI disease is the primary focus of this chapter, we are also interested in the methods by which Perkinsea infection can spread among tadpoles. Tadpoles are opportunistic feeders and are known to cannibalise other tadpoles, particularly when resources are scarce (Collins & Cheek 1983, Crump 1983). Cannibalism among amphibians has been linked to pathogen transmission. Brunner et al. (2007) found that 80% of naïve *Ambystoma tigrinium* larva became infected with ranavirus after consuming tail clips from infected conspecific larva. Pizzatto & Shine (2011) found that 62.5% of *Rhinella marina* adults (previously treated with antiparasitics) became infected with lungworms after consuming infected conspecific metamorphs. Interestingly, Pfenning et al. (1998) found that *A. tigrinium* larvae were less likely to survive to metamorphosis after consuming diseased conspecifics compared to diseased heterospecifics (both infected by *Clostridium*), and exhibited a preference for (healthy) heterospecifics over conspecifics. We inferred that cannibalism is a conceivable transmission route for Perkinsea, and we examined this

possibility by feeding *L. sphenocephalus* tadpoles liver tissue from other *L. sphenocephalus* tadpoles that had been experimentally exposed to Perkinsea cells.

2.2. METHODS

2.2.1. Sample collection

In June and July 2016, researchers from the University of Exeter and the US Fish and Wildlife Service Anchorage Field Office surveyed tadpoles at three Perkinsea-positive sites in the Kenai Peninsula Borough of Alaska (Table S2.1), one of which was experiencing a tadpole mass mortality event at the time of sampling. *Lithobates sylvaticus* tadpoles that appeared both healthy and symptomatic (Figure 2.1) were collected from multiple sites. Tadpoles were euthanized using an overdose of tricaine methane-sulfonate (MS-222). Livers were removed with tools that were sterilized between each tadpole using ethanol followed by lighter flame. Liver tissue containing Perkinsea organisms was preserved in either Dulbecco's Modified Eagle Medium/Nutrient Mixture F-12 (DMEM/F-12) or Ray's fluid thioglycollate medium (Figure 2.2).

In March and April 2017, *R. dalmatina* egg clutches were collected from ponds in the natural areas surrounding České Budějovice, Czech Republic. Tadpoles were reared from these clutches at the Czech Academy of Science Institute of Parasitology in 10 L tanks containing dechlorinated tap water until reaching Gosner stages (Gosner 1960) 24-33 (prior to limb development). These stages appear to be predominantly affected by the parasite (Davis et al. 2007).

In April 2019, *L. sphenocephalus* tadpoles were collected from a single site at the University of Central Florida in Florida, USA. These tadpoles included both the group that was exposed to Perkinsea cells in order to obtain infected tissue for feeding (Group A) (Table S2.3), as well as the group that was subsequently fed the tissue (Group B) (Table S2.4).

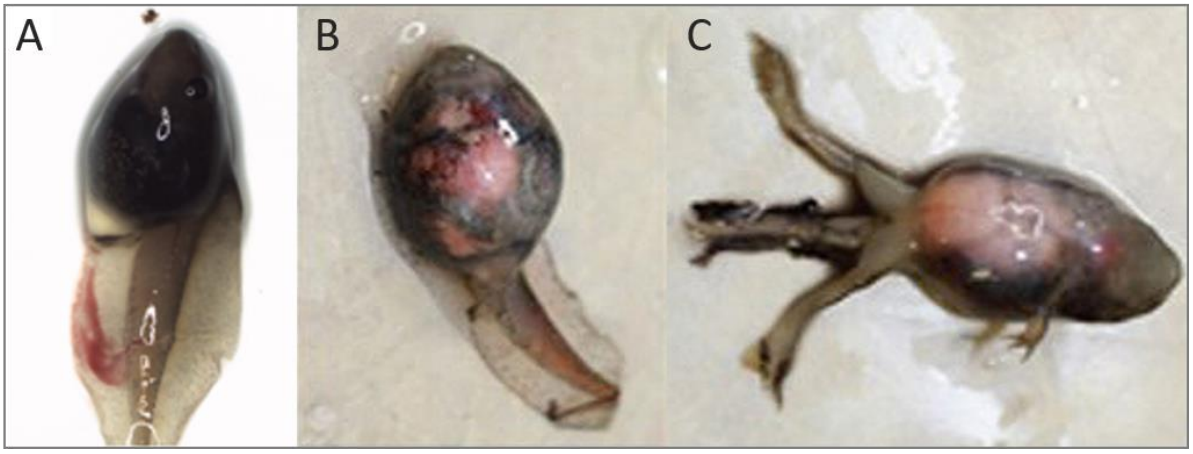

Figure 2.1. *Lithobates sylvaticus* tadpoles and metamorph.
A. 'Healthy' tadpole **B.** Perkinsea-infected tadpole **C.** Perkinsea-infected metamorph (Credit: A. Chambouvet & T. Richards)

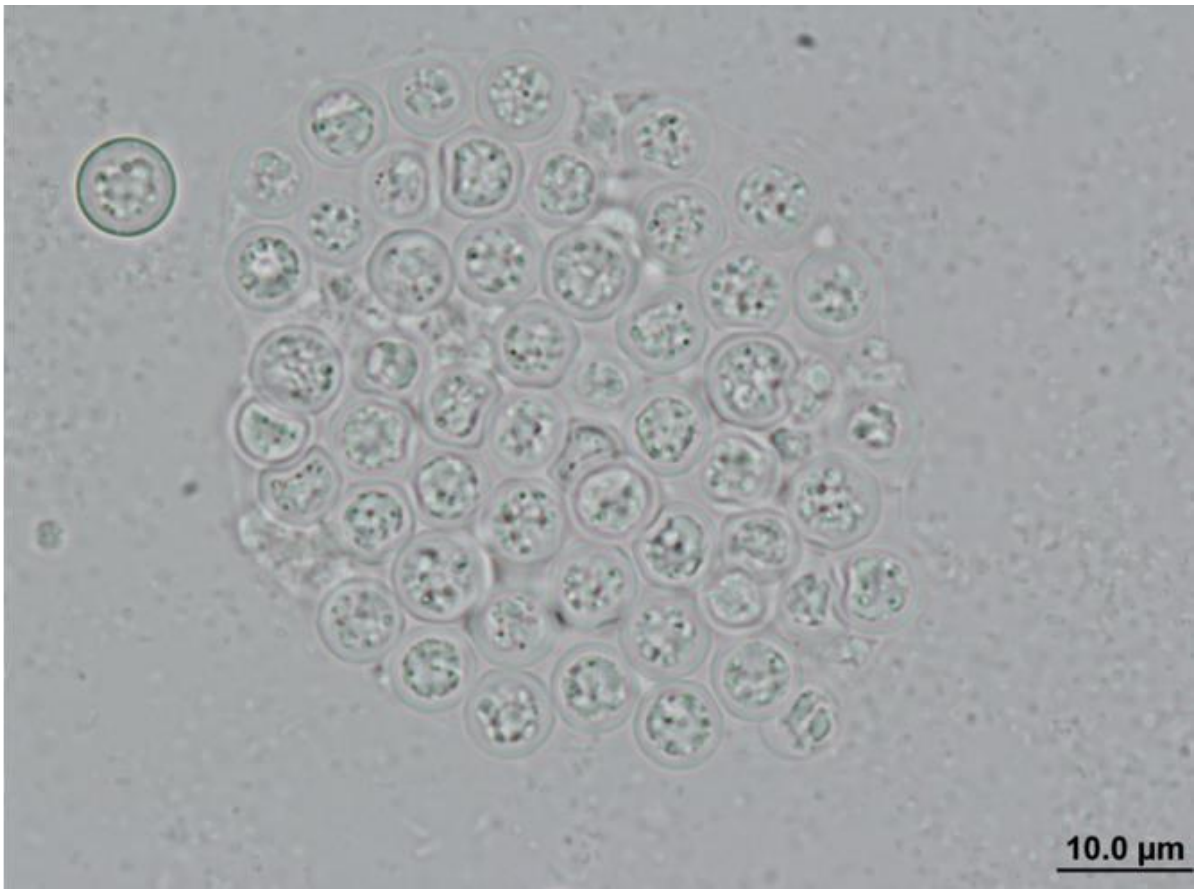

Figure 2.2. Perkinsea parasites recovered from the liver of a *Lithobates sylvaticus* tadpole (Credit: M. Jirků)

2.2.2. Experimental infections of *Rana dalmatina*

Direct injections and tank exposures were conducted at the Czech Academy of Science Institute of Parasitology using Perkinsea cells recovered from tadpoles from three sites (KNA03, KNA14, and KNA21) and preserved in DMEM/F-12 or Ray's fluid thioglycollate medium. One of the sites (KNA21) had mass tadpole mortality. Cells were separated into three tubes according to site, and an aliquot from each tube was counted on a hemocytometer. An aliquot from the KNA03 tube was triple-washed with amphibian Ringer's solution (a solution containing several salts in the same concentrations that occur in amphibian body fluids), and resuspended in Ringer's solution to bring the concentration to 1.8×10^6 cells/ml. For the direct injections, 43 tadpoles were injected in their coelomic cavities with 15 µl of the triple-washed KNA03 cell suspension (~27,000 cells per tadpole) using a hypodermic needle. Forty-three controls were injected in their coleomic cavities with 15 µl Ringer's solution. For the tank exposures, we placed 60 tadpoles into three 1 L beakers with approximately 1×10^6 total cells from each of the three sampling sites. In order to maximize spore ingestion, we let them graze for two days in the beakers before transferring to 10 L tanks. Controls were handled in the same manner without the addition of cells. We repeated this set up using increased parasite loads of 3×10^6 cells/l and 6×10^6 cells/l from KNA14. There were no chemical differences between the injection, exposure, and control treatments, aside from possible residual growth medium or thioglycollate medium (following the saline washes).

The tadpoles were monitored in their tanks for a period of 40 days. During the monitoring period, a subset of tadpoles was intermittently euthanized with an overdose of MS-222 from each of the treatments (Table S2.2) and microscopically examined (focusing on their livers) for symptoms of SPI disease and/or the presence of Perkinsea organisms. Tadpoles that died naturally during the monitoring period were examined in the same manner; however, many of these tadpoles were cannibalised by the surviving tadpoles before they could be examined. Because of the high rate of cannibalism, some subsets were decreased from 2 to 1 to prevent premature depletion (Table S2.2). At one time point, a subset of 3 tadpoles was taken from the control injection tank and the KNA03 injection tank for formalin preservation (Table S2.2). At the end of the monitoring period, all the surviving tadpoles (Table S2.2) were euthanized with an overdose of MS-222. A subset of 1-3 tadpoles was collected (randomly, if more than three remained) from each treatment and preserved whole in

RNA*later* (Sigma-Aldrich) at -20°C for downstream molecular screening (Table S2.6). Whenever possible, a separate subset of 2 tadpoles from each treatment was microscopically examined (focusing on their livers). We used a chi-square test of independence to measure the differences between the survivorships of the control and experimental groups.

2.2.3. Evaluation of Perkinsea cell viability using propidium iodide

The cells used for the *R. dalmatina* experimental infections were tested for viability using propidium iodide (PI). PI is a fluorescent intercalating agent that binds to nucleic acids (Crompton et al. 1992). It distinguishes live intact cells from dead cells because it cannot penetrate intact cell membranes, meaning only dead cells will fluoresce when stained (Figure 2.4). In this way, it was used to confirm that the absence of morbidity and mortality in the infected tadpoles was not due to loss of viable Perkinsea cells in the inoculum. PI staining was conducted at the University of Exeter in August 2017, approximately five weeks after the end of the infection experiment.

2.2.4. Cannibalism feeding experiment with *Lithobates sphenocephalus*

The cannibalism feeding experiment was conducted at the University of Central Florida. A subset of Group A tadpoles (GroupA_infected: n = 6) were incubated in 250 ml of amphibian Ringer's solution for 1 hour containing approximately 3 x 10^5 cells/ml. They were then transferred to individual containers with pond water from their collection site. As a control group, the second subset (GroupA_control: n = 6) were placed directly into individual containers without prior exposure to Perkinsea cells. The tadpoles were euthanized after 10 days, except for three that were euthanized earlier due to metamorphosis. Livers were removed from each tadpole using sterile tools. Samples were taken from each liver using sterile swabs. The livers from GroupA_control were combined into a tube, and the livers from GroupA_infected were combined into a tube. Using sterile tools, tail clips were taken from all Group B tadpoles before placing them in individual tanks. A subset of Group B tadpoles (GroupB_infected, n = 16) were fed an approximately equal sized portion from the infected liver tube. The same was repeated with the control liver tube for a second subset of Group B tadpoles (GroupB_control1, n = 14). A third subset of Group B

tadpoles was fed only algae wafers (GroupB_control2, n = 10). Tadpoles were monitored for approximately five weeks. During this monitoring period, tadpoles were continually processed when they died or were euthanized (due to metamorphosis). This involved extracting their livers using sterile tools, which were preserved in RNA*later* (Sigma-Aldrich) and stored at -20°C. After 1.5 weeks, tissues from all processed tadpoles up to that point (n = 19) were transported back to the University of Exeter in an insulated medical cooler and transferred to -20°C, whilst the remaining tadpoles (n = 21) were processed at the University of Central Florida. At the end of the monitoring period, the remaining tadpoles were euthanized with MS-222. We used a chi-square test of independence to measure the differences between the survivorships of the control and experimental groups.

2.2.5. Nucleic acid extraction and NAG01 molecular screening, cloning, and sequencing

- *Rana dalmatina*

Whole livers were removed from the harvested tadpoles using sterile tools and preserved in RNA*later* (Sigma-Aldrich). Liver tissue was flash frozen in liquid nitrogen, disrupted by grinding with a microcentrifuge pestle, and homogenized with QIAshredder spin-columns (Qiagen). Total DNA and total RNA were extracted from each tissue sample using the AllPrep DNA/RNA Micro Kit (Qiagen) following the manufacturer's protocol.

DNA samples were screened for Perkinsea using conventional PCR to confirm that our delivery methods were effective (i.e. the parasites were successfully inoculated and retained in the host tissues). Screening was conducted at the University of Exeter from September 2017 – February 2018. We used a combination of four primers to target a portion of the parasite's 18S SSU rRNA gene (Table 2.1). Two of our primer pairs were designed to target NAG01 Clades A-D (NAG01a-d) and one pair was designed to target PPC. DNA samples were first screened using the NAG01a-d-specific primer pairs, followed by the PPC-specific primer pair. The reaction mixture included 1x PCR MasterMix (Promega), 0.5 µM of each primer, 1 µl of template DNA, and molecular-grade water to bring the total reaction volume to 25 µl. Each PCR included a negative control (molecular-grade H_2O) and a positive

control (10 ng DNA from PPC-infected Alaska *L. sylvaticus* tadpole liver). Cycling reactions were as follows: 2 min at 95°C, followed by 35 cycles of 30 s at 95°C, 30 s at 56°C, and 60 s at 72°C, with an additional 10 min extension at 72°C.

RNA samples were screened using reverse transcriptase PCR (RT-PCR) in order to test if the parasites were ribosomally active. Prior to performing the RT-PCRs, RNA samples were DNase-treated using the TURBO DNA-free Kit (Ambion) according to the manufacturer's protocol for routine treatment. All RT-PCRs were performed using the OneStep RT-PCR Kit (Qiagen) according to the manufacturer's protocol. The reaction mixture included 1x OneStep RT-PCR Buffer, 1x Q-Solution, 400 µM of each dNTP, 0.6 µM of each primer, 1 µl of OneStep RT-PCR Enzyme Mix, 1 µl of template DNA, and AnalaR water (VWR) to bring the total reaction volume to 25 µl. Each reaction included a negative control (molecular-grade H_2O) and a positive control (10 ng DNA from PPC-infected Alaska *L. sylvaticus* tadpole liver). Cycling reactions were as follows: 30 min at 50°C, 15 min at 95°C, followed by 30 cycles of 60 s at 94°C, 60 s at 50°C, and 60 s at 72°C, with an additional 10 min extension at 72°C.

PCR products were checked on a 2% agarose gel and purified using the GeneJET PCR Purification Kit (Thermo Fisher). Purified PCR products were cloned into the plasmid vector pSC–A–amp/kan using the Strata Clone PCR Cloning Kit (Agilent Technologies) following the manufacturer's protocol. Plasmids were transformed into StrataClone SoloPack Competent Cells (Agilent Technologies) and blue-white screened on LB-ampicillin plates with 2% X-gal. White mono-colonies were cultured in LB-ampicillin broth at 37°C overnight. Plasmid DNA was extracted from the cultures using the GeneJET Plasmid Miniprep Kit (Thermo Fisher) according to the manufacturer's protocol. Extractions were sent to Eurofins Genomics (Wolverhampton, UK) for sequencing using the M13 reverse primer.

Table 2.1. Primers designed to target NAG01 Perkinsea and applied to total DNA extracted from *Rana dalmatina* tadpole livers to assess the efficacy of the delivery method for our experimental infections.

Primer	Sequence (5' - 3')	Specificity	Reference
300F-B	GGG CTT CAY AGT CTT GCA AT	NAG01 Clades A-D	Chambouvet et al. (2015)
PPC_R2	ACG GTC CAA AAA GGT AGG AC	NAG01 Clade D (PPC)	This study
Perk R1	CTG CTG GCA CCA GAC TTG	eukaryotes	This study
Perk R2	ART ATA CGC TAT TGG AGC TGG	eukaryotes	This study

- *Lithobates sphenocephalus*

Whole livers were removed from *L. sphenocephalus* tadpoles using sterile tools and preserved in RNA*later* (Sigma-Aldrich). Total DNA was extracted from the tail clips and liver swabs of Group A tadpoles, and from the livers and tail clips of Group B tadpoles. Tail clips were used here as secondary sample to identify tank-based exposure to the Perkinsea group, in addition to that from feeding. Extractions were carried out using the DNeasy Blood and Tissue Kit (Qiagen) according to the manufacturer's protocol.

DNA samples processed at the University of Central Florida were screened with a qPCR assay designed to detect PPC, the putatively pathogenic lineage of NAG01 Perkinsea. The assay uses a primer pair that targets a 133 bp fragment of the 18S rRNA gene of NAG01a-d, and a PPC-specific TaqMan probe (Table 2.2). The qPCRs were carried out according to the method of Karwacki et al. (2018).

DNA samples processed at the University at Exeter were also screened with a qPCR assay designed to detect PPC. This assay uses a primer pair that targets a larger fragment (287-290 bp) of the 18S rRNA gene of NAG01a-d, and a PPC-specific TaqMan probe (Table 2.2). All qPCRs were performed on the CFX96 real-time PCR detection system (Bio-Rad). The reaction mixture included 1x TaqMan Gene Expression Master Mix (Thermo Fisher Scientific), 500 nM of each primer, 250 nM of probe, 1 or 5 µl of template DNA, 5% DMSO, and molecular-grade water to bring the total reaction volume to 25 µl. Each qPCR included a negative control (molecular-grade H_2O) and 1 ng of plasmid DNA containing sequence from PPC. Cycling reactions were as follows: 10 minutes at 95°C followed by 40 cycles of 15 seconds at 95°C and 2 minutes at 60°C.

DNA samples were then subjected to conventional PCR using the same set of primers targeting the 287-290 bp fragment of the 18S rRNA gene of NAG01a-d (Table 2.2). The reaction mixture included 1x concentration PCR MasterMix (Promega), 500

nM of each primer, 1 or 2 µl of template DNA, and molecular-grade water to bring the total reaction volume to 25 µl. Each PCR included a negative control (molecular-grade H_2O) and 1 µl of template DNA from a positive control (DNA from PPC-infected Alaska *L. sylvaticus* tadpole liver). Cycling reactions were as follows: 2 min at 95°C, followed by 35 cycles of 30 s at 95°C, 30 s at 56°C, and 60 s at 72°C, with an additional 10 min extension at 72°C. PCR products were checked on a 2% agarose gel.

Table 2.2. Primers designed to target NAG01 Perkinsea, and probes designed to target the PPC lineage of NAG01 Perkinsea. PCR and qPCR assays utilizing the primers and probes were applied to total DNA extracted from *Lithobates sphenocephalus* tadpole tissues to test cannibalism as a route of transmission. "_P1" indicates an oligonucleotide probe sequence.

Primer/probe	Sequence (5' - 3')	Specificity	Reference
300F-B	GGG CTT CAY AGT CTT GCA AT	NAG01 Clades A-D	Chambouvet et al. (2015)
NAG01R_1	GCC TGC TTG AAA CRC TCT AA	NAG01 Clades A-D	This study
PPC_P1	FAM-TGC CAA GAA CGA CCG TCC TAC-BHQ-1	NAG01 Clade D (PPC)	This study
PerF	GAA CGA CCG TCC TAC CTT GG	NAG01 Clades A-D	Karwacki et al. (2018)
PerR	AGG CCT GCT TGA AAC ACT CT	NAG01 Clades A-D	Karwacki et al. (2018)
PerkinseaP	6-FAM-ACC GTG TTG ATC GAG GCA TT-Tamra	NAG01 Clade D (PPC)	Karwacki et al. (2018)

2.3. RESULTS

2.3.1. Experimental infections of *Rana dalmatina*

Rana dalmatina tadpoles were monitored for 40 days after being experimentally infected with Perkinsea. During the monitoring period, none of the tadpoles developed symptoms of SPI disease and there was no increase in the mortality of infected tadpoles compared to the controls (Figure 2.3). Surprisingly, both the injection and exposure controls had decreased survivorships relative to the experimental treatments (Figure 2.3). Differences between the survivorships of the control and experimental infection groups were statistically significant based on the chi-square test of independence (Figure 2.3). Increasing the parasite dose did not affect mortality nor did using source material (Perkinsea cells) from a site with high tadpole mortality (i.e. KNA21) (Figure 2.3). The microscopic examinations of tadpoles that were euthanized or died during the monitoring period, and those that were euthanized at the end of

monitoring period, did not reveal symptoms of SPI disease nor the presence of Perkinsea organisms.

The frequent cannibalism that occurred within our treatment groups, specifically the control group, hindered our ability to maintain accurate daily mortality counts. Therefore, we could not represent our mortality data using a survival curve, which is a standard for experimental infections (e.g. Lorch et al. 2011). Instead, we opted to show survivorship as the proportion of tadpoles that survived until the end of the monitoring period (Table S2.2 & Figure 2.3). The tadpoles that were collected and euthanized throughout the monitoring period for microscopic examination were removed from the survivorship calculations (Table S2.2).

A

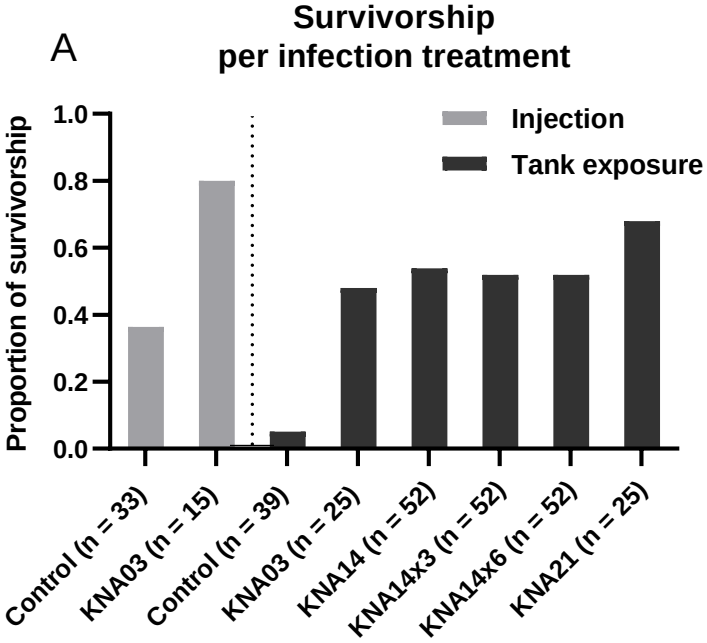

B

Treatment comparison	X^2	df	N	p-value
Control_I vs. KNA03_I	7.85	1	48	< 0.01
Control_Te vs. KNA03_Te	16.38	1	64	< 0.001
Control_Te vs. KNA14_Te	23.94	1	91	< 0.001
Control_Te vs. KNA14x3_Te	22.48	1	91	< 0.001
Control_Te vs. KNA14x6_Te	22.48	1	91	< 0.001
Control_Te vs. KNA21_Te	28.85	1	64	< 0.001

Figure 2.3. A. Proportion of *Rana dalmatina* tadpoles that survived until the end of the 40-day monitoring period following eight experimental treatments. Values along the x-axis (i.e. n = xx) correspond to the number of tadpoles per treatment, excluding those collected before the end of the monitoring period (see Table S2.2 for details). **B.** Results of the chi-square test for each pairwise comparison of the controls and their corresponding infection treatment (I = injection, Te = tank exposure).

2.3.2. Evaluation of Perkinsea cell viability and a possible correlation between survivorship and viable cell dose

Our PI stain revealed that the cell suspensions from KNA03, KNA14, and KNA21 had viable cell proportions of 68%, 26%, and 12%, respectively (Figure 2.5). Although cell viability varied dramatically between the three sources, each contained a high number of viable cells per tadpole (Figure 2.5), indicating that the quality of the source material was not a likely factor in the outcome of the experiments. We plotted the survivorship data for our tank exposure treatments against their corresponding counts of viable cells per tadpoles (in increasing order) to test for a possible dose effect on survivorship (Figure 2.6). We decided to omit the injection treatment because of inherent variability in the method of infection. A linear regression analysis of the data suggested a possible correlation between viable cell dose and survivorship ($y = 0.6 + -0.004x$); however, the relationship was not significant ($p = 0.33$). An R-squared value of 0.31 indicated that approximately 31% of the survivorship variance can be attributed to viable cell dose (Figure 2.6).

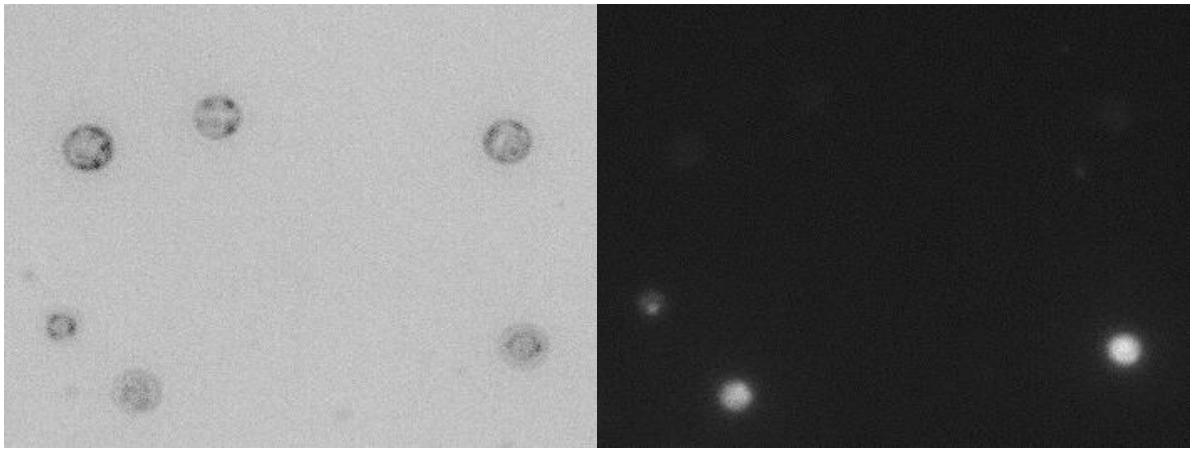

Figure 2.4. Perkinsea cells stained with propidium iodide (40X magnification).

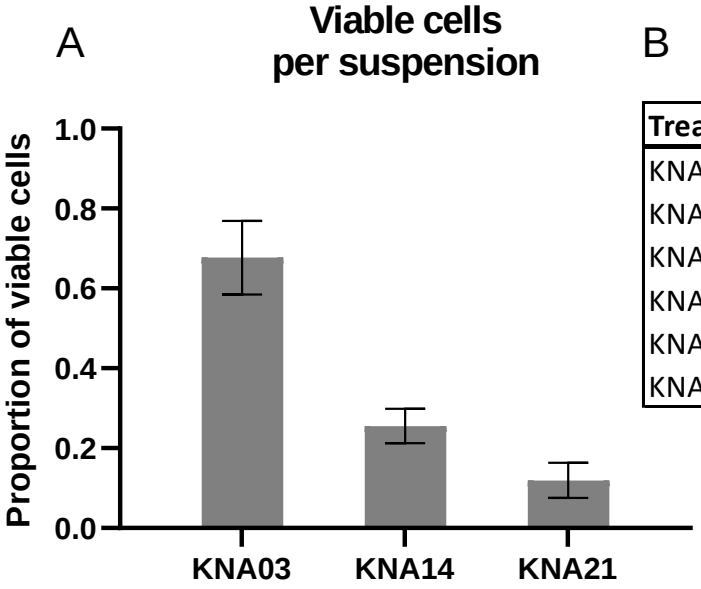

B

Treatment	Viable cells per tadpole
KNA03 injection	18,421
KNA03 tank exposure	11,413
KNA14 tank exposure	4,614
KNA14x3 tank exposure	13,842
KNA14x6 tank exposure	27,685
KNA21 tank exposure	2,025

Figure 2.5. A. Proportion of viable Perkinsea cells from the three cell suspensions used for experimental infections of *Rana dalmatina*. Error bars represent SEM values of technical replicates (KNA03: n = 4, KNA14: n = 10, KNA21: n = 4). **B.** Number of viable Perkinsea cells per tadpole used for each of the infection treatments.

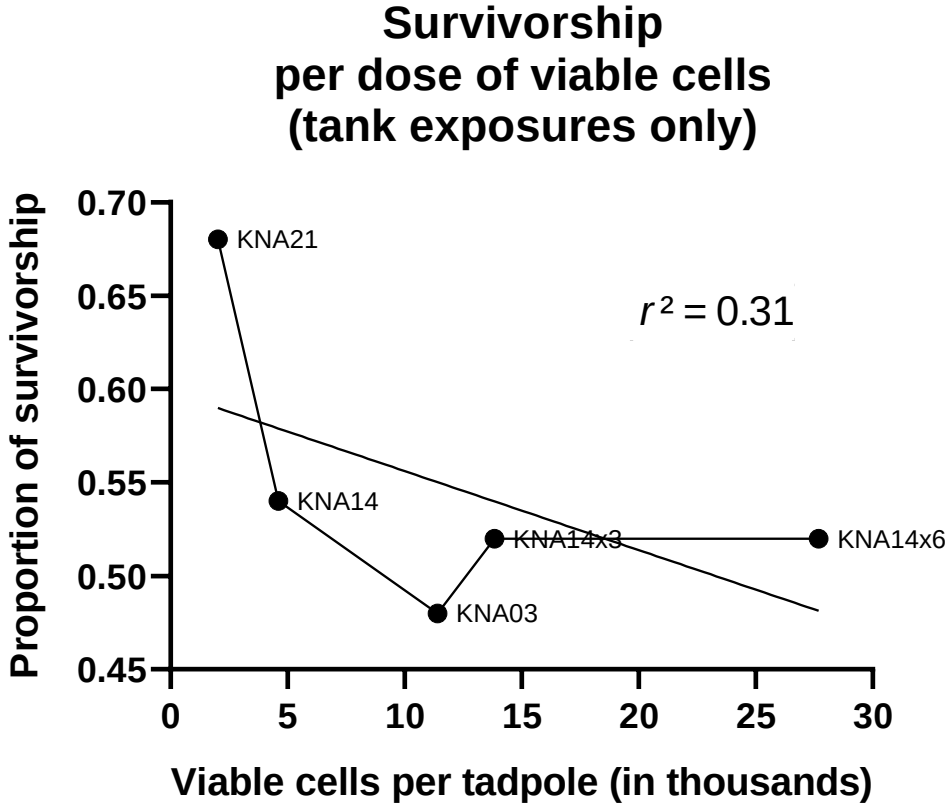

Figure 2.6. Proportion of survivorship as a function of viable cell dose per tadpole. Viable cells counts were derived from the five tank exposure treatments.

2.3.3. Cannibalism feeding experiment with *Lithobates sphenocephalus*

Lithobates sphenocephalus tadpoles were fed from three different sources: algae wafers (n = 10), control liver tissue (i.e. liver tissue from tadpoles not exposed to Perkinsea, n = 14), and infected liver tissue (i.e. liver tissue from tadpoles exposed to Perkinsea, n = 16). Tadpoles were monitored for five weeks (many of which had to be euthanized prior to the end of the monitoring period due to metamorphosis – indicating the likely absence of disease progression). During this period, no tadpoles developed symptoms of SPI disease. Those fed with infected liver tissue had a slightly lower survivorship than those fed with algae wafers, but a slightly higher survivorship than those fed with control liver tissue (Figure 2.7). However, these differences were not statistically significant based on the chi-square test of independence (Figure 2.7).

A

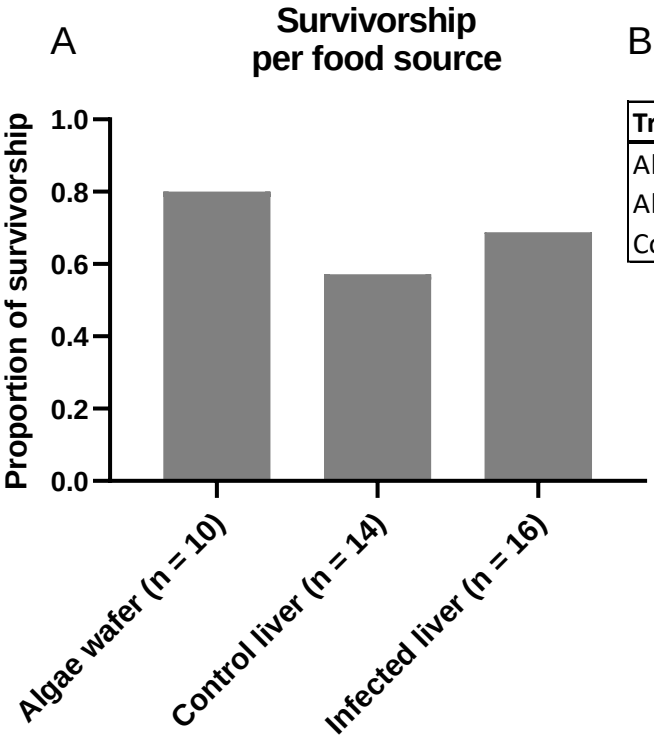

B

Treatment comparison	X^2	df	N	p-value
Algae wafer vs. Control liver	1.37	1	24	> 0.1
Algae wafer vs. Infected liver	0.4	1	26	> 0.25
Control liver vs. Infected liver	0.43	1	30	> 0.25

Figure 2.7. A. Proportion of *Lithobates sphenocephalus* tadpoles that were fed from three different sources and survived to either metamorphosis or the end of the five-

week monitoring period. Ten tadpoles were fed algae wafers, 14 tadpoles were fed liver tissue from other tadpoles not exposed to Perkinsea (i.e. control liver), and 16 tadpoles were fed liver tissue from other tadpoles exposed to Perkinsea (i.e. infected liver). Each tadpole was maintained in a separate tank during both feeding and monitoring. **B.** Results of the chi-square test for each pairwise comparison.

2.3.4. NAG01 molecular screening, cloning, and sequencing

- *Rana dalmatina*

Total DNA was extracted from a subset of 1-3 tadpoles from each experimental infection treatment, at the end of the 40-day monitoring period. Because we designed our experiment to maximise the success of infection (i.e. by directly injecting tadpoles with Perkinsea cells and by maximising their exposure to Perkinsea cells in tanks), we surmised that our small subset would be sufficient for detecting the presence/absence of a NAG01 DNA signal. Analysis of these extractions revealed that 1-3 tadpoles from each treatment were positive for both NAG01a-d and PPC DNA, except for the controls and the exposure treatment using 3 x 10^6 cells from KNA14, both of which had no positive samples (Table S2.6). The positive DNA results were as follows: KNA03 injection = 2/3, injection control = 0/2, KNA03 tank exposure = 2/3, KNA14 tank exposure = 2/3, KNA14x3 tank exposure = 0/3, KNA14x6 = 1/3, KNA21 tank exposure = 2/3, tank exposure control = 0/1 (Table S2.6). NAG01a-d RT-PCRs were negative for all treatments; for this reason, PPC-specific RT-PCRs were not performed (because PPC is part of NAG01a-d).

- *Lithobates sphenocephalus*

The PPC-specific qPCR assays revealed late-stage amplification in all of the liver and tail tissue sampled from Group A (tadpoles from which livers were harvested as a food source) (Table S2.3) and Group B (tadpoles that were fed infected liver, control liver, or algae wafers) (Table S2.5). PCR products from the NAG01a-d PCR were checked on a 2% agarose gel, which revealed bands of the correct size in the majority of samples (excluding the liver samples from specimens processed at UCF, which were not included in the screen) (Tables S2.3 & S2.5). Most of the bands were very faint in appearance.

2.4. DISCUSSION

There is evidence of the existence of two lineages of Perkinsea capable of infecting amphibians (Chambouvet et al. 2015, Isidoro-Ayza et al. 2017): a putatively pathogenic lineage (PPC) and a putatively non-pathogenic lineage (NAG01a-c). PPC has been linked to disease and die-offs in North American ranids. However, the exact relationship between infection and the development of disease is unclear. We investigated the aetiology of SPI disease by addressing Koch's postulates through experimental infections (direct injections and tank exposures) of *R. dalmatina* tadpoles with Perkinsea cells recovered from *L. sylvaticus* tadpoles. We also investigated the possibility that cannibalism provides a route of transmission for Perkinsea infection by feeding (apparently) healthy *L. sphenocephalus* tadpoles with tissue from other *L. sphenocephalus* tadpoles that had been experimentally exposed to Perkinsea.

2.4.1. Experimental infections of *Rana dalmatina*

Rana dalmatina tadpoles that were experimentally infected with Perkinsea did not develop symptoms of SPI disease, nor did they experience an increase in mortality relative to the controls. There was no detectable RT-PCR-based evidence for rRNA transcription of the target Perkinsea group at the point of tadpole sampling. A strong band of the correct size was observed in the positive control upon agarose gel inspection, indicating that the RT-PCR assay was effective. The combination of positive DNA and negative RNA Perkinsea PCR results suggests that bona-fide exposure was occurring but that the infecting population was not ribosomally active at the point of tadpole sampling.

Interestingly, the opposite effect was seen due to high mortality in the control treatments, suggesting a complex unforeseen effect. We speculated that this effect might be the distortion of eating behaviour in our infection treatments (i.e. cannibalism is reduced among tadpoles exposed to Perkinsea). Indeed, we found that the proportion of cannibalised tadpoles per treatment was significantly lower in the infection treatments compared to their corresponding controls based on the chi-square test of independence (Figure S2.1). Several studies have suggested that pathogen transmission acts as a selective force against cannibalism in some animals (Elgar & Crespi 1992, Curtis 2014), including amphibians (Pfenning et al. 1998). In this way,

conspecifics avoid the enhanced virulence associated with host specificity (e.g. resistance to host immune defences among pathogens) (Burdon & Jarosz 1988). The decrease in cannibalism observed in our pathogen-exposed tadpoles suggests such a phenomenon might have transpired in our experiment. Confirmation would require a follow up experiment similar to the one used by Pfenning et al. (1998) in which *A. tigrinum* larvae were fed both healthy and diseased conspecifics and heterospecifics, revealing an increase in mortality when preying upon diseased conspecifics, and a preference for healthy heterospecifics over heathy conspecifics (in a complementary experiment). Our *L. sphenocephalus* cannibalism feeding experiment (coincidentally) emulated this set-up (albeit using liver tissue rather than whole larvae as a food source); unfortunately, molecular evidence of a pre-existing cryptic PPC infection in our experimental tadpoles impeded our assessment of the results.

The results of the PI stain indicated that the Perkinsea cells used for our experimental infections were viable. Survivorship (in the tank exposure treatments) appeared to be negatively correlated to viable cell dose based on linear regression (Figure 2.6); however, this effect was only slight (r^2 = 0.31). In addition, our sample size (N = 5) was likely too small to accurately capture this effect in its entirety, which would require increasing the dose range and ideally including replicates for each dose. Our PCR screen confirmed the presence of NAG01 Perkinsea DNA in a subset of samples from each of our infection treatments, excluding the KNA14x3 tank exposure (Table S2.6). These results indicated that our infection methods were indeed effective. However, the lack of concomitant RNA amplification (identified using RT-PCR screening) indicated that the Perkinsea were not ribosomally active, and therefore not actively infectious. Overall, our results can be explained by one or more of the following reasons: an incompatibility between host and pathogen preventing parasite activity and proliferation post exposure, the contribution of unknown biotic and abiotic co-factors to the development of disease not recapitulated in the experimental set up, and a reduced infectivity of the Perkinsea life stage used for inoculation.

Despite the similarity between the species from which the parasites were harvested (*L. sylvaticus*) and the species into which they were inoculated (*R. dalmatina*), the latter did not develop the symptoms that were observed in the former. It is possible that Nearctic ranids (e.g. *Lithobates* spp.) are more susceptible to SPI disease than their Palearctic counterparts (e.g. *Rana* spp.). Such disparate patterns

in response to infectious disease are evident, for example, in the increased susceptibility of hibernating bats in North America to white-nose syndrome (the disease caused by *Pseudogymnoascus / Geomyces destructans*) compared to those in Europe (Lorch et al. 2011, Zukal et al. 2016). *Pseudogymnoascus destructans* was shown to have been recently introduced to North America (likely by European visitors in Upstate New York), meaning that its chiropteran hosts have not had time to evolve tolerance to infection (Zukal et al. 2016). It is possible that PPC has been recently introduced to North America, where it thrives among naïve hosts. However, the scarcity of PPC infections outside of North America (Chambouvet et al. 2015) indicates that it might be endemic to North America. In this regard, the emergence of SPI disease is probably not due to host naivety, but instead due to changes in the immunological and ecological aspects of the host-parasite relationship that transition the relationship from benign to pathogenic (Rachowicz et al. 2005).

A second explanation for our results is that SPI disease might only develop in association with other factors that increase host stress. It is likely that certain environmental conditions increase a hosts' susceptibility to infection, either by directly inhibiting immune cell function or by increasing stress hormone levels (Carey et al. 1999). Their susceptibility could be further augmented by natural, stress-inducing events such as metamorphosis, intensive breeding, and food deprivation (Rollins-Smith et al. 2011). Increased disease prevalence and severity have been shown to correlate with changes in environmental conditions (e.g. temperature, ultraviolet radiation) and pollution levels (Carey et al. 1999, Daszak et al. 1999, Collins & Storfer 2003, Stuart et al. 2004). Exposure to pollution has been linked to an increase in Perkinsea infection and the severity of dermo disease in oysters (Chu & Hale 1994). Water-borne agrochemicals have been linked to an increase in trematode infections and limb deformities in ranids in the USA (Kiesecker 2002, Rohr et al. 2008). Increases in temperature and ultraviolet radiation can promote the proliferation of parasites in the environment (Gleason et al. 2014), thereby increasing the odds of host exposure (a trend which is especially alarming with regard to climate change). For example, increased UV-B exposure was linked to an outbreak of *Saprolegnia ferax* (the agent of saprolegniasis) that resulted in the mass mortality of anuran embryos in Oregon, USA (Kiesecker & Blaustein 1995).

Of course, infections with multiple pathogens can further stress the host immune system and increase susceptibility to disease, as evidenced in the report of co-infection by PPC and ranavirus in a multispecies tadpole mortality event in Florida, USA (one of these species was *L. sevosus*, the critically endangered dusky gopher frog) (Landsberg et al. 2013). Furthermore, interactions between multiple strains of the same pathogen can strengthen their pathogenicity (Balmer & Tanner 2011), which has been demonstrated in frogs exposed to multiple strains of ranavirus (Mihaljevic et al. 2018). It is unclear what effect mixed Perkinsea infections (i.e. infection with both the putatively pathogenic lineage and the putatively non-pathogenic lineage) might have on pathogenicity, nor is it clear how frequently these co-infections occur. Enhanced surveillance methods are needed to assess the prevalence of co-infection and provide a better overall understanding of host-pathogen dynamics.

A third explanation for our results is that the life stage of the cells that were used for inoculation have reduced infectivity. In order to maximize infectivity, controlled infections should be done using pathogens that are in their log-phase of growth. Unfortunately, we were unable to induce growth of amphibian Perkinsea in culture, despite numerous attempts using various types of growth media, ambient temperatures, antibiotic and antifungal treatments, and carbon sources and nutrient supplements. As an alternative, we used the original source material for our infections: cells preserved in DMEM/F-12 or Ray's fluid thioglycollate medium. In these storage conditions, we inferred that the parasites were in a spore-like 'resting' stage (i.e. hypnospores) and that introducing them to potential hosts would trigger their transition into a pathogenic feeding stage (i.e. trophozoites); however, the results of our experimental infections indicate that this transition likely did not occur on a meaningful scale.

2.4.2. Cannibalism feeding experiment with *Lithobates sphenocephalus*

Studies have indicated that amphibian pathogens can be transmitted by cannibalism (Pfenning et al. 1998, Brunner et al. 2007, Pizzatto & Shine 2011). We investigated cannibalism as a possible mode of Perkinsea transmission by feeding (apparently) healthy *L. sphenocephalus* tadpoles with liver tissue from other *L. sphenocephalus* tadpoles that had been experimentally exposed to Perkinsea. Our control groups were fed algae wafers and liver tissue from unexposed tadpoles. The results of our

molecular screen indicate that a cryptic PPC infection pre-existed in a majority of tadpoles in every group (including those that were used as a food source). The tadpoles used for our experiment were collected from Florida, USA, a state with numerous reports of PPC infection and SPI disease in tadpoles (Landsberg et al. 2013, Isidoro-Ayza et al. 2017, Karwacki et al. 2018). Many of the tadpoles were collected at Gosner stages preceding limb development, which appear to be the stages predominantly affected by Perkinsea (Davis et al. 2007). We were unable to locate an anuran egg mass in Central Florida from which we could rear tadpoles in a laboratory setting in order to prevent them from being exposed to Perkinsea.

These results obscure our ability to accurately assess if consuming infected tissue is indeed a means of Perkinsea transmission. However, the results are somewhat interesting because they contradict the findings of Isidoro-Ayza et al. (2017), which found cryptic PPC infections in only 2 out of 81 (2.5%) apparently normal tadpoles surveyed. These two tadpoles were identified as *R. sphenocephala*; one was collected in 2008 from a site in Prince George's County, Maryland, USA, and the other was collected from a site in Wakulla County, Florida, USA (Isidoro-Ayza et al. 2017). Both of these sites were experiencing an SPI outbreak at the time of collection (Isidoro-Ayza et al. 2017). Wakulla County is located in the northern part of Florida, approximately 350 km from our collection site in Central Florida.

Our results are more consistent with the Florida tadpole survey conducted by Karwacki et al. (2018), which paired a PPC-specific qPCR assay (the same assay applied to our UCF-processed samples) with histopathology in order to measure Perkinsea infection. They detected PPC in 17 out of 18 (94%) tadpoles collected from Pebble Lake at Mike Roess Gold Head Branch State Park (29° 50'52'' N, 81° 57' 43''W), a site at which a Perkinsea-associated tadpole mortality event had been previously reported (Landsberg et al. 2013). Karwacki et al. (2018) found a positive correlation between qPCR intensity (measured by PPC 18S rRNA gene copy number) and infection severity (based on histopathological observation of Perkinsea cells in tadpole tissue). The PPC-positive samples with the lowest qPCR intensities showed little to no evidence of Perkinsea infection at the tissue level (Karwacki et al. 2018), indicating that there is indeed a prevalence of cryptic PPC infection in amphibians. We note that their article does not state if the tissue samples were from larval or adult frogs, as both life stages were included in their survey.

The prevalence of cryptic PPC infection undermines the first of Koch's postulates: that the microbe must be present in every case of the disease, but not in the absence of disease. It indicates that PPC is most likely a commensal microorganism, present in an abundance of amphibian hosts, which only becomes pathogenic under certain conditions. This relates to our second explanation for the results we observed in our *R. dalmatina* experimental infections, which suggests that SPI disease might only develop in association with other factors that increase host stress (and reduce host immunity) (e.g. exposure to pollution, food deprivation, co-infections). As a commensal, PPC would likely be managed effectively with strategies that focus on reducing the impact of the conditions that increase its pathogenicity and/or reduce host immunity. These conditions could be identified and monitored by routinely combining comprehensive amphibian disease diagnostics (i.e. testing for multiple pathogens) with comprehensive water quality assessments (e.g. measuring levels of ultraviolet radiation, nutrients, and pollutants). This might reveal a connection between specific environmental conditions and SPI disease outbreaks, as has been the case for other amphibian diseases (e.g. Kiesecker & Blaustein 1995, Kiesecker 2002, Rohr et al. 2008).

Information in this chapter went toward the following publications:

Smilansky V, Chambouvet A, Reeves M, Richards TA, Milner DS (2021) A novel duplex qPCR assay for stepwise detection of multiple Perkinsea protistan infections of amphibian tissues. *R Soc Open Sci* 8: 202150

Chapter 3. Development of a novel duplex qPCR assay to detect multiple clades of Perkinsea in amphibian tissues

ABSTRACT

Alveolate parasites in the class Perkinsea have been found to infect amphibians across a broad taxonomic and geographic range. Phylogenetic analysis has suggested the existence of two distinct lineages of amphibian Perkinsea: NAG01a-c, a putatively non-pathogenic lineage (comprised of three clades/phylotypes) linked to putatively asymptomatic infections of tadpoles in Africa, Europe, and South America, and PPC, a putatively pathogenic lineage linked to disease and mass mortality events of tadpoles in North America. We describe the development of a novel duplex TaqMan qPCR assay to simultaneously detect both lineages of amphibian Perkinsea. A single primer pair was designed to target a fragment of the 18S rRNA gene shared between the two lineages, and two dual-labelled TaqMan probes were designed to target a region within this fragment that is distinctive to each lineage. We tested the specificity, efficiency, and sensitivity of the assay in unixplex and duplex conditions using plasmid DNA and DNA derived from symptomatic and asymptomatic amphibian tissues. Our results reveal that the assay is indeed specific, efficient, and sensitive in most conditions, thereby supporting its application as an effective tool for the rapid detection of the two amphibian Perkinsea lineages. One caveat is the potential for mixed infections to result in a false negative NAG01a-c signal, as the typically more abundant PPC template can 'overwhelm' the signal emitted by the NAG01a-c template. Therefore, PPC+ samples tested in duplex conditions should be subsequently tested in NAG01a-c uniplex conditions to provide the most accurate mixed infection assessment. By incorporating our novel qPCR assay into the routine surveillance of amphibian populations, it is possible to assess the prevalence of one or both of these phylotype groups (possibly as a product of co-infection), and therefore provide improved understanding of infection dynamics.

3.1. INTRODUCTION

There is a consensus (among scientists) that the Earth is currently experiencing a mass extinction as a result of climate change and the burgeoning human population (Thomas et al. 2004, Wake & Vredenburg 2008). Amphibians are at the forefront of this extinction as the most threatened of the vertebrate taxa (Wake & Vredenburg 2008). According to the latest global assessment, nearly one-third (32.4%) of known species are classified as threatened or extinct, whilst at least 42% of all species are declining in population (Stuart et al. 2004). Major factors contributing to amphibian decline are habitat loss, pollution, invasive species, and infectious disease (Figure 3.1). Amphibians are particularly susceptible to infectious disease due to their unique life history, multi-phase development dependent immune system, and permeable skin. Infectious disease appears to disproportionately affect threatened species (whilst the other factors are more or less indiscriminate) (Chanson et al. 2008), although it is unclear if this is due to greater sampling efforts of threatened species, or an actual biological phenomenon. For example, threatened species with declining populations are at greater risk of loss of genetic diversity. Reduced genetic diversity (particularly MHC diversity) can increase a population's susceptibility to infectious disease (Spielman et al. 2004, Pearman & Garner 2005). These "bottlenecked" populations can remain vulnerable even if their numbers recover, unless reinforced by gene flow from other populations.

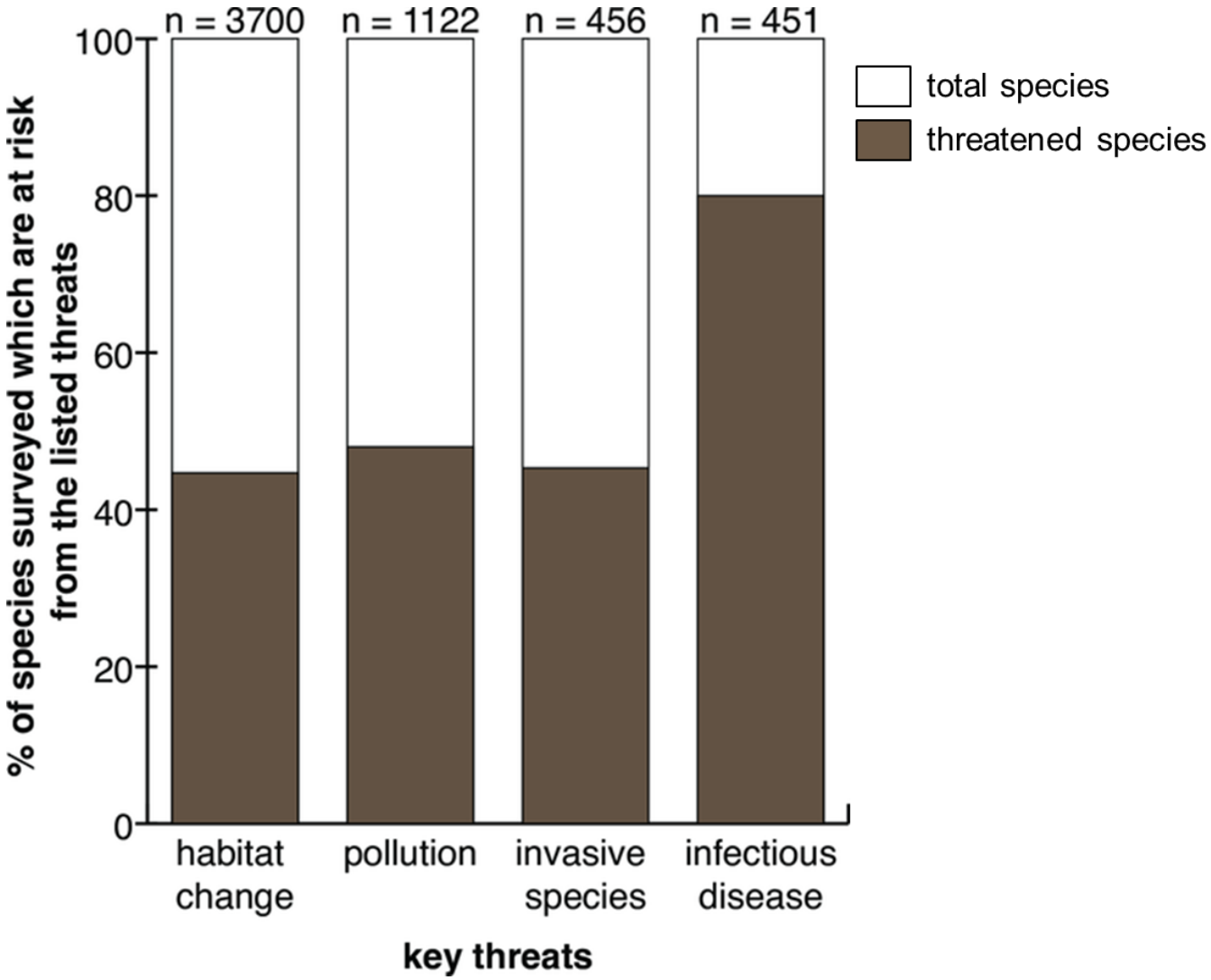

Figure 3.1. Graph illustrating key threats to amphibians (taken from Chambouvet et al. 2020).

Larval anurans (tadpoles) have a unique susceptibility to parasites due to their reduced immunity compared to adults and their habitation of aquatic environments (Pasquier et al. 1989, Chambouvet et al. 2020). Tadpole die-offs associated with an alveolate protist in the class Perkinsea have been reported across a broad range of US states, including Alaska (Green et al. 2002, Green et al. 2003, Davis et al. 2007, Landsberg et al. 2013, Isidoro-Ayza et al. 2017). Most of those affected are in the Ranidae family, including endangered species (Davis et al. 2007, Isidoro-Ayza et al. 2017). High mortalities (as high as 95%) have been recorded in some populations (Green et al. 2002, Davis et al. 2007, Isidoro-Ayza et al. 2017).

Macroscopic and histological examination of tissues from severely infected tadpoles reveals extensive haemorrhaging of the skin and enlargement and yellowing

of the liver, as well as the invasion of the liver (preferentially), kidney, spleen, and pancreas by myriad Perkinsea organisms (Isidoro-Ayza et al. 2017, 2018). Collectively these symptoms have been used to describe Severe Perkinsea Infection (SPI) associated disease (Isidoro-Ayza et al. 2017). SPI is purported to be the third most common infectious amphibian disease in North America, after chytridiomycosis and ranavirosis (Isidoro-Ayza et al. 2017).

Recent phylogenetic analysis of Perkinsea 18S rDNA clone sequences based on a targeted PCR protocol identified these putative pathogens as a distinctive clade (Clade D) within a broad monophyletic group of alveolates known as Novel Alveolate Group 01 (NAG01; Chambouvet et al. 2015). NAG01 includes three other clades/phylotypes (Clades A-C) known to infect tadpoles from a broad range of taxa in Africa, Europe, and South America without causing identifiable gross or tissue-level symptoms of disease (Chambouvet et al. 2015) (Table 3.1). However, we note that many of these samples were collected from early development phases or museum samples meaning that the potential to identify pathologies is limited. Hereafter, these clades/phylotypes are referred to as a single clade: NAG01a-c. The absence of evidence of pathologies in NAG01a-c suggests that pathogenicity might be restricted to the North America clade, which was designated Pathogenic Perkinsea Clade (PPC) by Isidoro-Ayza et al. (2017) and is hereafter referenced by this name (Table 3.1). PPC sequences have been recovered from moribund tadpoles from all known SPI-associated mortality events in the USA (Davis et al. 2007, Isidoro-Ayza et al. 2017), whereas they have only been recovered from 2.5% (2/81) of normal tadpoles surveyed (in localities with current or historical SPI outbreaks) (Isidoro-Ayza et al. 2017). These findings provide further support that PPC is indeed a disease-causing pathogen; however, the exact relationship between PPC and SPI-associated disease remains unclear (particularly in the absence of the fulfilment of Koch's postulates).

Furthermore, it is unclear what role PPC and NAG01a-c co-infection might play in pathogenesis. To date, there have not been any reports of co-infection by the two clades (i.e. PPC and NAG01a-c). Interestingly, Chambouvet et al. (2015) recovered sequences from both NAG01 clades/phylotypes A and B in 55% (22/38) of tadpole livers sampled, suggesting that the livers were either infected by both NAG01 A and B clades/phylotypes or that there is "intranuclear 18S rDNA variation within NAG01 genomes sampled", meaning that a single lineage of NAG01 encodes both

representatives of NAG01 A and B clades/phylotypes. Isidoro-Ayza et al. (2017) is the only paper thus far to produce a (comprehensive) phylogeny of PPC 18S rDNA sequences (from multiple locations), which showed no evidence of co-infection by NAG01a-c. In their study, clones were generated from a single PCR per tadpole liver, which implies that co-infection might have gone undetected due to limited replication and incomplete PCR library screening.

Irrespective, the reliance on DNA sequencing followed by phylogenetic analysis as a means to detect incidences of co-infection is not practical in many cases because this approach is labour intensive, time-consuming, and requires extensive laboratory facilities. Quantitative PCR (qPCR) is a sensitive method that uses fluorescent reporter dyes to detect DNA, providing presence/absence confirmation in a matter of hours, and also allowing for the quantification of target DNA by comparison to standards of known concentrations (Bustin et al. 2009). This method has been applied as a means of detection for *Batrachochytrium dendrobatidis* (e.g. Retallick et al. 2006) and ranavirus (e.g. Picco et al. 2007), the respective agents of chytridiomycosis and ranavirosis. Karwacki et al. (2018) developed a qPCR assay specific to PPC; however, similar methods have yet to be developed for NAG01a-c. Such approaches would allow for simultaneous assessment of the presence of different template(s) that could be indicative of mixed infections. With increasing development of field-based qPCR technologies (e.g. the *Biomeme* platform), such approaches also require reduced laboratory systems, making them increasingly viable in the field (Marx 2015).

Quantitative PCR assays commonly feature sequence-specific hydrolysis probes (e.g. TaqMan probes). These probes are labelled with two fluorescent dyes with different spectral profiles. In close proximity, the absorption spectrum of the dye at the 3' end (the quencher) overlaps the emission spectrum of the dye at the 5' end (the reporter). Fluorescence occurs when *Taq* polymerase cleaves the reporter and frees it from the quencher. As the amplicon concentration increases so does fluorescence, to the point where it can be detected (by a qPCR machine). TaqMan assays are more specific than assays that use fluorescent DNA-intercalating dyes (e.g. SYBR green), which bind any double-stranded DNA present, and therefore rely solely on primers for specificity. Furthermore, TaqMan probes enable duplexing and multiplexing without the need for multiple primer pairs, which is useful for highly similar targets such as the clades in this study.

This study aims to develop a method for assessing the prevalence of one or both clades of amphibian Perkinsea (i.e. PPC and NAG01a-c; Tables 3.1 & 3.2), thereby providing an improved understanding of infection dynamics. We describe the development of a novel duplex TaqMan qPCR assay designed to rapidly and simultaneously detect multiple clades in amphibian tissues. A single primer pair was designed to target a fragment of the 18S small subunit (SSU) rRNA gene shared between the two clades, and two dual-labelled TaqMan probes were designed to target a region within this fragment which is distinctive to each clade (Table 3.2). The assay was first optimised using plasmid DNA containing a sequence specific to each clade under uniplex conditions (i.e. using only a single clade-specific probe) and then in duplex conditions. Optimisation was conducted in accordance with MIQE guidelines (Bustin et al. 2009). After optimisation, we validated the assay on tissue samples using DNA from tadpole livers that had been previously confirmed positive for either PPC or NAG01 clade/phylotype A (NAG01a). The assay was also validated on a field-compatible qPCR platform using both plasmid DNA and DNA from liver tissue samples.

Table 3.1. Clades/phylotypes within the Novel Alveolate Group 1 (NAG01) that are known infectious agents of amphibians.

NAG01 Clade	Affiliated region	Associated with morbidity	Reference
Clade A	Africa, Europe, South America	No	Chambouvet et al. (2015)
Clade B	Africa, Europe, South America	No	Chambouvet et al. (2015)
Clade C	Europe, South America	No	Chambouvet et al. (2015)
Clade D (PPC)	North America	Yes	Isidoro-Ayza et al. (2017)

3.2. METHODS

3.2.1. Development of primers and probe

- qPCR target

The gene that is targeted by our qPCR assays is the small subunit (18S) ribosomal RNA encoding gene (18S rDNA). We based our PPC qPCR assay on an 18S rDNA sequence from a *Rana sphenocephala* pathogen (NCBI accession number EF675616) from Davis et al. (2007). We based our NAG01a-c qPCR assay on an 18S

rDNA sequence from a randomly selected NAG01 targeted clone library (NCBI accession number KP122572 from Clade B) from Chambouvet et al. (2015). Alignments of these and other NAG01 18S rDNA sequences are available at doi 10.5281/zenodo.12712. Secondary structure of the 18S rDNA amplicons targeted by each of our assays was analysed using mfold with default settings (Zuker 2003). For the amplicon targeted by the PPC qPCR assay, four structures were predicted with ΔG values ranging from -22.01 to -20.92 kcal/mol and Tm values ranging from 50.5°C to 53.2°C. For the amplicon targeted by the NAG01a-c qPCR assay, four structures were predicted with ΔG values ranging from -26.37 to -25.36 kcal/mol and Tm values ranging from 52.0°C to 56.2°C.

- qPCR oligonucleotides

The primers used in this study (Table 3.2) target a fragment of the 18S rRNA gene of NAG01 Perkinsea. The fragment is 290 bp long in PPC and ~287 bp long in NAG01a-c. The probes used in this study (Table 3.2) target a ~113-116 bp variant region within this fragment that can be used to distinguish PPC from NAG01a-c (Figure S3.1). This region spans position ~140-255 (ignoring gap sites) based on the alignment S1_Perkinsus_18S_full_seq_alignment_and_mask (doi 10.5281/zenodo.12712). The 300F-B and NAG01R_1 primers are respectively located at positions 1-17 and ~268-290 in the alignment, whilst the PPC and NAG01a-c probes are respectively located at positions 154-174 and ~157-179 (Figure S3.1) in the alignment. Primers and probes were manufactured by Eurofins Scientific and purified using high-performance liquid chromatography. The PPC probe is identical to 93/93 (100%) PPC clone libraries recovered from tadpole liver and generated for the alignment by Isidoro-Ayza et al. (2017). The NAG01a-c probe is identical to 172/177 (97%) NAG01a-c clone libraries recovered from tadpole liver and generated for the alignment by Chambouvet et al. (2015).

Table 3.2. Primers and probes developed to target two clades of NAG01 Perkinsea: PPC (associated with morbidity) and NAG01a-c (associated with putatively asymptomatic infection). "_P1" indicates an oligonucleotide probe sequence.

Primer/probe	Sequence (5' - 3')	Specificity	Reference
300F-B	GGG CTT CAY AGT CTT GCA AT	NAG01 Clades A-D	Chambouvet et al. (2015)
NAG01R_1	GCC TGC TTG AAA CRC TCT AA	NAG01 Clades A-D	This study
PPC_P1	FAM-TGC CAA GAA CGA CCG TCC TAC-BHQ-1	NAG01 Clade D (PPC)	This study
NAG01_P1	Cy5-CAA GGA CGA CCT ACC CAC CTT AG-BHQ-2	NAG01 Clades A-C	This study

3.2.2. Preparation of the qPCR template DNA

To obtain template for the PPC qPCR assay, total DNA was extracted from the pooled livers of nine PPC-infected tadpoles (Table S3.2) using the RNeasy PowerSoil DNA Elution Kit (Qiagen) following the manufacturer's protocol. The (total) DNA sample was amplified using primers 300F-B and NAG01R_1 (Table 3.2). The reaction mixture included 1x concentration PCR MasterMix (Promega), 500 nM of each primer, 1 µl of template DNA, and molecular-grade water to bring the total reaction volume to 25 µl. Each reaction included a negative control (molecular-grade H2O). Cycling conditions were as follows: 2 min at 95°C, followed by 35 cycles of 30 s at 95°C, 30 s at 56°C, and 60 s at 72°C, with an additional 10-min extension at 72°C. PCR products were checked on a 2% agarose gel and purified using the GeneJET PCR Purification Kit (Thermo Fisher). Purified PCR products were cloned into the plasmid vector pSC–A–amp/kan using the Strata Clone PCR Cloning Kit (Agilent Technologies) following the manufacturer's protocol. Plasmids were transformed into StrataClone SoloPack Competent Cells (Agilent Technologies) and blue-white screened on LB-ampicillin plates with 2% X-gal. White mono-colonies were cultured in LB-ampicillin broth at 37°C overnight. Plasmid DNA was extracted from the cultures using the GeneJET Plasmid Miniprep Kit (Thermo Fisher) according to the manufacturer's protocol, linearized using the NcoI restriction enzyme, and purified using the GeneJET PCR Purification Kit (Thermo Fisher). At the time of optimisation, we did not have access to viable specimens to provide template for the NAG01a-c qPCR assay. Instead, we opted to have the portion of the 18S rRNA gene specific to this clade synthesized into the pUC57-Amp plasmid vector by Synbio Technologies.

3.2.3. qPCR assay optimisation

All qPCRs were performed on the CFX96 real-time PCR detection system (Bio-Rad). For both assays, the (optimal) reaction mixture included 1x concentration TaqMan

Gene Expression Master Mix (Thermo Fisher Scientific), 500 nM of each primer, 250 nM of each probe, 1 µl of template DNA, 5% DMSO, and molecular-grade water to bring the total reaction volume to 25 µl. The (optimal) qPCR conditions were 10 minutes at 95°C followed by 40 cycles of 15 seconds at 95°C and 2 minutes at 60°C (PPC), 62°C (NAG01a-c), or 61°C (duplex).

- Annealing temperature

Optimal annealing temperature (Ta) is the Ta that yields the lowest quantitation cycle (Cq), which is the cycle at which fluorescence is first detected. Both the PPC and NAG01a-c qPCR assays were tested with six different Ta's ranging from 55.6°C to 64°C. The reaction mixture contained 1x concentration TaqMan Gene Expression Master Mix (Thermo Fisher Scientific), 500 nM of each primer, 250 nM of probe, 1 µl of plasmid DNA (1 ng total), and molecular-grade water to bring the total volume to 25 µl. The qPCR program settings were as follows: initial denaturation step at 95°C for 10 min, followed by 40 cycles of 15 seconds at 95°C and 1 minute at 55.6°C, 57.6°C, 60.2°C, 62.3°C, 63.4°C, and 64°C. Each Ta was tested with three replicates. A no-template control (NTC) was run with each of the four highest Ta's, using molecular-grade water instead of plasmid DNA.

- qPCR assay efficiency and sensitivity

Two crucial aspects of assay performance are amplification efficiency and analytical sensitivity (Bustin et al. 2009). Amplification efficiency is the (percent) increase in the number of target gene copies during each replication cycle (ideally doubling with each cycle). For an assay with ~100% efficiency, ΔCq is expected to be ~3.3 for a 1:10 dilution series, measured as the difference between the average Cq of each subsequent dilution. Amplification efficiency can be expressed as the range of (quantifiable) target gene copies over which the reaction is linear, as established by means of a calibration curve (i.e. linear dynamic range). Analytical sensitivity is the minimum number of copies in a sample that can be accurately measured by an assay, and is typically defined as the lower limit of detection (LoD). The counterpart is the upper LoD, which corresponds to the maximum number of copies that can be accurately measured. The linear dynamic range and LoDs can be expressed as the number of target gene copies, which is calculated using the following formula: number

of copies = (amount x $6.022*10^{23}$) / (length x $1*10^{9}$ x 650). In this formula, amount = template concentration (ng) and length = template length. The template length for the PPC qPCR assay was 4,590 bp (the 4.3 kb length of the pSC-A-amp/kan plasmid vector + the 290 bp length of the insert). The template length for the NAG01a-c qPCR assay was 2,916 bp (the 2,710 bp length of the pUC57-Amp vector + the 287 bp length of the insert – 81 bp that were removed upon ligation of the insert into the multiple cloning site).

In order to assess these performance criteria, a preliminary qPCR was tested with the PPC uniplex assay using a 5-point 10-fold template dilution series, starting with 10 ng of plasmid DNA. This was followed by a qPCR using an 11-point 10-fold template dilution series, starting with 1 ng of plasmid DNA. Optimization for the NAG01a-c assay was streamlined into a single 12-point 10-fold dilution series, starting with 10 ng of plasmid DNA. Due to high variation between replicates, a second qPCR was conducted using a 7-point 10-fold dilution series based on the predetermined linear dynamic range (to calculate efficiency). Finally, a duplex qPCR was run with an 8-point 10-fold dilution series based on the wider of the two linear dynamic ranges determined in the uniplex assays, starting with a total of 2 ng of plasmid DNA (1 ng specific to each of the assays). The reaction mixture contained 1x concentration TaqMan Gene Expression Master Mix (Thermo Fisher Scientific), 500 nM of each primer, 250 nM of each probe, 1 µl of plasmid DNA, 5% DMSO, and molecular-grade water to bring the total volume to 25 µl. Cycling conditions were as follows: initial denaturation step at 95°C for 10 min, followed by 40 cycles of 15 seconds at 95°C and 2 minutes at 60°C (PPC), 62°C (NAG01a-c), or 61°C (duplex). The annealing step was first set at 1 minute, but was increased to 2 minutes after the first preliminary 5-point dilution PPC qPCR yielded a low efficiency. Increasing annealing step duration improves efficiency for longer amplicons (Debode et al. 2017). Each qPCR was run with four replications for each template dilution. A no-template control (NTC) was run with a minimum of three replications, using molecular-grade water instead of plasmid DNA.

3.2.4. Applying the assay to tissue samples

The assay was applied to PPC+ tadpole liver tissue from Alaska, USA and NAG01a+ tadpole liver tissue from French Guiana, using both uniplex and duplex conditions.

Tissue samples used to validate the PPC assay were derived from tadpoles collected from three Perkinsea-positive sites in the Kenai Peninsula Borough in Alaska, USA in June and July 2016 by researchers from the University of Exeter and the US Fish and Wildlife Service Anchorage Field Office (Table S3.2). Whole livers were removed and placed in LifeGuard™ preservation solution (Qiagen), transported to the University of Exeter, and stored at -80°C. The livers were enlarged and yellow in appearance, and were revealed to be heavily infected with Perkinsea organisms upon microscopic observation. The livers of nine tadpoles were pooled into a single group (Table S3.2) from which total DNA was extracted using the RNeasy PowerSoil DNA Elution Kit (Qiagen) according to the manufacturer's protocol. The DNA sample was labelled "KNA_DNA". For the purpose of PPC-specific primer validation (not related to this study), KNA_DNA has been PCR-amplified, TA-cloned into a plasmid vector using the Strata Clone PCR Cloning Kit (Agilent Technologies), and sequenced by Eurofins Genomics (Wolverhampton, UK), thereby confirming that it is indeed positive for PPC DNA. Furthermore, KNA_DNA is the same sample used to generate PPC plasmid DNA for this study (see "Preparation of the qPCR template DNA"), which consistently amplified with our PPC assay, but not the NAG01a-c assay.

Tissue samples used to validate the NAG01a-c assay were derived from two (ethanol-preserved) tadpoles collected in 2013 from French Guiana: G2.13 and G8.1 (Table S3.2). Whole livers were removed and processed for DNA extraction by Chambouvet et al. (2015). Like the rest of the liver tissue samples processed by Chambouvet et al. (2015), these samples did not display gross or tissue-level symptoms (although their early development phases and/or museum preservation might have hindered pathology assessment). NAG01-specific 18S rDNA clone libraries were constructed from the DNA extractions and sequenced for phylogenetic analysis, thereby confirming that they were indeed positive for NAG01a DNA (Chambouvet et al. 2015).

3.2.5. Applying the assay on a field-compatible qPCR platform

Assay performance was tested in both uniplex and duplex conditions on a handheld, field-compatible qPCR device, the *Biomeme two3*. The device is battery-powered and docks to an Apple iPhone 5S that runs a custom app for controlling the device's electronics (Marx 2015). It features two fluorescence channels and three wells (hence

the name "*two3"*). The reaction mixture used with the *Biomeme two3* was consistent with the previous assays run on the CFX96 real-time PCR detection system (BioRad), except that TaqMan Gene Expression Master Mix (Thermo Fisher Scientific) was substituted with LyoDNA 2.0 Master Mix (Biomeme). Cycling conditions were the same on both qPCR platforms. The upper and lower LoDs of each uniplex assay and the duplex assay were tested using plasmid DNA. Subsequently, the uniplex and duplex assays were tested using DNA from KNA_DNA and G8.1.

3.3. RESULTS

3.3.1. Specificity of the assays

Specificity was tested both in silico and in vitro. A BLASTn search of the primer and probe sequences against the NCBI nr database confirmed that the oligonucleotides fully aligned to their intended targets (i.e. they shared 100% identity across the entire query). A second BLASTn search that excluded the targets showed no overlap between the (non-specific) hits of the primers, indicating that they have pairwise specificity to the targets. This specificity is further strengthened by the probes, which did not (fully) align with any non-specific sequences bioinformatically surveyed. Assay specificity was tested at each stage of development by including three or four replications of the reaction using non-target plasmid template (1 ng). For the annealing temperature assays, two non-target reactions were included at every tested Ta. There was no signal detected in any of the non-target reactions, confirming specificity for the distinct template.

3.3.2. Optimisation of the annealing temperature

The PPC qPCR assay successfully amplified a fragment at five Ta's ranging from 55.6°C to 63.4°C and resulted in average Cq values of 20.8, 16.49, 14.3, 17.54 and 29.33, respectively (Figure 3.2). Consequently, 60°C was retained as Ta for the PPC qPCR assay. No fluorescent signal was detected in the NTCs. The NAG01a-c qPCR assay successfully amplified a fragment at six Ta's ranging from 55.6°C to 64°C and resulted in average Cq values of 24.57, 16.27, 13.26, 13.09, 15.76 and 17.82, respectively (Figure 3.2). Consequently, 62°C was retained as the Ta for the NAG01a-

c qPCR assay. No fluorescent signal was detected in the NTCs. We note that the Ta's retained for each of the assays was at least 5.8°C higher than the highest Tm of the secondary structures predicted in their target amplicons. This suggests that all potential secondary structures in the amplicons destabilize prior to primer/probe annealing and therefore do not (significantly) interfere with assay function.

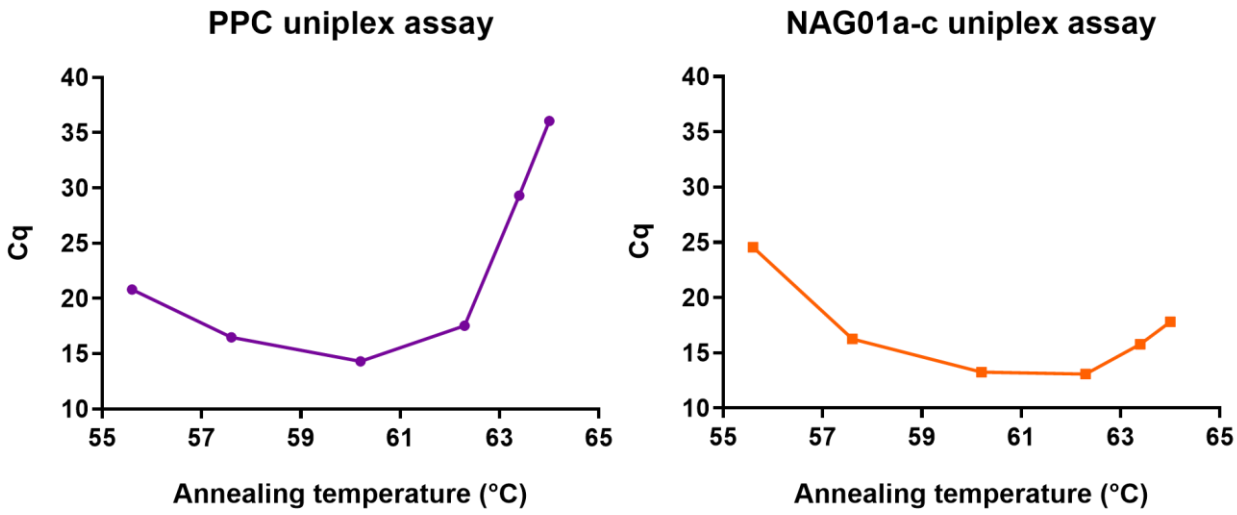

Figure 3.2. Quantitation cycle (Cq) plotted against a 6-point temperature gradient used to determine the optimal annealing temperatures for each of the NAG01 Perkinsea clade-specific assays. Reactions were conducted with 1 ng of plasmid template.

3.3.3. Efficiency and sensitivity of the assays

- PPC uniplex assay

The preliminary 5-point dilution qPCR successfully amplified at every dilution with an overall amplification efficiency of 96.45% (m = -3.41, b = 9.37, r^2 = 0.99) (Table S3.1). However, the distance between the 10 and 1 ng dilutions was 2.5 cycles, indicating abnormal amplification at target concentrations > $2.02*10^8$ target copies (1 ng). For this reason, the upper LoD was determined to be $2.02*10^8$ target copies (1 ng).

The 11-point dilution qPCR had a linear dynamic range of 20 → $2.02*10^8$ target copies ($1*10^{-7}$ ng → 1 ng). There was minimal variation between replicates and no signal detected in the NTCs (Table S3.1). Because one of the replicates was not

detected at 20 copies ($1*10^{-7}$ ng), the lower LoD was determined to be 202 target copies ($1*10^{-6}$ ng). To determine efficiency of the PPC assay, Cq was plotted against the 8-point 10-fold dilution series corresponding to the linear dynamic range (Figure 3.3). The assay efficiency was 89.57% (m = -3.6, b = 12.07, r^2 = 1).

- NAG01a-c uniplex assay

The 12-point dilution qPCR had a linear dynamic range of 318 → $3.18*10^8$ target copies ($1*10^{-6}$ ng → 1 ng). The distance between the 10 and 1 ng dilutions was 5.2 cycles, indicating low efficiency at target concentrations > $3.18*10^8$ target copies (1 ng). For this reason, the upper LoD of the assay was determined to be $3.18*10^8$ target copies (1 ng). The lower LoD of the NAG01a-c assay corresponds to the lowest point of the linear dynamic range: 318 copies ($1*10^{-6}$ ng). There was no signal detected in the NTCs (Table S3.1). Due to high variation between replicates (Table S3.1), a second qPCR was conducted using a 7-point 10-fold dilution series based on the predetermined linear dynamic range in order to calculate efficiency.

The 7-point dilution qPCR had a linear dynamic range that was consistent with the preceding 12-point dilution qPCR: 318 → $3.18*10^8$ target copies ($1*10^{-6}$ ng → 1 ng). There was minimal variation between replicates and no signal detected in the NTCs (Table S3.1). To determine efficiency of the NAG01a-c assay, Cq was plotted against the 7-point 10-fold dilution series corresponding to the linear dynamic range (Figure 3.3). The assay efficiency was 102.21% (m = -3.27, b = 15.1, r^2 = 0.99).

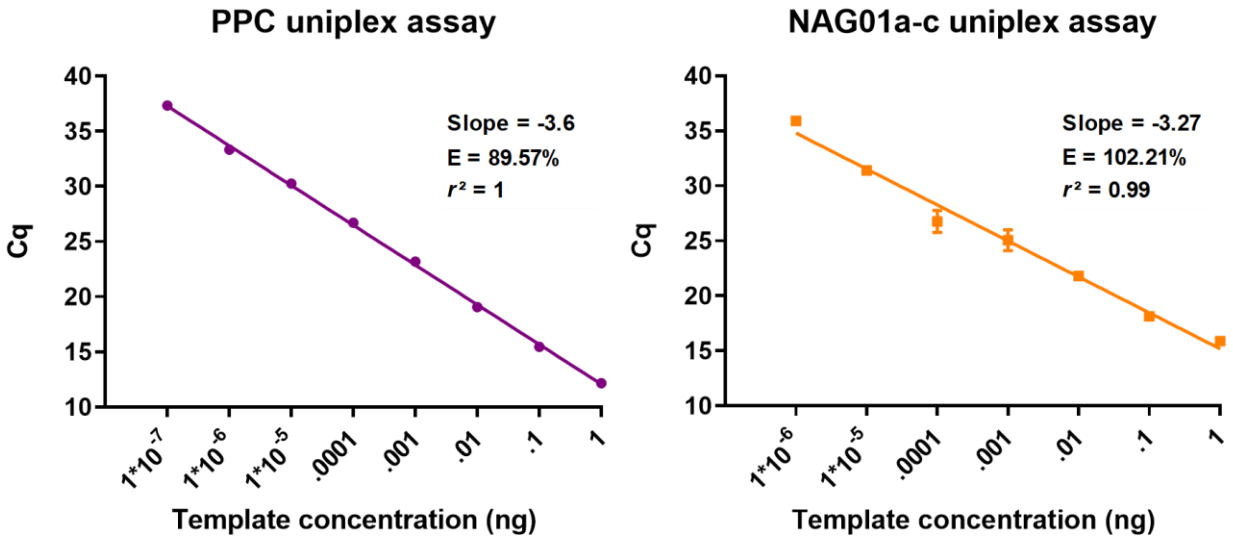

Figure 3.3. Calibration curves of the PPC uniplex and NAG01a-c uniplex assays: quantitation cycle (Cq) plotted against a 10-fold plasmid template dilution series. The graphs depict the linear dynamic range for each assay (i.e. the range of template concentrations over which the fluorescent signal (expressed as Cq) is linear). The linear dynamic range corresponds to the range of template concentrations in which the assay has high amplification efficiency (E; the percent increase in the number of target gene copies during each replication cycle).

- PPC / NAG01a-c duplex assay

The duplex qPCR was run with an 8-point 10-fold dilution series based on the linear dynamic range determined in the PPC uniplex assay (i.e. the wider range of the two uniplex assays) (Figure 3.4). Both assays successfully amplified at each of these dilutions, and there was no signal detected in the NTCs (Table S3.1). Both assays had higher variation between replicates in duplex conditions compared to uniplex conditions, particularly the NAG01a-c assay (Table S3.1). However, there were no statistically significant differences between the average Cq values of the uniplex and duplex assays at any of the dilutions based on the two-sample t-test (Table S3.1).

The overall amplification efficiencies for the PPC and NAG01a-c assays in duplex conditions were 102.21% (m = -3.27, b = 12.53, r^2 = 1) and 90.94% (m = -3.56, b = 10.52, r^2 = 0.99), respectively. The upper LoD for both the PPC and NAG01a-c assays in duplex conditions was determined to be $2.02*10^8$ target copies (1 ng) and $3.18*10^8$ target copies (1 ng), respectively. The lower LoD for the PPC assay in duplex conditions was determined to be 20 target copies ($1*10^{-7}$ ng). The lower LoD for the NAG01a-c assay in duplex conditions was determined to be 32 target copies ($1*10^{-7}$ ng).

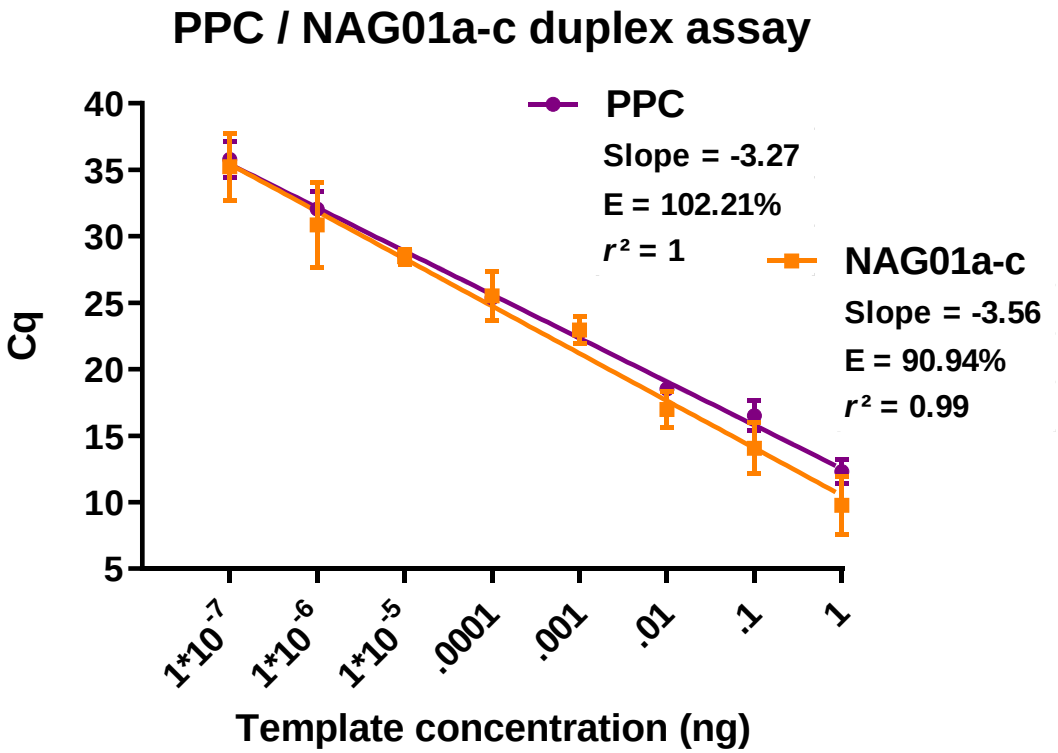

Figure 3.4. Standard curve of the PPC / NAG01a-c duplex qPCR assay: quantitation cycle (Cq) plotted against a 10-fold plasmid template dilution series.

3.3.4. Applying the assay to tissue samples

KNA_DNA was run in duplicate (10 ng each) to test the performance of the PPC uniplex assay. It amplified successfully, yielding an average Cq of 20.23 (Table S3.1). This value is within the LoDs of the PPC uniplex assay, and corresponds to approximately $2.02*10^6$ target gene copies (0.01 ng) based on the results of the optimisation (Table S3.1). The French Guiana extractions were run in triplicate to test the performance of the NAG01a-c uniplex assay. One of the French Guiana samples (G8.1) amplified successfully, yielding an average Cq of 33.89 (Table S3.1) (G2.13 did not produce a detectable signal; possible reasons for this are discussed later). This value is within the LoDs of the NAG01a-c uniplex assay, and corresponds to approximately 318 target gene copies ($1*10^{-6}$ ng) based on the results of the optimisation (Table S3.1). KNA_DNA and G8.1 were run together in triplicate in order to test the performance of the duplex assay. KNA_DNA was detected by the PPC probe, yielding an average Cq of 21.41 (similar to the result of the PPC uniplex assay)

(Table S3.1). G8.1 was not detected by the NAG01a-c probe when it was run with KNA_DNA. Possibly, this was due to the DNA polymerase being saturated by the PPC template (i.e. KNA_DNA), as KNA_DNA was derived from symptomatic tissue (presumably) containing many copies of the target gene. To test this possibility, G8.1 was run in triplicate with concentrations of PPC plasmid corresponding to the amount of NAG01a DNA contained in G8.1 ($1*10^{-6}$ ng; as determined by the NAG01a-c uniplex assay). In this case, G8.1 was detected by the NAG01a-c probe, yielding an average Cq of 32.89 (similar to the result of the NAG01a-c uniplex assay).

3.3.5. Applying the assay on a field-compatible qPCR platform

Assay performance was tested in both uniplex and duplex conditions on a handheld, field-compatible qPCR device, the *Biomeme two3*. The device is battery-powered and docks to an Apple iPhone 5S that runs a custom app for controlling the device's electronics (Marx 2015). It features two fluorescence channels and three wells (hence the name "*two3"*). The reaction mixture used with the *Biomeme two3* was consistent with the previous assays run on the CFX96 real-time PCR detection system (BioRad), except that TaqMan Gene Expression Master Mix (Thermo Fisher Scientific) was substituted with LyoDNA 2.0 Master Mix (Biomeme). Cycling conditions were the same on both qPCR platforms. The upper and lower LoDs of each uniplex assay and the duplex assay were tested using plasmid DNA. Subsequently, the uniplex and duplex assays were tested using DNA from KNA_DNA and G8.1.

The upper and lower LoDs for the PPC uniplex assay amplified successfully on the *Biomeme two3*, yielding respective Cq values of 10.93 and 30.54. KNA_DNA amplified with the PPC uniplex assay, yielding a Cq of 18.46. The upper and lower LoDs for the NAG01a-c uniplex assay amplified successfully on the *Biomeme two3*, yielding respective Cq values of 10.84 and 37.82. G8.1 amplified with the NAG01a-c uniplex assay, yielding a Cq of 32.67. The upper and lower LoDs for PPC and NAG01a-c assays in duplex conditions amplified successfully, yielding respective Cq values of 11.47 and 37 (PPC), and 13.66 and 38.25 (NAG01a-c). When KNA_DNA (i.e. PPC-specific template) and G8.1 (i.e. NAG01a-c-specific template) were run in duplex conditions, KNA_DNA was detected with the PPC probe (Cq = 17.68); however, G8.1 was not detected by the NAG01a-c probe. These results provided a serendipitous specificity check, as they confirm that the duplex assay can discriminate

a PPC+ tissue sample (i.e. the absence of NAG01a-c signal suggests there is no "cross-talk" between the NAG01a-c probe and the PPC template). G8.1 was subsequently run with a PPC plasmid concentration of $1*10^{-6}$ ng (i.e. the template concentration corresponding to that of G8.1). In this case, it was detected by the NAG01a-c probe, yielding a Cq of 34.2, similar to the result of the NAG01a-c uniplex assay. In most cases, the results of the tests run on the *Biomeme two3* were similar to the results of the tests run on the CFX96 qPCR platform (BioRad) (Table S3.3).

3.4. DISCUSSION

3.4.1. Critical assessment of our novel duplex qPCR assay

Quantitative PCR (qPCR) is a sensitive tool for diagnosing infection and has been routinely applied to various amphibian (and wildlife) populations leading to a better understanding of host−pathogen dynamics (Kriger et al. 2006, Retallick et al. 2006, Picco et al. 2007, Dong et al. 2008, Vredenburg et al. 2010, Karwacki et al. 2018). Duplexing and multiplexing greatly increases the power of qPCR analysis (Wittwer et al. 2001, Bustin et al. 2009): with regard to (wildlife) epidemiology, by allowing for the rapid and simultaneous detection of multiple pathogens/infectious agents. We developed a qPCR assay that can rapidly and simultaneously detect two clades (i.e. PPC and NAG01a-c) of an emerging alveolate pathogen of amphibians, which are respectively associated with either symptomatic or putatively asymptomatic infections.

Our assay uses primers that target a ~287/290 bp fragment of the NAG01 Perkinsea 18S rRNA gene. The PPC-specific uniplex assay developed by Karwacki et al. (2018) uses primers that target a 126 bp fragment of the same gene (this 126 bp fragment falls within the 290 bp fragment targeted by our assay). Both primer pairs amplify PPC and NAG01a-c. Our assay uses two probes to simultaneously detect both PPC and NAG01a-c, whereas the Karwacki assay uses a single probe to detect only PPC. The sequence of the Karwacki PPC probe differs from the PPC probe developed for this study; however, both probes target the same ~113-116 bp region that we use to distinguish PPC and NAG01a-c.

- Amplification efficiency

Our assay approximates the recommended amplification efficiency range of 90 – 100% (Bustin et al. 2009) in both uniplex and duplex conditions. Efficiency exceeded 100% in the NAG01a-c uniplex assay (E = 102.21%) and PPC duplex assay (E = 102.21%). Our data shows that template concentrations were more than doubling (i.e. ΔCq < 3.3) at certain dilutions (Table S3.1). This can happen due to the presence of primer dimers or nonspecific amplicons (Taylor et al. 2010); however, the absence of signal in the NTCs and the results of our in silico specificity checks suggest this is not a problem for our assay. It appears that our efficiency calculations were (artificially) elevated due to variation in technical replicates at certain template concentrations (Table S3.1). This can happen as a result of pipetting error or interference with fluorescence detection, which is measured by relative fluorescence units. Overall, this variation does not appear to have a drastically negative effect on the efficiency of our assay; in fact, many references recommend an efficiency range of 90 – 110% (e.g. Taylor et al. 2010).

The PPC uniplex assay developed by Karwacki et al. (2018) had an efficiency of 97.3% (m = -3.39, b = 37.24, r^2 = 1), compared to our PPC uniplex assay efficiency of 89.57%. The higher efficiency of the Karwacki assay is likely due to the smaller size of their target amplicon (126 bp compared to 290 bp), as smaller amplicons tend to amplify more efficiently (Debode et al. 2017). During the initial optimisation, the amplification efficiency (of both uniplex assays) was well below 90%. We compensated for this shortcoming by increasing the annealing step in our qPCR reaction from 1 to 2 minutes, as increasing annealing step duration improves efficiency for longer amplicons (Debode et al. 2017).

- Analytical sensitivity

In uniplex conditions, our assay is sensitive down to 202 and 318 copies of the targeted PPC and NAG01a-c gene, respectively. In duplex conditions, it is sensitive down to 20 and 32 copies of the targeted PPC and NAG01a-c gene, respectively. The duplex assay appears to be more sensitive than either of the uniplex assays, as the lower LoDs for the former were determined to be one order of magnitude lower than the latter. This finding should be interpreted with caution, as there is large variation among the technical replicates in the template concentrations at or near the lower LoDs in duplex conditions, particularly in the NAG01a-c duplex assay (Table S3.1). It appears

that fluorescence detection is less stable at lower template concentrations in duplex conditions compared to uniplex conditions. For this reason, it is advisable to designate the duplex assay as a means of rapid presence/absence detection for the two clades of amphibian Perkinsea. Samples that are positive for either clade (especially if their Cq values are low) should then be amplified with the corresponding uniplex assay to get a more reliable estimate of template concentration.

The PPC uniplex assay developed by Karwacki et al. (2018) is sensitive down to 20 copies of the target gene, compared to a sensitivity of 202 target copies ($1*10^{-6}$ ng) in our PPC uniplex assay. The lower LoD of our PPC uniplex assay was parsimoniously set to 202 target copies because one of the four replicates was not detected at 20 target copies ($1*10^{-7}$ ng) (Table S3.1). For the three replicates that amplified successfully, the average Cq was 37.35 (SD = 0.31) (Table S3.1). Our lower LoD was assigned in accordance with the MIQE guidelines, which states that "within a group of replicates containing the target at concentrations at the LOD, no more than 5% failed reactions should occur" (Bustin et al. 2009).

- Applying our assay to tissue samples

The symptomatic tissue samples used in this study (i.e. those combined into KNA_DNA: Table S3.2) consistently amplified with the PPC assay (in both uniplex and duplex conditions and on both qPCR platforms), yielding relatively low Cq values. Our duplex assay accurately distinguished KNA_DNA (i.e. KNA_DNA was detected by the PPC probe, but not the NAG01a-c probe), as evidenced by the duplex experiment using template from KNA_DNA and G8.1. Symptomatic samples typically contain many Perkinsea organisms and therefore a large amount of target DNA is likely available for detection. In contrast, putatively asymptomatic tissue samples likely contain fewer Perkinsea organisms and therefore less target DNA. Consequently, our results obtained from putatively asymptomatic samples (i.e. G2.13 and G8:1, both NAG01a+) are much more ambiguous. Indeed, only one of these samples (i.e. G8.1) amplified with the NAG01a-c assay (in both uniplex and duplex conditions and on both qPCR platforms), and the Cq values were relatively high (Table S3.1). Our duplex assay accurately distinguished G8.1 (i.e. G8.1 was detected by the NAG01a-c probe, but not the PPC probe), as evidenced by a duplex experiment using only G8.1 template (data not shown). Based on these Cq values, we determined that G8.1

contains a low amount of target DNA (approximately 318 target gene copies/1*10^{-6} ng), which corresponds to the lower LoD of the NAG01a-c uniplex assay (Table S3.1). We can presume that either the amount of target DNA in G2.13 (i.e. the NAG01a+ sample that was not detected with the assay) is less than 318 target gene copies/1*10^{-6} ng, or that the sample has degraded from the time when it was screened for NAG01 DNA by Chambouvet et al. (2015). The low amount of target DNA contained by putatively asymptomatic samples is especially important to consider when applying the duplex assay, as our results suggest that large amounts of PPC template might saturate the DNA polymerase, thereby curbing amplification of the NAG01a-c template and resulting in a false negative. Indeed, G8.1 could not be detected on either qPCR platform when it was run with KNA_DNA (i.e. a symptomatic sample containing a large amount of PPC DNA) in duplex conditions. A solution to DNA polymerase saturation is to reduce the concentration of primers that target the more abundant template; however, this is not an option for our duplex assay because it uses the same primer pair for both templates. This could potentially be a problem for symptomatic co-infected samples, but likely less of a problem for putatively asymptomatic co-infected samples. Therefore, PPC+ samples tested in duplex conditions should be subsequently tested in NAG01a-c uniplex conditions to provide the most accurate mixed infection assessment.

3.4.2. The potential for amphibian Perkinsea to be a major contributor to global amphibian decline

PPC and the mortality events with which it has been associated exhibit certain attributes that suggest it is “capable of causing local population declines and extinctions” (Isidoro-Ayza et al. 2017). Most prominently, outbreaks associated with PPC exhibit high mortality; in some cases, sparing only a small fraction of the population (Green et al. 2002, Davis et al. 2007, Isidoro-Ayza et al. 2017). PPC-tadpole associations have been shown to persist even at low host population densities; this is likely due to the resistance of the parasite in its spore phase (Cook 2008) and/or its capacity to exist in a free-living phase or in association with other host species, as evidenced by the presence of NAG01 sequences (closely related to NAG01 sequences derived from putatively asymptomatic infected tadpoles) recovered from planktonic freshwater samples in the UK, France, French Guiana and Upstate New

York, USA (Richards et al. 2005, Lefèvre et al. 2007, 2008, Chambouvet et al. 2015). It can infect a wide range of host taxa (species from both Ranidae and Hylidae, which are found globally), most of which are common species, but also endangered species (e.g. the dusky gopher frog) (Isidoro-Ayza et al. 2017).

Increased surveillance efforts are needed to fully expose the extent of PPC's range. Certain aspects suggest that it has the capacity for widespread transmission and its current distribution is likely broader than we realise. PPC has not yet been reported outside the USA; however, the fact that it has been found in Alaska suggests that it is distributed throughout much of the Nearctic region. The parasite's putative life history (i.e. it exists in a free-living phase) further increases its chances of spreading through contaminated water and its potential association with avian vectors. Until recently, there has only been one report of PPC in an adult frog (Jones et al. 2012); however, a survey in Florida, USA by Karwacki et al. (2018) indicates that it occurs in adults more frequently than previously thought. Adult frogs have greater mobility than tadpoles which increases the likelihood of PPC transmission between (local) sites. The international amphibian pet trade also poses a potential risk of transmission on a global scale.

3.4.3. Support for the incorporation of our assay into the routine surveillance of amphibian populations

Interaction by multiple strains of the same pathogen can lead to their increased pathogenicity (Balmer & Tanner 2011). This phenomenon has been implicated in frogs exposed to multiple strains of ranavirus (Mihaljevic et al. 2018). Evidence of these synergistic interactions in other amphibian pathogens suggests that the pathogenicity of PPC could be increased by its potential to interact with the NAG01a-c clade / other NAG01 clades (and of course other non-Perkinsea pathogens). For this reason (as well as those previously mentioned), it is important that we expand our surveillance of amphibian populations to routinely account for both clades of amphibian Perkinsea.

The duplex qPCR assay reported here can be used to assess the prevalence of PPC / NAG01a-c co-infection and provide a better understanding of the dynamics of amphibian Perkinsea infection, which could be used to inform management

strategies and possibly prevent disease outbreaks. For this reason, we also validated it for use with field-compatible qPCR equipment. Duplex qPCR has been developed for other amphibian pathogens, including an assay to distinguish different types of ranavirus (e.g. European vs. Australian) (Pallister et al. 2007), and another assay to simultaneously detect *B. dendrobatidis* (*Bd*) and *B. salamandrivorans* (*Bsal*), the agents of chytridiomycosis in frogs and salamanders, respectively (Blooi et al. 2013). Of course, numerous studies have described co-infection of amphibians by different species of pathogen, including a report of co-infection by PPC and ranavirus frog virus 3 (FV3) in a multispecies tadpole mortality event in Florida (one of these species was the critically endangered dusky gopher frog) (Landsberg et al. 2013). In this regard, a multiplex qPCR assay that simultaneously detects a wide range of amphibian pathogens seems an important goal; indeed, a recent multiplex assay was developed for *Bd*, *Bsal,* and FV3 (although amphibian Perkinsea was neglected) (Standish et al. 2018).

Chapter 4. Phylogenetic analysis of amphibian disease associated Perkinsea expands the identified geographic and host range of infections

ABSTRACT

Severe Perkinsea infection (SPI) is identified as an emerging infectious disease of amphibians and has been linked to a specific lineage of Perkinsea named Pathogenic Perkinsea Clade (PPC). PPC groups within a large cluster of mostly environmentally sampled SSU rDNA sequences named Novel Alveolate Group 01 (NAG01; Chambouvet et al. 2015). PPC and SPI-associated tadpole mortality events have been reported across a broad geographic range in North America, as far north as Alaska, USA and as far south as Florida, USA (Isidoro-Ayza et al. 2017), but they have not been reported outside of this range. Most of these mortality events have occurred in tadpoles of the *Lithobates* genus. In this study, we further investigate the geographic and host range of amphibian-associated Perkinsea (and SPI-associated disease) by screening for NAG01 Perkinsea in multiple species of tadpoles sampled from natural environments in Panama, and *Hyla arborea* (family Hylidae) tadpoles demonstrating symptoms of SPI recovered from hobbyist aquaculture in the UK. We used targeted tissue SSU rRNA PCR and cloning, combined with phylogenetic analyses, to investigate the prevalence of Perkinsea infections. Liver tissue samples from a total of 91 tadpoles were screened for NAG01 Perkinsea using PCR detection: 81 from Panama and 10 from the UK. NAG01 Perkinsea SSU rDNA was detected in 10 Panama samples, and a UK sample from the pooled liver tissue of five *H. arborea* tadpoles. Phylogenetic analysis of newly generated NAG01 Perkinsea SSU rDNA sequences revealed that the detected sequences are highly similar to previously published PPC sequences from mortality events in the USA, suggesting a rapid global radiation of this putative pathogen (at least on the scale of SSU-rRNA gene variation). We then used mitochondrial SSU rRNA phylogenetics to identify the taxonomic grouping of the Panama sampled tadpoles, demonstrating six anuran families: Bufonidae, Phyllomedusidae, Aromobatidae, Hylidae, Leptodactylidae, and Dendrobatidae. The 10 PPC-positive samples were distributed among three families: Bufonidae (n = 2), Aromobatidae (n = 4), and Hylidae (n = 4). These results expand PPC's known geographic range to include wild Panama populations and UK aquaculture, and further expand the known host range within the Hyloidea superfamily. These data add to a fuller understanding of the biogeography of this putatively pathogenic lineage and its host range, factors that will likely prove important for assessing the risk of this group for amphibian conservation.

4.1. INTRODUCTION

Severe Perkinsea infection (SPI) has been correlated to mass die-offs in a broad taxonomic and geographic diversity of tadpoles. A recent amphibian health survey found that it might represent the third most common infectious amphibian disease in North America, after ranavirus and chytridiomycosis (Isidoro-Ayza et al. 2017). It has been linked to a specific lineage of Perkinsea called Pathogenic Perkinsea Clade (PPC; Isidoro-Ayza et al. 2017), which is part of a broad monophyletic group of alveolates named Novel Alveolate Group 01 (NAG01; Chambouvet et al. 2015). PPC sequences have been recovered from moribund tadpoles from all known SPI-associated mortality events in the USA (Davis et al. 2007, Isidoro-Ayza et al. 2017), whereas they have only been recovered from 2.5% (2/81) of normal tadpoles surveyed (in localities with current or historical SPI outbreaks) (Isidoro-Ayza et al. 2017). NAG01 also includes three putatively nonpathogenic clades (Clades A-C) sampled from tadpoles from a broad range of taxa in Africa, Europe, and South America (Chambouvet et al. 2015). The absence of evidence of pathologies in NAG01 Clades A-C (NAG01a-c), combined with the pervasiveness of PPC among tadpoles with SPI, suggests that severe pathogenicity might be restricted to PPC. In Chapter 2, we attempted to elucidate the relationship between NAG01 Perkinsea and SPI-associated disease by addressing Koch's postulates (Koch 1884a) through experimental infection of *Rana dalmatina* tadpoles; however, our results could not confirm disease causation and therefore this relationship remains unclear.

The currently recognized geographic and host ranges of amphibian Perkinsea are based on eight studies (Green et al. 2002, Davis et al. 2007, Cook 2008, 2009, Landsberg et al. 2013, Chambouvet et al. 2015, Isidoro-Ayza et al. 2017, Karwacki et al. 2018). The most geographically comprehensive of these studies are Chambouvet et al. (2015), which sampled Africa, Europe, and South America, and Isidoro-Ayza et al. (2017), which sampled North America. Chambouvet et al. (2015) screened 182 healthy tadpoles (from six regions: French Guiana, Cameroon, Tanzania, Sao Tome, the UK, and the Czech Republic) and found 38 (21%) were positive for the putatively nonpathogenic NAG01 clades but did not find evidence for the PPC clade. These 38 specimens represented eight anuran families, including Ranidae (*Rana temporaria*), Hylidae (*Hypsiboas geographicus*, *Hyla helenae*), Phyllomedusidae *Phyllomedusa tomopterna*, *Leptopelis* sp.), Arthroleptidae (*Leptopelis vermiculatus*, *L. barbouri,*

Astylosternus schioetzi, Trichobatrachus robustus), Phrynobatrachidae (*Phrynobatrachus* sp., *P. steindachneri, P. dispar*), Hyperoliidae (*Hyperolius riggenbachi*, *H. lamottei, Kassina maculosa*), Bufonidae (*Bufo bufo, Amietophrynus regularis*), and Pyxicephalidae (*Amietia angolensis*). Interestingly, 21 of these specimens (55%) yielded sequences from both clades A and B, "suggesting that these livers harboured representatives from different non-clonal strains/species or that there is intranuclear SSU rDNA variation within NAG01 genomes sampled" (Chambouvet et al. 2015). Similar patterns of highly divergent multi-copy rRNA gene clusters have been seen in other alveolate parasites such as the malaria parasite *Plasmodium falciparum* (McCutchan et al. 1988, Nishimoto et al. 2008).

In North America, the first documented mass mortality events (MMEs) associated with SPI were recorded in New Hampshire in 1999 (Green et al. 2003). Since then, SPI-associated MMEs have been reported in seven other states across a broad geographic range: Florida, Mississippi, Virginia, Maryland, New York, Minnesota, and Alaska (Green et al. 2002, Davis et al. 2007, Landsberg et al. 2013, Isidoro-Ayza et al. 2017). Most of the SPI-associated MMEs have occurred in tadpoles of the *Lithobates* genus (family Ranidae), including *L. sylvaticus* (wood frog), *L. pipiens* (northern leopard frog), *L. sphenocephalus* (southern leopard frog), *L. catesbeianus* (American bullfrog), *L. clamitans* (green frog), *L. septrionalis* (mink frog), and the critically endangered *L. sevosus* (Mississippi gopher frog) (Green et al. 2003, Davis et al. 2007, Cook 2008, 2009, Landsberg et al. 2013, Isidoro-Ayza et al. 2017). SPI-associated MMEs have also occurred in larval hylids (family Hylidae), including *Pseudacris crucifer* (spring peeper) and *Acris gryllus* (southern cricket frog) (Isidoro-Ayza et al. 2017). Reports of asymptomatic PPC infection are rare. Isidoro-Ayza et al. (2017) conducted a NAG01 Perkinsea molecular screen on 81 apparently normal tadpoles from 12 US states, representing 11 species from three families (Hylidae, Ranidae and Pipidae). Only two of these tadpoles tested positive for PPC DNA, both of which were identified as *R. sphenocephala*: one from Wakulla, Florida (2010), and another from Prince George's, Maryland (2008). Both of these sites were experiencing an SPI outbreak at the time of specimen collection (Isidoro-Ayza et al. 2017). Although PPC is referred to as the North American clade, the extent to which it occurs across the continent is unclear because amphibian health surveys have been limited. Based

on its known distribution, it is highly likely that PPC (and SPI disease) has been occurring throughout the Nearctic region.

There has been no record of PPC (or SPI disease) outside North America. Only a single amphibian Perkinsea survey has been conducted south of Florida: 80 tadpoles (from 8 sites) in French Guiana, all of which were negative for PPC (although four were positive for NAG01a-c: Clade A = 2, Clade B = 1, Clades A, B & C = 1) (Chambouvet et al. 2015). Furthermore, the fact that it has been found in a variety of forested habitats with different climates, including marine west coast forest, eastern temperate forest, and northern forest, suggests that it has the capacity for a much broader distribution. This is further supported by its broad range of hosts, which includes species from two anuran families with near cosmopolitan distributions: Ranidae and Hylidae. A portion of samples screened from Africa, Europe, and South America were positive for NAG01a-c (the putatively nonpathogenic strain of amphibian Perkinsea) (Chambouvet et al. 2015). However, we note that many of the NAG01a-c samples were collected from early development phases or museum samples; therefore, it is possible that NAG01a-c pathologies had not developed or had gone undetected.

In this study, we further investigate the geographic and host range of amphibian Perkinsea (and SPI-associated disease) by screening tadpoles for NAG01 Perkinsea in Panama and the UK. Panama is particularly well-known for its recent loss of amphibian biodiversity due to chytridiomycosis (Lips et al. 2006); our sampling effort here allows us to further assess wider potential threats to the critical status of this country's amphibian community. Our UK sampling effort allows us to extend the relatively limited scope of Palearctic screenings and investigate a potential outbreak of this infection in (hobbyist) aquaculture, a potential route for further geographical transmission as hypothesised for other amphibian disease outbreaks (Mazzoni et al. 2003, Miller et al. 2011).

Surveys were conducted using phylogenetics based on sequences from ribosomal RNA (rRNA), a type of non-coding RNA that partially comprise ribosomes, the complexes responsible for protein synthesis. rRNA is arranged in two subunits that differ in size, measured as Svedberg units (S). The eukaryotic small subunit (SSU) rRNA is 18S and the large subunit (LSU) rRNA is 60S (comprised of 28S, 5.8S

and 5S). The prokaryotic SSU rRNA is 16S and the LSU rRNA is 50S (comprised of 23S and 5S). In the mitochondrion, mitochondrial SSU and LSU rRNA are 12S and 16S, respectively. All these genes have proven popular targets for sequencing projects in order to identify biodiversity of numerous taxonomic groups. As such, an extensive database of homologous sequences is now available supporting extensive downstream phylogenetic and biogeographical analysis.

There are certain criteria that a gene must meet for the construction of accurate species-phylogenies. The gene must occur in all organisms of interest and it must be conserved (that is, it must not have undergone lateral transfer between different genetic lineages), and it must not have been randomized over the course of evolution due to high rates of mutational saturation (Woese 1987, Pace 2009). rRNA genes are well-suited to these criteria as they are indeed ubiquitous in all living organisms. They contain some of the most conserved regions of DNA sequence (partly because they are not translated into protein). For example, the eukaryotic and bacterial SSU rRNA genes typically share about 50% similarity over their alignable lengths, providing consensus sites for sequence alignments (Pace 2009). rRNA genes also form complex secondary structures composed of double stranded regions, allowing for identification of regions suitable for comprehensive primer design (Pace 2009).

SSU rRNA sequences were used to create the first sequence-based tree of life, which traced all living organisms to three ‘aboriginal’ lines of descent: the eubacteria (or Bacteria), the archaebacteria (or Archaea), and the eukaryotes (Woese & Fox 1977). Since that time, the use of the SSU rRNA gene in phylogenetic research has grown rapidly (Woese et al. 1990, Cavalier-Smith 2004, Yarza et al. 2017), leading to the vast expansion of SSU rRNA databases. For example, the SILVA database currently (2020) contains nearly 10 million aligned SSU rRNA sequences (about 10x the number of aligned LSU rRNA sequences). SSU rDNA sequences were used to identify the different clades of NAG01 Perkinsea, and to link SPI disease specifically to PPC (Chambouvet et al. 2015, Isidoro-Ayza et al. 2017). This study aims to further explore the geographic and host ranges of NAG01 Perkinsea, and the co-association of the two clades. We used SSU rRNA sequences to construct a phylogeny for NAG01 Perkinsea recovered from tadpoles in Panama and the UK, and mitochondrial rRNA phylogenetics to identify the tadpoles (Panama only), demonstrating a wider biogeographical provenance of this putative pathogenic association.

4.2. METHODS

4.2.1. Sample collection and DNA extraction

Fieldwork was carried out in Panama in November 2018. Tadpoles with unknown pathology were captured using dip nets from seven sites spanning three regions: Soberania National Park, Altos de Campana National Park, and El Valle de Anton (Table S4.1 – GPS data provided). They were transported to the Gamboa Amphibian Research and Conservation Center where they were euthanized using an overdose of MS-222 and dissected. Their livers were stored in LifeGuard™ solution (Qiagen) at -20°C for 1-2 weeks before being transferred to -80°C. All of the livers appeared normal upon gross examination (i.e. there were no signs of enlargement or discoloration).

Hyla arborea tadpoles were collected from a single 'pathology' event in Surrey, UK in July 2019 (Table S4.1) and stored whole in LifeGuard™ preservation solution. They were delivered to the University of Exeter in an insulated cooler and stored at -80°C prior to dissection. Livers were removed from 10 tadpoles and immediately processed for DNA extraction. All of the livers showed signs of SPI disease upon gross examination, including enlargement and yellow discoloration; however, microscopic examination of two (symptomatic) samples did not reveal the presence of Perkinsea organisms.

Total DNA was extracted from the liver tissue of 91 tadpoles in total: 81 from Panama and 10 from the UK (Table S4.1). All of the UK tadpoles and some of the Panama tadpoles had very small livers, so in order to ensure that an adequate amount of starting material was used for the extractions, the 10 UK liver tissue samples were pooled into two groups of five, and 15 of the 81 Panama samples were pooled into three groups of five (the remaining 66 Panama samples were processed as single livers) (Table S4.1). Since the species of the Panama tadpoles were unknown at the time of dissection, their livers were pooled according to the external morphology of the tadpoles and their collection site (i.e. they shared the same morphology and came from the same site). Extractions were carried out using the DNeasy Blood and Tissue Kit (Qiagen) according to the manufacturer's protocol with an overnight lysis step at 37°C, followed by one minute of disruption with 425-600 µm acid-washed glass beads (Sigma-Aldrich) on a *FastPrep-24* tissue homogenizer (MP Biomedicals).

4.2.2. NAG01 Perkinsea molecular screening, cloning, and sequencing

DNA samples were subjected to conventional PCR using a published forward primer (300F-B; Chambouvet et al. 2015) and a reverse primer (NAG01R_1) designed for this study (Table 4.1). The primer pair targets a 287-290 bp fragment of the SSU rRNA gene of the NAG01 Perkinsea. The reaction mixture included 1x concentration PCR MasterMix (Promega), 500 nM of each primer, 5 µl of template DNA, and molecular-grade water to bring the total reaction volume to 25 µl. Each PCR assay included a negative control (molecular-grade H_2O) and 1 µl of template DNA from a positive control (DNA from PPC-infected Alaska *L. sylvaticus* tadpole liver). Cycling conditions were as follows: 2 min at 95°C, followed by 35 cycles of 30 s at 95°C, 30 s at 56°C, and 60 s at 72°C, with an additional 10-min extension at 72°C. PCR products were checked on a 2% agarose gel and purified using the GeneJET PCR Purification Kit (Thermo Fisher).

Purified PCR products were cloned into the plasmid vector pSC–A–amp/kan using the Strata Clone PCR Cloning Kit (Agilent Technologies) following the manufacturer's protocol. Plasmids were transformed into StrataClone SoloPack Competent Cells (Agilent Technologies) and blue-white screened on LB-ampicillin plates with 2% X-gal. White mono-colonies were cultured in LB-ampicillin broth at 37°C overnight. Plasmid DNA was extracted from the cultures using the GeneJET Plasmid Miniprep Kit (Thermo Fisher) according to the manufacturer's protocol. Extractions were sent to Eurofins Genomics (Wolverhampton, UK) for sequencing with primers T3 forward and T7 reverse. The program Sequencher (version 5.4.6) was used to remove vector sequences, assemble the forward and reverse reads into consensus sequences, and correct ambiguous sites. In order to determine if the DNA samples contained multiple clades of NAG01 Perkinsea (and to generate a larger number of sequences for phylogenetic analysis), we attempted to triplicate the (PCR, cloning, and sequencing) process on every sample that yielded a product in the first round of PCR (n = 11; Table S4.2). One of these samples (UK_HA01-5) was subjected to a second triplication process with a lower PCR annealing temperature (54°C) to further test for clade diversity by decreasing primer-specificity.

Table 4.1. Primers used in this study.

Primer	Sequence (5' - 3')	Specificity	Reference
300F-B	GGG CTT CAY AGT CTT GCA AT	NAG01 Perkinsea	Chambouvet et al. (2015)
NAG01R_1	GCC TGC TTG AAA CRC TCT AA	NAG01 Perkinsea	This study
16SAR-L	CGC CTG TTT ATC AAA AAC AT	vertebrates	Palumbi et al. (1991)
16SBR-H	CCG GTC TGA ACT CAG ATC ACG T	vertebrates	Palumbi et al. (1991)
MCP-F	TAC TTT GTC AAG GAG CAY TAC T	ranavirus	This study
MCP-R	TCA TGT TAT AGT AGC CTR TGC	ranavirus	This study

4.2.3. SSU rDNA-based phylogeny of NAG01 Perkinsea

The novel clone sequences generated in this study (Table S4.2) were assembled into a multiple sequence alignment (MSA), along with 116 SSU rDNA sequences recovered from the NCBI nr database (accessed August 2019), including 100 PPC sequences, 5 sequences representing NAG01 Clades A, B and C, 5 NAG01 environmental sequences, 2 (non-NAG01) Perkinsea-like environmental sequences, and 4 *Perkinsus* species (Table S4.3). Reference sequences for the four *Perkinsus* species were used to root the tree. An alignment of the sequence data was generated using MUSCLE in the program SeaView (version 4.6.2) (Gouy et al. 2010). The alignment was manually checked and masked to generate a final data matrix of 188 sequences with 288 nucleotide sites. Maximum likelihood (ML) and neighbour-joining (BioNJ; Gascuel 1997) were performed using IQ-TREE (version 1.6.5) (Nguyen et al. 2015) and SeaView, respectively. For the ML analysis, a TIM3e+G4 model was used (the best model for the alignment according to ModelFinder (Kalyaanamoorthy et al. 2017) implemented in IQ-TREE) and 1,000 bootstrap iterations were performed. For the BioNJ analysis, a Log-Det distance model was used and 1,000 bootstrap iterations were performed. All Perkinsea sequences that were newly generated in this study have been deposited in GenBank (Table S4.2). The Perkinsea alignments have been made available in the SeaView Mase format with the alignment mask information retained (available at DOI: 10.6084/m9.figshare.13108136).

4.2.4. Host species genetic identification using mitochondrial rDNA amplification

Tadpoles can be difficult to identify based on their morphology, particularly in their early stages. The broad diversity of species in Panama further complicates their

identification. In order to classify our specimens, we PCR amplified a ~600 bp fragment of the mitochondrial rDNA gene using mitochondrial AR-L and mitochondrial BR-H primers obtained from Palumbi et al. (1991) (Table 4.1). The primers were designed to incorporate 'ID-tags' comprised of random 12-nt sequences added to the 5' end of the primers with a "GC" in between, thereby generating twenty unique identifiers to use for sample pooling. The reaction mixture included 1x concentration PCR MasterMix (Promega), 500 nM of each primer, 1 µl of template DNA, and molecular-grade water to bring the total reaction volume to 25 µl. Each PCR included a negative control (molecular-grade H_2O) and 1 µl of template DNA from a positive control (DNA from PPC-infected Alaskan *L. sylvaticus* tadpole liver). Cycling conditions were as follows: 2 min at 95°C, followed by 35 cycles of 30 s at 95°C, 30 s at 56°C, and 60 s at 72°C, with an additional 10 min extension at 72°C. PCR products were checked on a 1.5% agarose gel; those that failed to amplify were rerun with 5 µl of template DNA.

4.2.5. Library preparation and sequencing of SSU rDNA amplicons

For the purpose of mitochondrial SSU rRNA amplicon sequencing we prepared amplicon libraries for MinION (Oxford Nanopore) sequencing following the 1D Amplicon by ligation protocol (SQK-LSK108). A total of 69 uniquely-tagged amplicons (~100 ng each) were combined into a total of five pools. The amplicon pools were processed for end-repair using the NEBNext Ultra II End Repair/dA-Tailing Module (New England Biolabs), followed by purification with Agencourt AMPure XP beads (Beckman Coulter) with a ratio of beads to PCR product volume of 0.8. Adapters were ligated to the end-prepped amplicons with Blunt/TA Ligase Master Mix (New England Biolabs) and re-purified with Agencourt AMPure XP beads to obtain the final libraries. The libraries were loaded into FLO-MIN106 flow cells (R9.4.1) and sequenced on a MinION nanopore sequencer using MinKNOW software.

Sequence reads were demultiplexed based on their unique tags using MiniBar software (version 0.21), allowing a maximum of two mismatches between the tags. Low quality reads were filtered using NanoFilt (version 2.5) (De Coster et al. 2018) using the script filter.sh. Out of the 69 uniquely-tagged samples, seven did not yield any reads ("NR" in Table S4.1), and were excluded from subsequent analysis. Reads

from the remaining 62 samples were subsampled to 150x (where applicable) and then assembled into contigs (consensus sequences) using Canu (version 1.8) (Koren et al. 2017) using the script canu.sh. Out of the 62 samples, 39 successfully assembled into contigs. Two of these samples yielded multiple contigs from multiple species, indicating possible contamination, and were excluded from phylogenetic analysis ("MC" in Table S4.1). None of the nine samples excluded from phylogenetic analysis (for either lack of reads or multiple contigs) were PCR-positive for Perkinsea DNA.

For the 23 samples that failed to assemble into contigs, the demultiplexed, filtered reads were examined. Six of these samples yielded reads with high rates of sequencing errors in conserved regions ("SE" in Table S4.1). A search of these reads against the NCBI nr database, as well as their partial alignments (not including the error regions), indicated they were redundant sampling covered by other tadpoles, and were therefore excluded from the final analysis. An exception was PA_T135, as this sample was PCR-positive for Perkinsea DNA and therefore of greater importance to the study. For this sample, the PCR was repeated and the product was sequenced using Sanger sequencing following the same methods outlined for the NAG01 sequences. This sequence was added to the alignment for phylogenetic analysis. For the remaining 17 samples (i.e. those without high rates of sequencing errors), the top read was retained for phylogenetic analysis.

4.2.6. Mitochondrial rDNA-based phylogeny of host species

A total of 60 amphibian mitochondrial rDNA sequences were searched against the NCBI nr database using BLASTn MegaBLAST (accessed 18 June 2019). Details for the hits with the highest identity percentage for each of the newly generated sequences are presented in Table S4.4. The database search yielded a total of 16 unique sequences (Table S4.4), 12 of which were assembled into an MSA (Table S4.5) along with the newly generated sequences (excluding the six samples with high rates of sequencing errors). Also included in the MSA were 12 sequences representing taxa closely related to those identified in the database search and a single sequence representing *Hyla arborea* (i.e. the species of the UK specimens) (Table S4.5). A total of five reference sequences representing *Xenopus laevis*, *Ambystoma* spp., and *Pleurodeles* spp. were chosen as outgroups for the phylogeny.

An alignment of the sequence data was generated using MUSCLE in the program SeaView (Gouy et al. 2010). The alignment was manually checked and masked to generate a final alignment of 84 sequences with 410 nucleotide sites. Maximum likelihood (ML) and neighbour-joining (BioNJ; Gascuel 1997) were performed using IQ-TREE (Nguyen et al. 2015) and SeaView, respectively. For the ML analysis, a GTR+F+I+G4 model was used (the best model for the alignment according to ModelFinder (Kalyaanamoorthy et al. 2017), implemented in IQ-TREE) and 1,000 bootstrap iterations were performed. For the BioNJ analysis, a Log-Det distance model was used and 1,000 bootstrap iterations were performed. All tadpole sequences that were newly generated in this study have been deposited in GenBank (Table S4.1). The tadpole alignments have been made available in the SeaView Mase format with the alignment mask information retained (available at DOI: 10.6084/m9.figshare.13108136).

4.2.7. Ranavirus molecular screening

The Panama and UK samples were tested for the presence of ranavirus by PCR. A primer pair was designed to target a 358 bp sequence of the major capsid protein (MCP) encoding gene (Table 4.1). In order to obtain template DNA for a positive control, this sequence was synthesized into a plasmid vector (pUC57-Amp) by Synbio Technologies. The reaction mixture included 1x concentration PCR MasterMix (Promega), 500 nM of each primer, 1 µl of template DNA, and molecular-grade water to bring the total reaction volume to 25 µl. The reaction included a negative control (molecular-grade H_2O) and 1 ng of plasmid DNA as a positive control. Cycling conditions were as follows: 2 min at 95°C, followed by 35 cycles of 30 s at 95°C, 30 s at 56°C, and 60 s at 72°C, with an additional 10-min extension at 72°C. PCR products were checked on a 2% agarose gel.

4.3. RESULTS

4.3.1. NAG01 Perkinsea molecular screening, cloning, and sequencing

Liver tissue samples from a total of 91 tadpoles were screened for NAG01 Perkinsea using PCR detection: 81 from Panama and 10 from the UK (Table S4.1). The 10 UK

samples were pooled into two groups of five, and 15 of the 81 Panama samples were pooled into three groups of five. NAG01 Perkinsea SSU rDNA was detected in 10 of the Panama samples (all of which were single tadpole-specimens processed separately), and one of the pooled UK samples, which contained tadpoles from the same population (Table S4.1). PCR products were purified, cloned, and sequenced; this process yielded 1-10 clones for each sample in the first round (Table S4.2). To improve clone-sequence sampling and further test for the possibility of contamination we then replicated the PCR and cloning steps for three samples for the purpose of additional sequence sampling (PA_T135, PA_T139, and UK_HA01-5). The number of recoverable clones varied between samples and PCRs, resulting in a total of 72 novel clone sequences (Table S4.2). These sequences were incorporated into an MSA, along with Perkinsea sequences recovered from the NCBI nr database, and used to generate an SSU rDNA-based phylogeny.

4.3.2. SSU rDNA-based phylogeny of NAG01 Perkinsea

Phylogenetic analysis revealed that the 72 newly generated NAG01 Perkinsea SSU rDNA sequences from Panama and the UK were identical or nearly identical to previously published PPC sequences from mortality events in the USA (Davis et al. 2007, Isidoro-Ayza et al. 2017). These sequences formed a strongly supported clade (labelled PPC) that was distinct from other NAG01 sequences, including representatives from Clades A, B, and C, associated with cryptic infections of tadpoles (Chambouvet et al. 2015) (Figure 4.1). All of the UK sequences and most of the Panama sequences were more closely related to each other than they were to previously published sequences from the USA, as evidenced by their discrete moderately supported grouping (Figure 4.1). Two sequences from PA_T135 grouped more closely with a subset of USA sequences (Figure 4.1). There was evidence of micro-diversity within the PA/UK group, including an exclusive subgroup of Panama sequences (Figure 4.1). This subgroup was also detected by the neighbour joining analysis; however, both of the analyses had low node support. Examination of the masked MSA used to calculate the phylogeny revealed that the PA/UK group was distinguished by a single SNP at a single locus (position 275), whereas the Panama subgroup within the PA/UK radiation was distinguished by a SNP at position 233. The sequences generated from the UK samples that were PCR amplified at different

annealing temperatures (i.e. “_54°” and “_56°”) were identical or nearly identical (Figure 4.1).

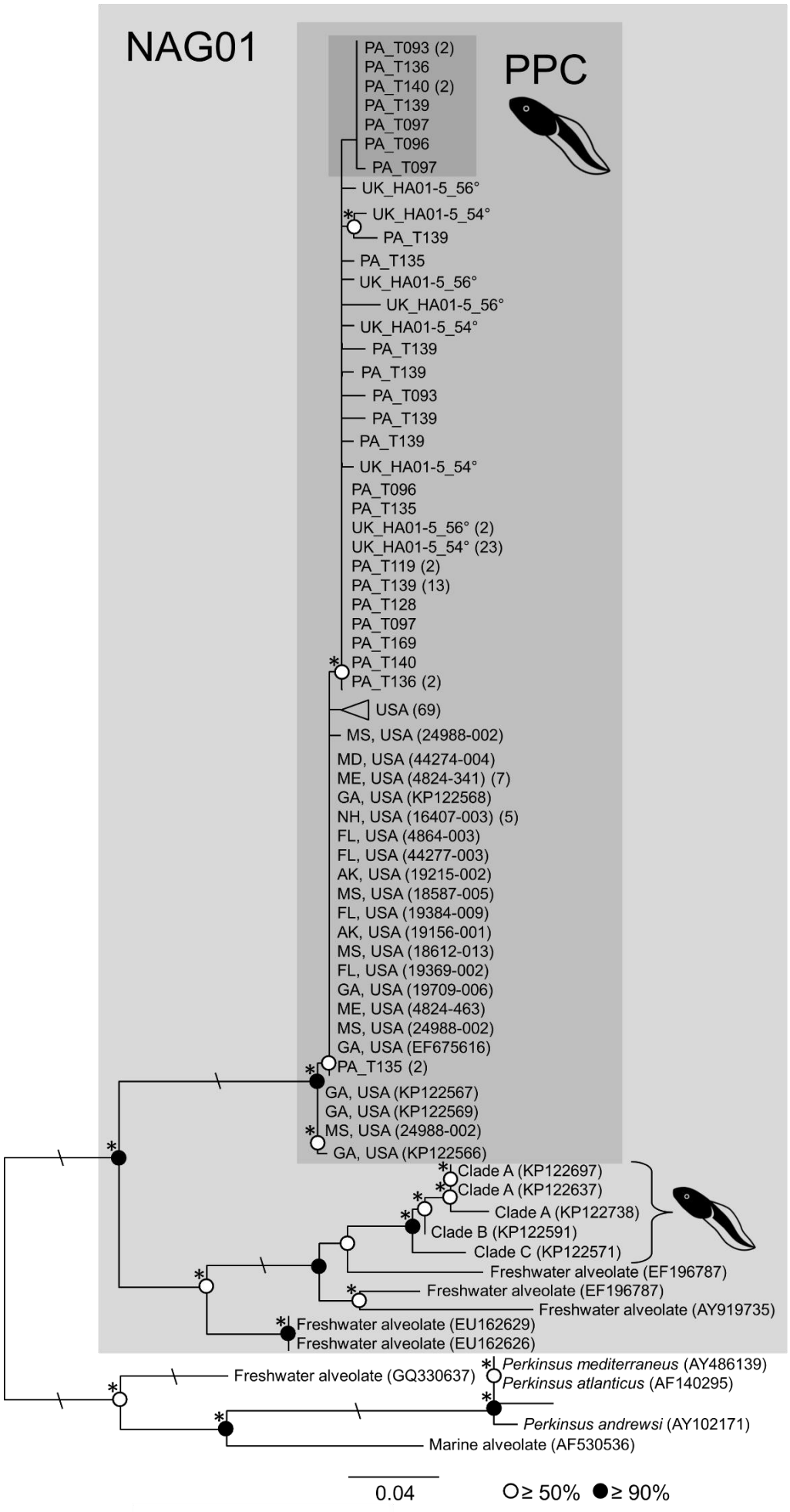
NAG01
PPC
PA_T093 (2)
PA_T136
PA_T140 (2)
PA_T139
PA_T097
PA_T096
PA_T097
UK_HA01-5_56°
UK_HA01-5_54°
PA_T139
PA_T135
UK_HA01-5_56°
UK_HA01-5_56°
UK_HA01-5_54°
PA_T139
PA_T139
PA_T093
PA_T139
PA_T139
UK_HA01-5_54°
PA_T096
PA_T135
UK_HA01-5_56° (2)
UK_HA01-5_54° (23)
PA_T119 (2)
PA_T139 (13)
PA_T128
PA_T097
PA_T169
PA_T140
PA_T136 (2)
USA (69)
MS, USA (24988-002)
MD, USA (44274-004)
ME, USA (4824-341) (7)
GA, USA (KP122568)
NH, USA (16407-003) (5)
FL, USA (4864-003)
FL, USA (44277-003)
AK, USA (19215-002)
MS, USA (18587-005)
FL, USA (19384-009)
AK, USA (19156-001)
MS, USA (18612-013)
FL, USA (19369-002)
GA, USA (19709-006)
ME, USA (4824-463)
MS, USA (24988-002)
GA, USA (EF675616)
PA_T135 (2)
GA, USA (KP122567)
GA, USA (KP122569)
MS, USA (24988-002)
GA, USA (KP122566)
Clade A (KP122697)
Clade A (KP122637)
Clade A (KP122738)
Clade B (KP122591)
Clade C (KP122571)
Freshwater alveolate (EF196787)
Freshwater alveolate (EF196787)
Freshwater alveolate (AY919735)
Freshwater alveolate (EU162629)
Freshwater alveolate (EU162626)
Freshwater alveolate (GQ330637)
Perkinsus mediterraneus (AY486139)
Perkinsus atlanticus (AF140295)
Perkinsus andrewsi (AY102171)
Marine alveolate (AF530536)
0.04
≥ 50%
≥ 90%

Figure 4.1. Maximum likelihood phylogenetic tree of Perkinsea SSU rDNA estimated from an alignment consisting of 188 sequences and 288 nucleotide sites. Bootstrap values are summarized by black circles when the node support is greater than or equal to 90%, and white circles when the node support is less than 90% but equal to or greater than 50%. Asterisks (*) indicate node support was consistent with the Log-Det neighbour joining analysis. Slashes (\) indicate branch length was reduced by half. The phylogeny focuses on the NAG01 groups of Perkinsea known to infect tadpoles, including the lineage associated with disease and mortality (PPC), and the lineage associated with cryptic infections (Clades A, B, and C). Newly generated PPC sequences are labelled with geographic location (PA or UK) and sample ID. Sequences derived from the same sample were combined for simplicity. PPC sequences composing the exclusive Panama subgroup are highlighted in the dark grey box. Reference PPC sequences are labelled with geographic location and GenBank accession number or sample ID. (For all PPC sequences derived from Isidoro-Ayza et al. (2017), accession number was replaced with sample ID, and sequences with the same sample ID were combined for simplicity). All other reference sequences are labelled with their GenBank accession number and either their NAG01 clade, environmental origin (i.e. freshwater or marine alveolate), or species (i.e. *Perkinsus* spp.). The sequences outside of the NAG01 group were used to root the tree. The triangle represents a large subset of reference PPC sequences from the USA; the number of sequences is listed in parentheses. All other parenthesized numbers correspond to the number of sequences represented by a sample. Details for the newly generated sequences used in this analysis can be found in Table S4.2. Details for the published sequences can be found in Table S4.3. This figure was created using a combination of FigTree (version 1.4.4) (Rambaut 2018) and Microsoft PowerPoint 2016.

4.3.3. Mitochondrial rDNA-based phylogeny of host species

Phylogenetic analysis revealed that the 54 newly generated amphibian mitochondrial rDNA sequences included in the final alignment represented six anuran families: Bufonidae, Phyllomedusidae, Aromobatidae, Hylidae, Leptodactylidae, and Dendrobatidae (Figure 4.2). The 10 PPC-positive samples included in the alignment were distributed among three families: Bufonidae (n = 2), Aromobatidae (n = 4), and

Hylidae (n = 4) (Figure 4.2). All 10 samples grouped in strongly supported clades with a reference sequence for a particular species: PA_T128: *Rhinella marina* (Bufonidae); PA_T169: *Rhinella atlata* (Bufonidae); PA_T136, PA_T139, PA_T140: *Allobates talamancae* (Aromobatidae); PA_T097, PA_T096, PA_T093: *Boana rosenbergi* (Hylidae), and PA_T119: *Dendrosophus ebraccatus* (Hylidae). Many of the nodes in the phylogeny have moderate to strong support (i.e. their bootstrap values are either equal/greater than 50% and less than 90%, or equal/greater than 90%, respectively). This includes most of the distal interior nodes (i.e. the nodes resolving relationships at the genus and species level) and the ancestral interior nodes (i.e. the nodes at the order and superfamily level). However, most of the intermediate interior nodes (i.e. the nodes at the family level) have comparatively low support (i.e. their bootstrap values are less than 50%). For this reason, the phylogenetic relationships at the family level should be interpreted with caution. For example, both the ML and Log_Det neighbour analyses failed to recognize the close relationship between the families Hylidae and Phyllomedusidae, which have recently been combined into the unranked taxon Arboranae (Duellman et al. 2016).

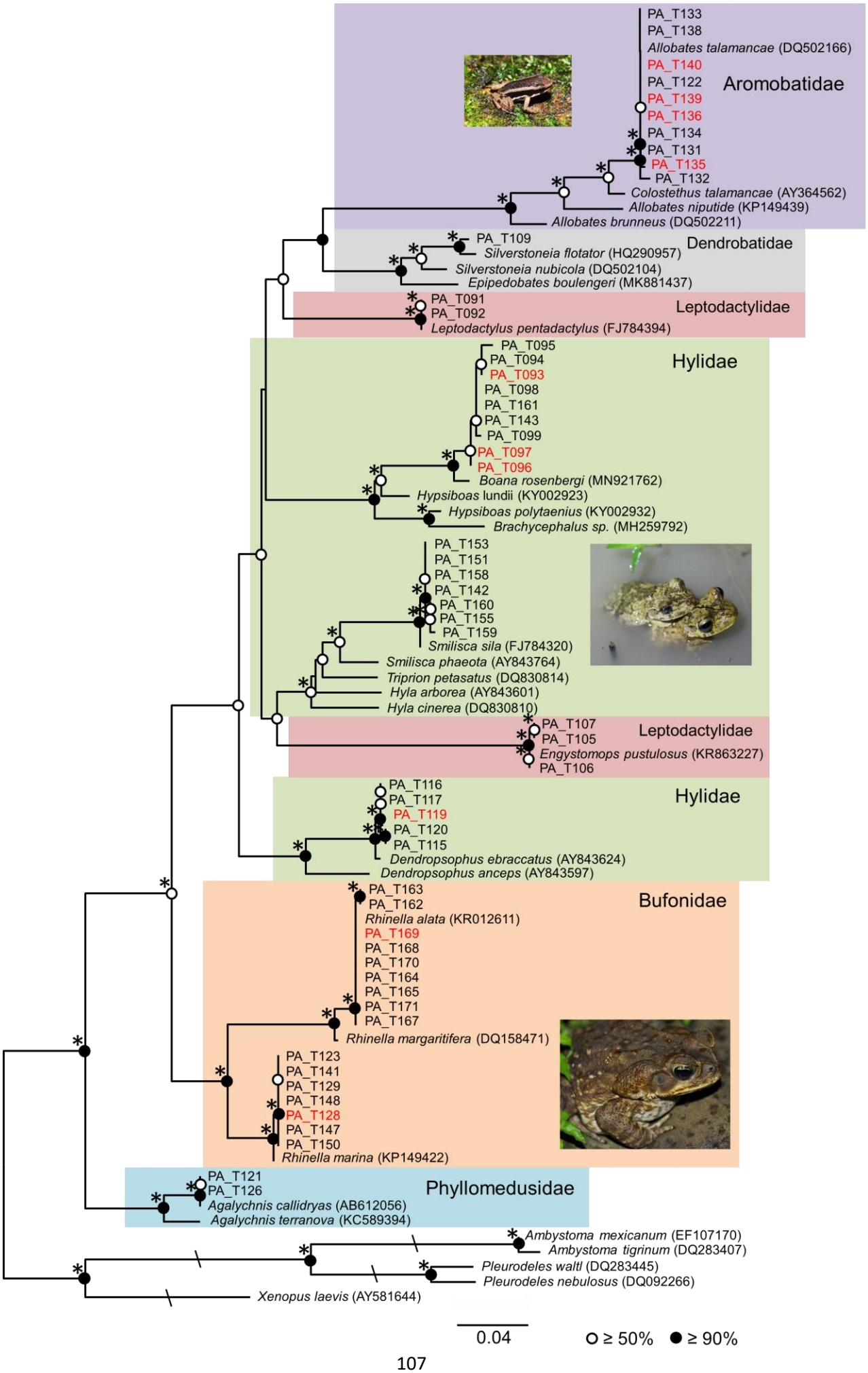
PA_T133
PA_T138
Allobates talamancae (DQ502166)
PA_T140
PA_T122
Aromobatidae
PA_T139
PA_T136
PA_T134
PA_T131
PA_T135
PA_T132
Colostethus talamancae (AY364562)
Allobates niputide (KP149439)
Allobates brunneus (DQ502211)
PA_T109
Dendrobatidae
Silverstoneia flotator (HQ290957)
Silverstoneia nubicola (DQ502104)
Epipedobates boulengeri (MK881437)
PA_T091
PA_T092
Leptodactylidae
Leptodactylus pentadactylus (FJ784394)
PA_T095
PA_T094
Hylidae
PA_T093
PA_T098
PA_T161
PA_T143
PA_T099
PA_T097
PA_T096
Boana rosenbergi (MN921762)
Hypsiboas lundii (KY002923)
Hypsiboas polytaenius (KY002932)
Brachycephalus sp. (MH259792)
PA_T153
PA_T151
PA_T158
PA_T142
PA_T160
PA_T155
PA_T159
Smilisca sila (FJ784320)
Smilisca phaeota (AY843764)
Triprion petasatus (DQ830814)
Hyla arborea (AY843601)
Hyla cinerea (DQ830810)
PA_T107
PA_T105
Leptodactylidae
Engystomops pustulosus (KR863227)
PA_T106
PA_T116
PA_T117
Hylidae
PA_T119
PA_T120
PA_T115
Dendropsophus ebraccatus (AY843624)
Dendropsophus anceps (AY843597)
PA_T163
PA_T162
Bufonidae
Rhinella alata (KR012611)
PA_T169
PA_T168
PA_T170
PA_T164
PA_T165
PA_T171
PA_T167
Rhinella margaritifera (DQ158471)
PA_T123
PA_T141
PA_T129
PA_T148
PA_T128
PA_T147
PA_T150
Rhinella marina (KP149422)
PA_T121
PA_T126
Phyllomedusidae
Agalychnis callidryas (AB612056)
Agalychnis terranova (KC589394)
Ambystoma mexicanum (EF107170)
Ambystoma tigrinum (DQ283407)
Pleurodeles waltl (DQ283445)
Pleurodeles nebulosus (DQ092266)
Xenopus laevis (AY581644)
0.04
≥ 50%
≥ 90%

Figure 4.2. Maximum likelihood phylogenetic tree of mitochondrial rDNA representing the Panama tadpole diversity sampled in this study. The final alignment used for the analysis consisted of 85 sequences and 410 nucleotide sites. Bootstrap values are summarized by black circles when the node support is greater than or equal to 90%, and white circles when the node support is less than 90% but equal to or greater than 50%. Asterisks (*) indicate node support was consistent with the Log-Det neighbour joining analysis. Newly generated sequences are labelled with geographic location (PA) and sample ID. Reference sequences are labelled with species and GenBank accession number. Samples with PCR and sequencing evidence for PPC infections are coloured in red. Photographs depict *Allobates talamancae* (Aromobatidae) (Credit*: P. Kirillov), *Boana rosenbergi* (Hylidae) (Credit: the author), and *Rhinella marina* (Bufonidae) (Credit: the author). Details for the newly generated sequences used in this analysis can be found in Table S4.1. Details for the published sequences can be found in Table S4.5. This figure was created using a combination of FigTree (version 1.4.4) (Rambaut A 2018) and Microsoft PowerPoint 2016.

*License: https://creativecommons.org/licenses/by-sa/2.0/deed.en

4.3.4. Ranavirus molecular screening

Ranavirus DNA was not detected by MCP-specific PCR in any of the samples in this study. The agarose gel analysis revealed a strong band of the correct size in the positive control (1 ng of plasmid DNA containing MCP sequence), indicating that the assay was functional.

4.4. DISCUSSION

4.4.1. Expansion of PPC's known geographic range based on SSU rDNA phylogenetics

We screened tadpoles from Panama and the UK in order to further investigate the geographic range of amphibian Perkinsea infection. We used PCR to screen 91 tadpoles for NAG01 Perkinsea SSU rDNA; 10 of which were positive for the pathogenic lineage (PPC) (Table S4.1). PCR products were cloned and sequenced,

and used to construct a phylogeny with previously published NAG01 sequences for comparison (Figure 4.1). Our results revealed that the newly generated PPC sequences from Panama and the UK were identical or nearly identical to previously published PPC sequences from mortality events in the USA (Davis et al. 2007, Isidoro-Ayza et al. 2017).

Prior to this study, PPC had only been detected in tadpoles from North America, as far south as Florida (Isidoro-Ayza et al. 2017). Our results reveal that PPC can be found at least as far south as Panama, and close to the equator. PPC was also detected in specimens from the UK. In order to exclude the possibility that the UK-Panama similarities were the product of contamination, we replicated a subset of the PCR and cloning steps, confirming this shared SSU rDNA micro-diversity. On all occasions, including the initial PCR survey, the negative controls (molecular-grade H_2O) in each PCR step were clear and therefore likely free from contamination, and the PCRs for each of the locations were completed on different dates. The majority of PPC sequences from Panama and the UK are more closely related to each other than either are to the other previously published PPC sequences from the USA (Figure 4.1), but the evidence for this is limited to a single shared single nucleotide polymorphism (position 275 in the MSA used to estimate the phylogeny in Figure 4.1). Further biogeographic complexity would likely be resolved by additional sequencing. Furthermore, our sequencing identified putative evidence of a Panama specific clade (Figure 4.1), also marked by a single nucleotide polymorphism (position 233 in the MSA used to estimate the phylogeny in Figure 4.1).

Our results suggest that there is micro-diversity in the PPC data that cannot be fully resolved by sequencing the target 290 bp of the SSU rRNA gene sampled here. Evidence of this can be seen in the detection of an unsupported subgroup composed exclusively of Panama sequences in both the ML and BioNJ analyses. The evolutionary conservation that makes SSU rRNA such an appealing target for phylogenetics and, specifically, molecular sampling also hinders its ability to distinguish close relatives with few differences in their rRNA sequence (e.g. those at strain or species level) (Pace 2009). For example, SSU rRNA sequences do not reliably distinguish species of naked lobose amoebae (Nassonova et al. 2010), or *Escherichia coli* from *Shigella* spp. (Pace 2009, Devanga Ragupathi 2017). The SSU rRNA gene is only about 1,500 to 2,000 bp, half of which are invariant, meaning only

~1,000 bp are suited for resolving phylogenetic relationships (Pace 2009). Our SSU rDNA phylogeny was estimated from an MSA that included (only) 288 nucleotide sites. These sites span a region of the SSU rRNA gene with high-relative variation between the putatively pathogenic clade (PPC) and the putatively nonpathogenic clades (NAG01a-c) (Chambouvet et al. 2015), which has proven sufficient to distinguish these groups as evidenced in our SSU rDNA phylogeny (Figure 4.1). In the (masked) MSA used to estimate the phylogeny, PPC and NAG01a-c share only ~78% homology from position 137 to 253 (whereas they share ~97% homology in the rest of the alignment). It is possible that estimating a phylogeny from longer SSU rDNA sequences would help resolve the apparent micro-diversity within PPC. However, simply expanding an SSU rRNA phylogeny might not provide sufficient nucleotide variation for this resolution, due to abundant sequence conservation in the gene.

Another approach to solve the problem associated with SSU rRNA gene conservation would be to expand sequencing to other genes (ideally, less conserved genes in which a large number of differences occur among close relatives). Although SSU rRNA is the principal gene in protist diversity research, multiple other genes have proven useful for such investigation, including LSU 28S rRNA, internal transcribed spacer (ITS) rRNA, and mitochondrial cytochrome oxidase subunit I (COI) (Pawlowski et al. 2012). Sequences of the LSU rRNA gene, which is typically about twice the size of the SSU gene (Pace 2009), have been used to identify hundreds of novel haptophyte taxa (Liu et al. 2009), and have uncovered the existence of six main acantharian clades (Decelle et al. 2012). ITS rRNA, a region predominantly used in fungal diversity research (Schoch et al. 2012), has also been a source of species-level identification of oomycetes (Robideau et al. 2011) and chlorarachniophytes (Gile et al. 2010). COI, a demonstrable identifier for metazoans (Hebert et al. 2003), has been used to detect intraspecific diversity among ciliate isolates (Gentekaki & Lynn 2009) and species-level diversity among various other protists, including dinoflagellates (Stern et al. 2010), raphid diatoms (Evans et al. 2007), and naked lobose (Nassonova et al. 2010) and shelled amoebae (Kosakyan et al. 2012). Concatenations of multiple gene sequences can expand the number of informative sites, leading to phylogenies with increased resolution and statistical support that are better suited for discerning highly divergent sequences (Moreira et al. 2007, Marande et al. 2009).

Our results also indicate that there could be variant copies of the SSU rRNA gene in the genome of amphibian Perkinsea. This could explain why sequences from the same sample are not completely identical. Variant copies of SSU rRNA gene paralogues (e.g. ITS) are known to occur in alveolates (e.g. dinoflagellates) (Stern et al. 2012). *Plasmodium* spp. have structurally and functionally distinct (paralogous) copies of the SSU rRNA gene that are differentially expressed in their life cycle stages (Nishimoto et al. 2008), exhibiting 11% sequence dissimilarity (McCutchan et al. 1988). Single cell sequencing could be used to test amphibian Perkinsea for intranuclear variation in the SSU rRNA gene. This technique has been applied to the rRNA genes of ciliates (Gong et al. 2013) and dinoflagellates (Gribble & Anderson 2007). At most, the sequences in this study exhibit ~1% dissimilarity within samples, which is comparable to the intra-individual ITS variation observed in a *Vorticella* sp. (Gong et al. 2013). We note that our samples, which were derived from tadpole tissue, presumably contain many Perkinsea individuals.

4.4.2. Expansion of PPC's known host range based on mitochondrial rDNA phylogenetics

We PCR screened a diverse group of tadpoles from Panama for NAG01 Perkinsea in order to further investigate the putative pathogen's host range. We used mitochondrial rRNA phylogenetics for taxonomic identification of the tadpoles. Our phylogeny results revealed that 54 amphibian mitochondrial rDNA sequences generated in our study represented six anuran families: Bufonidae, Phyllomedusidae, Aromobatidae, Hylidae, Leptodactylidae, and Dendrobatidae (Figure 4.2). Ten PPC-positive samples were distributed among three families: Bufonidae (n = 2), Aromobatidae (n = 4), and Hylidae (n = 4) (Figure 4.2). Furthermore, a sample from the UK containing pooled DNA from five *Hyla arborea* tadpoles tested positive for PPC (species ID was provided by the supplier).

Previous NAG01 Perkinsea surveys identified the majority of infected tadpoles as members of the Ranoidea superfamily; this is true for both PPC (Isidoro-Ayza et al. 2017) and NAG01a-c (Chambouvet et al. 2015). Our results show that PPC's host range is broader than previously indicated, as the PPC-positive samples in our study include a larger number of Hyloidea species, including two within the Bufonidae family:

PA_T128 and PA_T169 (Figure 4.2). Prior to this study, PPC had not been detected in Bufonidae, which is one of the most widespread and speciose anuran families (Pramuk et al. 2008). We note that the molecular data for PPC in PA_T128 and PA_T169 are relatively weak. We attempted to triplicate the PCRs for all the samples in which NAG01 Perkinsea DNA was detected (in the initial PCR screen). Neither PA_T128 nor PA_T169 yielded subsequent PCR products (Figure S4.2). Furthermore, only one clone was successfully generated from the initial PCR product (Figure S4.2); however, we do not suspect contamination as the control PCRs were negative. We could not replicate this further due to low DNA extraction yield from the small liver sample, this is also likely to explain the low cloning yield.

The North America survey conducted by Isidoro-Ayza et al. (2017) found cryptic PPC infections to be a rarity; indeed, only 2 out of 81 tadpoles that appeared grossly and microscopically normal (both *R. sphenocephala*) were PCR-positive for PPC. However, our results show that cryptic PPC infections are more prevalent than previously indicated, as all 10 of the PPC-positive specimens from Panama appeared normal upon gross examination. Interestingly, most of the SPI-associated tadpole mortality events in North America have been documented in ranids (superfamily Ranoidea) (Green et al. 2002, Davis et al. 2007, Cook 2008, 2009, Landsberg et al. 2013, Chambouvet et al. 2015, Isidoro-Ayza et al. 2017, Karwacki et al. 2018), whereas the PPC-positive samples from this study were all members of the superfamily Hyloidea. This disparity suggests that Hyloidea species might be more tolerant of infection (i.e. infection is less likely to lead to disease in this superfamily). We note that the PPC-positive UK DNA sample was derived from symptomatic tissue from *H. arborea*, a member of Hyloidea. A putative Hyloidea tolerance could be tested by broader sampling of species in North America and Central America, which would respectively reveal cryptic PPC infections in hylids (but not ranids) and SPI disease in ranids (but not hylids). However, the disparity we observed might simply reflect the larger ratio of hylids to ranids in Central America compared to North America. In this case, broader sampling in Central America should reveal SPI disease in hylids (but not ranids), whereas broader sampling in North America should reveal cryptic infections in ranids (but not hylids).

Another inconsistency in our results is the fact that all the UK specimens displayed gross signs of SPI disease (i.e. enlargement and yellow discoloration of their

livers), yet microscopic examination of the liver tissue from a subset of samples did not reveal the presence of Perkinsea organisms (nor any other conspicuous infectious agents). This highlights the innate ambiguity of clinical symptoms, which are not necessarily indicative of infections. Furthermore, different infections can manifest symptoms similar to SPI disease. For example, both *Mycobacterium* spp. and *Chlamydophila* spp., which often infect captive amphibians (such as the *Hyla arborea* specimens from this study), are associated with enlargement of the liver (Densmore & Green 2007). Since NAG01 Perkinsea DNA was detected in only one of the two pooled samples (and no Perkinsea organisms were detected microscopically), it is possible that the UK specimens were infected with another unknown pathogen (which was affecting the observed symptoms), and a subset was cryptically infected with PPC.

4.4.3. Conservation implications

We recovered PPC DNA from *H. arborea* liver tissue exhibiting symptoms of SPI disease, derived from captive-bred tadpoles in Surrey, UK. The origin of infection for this particular pathology event is not traceable, as the *H. arborea* frogs were bred separately from any other amphibian. Potentally, the pathogen could have been introduced by tank water contamination from adult *H. arborea* frogs from a UK outlet (in 2018), or from another unidentified source. To the best of our knowledge, this is the first record of the putatively pathogenic lineage of NAG01 Perkinsea occurring in tadpoles in the UK, and indeed outside of North America. Chambouvet et al. (2015) recovered NAG01 Perkinsea DNA corresponding to the putatively nonpathogenic Clades A and B from one cryptically infected *Bufo bufo* (family Bufonidae) tadpole collected in London, UK and two cryptically infected *Rana temporaria* (family Ranidae) tadpoles collected in Kent, UK. Clade B was recovered from the *B. bufo* tadpole, and both Clades A and B were recovered from each of the *R. temporaria* tadpoles.

Our discovery of PPC in UK amphibian aquaculture leaves us with concerns regarding PPC transmission. Aquaculture disease outbreaks pose a threat to native species (Peeler et al. 2011), as captive-bred/farmed animals (and their pathogens) often spread from aquaculture to natural environments (Naylor et al. 2001). Pathogens can be unintentionally spread across a large scale when captive-bred (and

potentially infectious) amphibians are translocated for trade, food, stocking and commercial purposes; a phenomenon known as 'pathogen pollution' (Picco & Collins 2008, McKenzie & Peterson 2012). It has been hypothesized that pathogen transmission is accelerated in captive environments (e.g. aquaculture, captive survival assurance colonies) by high host density, which promotes the evolution of pathogen virulence (Ewald et al. 1994, Miller et al. 2011). Indeed, ranavirus strains isolated from captive bullfrogs (*R. catasbeiana*) have been shown to exhibit enhanced virulence compared to other ranaviruses when introduced into healthy hosts (Majji et al. 2006, Hoverman et al. 2011). Increased pathogen virulence poses a threat to amphibians in captivity, including those bred in survival assurance colonies (i.e. breeding groups maintained for the purpose of preventing extinction of critically endangered species) (Griffiths & Pavajeau 2008). Moreover, re-introducing captive-bred, infected amphibians can lead to the unwitting spread of disease in natural environments (Walker et al. 2008). This has alarming implications for amphibian conservation, as many amphibian species are currently suffering from catastrophic population decline (Stuart et al. 2004).

Central America is home to a large diversity of amphibian species, many of which are in decline (IUCN 2008). Panama has suffered recent loss of amphibian biodiversity due to chytridiomycosis (Lips et al. 2006), which has driven some species to near extinction or extinction the wild (e.g. *Atelopus* spp.) (Lewis et al. 2019). Many of these species now persist in local captive assurance colonies (Lewis et al. 2019). Our survey for NAG01 Perkinsea infection in Panama tadpoles did not yield evidence of SPI-associated disease or mortality. However, our detection of PPC DNA in a diverse group of amphibian hosts is cause for concern. PPC has been linked to tadpole morbidity and mass mortality (up to 95% of populations) in North America, as far south as Florida (Isidoro-Ayza et al. 2017). In light of the current imperilled state of Panama amphibians, and the threat that infectious disease outbreaks pose to captive assurance colonies (Griffiths & Pavajeau 2008), our findings encourage management strategies to consider routinely monitoring both wild and captive amphibian populations for this potential pathogen.

Chapter 5. Discussion

5.1. AETIOLOIGCAL ASPECTS OF PERKINSEA INFECTION AND SPI DISEASE IN AMPHIBIANS

In Chapter 2, we investigated the aetiology of SPI disease by addressing Koch's postulates (Koch 1884a) through experimental infections (direct injections and tank exposures) of *Rana dalmatina* tadpoles with Perkinsea cells recovered from *Lithobates sylvaticus* tadpoles. *Rana dalmatina* tadpoles that were experimentally infected with Perkinsea did not develop symptoms of SPI disease, nor did they experience an increase in mortality relative to the controls, despite the taxonomic similarity between the species from which the parasites were harvested (*L. sylvaticus*) and the species into which they were inoculated (*R. dalmatina*). The results of the PI stain indicated that the Perkinsea cells used for the infections were viable. Furthermore, the presence of NAG01 Perkinsea DNA, confirmed by our PCR screen, indicated that our infection methods (i.e. direct injections and tank exposures) were effective. However, the lack of detectable concomitant RNA amplification, confirmed by our RT-PCR screen, indicated that the Perkinsea were not ribosomally active, and therefore not actively infectious. Our experimental infection results do not necessarily mean that Perkinsea infection does not directly lead to SPI disease. As detailed in the Chapter 2 Discussion, it is possible that host incompatibility and/or a lack of infectivity in the hypnospore life stage (i.e. the stage used for infections) might have hindered disease progression; therefore, the relationship between NAG01 Perkinsea infection and SPI disease is still undetermined.

Future experimental infections should include using a different amphibian host and a different parasite life stage (i.e. trophozoite) ideally undergoing exponential growth. Of course, this necessitates first growing the parasite, which we have yet to do sustainably either in culture or in the presence of an amphibian host. Actively growing cells in culture could provide (suitable) material for use in experimental infections to address Koch's postulates for SPI disease. Successfully growing the parasite would also allow us to confirm our speculations about its life cycle, which is perceived to be similar to those of other *Perkinsus* spp. (Perkins 1966, 1988) based on its position in alveolate phylogeny as well as observations of both the hypnospore and trophozoite life stage in infected tadpole tissue.

Indeed, I made several attempts to grow the parasite prior to conducting the experimental infections; unfortunately, I was unable to induce growth during our trials. By providing details of these trials, we aim to provide guidelines for future culture attempts. Our culture attempts included using various types of growth media, ambient temperatures, antibiotic and antifungal treatments, and carbon sources and nutrient supplements. I used Perkinsea cells that had been harvested from the livers of four *Lithobates sphenocephalus* tadpoles (each representing a different site on the Kenai Peninsula Borough of Alaska) and stored in thioglycollate medium. I first attempted to grow the cells in DMEM/F-12 growth media. Aliquots of the thioglycollate-preserved cells were pelleted and washed 3x with fresh DMEM/F-12, and then transferred to 50 ml culture flasks containing 5-10 ml of fresh DMEM/F-12. Certain *Perkinsus* spp. (i.e. parasites of bivalves) have been shown to grow optimally in vitro at temperatures 20°C ≥ 28°C (Gauthier & Vasta 1995, Ordás & Figueras 1998). Therefore, the attempt to grow our cultures at 18°C and 25°C. At each temperature, they were kept stationary or at 140 rpm on a shaker incubator. We did not observe any growth or life cycle progression (i.e. hypnospores did not progress into trophozoites) in any of the conditions after 14 days. Some of our cultures became contaminated with bacteria and/or fungi, which we speculated might have had an inhibitory effect on the Perkinsea cells. I then attempted an experiment on a 96-well plate in which we added 50 µl of DMEM/F-12 containing Perkinsea cells to individual wells, followed by 50 µl of DMEM/F-12 containing either 0.02% penicillin (10,000 U/ml) or a combination of 0.02% penicillin + 0.004% µl Nystatin (25 mg/ml). Although the addition of the antibiotic and antifungal prevented the growth of contaminants, Perkinsea cell growth (or progression) was again absent.

We later attempted to grow the cells in ATCC medium: 1886 *Perkinsus* broth medium (substituting seawater with distilled water). This medium uses DMEM/F-12 as a base with additional nutrients, including JLP Carbohydrate Solution, Lipid Concentrate, and foetal bovine serum. Fresh aliquots containing Perkinsea cells from the thioglycollate tubes were pelleted and washed 3x with fresh ATCC medium, and then transferred to 50 ml culture flasks containing 5-10 ml of fresh medium and 0.005% PSN (i.e. an antibiotic mixture containing penicillin, streptomycin and neomycin) and 0.001% Nystatin (25 mg/ml). After this medium upgrade failed to induce cell growth (or progression), we tried to grow the cells in the OmniLog Phenotypic MicroArray

System (Biolog) using 96-well MicroPlates PM1 (carbon sources), PM2A (carbon sources), and PM5 (nutrient supplements). Aliquots containing 2,500 cells in 100 µl of ATCC medium were dispensed into the MicroPlates and incubated in the OmniLog for 7 days at room temperature. The OmniLog detects respiratory activity through a colour change (i.e. increased cell respiration corresponds with a reduction in a tetrazolium dye); unfortunately, this colour change was not observed in any of the MicroPlate wells.

We also attempted to grow the parasite in the presence of an amphibian host. Specifically, we attempted to trigger the transition from hypnospore to zoospore by incubating hypnospores in the presence of live *R. dalmatina* tadpoles. Our experimental setup was essentially a scaled-down version of our tank exposure experiment. We placed three tadpoles in individual wells on a 6-well cell culture plate. Each well contained approximately 2,250 Perkinsea cells/mL in ~15 mL of water. We microscopically observed the wells for changes in the hypnospores over the course of five days. We did not observe any changes in the hypnospores, which appeared to decline in number over the five days (most likely due to ingestion by the tadpoles). In order to avoid the loss of cells (due to ingestion), we repeated the experiment using clipped tail tissue from *R. dalmatina* tadpoles. Microscopic observations did not reveal any changes to the hypnospores. Like our experimental infections (i.e. tank exposures and direct injections), host incompatibility might have been a hindrance to these incubation experiments. Future research should include reattempting these experiments with another host species that is known to be susceptible to Perkinsea infection and SPI disease, such as one of the numerous *Lithobates* spp. that have been documented in North America (e.g. Isidoro-Ayza et al. 2017).

5.2. EPIDEMIOLOGICAL ASPECTS OF PERKINSEA INFECTION AND SPI DISEASE IN AMPHIBIANS

5.2.1. Transmission of Perkinsea and SPI disease between amphibian hosts

The transmission routes of SPI disease, and its (related) parasitic strategy, have yet to be determined. We speculate that amphibian Perkinsea likely utilise the direct transmission strategy shared by other Perkinsea species (e.g. *Perkinsus* spp.)

(Perkins 1966, 1988). This was addressed by our experimental infections with *R. dalmatina*. In a related experiment, we investigated the possibility that amphibian Perkinsea can also be trophically-transmitted between hosts through consumption of conspecifics (i.e. cannibalism). The experiment involved feeding (apparently) healthy *L. sphenocephalus* tadpoles with tissue from other *L. sphenocephalus* tadpoles that had been experimentally exposed to Perkinsea. This species is known to be susceptible to Perkinsea infection and SPI disease, as both have been reported in numerous populations of *L. sphenocephalus* in the USA (Davis et al. 2007, Isidoro-Ayza et al. 2017, Karwacki et al. 2018). The results of our molecular screen of tadpoles used in the cannibalism experiment indicate that a cryptic PPC infection pre-existed in a majority of tadpoles in every group, including the control groups. Consequently, we could not accurately assess if the consumption of infected liver tissue resulted in the transmission of Perkinsea to uninfected hosts.

Our experimental infections of *R. dalmatina* tadpoles led to an incidental finding that suggests exposure to Perkinsea alters the cannibalistic behaviour of tadpoles, which has consequences for transmission. We observed a decrease in the proportion of cannibalized tadpoles in groups that were exposed to Perkinsea cells compared to the control groups (Figure S2.1). This observation suggests that the tadpoles were refraining from consuming infected conspecifics. Trophically-transmitted parasites have been known to induce behavioural changes in their hosts that lead to an increase in (trophic) transmission (Lafferty 1999). For example, intermediate rat hosts infected by *Toxoplasma gondii*, lose their fear of cats (i.e. the definitive host of *T. gondii*) and become more to vulnerable to predation, which increases the chances that the parasite will complete its life cycle (Berdoy et al. 2000). Mosquito vectors infected by *Plasmodium falciparum* (i.e. the agent of malaria) alter their blood-seeking behaviour by increasing both the size of their blood meals and their number of feedings (among multiple humans), increasing the likelihood that the parasite will reach its definitive host (Koella et al. 1998).

The *T. gondii* and *P. falciparum* examples highlight a parasite's ability to alter host behaviour for its own benefit. Our experiment is a putative example of hosts changing their behaviour to protect themselves (i.e. to avoid infection by Perkinsea), which potentially changes the relative frequency uninfected tadpoles feed on infected tadpoles. Indeed, consumption of diseased conspecifics has been linked to increased

mortality in *Ambystoma tigrinum* larvae, which also exhibit a preference for (healthy) heterospecifics over conspecifics (Pfenning et al. 1998). The risk of pathogen transmission helps to explain why cannibalism is not more prevalent in nature (Elgar & Crespi 1992, Pfenning et al. 1998, Curtis 2014).

Future transmission experiments should reattempt our design with tadpoles reared from an egg mass, rather than collected at later developmental stages. Rearing tadpoles from an egg mass would help prevent them from being exposed to Perkinsea prior to experimentation (i.e. it would ensure that the controls are uncompromised). This was indeed the case for the *R. dalmatina* control tadpoles that were reared from an egg mass collected for our experimental infections in the Czech Republic (Table S2.6). Unfortunately, we were unable to locate an anuran egg mass in Central Florida for our cannibalism experiment.

5.2.2. Geographic and host range of amphibian Perkinsea and SPI disease

We further investigated the geographic and host range of amphibian Perkinsea (and SPI-associated disease) by screening tadpoles for NAG01 Perkinsea in Panama (a global centre of amphibian diversity) and the UK. We used SSU rRNA sequences to construct a phylogeny for NAG01 Perkinsea recovered from tadpoles in Panama and the UK, and mitochondrial rRNA phylogenetics to identify the tadpoles (Panama only) demonstrating a wider biogeographical provenance of this putative pathogenic association.

Our results reveal that PPC can be found at least as far south as Panama. The newly generated PPC sequences from Panama and the UK were identical or nearly identical to previously published PPC sequences from mortality events in the USA (Davis et al. 2007, Isidoro-Ayza et al. 2017). Our results also show that PPC's host range is broader than previously indicated. The PPC-positive samples in our study were all members of the superfamily Hyloidea, whereas the majority of the SPI-associated tadpole mortality events in North America have been reported in ranids (superfamily Ranoidea) (Green et al. 2002, Davis et al. 2007, Cook 2008, 2009, Landsberg et al. 2013, Chambouvet et al. 2015, Isidoro-Ayza et al. 2017, Karwacki et al. 2018). Furthermore, all 10 of the PPC-positive specimens from Panama appeared normal upon gross examination, suggesting that cryptic PPC infections are more

prevalent than previously indicated. This is further supported by the results of our Florida cannibalism experiment, which revealed a prevalence of pre-existing cryptic PPC infections in each experimental tadpole group.

Differences in host susceptibility to PPC infection might shape the distribution of SPI disease among amphibian populations. Indeed, the highest rates of *Bd*-associated mortality and decline are found among Neotropical Hyloidea and Brachycephaloidea species in Mesoamerica and South America (La Marca et al. 2005, Scheele et al. 2019). Our data suggest that Hyloidea species might be more tolerant of infection compared to Ranoidea species (i.e. infection is less likely to lead to disease in Hyloidea). This could help explain the prevalence of SPI disease in North America, which contains regions rich with ranid species. However, we would need to expand our global surveillance efforts to confirm that the disparity we observed is not simply a reflection of the larger ratio of hylids to ranids in Central America compared to North America, or more thorough amphibian survey efforts in North America.

Future epidemiological surveillance could incorporate the duplex qPCR assay that we designed to detect the two lineages of amphibian Perkinsea (i.e. PPC, the putatively pathogenic lineage, and NAG01a-c, the putatively non-pathogenic lineage). Indeed, a novel multiplex qPCR assay specific for amphibian pathogens (i.e. *Bd*, *Bsal*, and FV3) has been successfully applied to field samples throughout a range of habitats in Wisconsin, USA (Standish et al. 2018). Chapter 3 focused on the development of our duplex qPCR assay, which is both specific and sensitive in its rapid and simultaneous detection of the two Perkinsea lineages. The assay has also been validated in uniplex conditions, which can provide accurate measurements of the amount of lineage-specific Perkinsea DNA per sample. The assay has been validated on a mobile qPCR device, the *Biomeme two3*, therefore it can be taken directly into the field for analysis. This mobility is particularly helpful for surveying amphibians in remote areas where access to laboratory facilities is limited. Expanding our surveillance efforts with our novel duplex qPCR assay would allow us to gain information about the geographic and host range of PPC and SPI disease, and also provide insight in the infection dynamics of the two lineages.

5.2.3. Study on intestinal eukaryotic microbiomes of healthy and Perkinsea-infected tadpoles

The prevalence of cryptic PPC infections that we found in our Florida cannibalism experiment and our survey of Panama tadpoles undermines the first of Koch's postulates: that the microbe must be present in every case of the disease, but not in the absence of disease. It indicates that PPC is most likely a commensal microorganism, present in an abundance of amphibian hosts, which only becomes pathogenic under certain conditions. SPI disease might only develop in association with other factors that increase host stress (and reduce host immunity - e.g. exposure to pollution, food deprivation, co-infections). We investigated a possible micro-ecological link between amphibian Perkinsea infection and the intestinal eukaryotic microbiome of tadpoles using amplicon-based metagenomics, comparing the composition of these microbiomes between infected and healthy individuals.

- Sample collection and DNA extraction

We used gut tissue harvested from some of the same tadpoles collected for our Panama and UK phylogeny analysis and for our Florida cannibalism experiment. Fieldwork was carried out in Panama in November 2018. Tadpoles were captured from seven sites in Panama in November 2018 (Table S5.1). They were transported to the Gamboa Amphibian Research and Conservation Center where they were euthanized using an overdose of MS-222 and dissected. The liver and gut tissues were stored in LifeGuard™ preservation solution (Qiagen) at -20°C for 1-2 weeks. They were later transported to the University of Exeter in an insulated medical cooler and transferred to -80°C prior to DNA extraction.

Tadpoles were captured from six sites in Florida in March 2019 (Table S5.1). Tadpoles were euthanized and dissected at the University of Central Florida, and their liver and gut tissues were stored in LifeGuard™ preservation solution at -80°C. These samples were transferred to the University of Exeter in May 2019 and stored at -80°C prior to DNA extraction.

Hyla arborea tadpoles from a pathology event in Surrey, UK were collected in July and October 2019 (Table S5.1) and stored whole in LifeGuard™ preservation solution. They were delivered to the University of Exeter and stored at -80°C prior to dissection and isolation of the liver and gut tissues.

Total DNA was extracted from the gut tissues of 48 tadpoles in total: 21 from Panama, 23 from Florida, and 4 from the UK. Extractions were carried out using the DNeasy Blood and Tissue Kit (Qiagen) according to the manufacturer's protocol with an overnight lysis step at 37°C, followed by one minute of disruption with 425-600 µm acid-washed glass beads (Sigma-Aldrich) on a *FastPrep-24* tissue homogenizer (MP Biomedicals).

- 18S rDNA amplification of eukaryotic microbes in tadpole guts

A portion of the 18S rRNA gene was amplified from the tadpole gut tissue using a eukaryote-specific forward primer and a eukaryote-specific reverse primer that is biased against Metazoa (Table 5.1). This primer pair targets the hypervariable V4 region of the gene but does not amplify host (metazoan) DNA. Universal molecular identifiers (UMIs) that were 8, 10 or 12-nt in length were added to the 5' end of the primers, as were 33-nt pads (Table 5.2). The reaction mixture included 1x concentration PCR MasterMix (Promega), 500 nM of each primer, 1 µl of template DNA, and molecular-grade water to bring the total reaction volume to 25 µl. Each PCR included a negative control (molecular-grade H2O) and a positive control (DNA from PPC-infected Alaskan *L. sylvaticus* tadpole liver). Cycling conditions were as follows: 2 min at 95°C, followed by 35 cycles of 30 s at 95°C, 30 s at 56°C, and 60 s at 72°C, with an additional 10-min extension at 72°C. PCRs were triplicated using combinations of primers that differed in the lengths of their UMIs (Table 5.2).

PCR amplification was evaluated through the discernment of a ~700 bp fragment on a 1.5% agarose gel. Amplification was successful across the three PCRs in 15/23 Florida samples and 4/4 UK samples. Surprisingly, none of the Panama samples successfully amplified across all three PCRs. Only the PCR that combined primers 528F1 and 18S-EUK-1134-R3 yielded any amplification (5/21 samples). This could be due to the smaller amount of gut tissue used in the DNA extractions, as the Panama specimens were typically of smaller size compared to the Florida and UK specimens. Only successful triplicates were used for library preparation, which included 19 experimental samples (Table S5.1) and one negative.

Table 5.1. Primers used in this study

Primer	Sequence (5' - 3')	Specificity	Reference
300F-B	GGG CTT CAY AGT CTT GCA AT	wider NAG01 group	Chambouvet et al. (2015)
NAG01R_1	GCC TGC TTG AAA CRC TCT AA	wider NAG01 group	This study
528F	CGG TAA TTC CAG CTC C	eukaryotes	Elwood et al. (1985)
18S-EUK-1134-R	TTT AAG TTT CAG CCT TGC G	non-metazoan eukaryotes	Bower et al. (2004)
MCP-F	TAC TTT GTC AAG GAG CAY TAC T	ranavirus	This study
MCP-R	TCA TGT TAT AGT AGC CTR TGC	ranavirus	This study

Table 5.2. Adaptations to the 18S non-metazoan primers used in this study. The number of asterisks correspond to the primer pairs.

Primer	Sequence (5' - 3')
528F1*	TCGTCGGCAGCGTCAGATGTGTATAAGAGACAGNNNNNNNNNCGGTAATTCCAGCTCC
528F2**	TCGTCGGCAGCGTCAGATGTGTATAAGAGACAGNNNNNNNNNNNCGGTAATTCCAGCTCC
528F3***	TCGTCGGCAGCGTCAGATGTGTATAAGAGACAGNNNNNNNNNNNNNCGGTAATTCCAGCTCC
18S-EUK-1134-R1***	GTCTCGTGGGCTCGGAGATGTGTATAAGAGACAGNNNNNNNNTTTAAGTTTCAGCCTTGCG
18S-EUK-1134-R2**	GTCTCGTGGGCTCGGAGATGTGTATAAGAGACAGNNNNNNNNNNTTTAAGTTTCAGCCTTGCG
18S-EUK-1134-R3*	GTCTCGTGGGCTCGGAGATGTGTATAAGAGACAGNNNNNNNNNNNNTTTAAGTTTCAGCCTTGCG

- NAG01 Perkinsea molecular screening of tadpole livers

Total DNA was extracted from the liver tissue of the 19 specimens used for profiling intestinal eukaryotic microbes (Table S5.1) using the same method that was applied to the gut tissue. Extractions were screened for NAG01 Perkinsea DNA using primers that target a fragment of the 18S rDNA encoding gene (Table 5.1). The fragment is 290 bp long in PPC (i.e. the putatively pathogenic lineage) and ~287 bp long in NAG01a-c (i.e. the putatively non-pathogenic lineage). This fragment includes a ~113-116 bp variant region that can be used to distinguish PPC from NAG01a-c. The reaction mixture included 1x concentration PCR MasterMix (Promega), 500 nM of each primer, 1 µl of template DNA, and molecular-grade water to bring the total reaction volume to 25 µl. Each PCR included a negative control (molecular-grade H2O) and 1 µl of template DNA from a positive control (DNA from PPC-infected Alaskan *L. sylvaticus* tadpole liver). Cycling conditions were as follows: 2 min at 95°C, followed by 35 cycles of 30 s at 95°C, 30 s at 56°C, and 60 s at 72°C, with an additional 10-min extension at 72°C. PCR products were checked on a 2% agarose gel, revealing a band of the correct size in 6/19 specimens (Table S5.1). These samples were confirmed positive for PPC by TA-cloning and Sanger sequencing the PCR

products, or by running the samples with our novel PPC-specific (uniplex) qPCR assay (Table S5.1).

- Ranavirus molecular screening of tadpole guts

All the gut tissue extractions were tested for the presence of ranavirus by PCR. A primer pair was designed to target a 358 bp sequence of the major capsid protein (MCP) encoding gene (Table 5.1). In order to obtain template DNA for a positive control, this sequence was synthesized into a plasmid vector (pUC57-Amp) by Synbio Technologies. The reaction mixture included 1x concentration PCR MasterMix (Promega), 500 nM of each primer, 1 µl of template DNA, and molecular-grade water to bring the total reaction volume to 25 µl. The reaction included a negative control (molecular-grade H2O) and 1 ng of plasmid DNA as a positive control. Cycling conditions were as follows: 2 min at 95°C, followed by 35 cycles of 30 s at 95°C, 30 s at 56°C, and 60 s at 72°C, with an additional 10-min extension at 72°C.

PCR products were checked on a 2% agarose gel, which did not reveal (MCP-specific) amplification in any of the samples. The gel revealed a strong band of the correct size in the positive control (1 ng of plasmid DNA containing MCP sequence), indicating that the assay was functional.

- Library preparation and sequencing of 18S rDNA amplicons from tadpole guts

The non-metazoan 18S rDNA PCR products were purified using the Wizard PCR Clean-up System (Promega). The purified PCR products had dual sequencing indices attached using the Nextera XT Index Kit v2 (Illumina). The reaction mixture included 1x NEBNext PCR reaction mix (New England Biolabs), 2.5 µl of each index, 3 µl of template DNA, and molecular-grade water to bring the total reaction volume to 25 µl. The 3 µl of template DNA was a combination of 1 µl from each of the PCR triplicates. A unique pair of indices was attached to the 5’ and 3’ ends of each combined sample. Molecular-grade water was used as a negative control for the reaction. Cycling conditions were as follows: 3 min at 95°C, followed by 15 cycles of 30 s at 95°C, 30 s at 55°C, and 30 s at 72°C, with an additional 5-min extension at 72°C.

The PCR products were purified using the Wizard PCR Clean-up System (Promega) and quantified on a Qubit. An aliquot of 10 ng was taken from each sample and pooled. Quality analysis of the pooled samples was carried out on an Agilent 2200 Tapestation, which revealed a strong ~700 bp fragment (target amplicon) and a much fainter 200 bp fragment (primer dimers). In order to remove the primer dimers, the pool was cleaned using Agencourt AMPure XP beads (Beckman Coulter) with a ratio of beads to PCR product volume of 0.6. It was reanalysed on the Tapestation prior to sequencing. Sequencing was performed on an Illumina MiSeq at the Exeter Sequencing Service.

Sequences were demultiplexed into 20 sample files (19 experimental samples and one negative). Demultiplexed reads were adapter and quality-trimmed with a quality score of ≥ 20 and a minimum read length of 50 nt using TrimGalore! (version 0.6.5) (Krueger 2015). The 33-nt pads were trimmed using Cutadapt (version 1.1.5) (Martin 2011). A script was developed to sort the reads from each PCR replicate into three separate files based on the length of their UMIs whilst simultaneously trimming the UMIs from the reads. The script was implemented using MATLAB R2019b software. Cutadapt was then used to trim the primers and remove all remaining reads less than 200 nt.

Sequences were then processed using the pipeline for single-read big data in DADA2 (version 1.14) (Callahan et al. 2016). The pipeline was implemented in RStudio (version 1.2.5033). Amplicon sequence variants (ASVs) in the experimental samples were checked for contaminants based on the ASVs in the negative controls using decontam (version 1.6) (Davis et al. 2018). ASVs were aligned to the SILVA 18S database (version 132) and the pr2 18S database (version 4.12) and assigned to broad taxonomic ranks. Using ggplot2 (Wickham 2016) in RStudio, alignment files were used to create box plots (Figures 5.1 & 5.3) and stacked bar charts (Figure 5.2 & 4) depicting the taxon-based distribution of ASVs across samples.

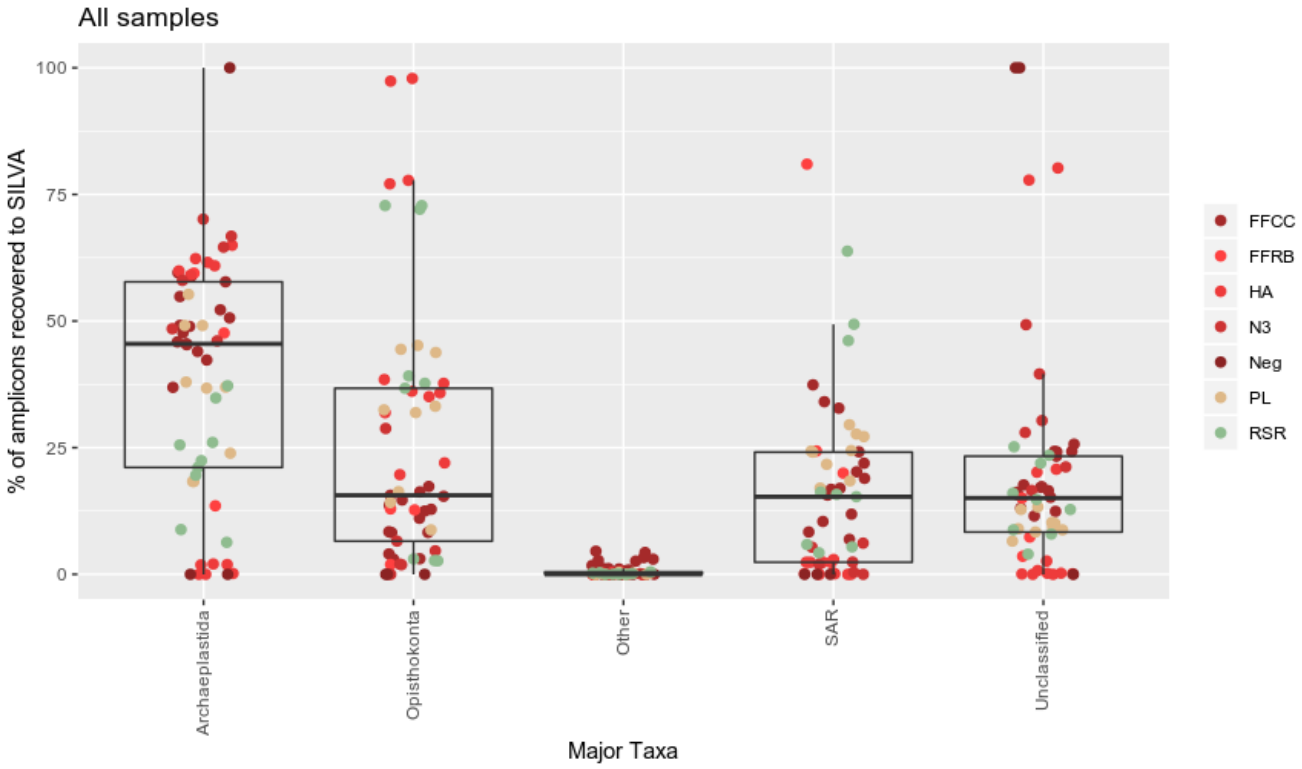

Figure 5.1. Taxon-based distribution of ASVs recovered from the intestinal eukaryotic microbiomes of tadpoles and aligned to the SILVA database.

Samples and their replicates were grouped according to the site from which they were collected (i.e. FFCC, FFRB, HA, N3, PL, RSR). SAR represents “Stramenopiles, Alveolata, Rhizaria”. “Other” includes ASVs with assignments outside the specified taxonomies. “Unclassified” includes ASVs with no identifiable taxonomy.

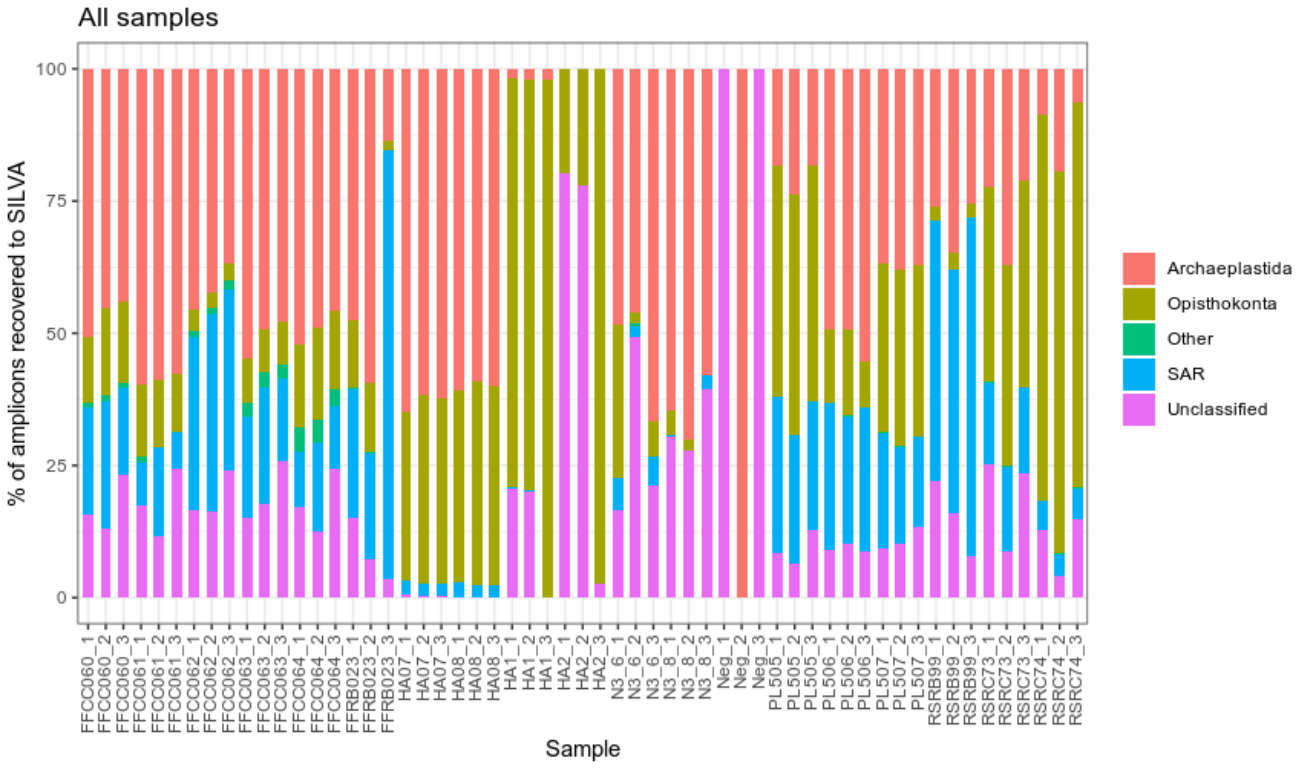

Figure 5.2. Taxon-based distribution of ASVs recovered from the intestinal eukaryotic microbiomes of tadpoles and aligned to the SILVA database. SAR represents "Stramenopiles, Alveolata, Rhizaria". "Other" includes ASVs with assignments outside the specified taxonomies. "Unclassified" includes ASVs with no identifiable taxonomy.

.

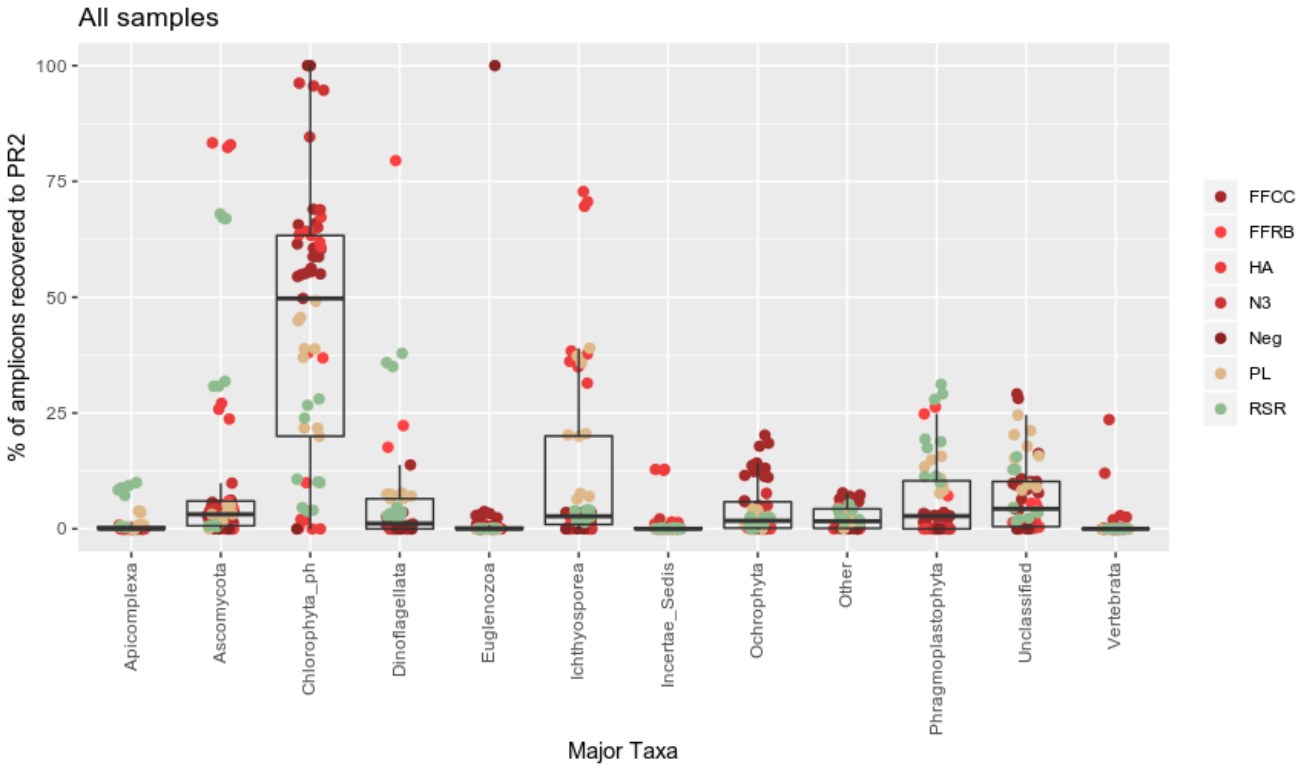

Figure 5.3. Taxon-based distribution of ASVs recovered from the intestinal eukaryotic microbiomes of tadpoles and aligned to the PR2 database. Samples and their replicates were grouped according to the site from which they were collected (i.e. FFCC, FFRB, HA, N3, PL, RSR). "Other" includes ASVs with assignments outside the specified taxonomies. "Unclassified" includes ASVs with no identifiable taxonomy.

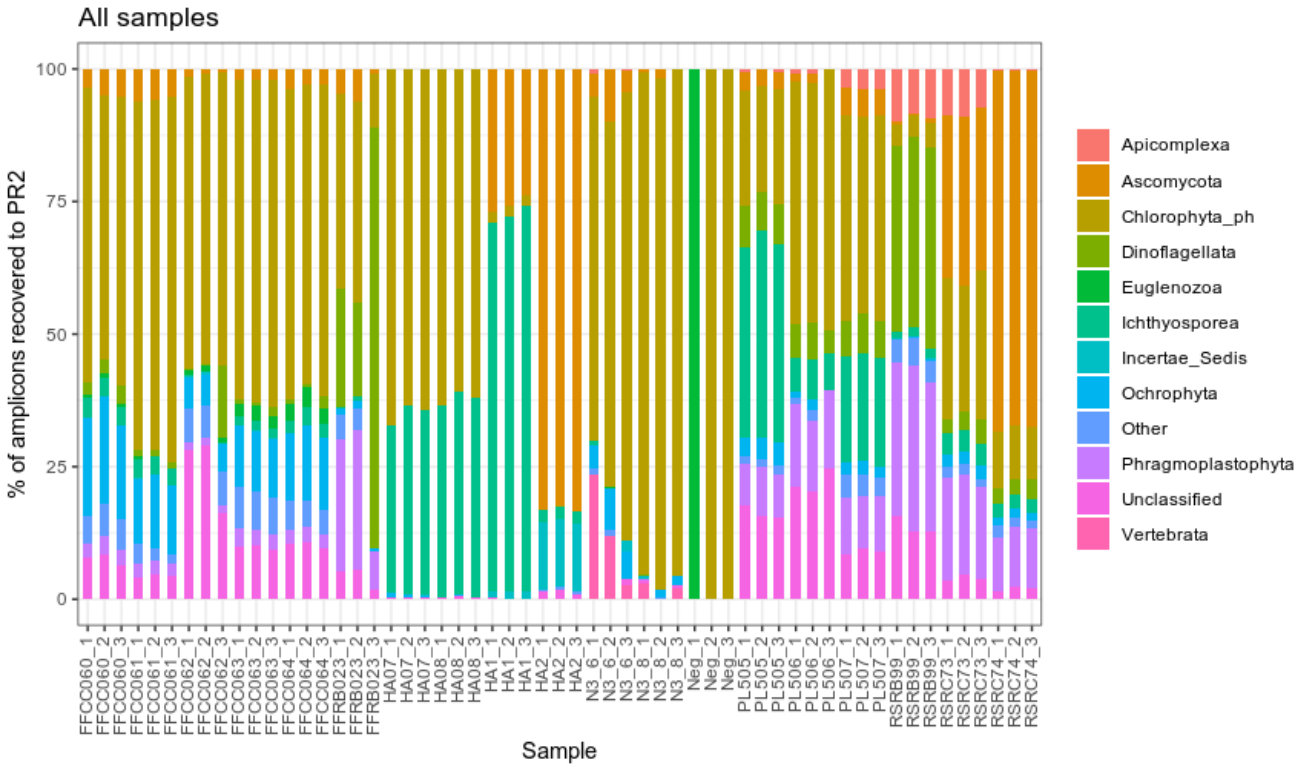

Figure 5.4. Taxon-based distribution of ASVs recovered from the intestinal eukaryotic microbiomes of tadpoles and aligned to the PR2 database. “Other” includes ASVs with assignments outside the specified taxonomies. “Unclassified” includes ASVs with no identifiable taxonomy.

- Comparison of the intestinal eukaryotic microbiomes between healthy and Perkinsea-infected tadpoles

Based on the results of our ASV alignments to the SILVA and PR2 databases (Figures 5.1-4), there do not appear to be any (consistent) compositional differences in the intestinal eukaryotic microbiomes between healthy and Perkinsea-infected tadpoles (at least at the broad taxonomic ranks that were investigated). Two of the samples that were confirmed positive for Perkinsea based on qPCR detection of PPC DNA in liver tissue (i.e. RSRB099 & RSRC073) had higher percentages of ASVs assigned to SAR and Apicomplexa compared to the rest of the samples. Since Perkinsea are alveolates (close relatives of Apicomplexa), these results suggest that Perkinsea organisms might have infected both the liver and gut tissue in these tadpoles and/or the tadpoles might have consumed Perkinsea cells.

The most obvious compositional differences among the tadpole intestinal eukaryotic microbiomes appear to be location-based (i.e. UK vs. Florida), which is especially clear in the stacked bar charts (Figures 5.2 & 5.4). We note that the UK samples (i.e. those beginning with "HA") were captive-bred, whereas the Florida samples were collected from the wild. These drastically different environments almost certainly would have affected the tadpoles' diet and overall exposure to microbes, which is reflected in our results. The UK samples have high percentages of ASVs assigned to Ascomycota and/or Ichthyosporea (Figure 5.4), which respectively include many known fungal and protistan pathogens of animals, including amphibians (Berbee 2001, Rowley et al. 2013). Interestingly, the UK samples all exhibited signs of SPI disease upon gross examination of their livers, including enlargement and yellow discoloration (although only HA1 and HA2 were positive for PPC DNA in liver tissue). We cannot fully resolve any links between Perkinsea infection and other potential pathogens without first classifying our ASVs to lower taxonomic ranks.

Classifying ASVs to lower taxonomic ranks would require more sequence information (i.e. larger amplicons) for database alignments. This could be achieved using long-read sequencing technology such as Oxford Nanopore. Indeed, we attempted to sequence our amplicons on a Flongle flow cell using a MinION (Oxford Nanopore); unfortunately, the Nextera indexes (Illumina) were distorted during the process and we were therefore unable to demultiplex the samples based on their unique identifiers. It is possible that the shorter length of the Nextera identifiers (i.e. 8 nt) relative to Nanopore-recommended identifiers (i.e. 12 nt) might have contributed to this problem, and future experiments should be cautioned against transferring oligos across platforms. Successfully obtaining long-read sequences could potentially allow us to classify ASVs to genus or species-level. With this amount of detail, we could confidently resolve any potential associations between Perkinsea infection and intestinal microbes in amphibians.

5.3. THESIS RECOMMENDATIONS WITH A VIEW TO CONSERVATION

This thesis aims to gain insight into aetiological and epidemiological aspects of Perkinsea infection and SPI disease in amphibians, and provide directions for future research in the field. The aims were addressed in the objectives of the three data

chapters and a study incorporated in the general Discussion that was intended to be a separate data chapter, but could not be brought to completion due to experimental complexities. In summary, we investigated the aetiology and transmission of SPI disease by addressing Koch's postulates through experimental infections of healthy tadpoles with Perkinsea cells, and with a feeding experiment in which healthy tadpoles were fed liver tissue from other tadpoles that had been experimentally exposed to Perkinsea cells. We further explored the biogeographical range of amphibian Perkinsea using using phylogenetic analyses. Finally, we used amplicon-based metagenomics to assess gut microbiome composition as a potential co-factor for Perkinsea infection in amphibians. Based on the outcomes of our experiments, we offer the following recommendations with a view to conservation:

- Cryptic Perkinsea infection (specifically, PPC) was prevalent among many of our tadpole specimens, which suggests that PPC is most likely a commensal microorganism that only becomes pathogenic under certain conditions. It is important to identify conditions (e.g. exposure to pollution, food deprivation, co-infections) that might increase PPC pathogenicity and/or reduce host immunity. PPC infection and SPI disease should be managed with strategies that focus on reducing the impact of these conditions. For example, amphibian health surveys could be combined with water quality assessments (e.g. measuring levels of ultraviolet radiation, nutrients, and pollutants) to expose possible correlations between disease prevalence and certain environmental conditions.

- Cannibalism was reduced among tadpoles exposed to Perkinsea in our experimental infections, suggesting that Perkinsea transmission might act as a selective force against the consumption of conspecifics. Therefore, efforts to control Perkinsea transmission should focus on maintaining healthy habitats with plentiful resources to prevent conditions (e.g. depletion of food sources) that increase rates of cannibalism in tadpoles.

- It is unclear what effect mixed Perkinsea infections (i.e. infection with both PPC and NAG01a-c) might have on pathogenicity, nor is it clear how frequently these

co-infections occur. Enhanced surveillance methods are needed to assess the prevalence of co-infection and provide a better overall understanding of host-pathogen dynamics. The duplex qPCR assay reported in Chapter 3 can be used to assess the prevalence of co-infection and provide a better understanding of these dynamics, which could be used to inform management strategies and possibly prevent disease outbreaks.

- Pathogenic Perkinsea have the capacity for widespread transmission among amphibians in not only wild but also captive-bred populations, as evidenced by our discovery of PPC in UK amphibian aquaculture. Increased surveillance efforts are needed to fully expose the extent of amphibian Perkinsea's geographic and host range (in both wild and captive-bred amphibian populations). Again, our duplex qPCR assay can be an effective tool for such efforts, especially if implemented with field-compatible qPCR equipment.

- We detected cryptic PPC infection in a broad taxonomic range of Panama tadpoles. Our findings encourage wildlife management strategies in Panama to incorporate routine monitoring for PPC in both wild and captive amphibian populations, considering the current imperilled state of Panama amphibians and the threat that infectious disease outbreaks pose to the country's captive assurance colonies.

Appendix

Chapter 2. Experimental infections of ranid tadpoles with putatively pathogenic amphibian Perkinsea

Table S2.1. Specimen data for tadpoles from which Perkinsea parasites were harvested and used for the experimental infections of *Rana dalmatina.*

Sample ID	Location	Region	Site	Collection date	Species	Gosner stage	Health
KNA03_01	AK, USA	Kenai	KNA03	03/07/2016	*Lithobates sylvaticus*	41	symptomatic
KNA03_02	AK, USA	Kenai	KNA03	03/07/2016	*L. sylvaticus*	41	symptomatic
KNA03_03	AK, USA	Kenai	KNA03	03/07/2016	*L. sylvaticus*	38	symptomatic
KNA03_04	AK, USA	Kenai	KNA03	03/07/2016	*L. sylvaticus*	38	symptomatic
KNA14_05	AK, USA	Kenai	KNA14	02/07/2016	*L. sylvaticus*	39	unknown
KNA21_01	AK, USA	Kenai	KNA21	08/06/2016	*L. sylvaticus*	25	symptomatic
KNA21_02	AK, USA	Kenai	KNA21	08/06/2016	*L. sylvaticus*	25	symptomatic
KNA21_03	AK, USA	Kenai	KNA21	08/06/2016	*L. sylvaticus*	25	symptomatic
KNA21_04	AK, USA	Kenai	KNA21	08/06/2016	*L. sylvaticus*	25	symptomatic
KNA21_05	AK, USA	Kenai	KNA21	08/06/2016	*L. sylvaticus*	25	normal
KNA21_06	AK, USA	Kenai	KNA21	08/06/2016	*L. sylvaticus*	25	normal
KNA21_07	AK, USA	Kenai	KNA21	08/06/2016	*L. sylvaticus*	25	normal
KNA21_08	AK, USA	Kenai	KNA21	08/06/2016	*L. sylvaticus*	25	normal
KNA21_09	AK, USA	Kenai	KNA21	08/06/2016	*L. sylvaticus*	25	normal

Table S2.2. Tally of tadpoles collected and euthanized for microscopic examinations during the monitoring period following the experimental infections of *Rana dalmatina* tadpoles with Perkinsea. The proportion of survivorship per treatment (depicted in Figure 2.3) was calculated by first subtracting the total number of tadpoles collected before the end of the monitoring period (i.e. Tc) from the total at the start of the monitoring period (i.e. Ts). This value (i.e. Ts - Tc) was then used to divide the total number of tadpoles remaining at the end of the monitoring period (i.e. Te).

Collection day	Control injection	KNA03 injection	Control exposure	KNA03 tank exposure	KNA14 tank exposure	KNA14x3 tank exposure	KNA14x6 tank exposure	KNA21 tank exposure
D1			2	2				2
D2			2	2				2
D4			2	2				2
D7			2	2	2	2	2	2
D11		1	1	1				1
D15		2	2	2	2	2	2	2
D19	3	3	2	2	2	2	2	2
D25		2	2	2	2	2	2	2
D32		20		20				20
D40	7		6					
Total at start (Ts)	43	43	60	60	60	60	60	60
Total collected before end (Tc)	10	28	21	35	8	8	8	35
Total at end (Te)	12	12	2	12	28	27	27	17
Ts - Tc	33	15	39	25	52	52	52	25
Proportion of survivorship (i.e. Te/(Ts - Tc))	0.363636364	0.8	0.051282051	0.48	0.538461538	0.519230769	0.519230769	0.68

Table S2.3. Specimen data and molecular screening results for tadpoles from which livers were harvested and used to feed *Lithobates sphenocephalus* tadpoles. Prior to the harvesting of their livers, a subset of tadpoles was exposed to Perkinsea cells (GroupA_infected), and a second subset was not exposed (GroupA_control). Swabs were taken from each liver, and total DNA was extracted and screened using a PPC-specific qPCR and a NAG01a-d-specific PCR. Cq values and gel electrophoresis results are shown.

Sample ID	Location	Region	Site	Collection date	Species	Health	Treatment	PPC qPCR	NAG01a-d PCR
FB04	FL, USA	Central	UCF	19/04/2019	*Lithobates sphenocephalus*	normal	GroupA_control	32.28	positive
FB05	FL, USA	Central	UCF	19/04/2019	*L. sphenocephalus*	normal	GroupA_control	33.36	positive
FB06	FL, USA	Central	UCF	19/04/2019	*L. sphenocephalus*	normal	GroupA_infected	31.79	positive
FB07	FL, USA	Central	UCF	19/04/2019	*L. sphenocephalus*	normal	GroupA_control	32.52	positive
FB08	FL, USA	Central	UCF	19/04/2019	*L. sphenocephalus*	normal	GroupA_control	31.12	negative
FB09	FL, USA	Central	UCF	19/04/2019	*L. sphenocephalus*	normal	GroupA_control	33.16	positive
FB10	FL, USA	Central	UCF	19/04/2019	*L. sphenocephalus*	normal	GroupA_infected	30.74	negative
FB11	FL, USA	Central	UCF	19/04/2019	*L. sphenocephalus*	normal	GroupA_infected	32.75	positive
FB12	FL, USA	Central	UCF	19/04/2019	*L. sphenocephalus*	normal	GroupA_infected	35.52	negative
FB13	FL, USA	Central	UCF	19/04/2019	*L. sphenocephalus*	normal	GroupA_infected	32.82	positive
FB14	FL, USA	Central	UCF	19/04/2019	*L. sphenocephalus*	normal	GroupA_infected	33.48	positive
FB16	FL, USA	Central	UCF	19/04/2019	*L. sphenocephalus*	normal	GroupA_control	34.38	positive

Table S2.4. Specimen data for tadpoles that were collected as subjects for the cannibalism feeding experiment.

Sample ID	Location	Region	Site	Collection date	Species	Gosner stage	Health
CE01	FL, USA	Central	UCF	29/04/2019	*Lithobates sphenocephalus*	35	normal
CE02	FL, USA	Central	UCF	29/04/2019	*L. sphenocephalus*	25	normal
CE03	FL, USA	Central	UCF	29/04/2019	*L. sphenocephalus*	35	normal
CE04	FL, USA	Central	UCF	29/04/2019	*L. sphenocephalus*	35	normal
CE05	FL, USA	Central	UCF	29/04/2019	*L. sphenocephalus*	30	normal
CE06	FL, USA	Central	UCF	29/04/2019	*L. sphenocephalus*	35	normal
CE07	FL, USA	Central	UCF	29/04/2019	*L. sphenocephalus*	25	normal
CE08	FL, USA	Central	UCF	29/04/2019	*L. sphenocephalus*	35	normal
CE09	FL, USA	Central	UCF	29/04/2019	*L. sphenocephalus*	35	normal
CE10	FL, USA	Central	UCF	29/04/2019	*L. sphenocephalus*	25	normal
CE11	FL, USA	Central	UCF	29/04/2019	*L. sphenocephalus*	35	normal
CE12	FL, USA	Central	UCF	29/04/2019	*L. sphenocephalus*	35	normal
CE13	FL, USA	Central	UCF	29/04/2019	*L. sphenocephalus*	35	normal
CE14	FL, USA	Central	UCF	29/04/2019	*L. sphenocephalus*	30	normal
CE15	FL, USA	Central	UCF	29/04/2019	*L. sphenocephalus*	35	normal
CE16	FL, USA	Central	UCF	29/04/2019	*L. sphenocephalus*	25	normal
CE17	FL, USA	Central	UCF	29/04/2019	*L. sphenocephalus*	25	normal
CE18	FL, USA	Central	UCF	29/04/2019	*L. sphenocephalus*	25	normal
CE19	FL, USA	Central	UCF	29/04/2019	*L. sphenocephalus*	25	normal
CE20	FL, USA	Central	UCF	29/04/2019	*L. sphenocephalus*	25	normal
CE21	FL, USA	Central	UCF	29/04/2019	*L. sphenocephalus*	35	normal
CE22	FL, USA	Central	UCF	29/04/2019	*L. sphenocephalus*	25	normal
CE23	FL, USA	Central	UCF	29/04/2019	*L. sphenocephalus*	35	normal
CE24	FL, USA	Central	UCF	29/04/2019	*L. sphenocephalus*	35	normal
CE25	FL, USA	Central	UCF	29/04/2019	*L. sphenocephalus*	25	normal
CE26	FL, USA	Central	UCF	29/04/2019	*L. sphenocephalus*	35	normal

CE27	FL, USA	Central	UCF	29/04/2019	*L. sphenocephalus*	30	normal
CE28	FL, USA	Central	UCF	29/04/2019	*L. sphenocephalus*	30	normal
CE29	FL, USA	Central	UCF	29/04/2019	*L. sphenocephalus*	25	normal
CE30	FL, USA	Central	UCF	29/04/2019	*L. sphenocephalus*	25	normal
CE31	FL, USA	Central	UCF	29/04/2019	*L. sphenocephalus*	25	normal
CE32	FL, USA	Central	UCF	29/04/2019	*L. sphenocephalus*	25	normal
CE33	FL, USA	Central	UCF	29/04/2019	*L. sphenocephalus*	30	normal
CE34	FL, USA	Central	UCF	29/04/2019	*L. sphenocephalus*	25	normal
CE35	FL, USA	Central	UCF	29/04/2019	*L. sphenocephalus*	25	normal
CE36	FL, USA	Central	UCF	29/04/2019	*L. sphenocephalus*	25	normal
CE37	FL, USA	Central	UCF	29/04/2019	*L. sphenocephalus*	25	normal
CE38	FL, USA	Central	UCF	29/04/2019	*L. sphenocephalus*	25	normal
CE39	FL, USA	Central	UCF	29/04/2019	*L. sphenocephalus*	25	normal
CE40	FL, USA	Central	UCF	29/04/2019	*L. sphenocephalus*	25	normal

Table S2.5. Molecular screening results of the *Lithobates sphenocephalus* cannibalism feeding experiment per tadpole, organized by treatment. GroupB_infected was fed with liver tissue from tadpoles that were deliberately exposed to Perkinsea cells and GroupB_control1 was fed with liver tissue from tadpoles that were not deliberately exposed (see Table S2.2). GroupB_control2 was fed only with algae wafers. Total DNA was extracted from liver (GroupA = swabs, all others = tissue) and tail clips and screened using a PPC-specific qPCR and a NAG01a-d-specific PCR (excluding those processed at UCF). Cq values and gel electrophoresis results are shown.

Sample ID	Treatment	Stage at start	Stage at end	PPC qPCR (liver)	NAG01a-d PCR (liver)	PPC qPCR (tail)	NAG01a-d PCR (tail)	Processed at:
CE01	GroupB_infected	35	metamorph	35.08	Positive	37.04	positive	Exe
CE03	GroupB_infected	35	35	33.19	NA	39.36	positive	UCF
CE05	GroupB_infected	30	30	33.85	NA	35.34	positive	UCF
CE07	GroupB_infected	25	metamorph	negative	NA	38.59	positive	UCF
CE09	GroupB_infected	35	30	37.44	Positive	39.92	negative	Exe
CE12	GroupB_infected	35	metamorph	37.36	Positive	38.96	negative	Exe
CE15	GroupB_infected	35	25	negative	NA	33.77	negative	UCF
CE18	GroupB_infected	25	metamorph	34.19	NA	36.14	positive	UCF
CE20	GroupB_infected	25	30	35.07	Positive	35.44	positive	Exe
CE23	GroupB_infected	35	25	34.55	Positive	36.29	positive	Exe
CE25	GroupB_infected	25	metamorph	28.5	Positive	34.99	negative	Exe
CE27	GroupB_infected	30	metamorph	33.08	NA	33.22	positive	UCF
CE30	GroupB_infected	25	35	33.42	Positive	33.64	positive	Exe
CE33	GroupB_infected	30	30	34.8	NA	32.25	positive	UCF
CE34	GroupB_infected	25	metamorph	37.27	Positive	29.17	negative	Exe
CE39	GroupB_infected	25	25	34.15	NA	36.29	positive	UCF
CE02	GroupB_control1	25	metamorph	33.94	NA	35.37	positive	UCF
CE06	GroupB_control1	35	metamorph	negative	NA	36.72	positive	UCF

CE10	GroupB_control1	25	30	32.81	NA	34.94	positive	UCF
CE13	GroupB_control1	35	metamorph	34.77	Negative	34.8	negative	Exe
CE16	GroupB_control1	25	25	negative	NA	37.5	positive	UCF
CE19	GroupB_control1	25	metamorph	35.55	NA	36.37	positive	UCF
CE22	GroupB_control1	25	25	29.14	Positive	34.26	positive	Exe
CE24	GroupB_control1	35	25	negative	NA	36.05	positive	UCF
CE28	GroupB_control1	30	metamorph	negative	NA	31.02	positive	UCF
CE31	GroupB_control1	25	metamorph	31.95	Positive	32.32	positive	Exe
CE36	GroupB_control1	25	metamorph	negative	NA	34.42	positive	UCF
CE37	GroupB_control1	25	25	35.57	Negative	32.47	positive	Exe
CE38	GroupB_control1	25	metamorph	35.1	Positive	29.79	positive	Exe
CE40	GroupB_control1	25	30	34.63	Positive	37.29	negative	Exe
CE04	GroupB_control2	35	metamorph	33.23	Positive	21.64	positive	Exe
CE08	GroupB_control2	35	25	30.55	NA	38.53	negative	UCF
CE11	GroupB_control2	35	25	35.02	Positive	35.44	positive	Exe
CE14	GroupB_control2	30	35	33.17	NA	36.15	positive	UCF
CE17	GroupB_control2	25	30	36.49	Positive	14.94	negative	Exe
CE21	GroupB_control2	35	25	38.05	Negative	35.83	positive	Exe
CE26	GroupB_control2	35	metamorph	33.56	Positive	35.03	positive	Exe
CE29	GroupB_control2	25	metamorph	negative	NA	32.24	positive	UCF
CE32	GroupB_control2	25	30	35.83	NA	34.07	positive	UCF
CE35	GroupB_control2	25	30	negative	NA	32.02	positive	UCF

Table S2.6. Molecular screening results of the *Rana dalmatina* (Rd) experimental infections, organized by treatment. Nucleic acid was extracted from livers harvested from each tadpole. Total DNA was screened using NAG01a-d-specific PCR and PPC-specific PCR, and total RNA was screened using NAG01a-d-specific RT-PCR. Gel electrophoresis results are shown.

Sample ID	Treatment	NAG01a-d PCR	PPC PCR	NAG01a-d RT-PCR
Rd_03_I_1	KNA03 injection	positive	positive	Negative
Rd_03_I_2	KNA03 injection	positive	positive	Negative
Rd_03_I_3	KNA03 injection	negative	negative	NA
Rd_C_I_1	Control injection	negative	negative	NA
Rd_C_I_2	Control injection	negative	negative	NA
Rd_03_E_1	KNA03 tank exposure	positive	positive	Negative
Rd_03_E_2	KNA03 tank exposure	positive	positive	Negative
Rd_03_E_3	KNA03 tank exposure	negative	negative	NA
Rd_14_E_1	KNA14 tank exposure	positive	positive	Negative
Rd_14_E_2	KNA14 tank exposure	positive	positive	Negative
Rd_14_E_3	KNA14 tank exposure	negative	negative	NA
Rd_14_x3_E_1	KNA14x3 tank exposure	negative	negative	NA
Rd_14_x3_E_2	KNA14x3 tank exposure	negative	negative	NA
Rd_14_x3_E_3	KNA14x3 tank exposure	negative	negative	NA
Rd_14_x6_E_1	KNA14x6 tank exposure	positive	positive	Negative
Rd_14_x6_E_2	KNA14x6 tank exposure	negative	negative	NA
Rd_14_x6_E_3	KNA14x6 tank exposure	negative	negative	NA
Rd_21_E_1	KNA21 tank exposure	positive	positive	Negative

Rd_21_E_2	KNA21 tank exposure	negative	negative	NA
Rd_21_E_3	KNA21 tank exposure	positive	positive	Negative
Rd_C_E_1	Control tank exposure	negative	negative	NA

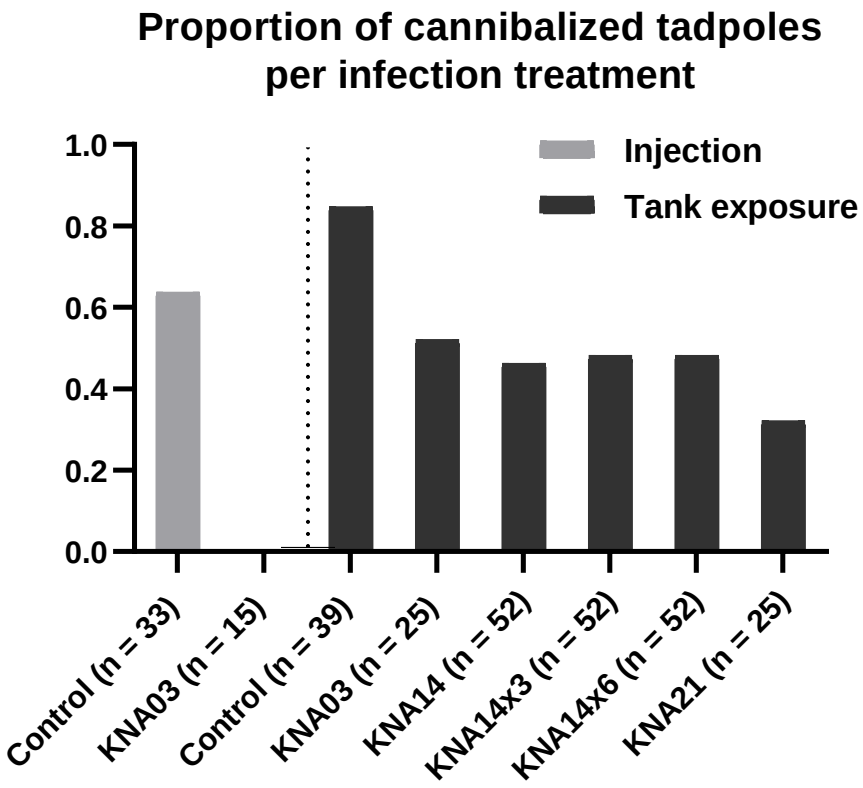

Treatment comparison	X^2	df	N	p-value
Control_I vs. KNA03_I	16.7	1	48	< 0.001
Control_Te vs. KNA03_Te	9.48	1	64	< 0.001
Control_Te vs. KNA14_Te	14.92	1	91	< 0.001
Control_Te vs. KNA14x3_Te	13.7	1	91	< 0.001
Control_Te vs. KNA14x6_Te	13.7	1	91	< 0.001
Control_Te vs. KNA21_Te	20.2	1	64	< 0.001

Figure S2.1. Proportion of *Rana dalmatina* tadpoles that were cannibalized by other *R. dalmatina* tadpoles during the 40-day monitoring period following eight experimental treatments. Values along the x-axis (i.e. n = xx) correspond to the number of tadpoles per treatment, excluding those collected before the end of the monitoring period (see Table S2.2 for details). The table shows the results of the chi-square test for each pairwise comparison of the controls and their corresponding infection treatment (I = injection, Te = tank exposure).

Table S3.1. Cq values per template dilution used to determine the efficiency and sensitivity of the NAG01 Perkinsea strain-specific qPCR assays in both uniplex and duplex conditions. Also presented are Cq values for PPC+ (KNA_DNA) and NAG01a+ (G2.13 and G8.1) DNA samples, extracted from tadpole livers. Grey highlights correspond to the linear dynamic ranges calculated for each assay. Dark grey highlights correspond to the upper and lower limits of detection calculated for each assay. "NA" in the Replicate columns indicates that the BioRad software was unable to calculate a Cq, likely due to interference with fluorescence detection. An asterisk (*) in the Replicate columns indicates that the regression method (as opposed to the default single threshold method) was used to determine Cq due to a high level of background noise. The regression method uses multiple data points to determine Cq and is therefore less sensitive to noise.

PPC uniplex assay

	Replicate 1	Replicate 2	Replicate 3	Replicate 4	Average Cq	SD	ΔCq
1*10-3 ng	23.28	23.59	23.5	23.38	23.4375	0.135739	NA
0.01 ng	19.63	19.21	19.34	19.24	19.355	0.191572	4.0825
0.1 ng	16.05	15.88	15.94	15.82	15.9225	0.098107	3.4325
1 ng	12.38	12.33	12.45	12.24	12.35	0.088318	3.5725
10 ng	10.45	9.56	10.15	9.38	9.885	0.500033	2.465
NTC	No amp.	No amp.	No amp.		NA	NA	NA

	Replicate 1	Replicate 2	Replicate 3	Replicate 4	Average Cq	SD	ΔCq
1*10-10 ng	36.74	No amp.	36.95	No amp.	36.845	0.148492	NA
1*10-9 ng	36.05	38.25	No amp.	37.63	37.31	1.134372	-0.465
1*10-8 ng	36.01	No amp.	38.03	36.42	36.82	1.067755	0.49
1*10-7 ng	No amp.	37.01	37.63	37.4	37.3466667	0.313422	-0.52667

1*10-6 ng	33.12	33.29	33.38	33.52	33.3275	0.167606	4.019167
1*10-5 ng	30.42	30.31	30.25	30.04	30.255	0.159687	3.0725
1*10-4 ng	26.64	26.73	26.66	26.83	26.715	0.085829	3.54
1*10-3 ng	23.17	23.3	23.13	23.17	23.1925	0.074106	3.5225
0.01 ng	19.05	19.16	19.04	18.99	19.06	0.071647	4.1325
0.1 ng	15.35	15.59	15.48	15.42	15.46	0.101653	3.6
1 ng	12.24	12.11	12.16	12.13	12.16	0.057155	3.3
NTC	No amp.	No amp.	No amp.	No amp.	NA	NA	NA

KNA_DNA	20.19	20.27			20.23	0.056569

NAG01 uniplex assay

	Replicate 1	Replicate 2	Replicate 3	Replicate 4	Average Cq	SD	ΔCq
1*10-10 ng	No amp.	No amp.	No amp.	No amp.	NA	NA	NA
1*10-9 ng	No amp.	NA	No amp.	No amp.	NA	NA	NA
1*10-8 ng	No amp.	No amp.	No amp.	No amp.	NA	NA	NA
1*10-7 ng	No amp.	No amp.	No amp.	No amp.	NA	NA	NA
1*10-6 ng	35.54	NA	34.43	34.77	34.9133333	0.568712	NA
1*10-5 ng	33.66	31.3	31.79	31.91	32.165	1.031003	2.748333
1*10-4 ng	30.09	28.85	27.8	28.2	28.735	1.001615	3.43
1*10-3 ng	26.51	NA	23.31	27.97	25.93	2.383527	2.805
0.01 ng	22.35	20.48	20.38	21.62	21.2075	0.946832	4.7225
0.1 ng	20.02	16.55	15.64	17.48	17.4225	1.88758	3.785
1 ng	15.19	13.46	14.75	13.43	14.2075	0.89868	3.215
10 ng	10.22	10.7	6.15	NA	9.02333333	2.499927	5.184167
NTC	No amp.	No amp.	No amp.	No amp.	NA	NA	NA

1*10-6 ng	35.68	36.13	NA	NA	35.905	0.318198	NA
1*10-5 ng	31.42	31.39	NA	32.75	31.405	0.021213	4.5

1*10-4 ng	30.33	27.48	26.05	27.67	26.765	1.011163	4.64
1*10-3 ng	25.39	23.99	25.8	24.68	25.06	0.949052	1.705
0.01 ng	21.95	21.42	22.03	20.17	21.8	0.331512	3.26
0.1 ng	18.41	17.86	NA	18.02	18.135	0.388909	3.665
1 ng	15.74	16.04	16.71	15.09	15.89	0.212132	2.245
NTC	No amp.	No amp.	No amp.	No amp.	NA	NA	NA

G2.13	NA	No amp.	No amp.		NA	NA
G8.1	33.97	NA	33.81		33.89	0.113137

PPC duplex assay

	Replicate 1	Replicate 2	Replicate 3	Replicate 4	Average Cq	SD	ΔCq	$\overline{Cq}$ uniplex vs. $\overline{Cq}$ duplex
1*10-7 ng	36.5	37.16	33.97	35.49	35.78	1.388404	NA	$t(5) = .12$, $p > .05$
1*10-6 ng	31.29	30.73	33.73	32.51	32.065	1.335802	3.715	$t(6) = .11$, $p > .05$
1*10-5 ng	28.6	28.44	28.58	28.53	28.5375	0.071356	3.5275	$t(6) = 1.1*10^{-6}$, $p > .05$
1*10-4 ng	25.35	25.42	25.23	25.5	25.375	0.114455	3.1625	$t(6) = 1.5*10^{-6}$, $p > .05$
1*10-3 ng	22.13	23.11	22.94	22.91	22.7725	0.437293	2.6025	$t(6) = .11$, $p > .05$
0.01 ng	19.21	18.15	18.43	18.26	18.5125	0.479053	4.26	$t(6) = .06$, $p > .05$
0.1 ng	17.5	16.05	17.32	15.16	16.5075	1.106085	2.005	$t(6) = .11$, $p > .05$
1 ng	11.4	12.15	13.55	12.08	12.295	0.90246	4.2125	$t(6) = .78$, $p > .05$
NTC	No amp.	No amp.	No amp.	No amp.	NA	NA	NA	NA

KNA_DNA	21.24	21.13	21.87		21.4133333	0.399291

NAG01 duplex assay

	Replicate 1	Replicate 2	Replicate 3	Replicate 4	Average Cq	SD	ΔCq	$\overline{Cq}$ uniplex vs. $\overline{Cq}$ duplex
1*10-7 ng	37.43	32.33	37.23	33.9	35.2225	2.517848	NA	NA
1*10-6 ng	NA	28.58	NA	33.11	30.845	3.203194	4.3775	$t(2) = .16$, $p > .05$
1*10-5 ng	28.01	28.13	29.25	28.44	28.4575	0.558532	2.3875	$t(5) = 1.1*10^{-3}$, $p > .05$

1*10-4 ng	27.62*	25.13	26.08	23.25*	25.52	1.828351	2.9375	$t(6) = .11$, $p > .05$
1*10-3 ng	22.06	24.1	22.13	23.52	22.9525	1.018475	2.5675	$t(6) = .03$, $p > .05$
0.01 ng	18.78	15.57	16.36	17.21	16.98	1.374215	5.9725	$t(6) = 1.6*10^{-3}$, $p > .05$
0.1 ng	13.95*	16.74	12.16*	13.43	14.07	1.93227	2.91	$t(5) = .02$, $p > .05$
1 ng	10.46*	8.82*	7.37*	12.46	9.7775	2.188948	4.2925	$t(6) = 1.8*10^{-3}$, $p > .05$
NTC	No amp.	No amp.	No amp.	No amp.	NA	NA	NA	NA
G8.1	33.01	32.77	NA		32.89	0.169706		

Table S3.2. Specimen data for livers harvested from Alaska and French Guiana tadpoles. Liver tissue from each of the Alaska tadpoles was pooled prior to DNA extraction, yielding a single DNA sample (KNA_DNA). DNA was extracted individually from each of the French Guiana liver tissue samples.

Sample ID	State, country	Region	Site	GPS	Collection date	Species	Life stage	Liver appearance
KNA03_01	AK, USA	Kenai	KNA03	60.72574, -150.89	03/07/2016	*Lithobates sylvaticus*	41	abnormal
KNA03_02	AK, USA	Kenai	KNA03	60.72574, -150.89	03/07/2016	*Lithobates sylvaticus*	41	abnormal
KNA03_03	AK, USA	Kenai	KNA03	60.72574, -150.89	03/07/2016	*Lithobates sylvaticus*	38	abnormal
KNA03_04	AK, USA	Kenai	KNA03	60.72574, -150.89	03/07/2016	*Lithobates sylvaticus*	38	abnormal
KNA05_01	AK, USA	Kenai	KNA05	60.70667, -150.891	03/07/2016	*Lithobates sylvaticus*	43	abnormal
KNA05_03	AK, USA	Kenai	KNA05	60.70667, -150.891	03/07/2016	*Lithobates sylvaticus*	38	abnormal
KNA14_05	AK, USA	Kenai	KNA14	60.75101, -150.502	02/07/2016	*Lithobates sylvaticus*	39	abnormal
KNA1090_01	AK, USA	Kenai	KNA1090	60.75212, -151.191	01/07/2016	*Lithobates sylvaticus*	35	abnormal
KNA1090_04	AK, USA	Kenai	KNA1090	60.75212, -151.191	08/06/2016	*Lithobates sylvaticus*	unknown	abnormal
G2.13	French Guiana	Near Patawa	FG2	4.5293889, -52.1516	14/04/2013	*Phyllomedusa tomopterna*	28/29	normal
G8.1	French Guiana	Patawa	FG7	4.5416667, -52.15	26/04/2013	*Hypsiboas geographicus*	37/38	normal

Table S3.3. Cq values for the upper and lower limits of detections (LoDs) for the novel PPC and NAG01a-c qPCR assays in uniplex and duplex conditions. Also presented are Cq values for PPC+ (KNA_DNA) and NAG01a+ (G8.1) DNA samples, extracted from tadpole livers. The Cq values shown are the results of screening on the *Biomeme two3* qPCR device, compared to the average Cq values (in parentheses) obtained on the CFX96 real-time PCR detection system (BioRad). *These values show the results of the duplex assay combining G8.1 with PPC plasmid ($1*10^{-6}$ ng), rather than G8.1 with KNA_DNA, as the latter G8.1 was not detected.

Sample ID	PPC uniplex Cq	Duplex Cq (PPC)	NAG01a-c uniplex Cq	Duplex Cq (NAG01a-c)
Upper LoD	10.93 (12.16)	11.47 (12.3)	10.84 (14.21)	13.66 (9.78)
Lower LoD	30.54 (33.33)	37 (35.78)	37.82 (34.91)	38.25 (35.22)
KNA_DNA	18.46 (20.23)	17.68 (21.41)	NA (NA)	NA (NA)
G8.1	NA (NA)	NA (NA)	32.67 (33.89)	34.2 (32.89)*

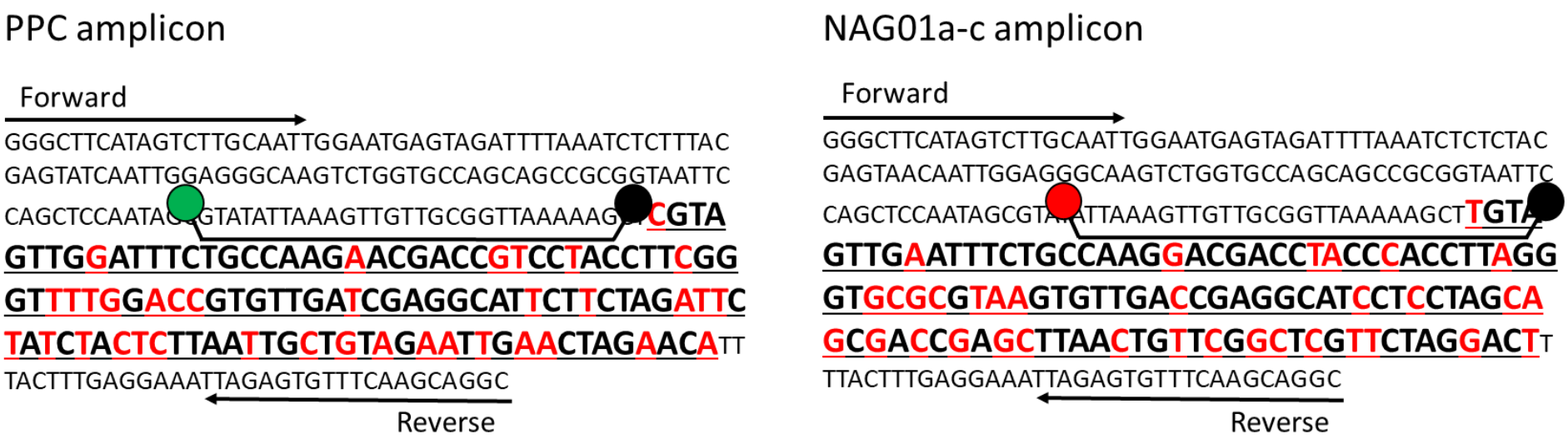

Figure S3.1. The (sense strand) sequence of the 18S rRNA gene fragment targeted by the NAG01 Perkinsea strain-specific assays. The bold sequence is the variant region used to distinguish the strains. The red nucleotides are the sites that differ between the two strains. The arrows represent the primers, and the probe-like shapes represent the FAM (green) and Cy5 (red) probes. The PPC probe is identical to 93/93 (100%) PPC clone libraries recovered from tadpole liver and generated for the alignment by Isidoro-Ayza et al. (2017). The NAG01a-c probe is identical to 172/177 (97%) NAG01a-c clone libraries recovered from tadpole liver and generated for the alignment by Chambouvet et al. (2015).

Chapter 4. Phylogenetic analysis of pathogenic amphibian Perkinsea expands its known geographic and host range

Table S4.1. Specimen data for all tadpoles sampled in this study and the corresponding NCBI accession number of the 16S rDNA sequence. Samples highlighted in grey are positive for PCR detection of NAG01 Perkinsea. Species are identified by the hit with the highest identity percentage from a NCBI BLASTn MegaBLAST search of the nr database using 16S rDNA sequences; the IDs are only estimates because identity percentages were less than 100 (see Table S4.4 for details). "NR" indicates that no reads were generated, "MC" indicates that assembly of the reads yielded multiple contigs from multiple species, and "SE" indicates that the reads contained high rates of sequencing errors in conserved regions; for these reasons, a BLASTn search could either not be completed or could not be relied upon for positive identification.

Sample ID	Single or pooled	Country	Region	Site	GPS	Collection date	Species	Family	Accession Number
PA_T091	Single	PA	Soberania	SNP6	9.071012, -79.656412	17/11/2018	*Leptodactylus pentadactylus*	Leptodactylidae	MW136603
PA_T092	Single	PA	Soberania	SNP6	9.071012, -79.656412	17/11/2018	*Leptodactylus pentadactylus*	Leptodactylidae	MW136604
PA_T093	Single	PA	Soberania	SNP6	9.071012, -79.656412	17/11/2018	*Hypsiboas lundii*	Hylidae	MW136605
PA_T094	Single	PA	Soberania	SNP6	9.071012, -79.656412	17/11/2018	*Hypsiboas lundii*	Hylidae	MW136606
PA_T095	Single	PA	Soberania	SNP6	9.071012, -79.656412	17/11/2018	*Hypsiboas lundii*	Hylidae	MW136607
PA_T096	Single	PA	Soberania	SNP6	9.071012, -79.656412	17/11/2018	*Boana rosenbergi*	Hylidae	MW136608
PA_T097	Single	PA	Soberania	SNP6	9.071012, -79.656412	17/11/2018	*Boana rosenbergi*	Hylidae	MW136609
PA_T098	Single	PA	Soberania	SNP6	9.071012, -79.656412	17/11/2018	*Boana rosenbergi*	Hylidae	MW136610
PA_T099	Pooled (x5)	PA	Soberania	SNP6	9.071012, -79.656412	17/11/2018	*Boana rosenbergi*	Hylidae	MW136611
PA_T105	Single	PA	Soberania	SNP6	9.071012, -79.656412	17/11/2018	*Engystomops pustulosus*	Leptodactylidae	MW136612
PA_T106	Single	PA	Soberania	SNP6	9.071012, -79.656412	17/11/2018	*Engystomops pustulosus*	Leptodactylidae	MW136613
PA_T107	Single	PA	Soberania	SNP6	9.071012, -79.656412	17/11/2018	*Engystomops pustulosus*	Leptodactylidae	MW136614

PA_T109	Single	PA	Altos de Campana	AC1	8.681981, -79.928944	20/11/2018	*Silverstoneia flotator*	Leptodactylidae	MW136615
PA_T115	Single	PA	Altos de Campana	AC2	8.677743, -79.928435	20/11/2018	*Dendropsophus anceps*	Hylidae	MW136616
PA_T116	Single	PA	Altos de Campana	AC2	8.677743, -79.928435	20/11/2018	*Dendropsophus anceps*	Hylidae	MW136617
PA_T117	Single	PA	Altos de Campana	AC2	8.677743, -79.928435	20/11/2018	*Dendropsophus anceps*	Hylidae	MW136618
PA_T118	Single	PA	Altos de Campana	AC2	8.677743, -79.928435	20/11/2018	NR	NA	NA
PA_T119	Single	PA	Altos de Campana	AC2	8.677743, -79.928435	20/11/2018	*Dendropsophus anceps*	Hylidae	MW136619
PA_T120	Pooled (x5)	PA	Altos de Campana	AC2	8.677743, -79.928435	20/11/2018	*Dendropsophus anceps*	Hylidae	MW136620
PA_T121	Single	PA	Altos de Campana	AC2	8.677743, -79.928435	20/11/2018	*Agalychnis callidryas*	Phyllomedusidae	MW136621
PA_T122	Single	PA	Altos de Campana	AC2	8.677743, -79.928435	20/11/2018	*Allobates talamancae*	Aromobatidae	MW136622
PA_T123	Single	PA	Altos de Campana	AC2	8.677743, -79.928435	20/11/2018	*Rhinella marina*	Bufonidae	MW136623
PA_T124	Single	PA	Altos de Campana	AC2	8.677743, -79.928435	20/11/2018	SE	NA	NA
PA_T125	Single	PA	Altos de Campana	AC2	8.677743, -79.928435	20/11/2018	MC	NA	NA
PA_T126	Pooled (x5)	PA	Altos de Campana	AC2	8.677743, -79.928435	20/11/2018	*Agalychnis callidryas*	Phyllomedusidae	MW136624
PA_T128	Single	PA	El Valle de Anton	EVA3	8.59757, -80.11545	22/11/2018	*Rhinella marina*	Bufonidae	MW136625
PA_T129	Single	PA	El Valle de Anton	EVA3	8.59757, -80.11545	22/11/2018	*Rhinella marina*	Bufonidae	MW136626
PA_T130	Single	PA	El Valle de Anton	EVA3	8.59757, -80.11545	22/11/2018	NR	NA	NA
PA_T131	Single	PA	El Valle de Anton	EVA4	8.601778, -80.115663	22/11/2018	*Allobates talamancae*	Aromobatidae	MW136627
PA_T132	Single	PA	El Valle de Anton	EVA4	8.601778, -80.115663	22/11/2018	*Allobates talamancae*	Aromobatidae	MW136628
PA_T133	Single	PA	El Valle de Anton	EVA4	8.601778, -80.115663	22/11/2018	*Allobates talamancae*	Aromobatidae	MW136629
PA_T134	Single	PA	El Valle de Anton	EVA4	8.601778, -80.115663	22/11/2018	*Allobates talamancae*	Aromobatidae	MW136630
PA_T135	Single	PA	El Valle de Anton	EVA4	8.601778, -80.115663	22/11/2018	*Allobates talamancae*	Aromobatidae	MW136631
PA_T136	Single	PA	El Valle de Anton	EVA4	8.601778, -80.115663	22/11/2018	*Allobates talamancae*	Aromobatidae	MW136632
PA_T137	Single	PA	El Valle de Anton	EVA4	8.601778, -80.115663	22/11/2018	NR	NA	NA
PA_T138	Single	PA	El Valle de Anton	EVA4	8.601778, -80.115663	22/11/2018	*Allobates talamancae*	Aromobatidae	MW136633
PA_T139	Single	PA	El Valle de Anton	EVA4	8.601778, -80.115663	22/11/2018	*Allobates talamancae*	Aromobatidae	MW136634
PA_T140	Single	PA	El Valle de Anton	EVA4	8.601778, -80.115663	22/11/2018	*Allobates talamancae*	Aromobatidae	MW136635
PA_T141	Single	PA	El Valle de Anton	EVA4	8.601778, -80.115663	22/11/2018	*Rhinella marina*	Bufonidae	MW136636
PA_T142	Single	PA	El Valle de Anton	EVA4	8.601778, -80.115663	22/11/2018	*Smilsca sila*	Hylidae	MW136637
PA_T143	Single	PA	El Valle de Anton	EVA4	8.601778, -80.115663	22/11/2018	*Boana rosenbergi*	Hylidae	MW136638
PA_T144	Single	PA	El Valle de Anton	EVA4	8.601778, -80.115663	22/11/2018	SE	NA	NA

PA_T145	Single	PA	El Valle de Anton	EVA4	8.601778, -80.115663	22/11/2018	NR	NA	NA
PA_T146	Single	PA	El Valle de Anton	EVA4	8.601778, -80.115663	22/11/2018	MC	NA	NA
PA_T147	Single	PA	El Valle de Anton	EVA4	8.601778, -80.115663	22/11/2018	*Rhinella marina*	Bufonidae	MW136639
PA_T148	Single	PA	El Valle de Anton	EVA4	8.601778, -80.115663	22/11/2018	*Rhinella marina*	Bufonidae	MW136640
PA_T149	Single	PA	El Valle de Anton	EVA4	8.601778, -80.115663	22/11/2018	SE	NA	NA
PA_T150	Single	PA	El Valle de Anton	EVA4	8.601778, -80.115663	22/11/2018	*Rhinella marina*	Bufonidae	MW136641
PA_T151	Single	PA	Soberania	SNP7	9.07812, -79.65118	24/11/2018	*Smilisca sila*	Hylidae	MW136642
PA_T152	Single	PA	Soberania	SNP7	9.07812, -79.65118	24/11/2018	NR	NA	NA
PA_T153	Single	PA	Soberania	SNP7	9.07812, -79.65118	24/11/2018	*Smilisca sila*	Hylidae	MW136643
PA_T154	Single	PA	Soberania	SNP7	9.07812, -79.65118	24/11/2018	NR	NA	NA
PA_T155	Single	PA	Soberania	SNP7	9.07812, -79.65118	24/11/2018	*Smilisca sila*	Hylidae	MW136644
PA_T156	Single	PA	Soberania	SNP7	9.07812, -79.65118	24/11/2018	SE	NA	NA
PA_T157	Single	PA	Soberania	SNP7	9.07812, -79.65118	24/11/2018	SE	NA	NA
PA_T158	Single	PA	Soberania	SNP7	9.07812, -79.65118	24/11/2018	*Smilisca sila*	Hylidae	MW136645
PA_T159	Single	PA	Soberania	SNP7	9.07812, -79.65118	24/11/2018	*Smilisca sila*	Hylidae	MW136646
PA_T160	Single	PA	Soberania	SNP7	9.07812, -79.65118	24/11/2018	*Smilisca sila*	Hylidae	MW136647
PA_T161	Single	PA	Soberania	SNP7	9.07812, -79.65118	24/11/2018	*Boana rosenbergi*	Hylidae	MW136648
PA_T162	Single	PA	Soberania	SNP8	9.09055, -79.61837	24/11/2018	*Rhinella atlata*	Bufonidae	MW136649
PA_T163	Single	PA	Soberania	SNP8	9.09055, -79.61837	24/11/2018	*Rhinella atlata*	Bufonidae	MW136650
PA_T164	Single	PA	Soberania	SNP8	9.09055, -79.61837	24/11/2018	*Rhinella atlata*	Bufonidae	MW136651
PA_T165	Single	PA	Soberania	SNP8	9.09055, -79.61837	24/11/2018	*Rhinella atlata*	Bufonidae	MW136652
PA_T166	Single	PA	Soberania	SNP8	9.09055, -79.61837	24/11/2018	NR	NA	NA
PA_T167	Single	PA	Soberania	SNP8	9.09055, -79.61837	24/11/2018	*Rhinella atlata*	Bufonidae	MW136653
PA_T168	Single	PA	Soberania	SNP8	9.09055, -79.61837	24/11/2018	*Rhinella atlata*	Bufonidae	MW136654
PA_T169	Single	PA	Soberania	SNP8	9.09055, -79.61837	24/11/2018	*Rhinella atlata*	Bufonidae	MW136655
PA_T170	Single	PA	Soberania	SNP8	9.09055, -79.61837	24/11/2018	*Rhinella atlata*	Bufonidae	MW136656
PA_T171	Single	PA	Soberania	SNP8	9.09055, -79.61837	24/11/2018	*Rhinella atlata*	Bufonidae	MW136657
UK_HA01-5	Pooled (x5)	UK	Surrey	NA		July 2019	*Hyla arborea*	Hylidae	NA
UK_HA06-10	Pooled (x5)	UK	Surrey	NA		July 2019	*Hyla arborea*	Hylidae	NA

Table S4.2. List of 18S rDNA sequences newly generated in this study from PPC-positive tadpoles, and their corresponding NCBI accession number.

Sample ID	Sequence/clone	PCR 1	PCR 2	PCR 3	Accession Number
PA_T093	PA_T093_1.1	X			MW136531
	PA_T093_1.2	X			MW136532
	PA_T093_1.3	X			MW136533
PA_T096	PA_T096_1.1	X			MW136534
	PA_T096_1.2	X			MW136535
PA_T097	PA_T097_1.1	X			MW136536
	PA_T097_1.2	X			MW136537
	PA_T097_1.3	X			MW136538
PA_T119	PA_T119_1.1	X			MW136539
	PA_T119_1.2	X			MW136540
PA_T128	PA_T128_1.1	X			MW136541
PA_T135	PA_T135_1.1_T3	X			MW136542
	PA_T135_1.2	X			MW136543
	PA_T135_1.3	X			MW136544
	PA_T135_2.1		X		MW136545
PA_T136	PA_T136_1.1	X			MW136546
	PA_T136_1.2	X			MW136547
	PA_T136_1.3	X			MW136548
PA_T139	PA_T139_1.1	X			MW136549
	PA_T139_1.2_T3	X			MW136550
	PA_T139_1.3	X			MW136551
	PA_T139_2.1		X		MW136552
	PA_T139_2.2		X		MW136553

	PA_T139_2.3		X		MW136554
	PA_T139_2.4		X		MW136555
	PA_T139_2.5_T3		X		MW136556
	PA_T139_2.6		X		MW136557
	PA_T139_2.7		X		MW136558
	PA_T139_2.8		X		MW136559
	PA_T139_2.9		X		MW136560
	PA_T139_3.1			X	MW136561
	PA_T139_3.2			X	MW136562
	PA_T139_3.3			X	MW136563
	PA_T139_3.4			X	MW136564
	PA_T139_3.5			X	MW136565
	PA_T139_3.6			X	MW136566
	PA_T139_3.7			X	MW136567
PA_T140	PA_T140_1.1	X			MW136568
	PA_T140_1.2	X			MW136569
	PA_T140_1.3	X			MW136570
PA_T169	PA_T169_1.1	X			MW136571
UK_HA01-5	UK_HA01-5_54_1.1	X			MW136572
	UK_HA01-5_54_1.2	X			MW136573
	UK_HA01-5_54_1.3	X			MW136574
	UK_HA01-5_54_1.4	X			MW136575
	UK_HA01-5_54_1.5	X			MW136576
	UK_HA01-5_54_1.6	X			MW136577
	UK_HA01-5_54_1.7	X			MW136578
	UK_HA01-5_54_1.8	X			MW136579
	UK_HA01-5_54_1.9	X			MW136580
	UK_HA01-5_54_1.10	X			MW136581
	UK_HA01-5_54_2.1		X		MW136582
	UK_HA01-5_54_2.2		X		MW136583

UK_HA01-5_54_2.3		X		MW136584
UK_HA01-5_54_2.4		X		MW136585
UK_HA01-5_54_2.5		X		MW136586
UK_HA01-5_54_2.6		X		MW136587
UK_HA01-5_54_2.7		X		MW136588
UK_HA01-5_54_2.8		X		MW136589
UK_HA01-5_54_2.9		X		MW136590
UK_HA01-5_54_2.10		X		MW136591
UK_HA01-5_54_2.11		X		MW136592
UK_HA01-5_54_3.1			X	MW136593
UK_HA01-5_54_3.2			X	MW136594
UK_HA01-5_54_3.3			X	MW136595
UK_HA01-5_54_3.4			X	MW136596
UK_HA01-5_54_3.5			X	MW136597
UK_HA01-5_56_1.1	X			MW136598
UK_HA01-5_56_1.2	X			MW136599
UK_HA01-5_56_2.1		X		MW136600
UK_HA01-5_56_3.1			X	MW136601
UK_HA01-5_56_3.2			X	MW136602

Table S4.3. Details of published Perkinsea 18S rDNA sequences used as references in the phylogenetic analysis presented in Figure 4.1. Sequences with a triangle (◁) are included in the subset that was collapsed into a representative triangle.

Accession Number	Sample ID	Description	Year	Host/source	City/county/parrish	State/country	Reference

KY679209	4824-341	NAG01 PPC	2003	*Rana sylvatica*	Hancock	Maine, USA	Isidoro-Ayza et al. 2017
KY679210	4824-463	NAG01 PPC	2003	*R. clamitans*	Hancock	Maine, USA	Isidoro-Ayza et al. 2017
KY679211 ◁	4957-311	NAG01 PPC	2005	*R. sphenocephala*	Union	Louisiana, USA	Isidoro-Ayza et al. 2017
KY679212	4864-003	NAG01 PPC	2003	*R. sphenocephala*	Wakulla	Florida, USA	Isidoro-Ayza et al. 2017
KY679213 ◁	4960-291	NAG01 PPC	2005	*R. clamitans*	Hancock	Maine, USA	Isidoro-Ayza et al. 2017
KY679214	16407-003	NAG01 PPC	1999	*R. catesbeiana*	Carroll	New Hampshire, USA	Isidoro-Ayza et al. 2017
KY679215 ◁	17272-015	NAG01 PPC	2001	*R. sylvatica*	Augusta	Virginia, USA	Isidoro-Ayza et al. 2017
KY679216 ◁	18587-005	NAG01 PPC	2003	*R. sevosa*	Harrison	Mississippi, USA	Isidoro-Ayza et al. 2017
KY679217	18612-013	NAG01 PPC	2003	*R. sevosa*	Harrison	Mississippi, USA	Isidoro-Ayza et al. 2017
KY679218 ◁	18709-002	NAG01 PPC	2003	*R. sphenocephala*	Prince George's	Maryland, USA	Isidoro-Ayza et al. 2017
KY679219 ◁	18761-005	NAG01 PPC	2003	*R. sphenocephala*	Prince George's	Maryland, USA	Isidoro-Ayza et al. 2017
KY679220	19156-001	NAG01 PPC	2004	*R. sylvatica*	Kenai Peninsula	Alaska, USA	Isidoro-Ayza et al. 2017
KY679221	19215-002	NAG01 PPC	2004	*R. sylvatica*	Kenai Peninsula	Alaska, USA	Isidoro-Ayza et al. 2017
KY679222	19369-002	NAG01 PPC	2005	*R. capito*	Hernando	Florida, USA	Isidoro-Ayza et al. 2017
KY679223	19384-009	NAG01 PPC	2005	*R. sphenocephala*	Putnam	Florida, USA	Isidoro-Ayza et al. 2017
KY679224	19709-006	NAG01 PPC	2006	*R. heckscheri*	Miller	Georgia, USA	Isidoro-Ayza et al. 2017
KY679225 ◁	22445-004	NAG01 PPC	2007	*R. sphenocephala*	Suffolk	New York, USA	Isidoro-Ayza et al. 2017
KY679226 ◁	24988-002	NAG01 PPC	2014	*R. sevosa*	Harrison	Mississippi, USA	Isidoro-Ayza et al. 2017
KY679227	44274-004	NAG01 PPC	2008	*R. sphenocephala*	Prince George's	Maryland, USA	Isidoro-Ayza et al. 2017
KY679228	44277-003	NAG01 PPC	2010	*R. sphenocephala*	Wakulla	Florida, USA	Isidoro-Ayza et al. 2017
KY679229 ◁	44277-011	NAG01 PPC	2010	*R. sphenocephala*	Wakulla	Florida, USA	Isidoro-Ayza et al. 2017
KY679230	4824-341 clone #2	NAG01 PPC	2003	*R. sylvatica*	Hancock	Maine, USA	Isidoro-Ayza et al. 2017
KY679231 ◁	4824-341 clone #4	NAG01 PPC	2003	*R. sylvatica*	Hancock	Maine, USA	Isidoro-Ayza et al. 2017
KY679232	4824-341 clone #6	NAG01 PPC	2003	*R. sylvatica*	Hancock	Maine, USA	Isidoro-Ayza et al. 2017
KY679233	4824-341 clone #7	NAG01 PPC	2003	*R. sylvatica*	Hancock	Maine, USA	Isidoro-Ayza et al. 2017
KY679234 ◁	4824-341 clone #8	NAG01 PPC	2003	*R. sylvatica*	Hancock	Maine, USA	Isidoro-Ayza et al. 2017
KY679235	4824-341 clone #9	NAG01 PPC	2003	*R. sylvatica*	Hancock	Maine, USA	Isidoro-Ayza et al. 2017
KY679236	4824-341 clone #10	NAG01 PPC	2003	*R. sylvatica*	Hancock	Maine, USA	Isidoro-Ayza et al. 2017
KY679237	4824-341 clone #11	NAG01 PPC	2003	*R. sylvatica*	Hancock	Maine, USA	Isidoro-Ayza et al. 2017
KY679238 ◁	4957-311 clone #2	NAG01 PPC	2005	*R. sphenocephala*	Union	Louisiana, USA	Isidoro-Ayza et al. 2017

KY679239 ◁	4957-311 clone #3	NAG01 PPC	2005	*R. sphenocephala*	Union	Louisiana, USA	Isidoro-Ayza et al. 2017
KY679240 ◁	4957-311 clone #5	NAG01 PPC	2005	*R. sphenocephala*	Union	Louisiana, USA	Isidoro-Ayza et al. 2017
KY679241 ◁	4957-311 clone #6	NAG01 PPC	2005	*R. sphenocephala*	Union	Louisiana, USA	Isidoro-Ayza et al. 2017
KY679242 ◁	4957-311 clone #9	NAG01 PPC	2005	*R. sphenocephala*	Union	Louisiana, USA	Isidoro-Ayza et al. 2017
KY679243 ◁	4957-311 clone #10	NAG01 PPC	2005	*R. sphenocephala*	Union	Louisiana, USA	Isidoro-Ayza et al. 2017
KY679244 ◁	4957-311 clone #11	NAG01 PPC	2005	*R. sphenocephala*	Union	Louisiana, USA	Isidoro-Ayza et al. 2017
KY679245 ◁	4957-311 clone #12	NAG01 PPC	2005	*R. sphenocephala*	Union	Louisiana, USA	Isidoro-Ayza et al. 2017
KY679246	16407-003 clone #4	NAG01 PPC	1999	*R. catesbeiana*	Carroll	New Hampshire, USA	Isidoro-Ayza et al. 2017
KY679247 ◁	16407-003 clone #7	NAG01 PPC	1999	*R. catesbeiana*	Carroll	New Hampshire, USA	Isidoro-Ayza et al. 2017
KY679248 ◁	16407-003 clone #18	NAG01 PPC	1999	*R. catesbeiana*	Carroll	New Hampshire, USA	Isidoro-Ayza et al. 2017
KY679249	16407-003 clone #20	NAG01 PPC	1999	*R. catesbeiana*	Carroll	New Hampshire, USA	Isidoro-Ayza et al. 2017
KY679250	16407-003 clone #32	NAG01 PPC	1999	*R. catesbeiana*	Carroll	New Hampshire, USA	Isidoro-Ayza et al. 2017
KY679251 ◁	16407-003 clone #33	NAG01 PPC	1999	*R. catesbeiana*	Carroll	New Hampshire, USA	Isidoro-Ayza et al. 2017
KY679252	16407-003 clone #34	NAG01 PPC	1999	*R. catesbeiana*	Carroll	New Hampshire, USA	Isidoro-Ayza et al. 2017
KY679253 ◁	16407-003 clone #36	NAG01 PPC	1999	*R. catesbeiana*	Carroll	New Hampshire, USA	Isidoro-Ayza et al. 2017
KY679254 ◁	17272-015 clone #1	NAG01 PPC	2001	*R. sylvatica*	Augusta	Virginia, USA	Isidoro-Ayza et al. 2017
KY679255 ◁	17272-015 clone #2	NAG01 PPC	2001	*R. sylvatica*	Augusta	Virginia, USA	Isidoro-Ayza et al. 2017
KY679256 ◁	17272-015 clone #3	NAG01 PPC	2001	*R. sylvatica*	Augusta	Virginia, USA	Isidoro-Ayza et al. 2017
KY679257 ◁	17272-015 clone #5	NAG01 PPC	2001	*R. sylvatica*	Augusta	Virginia, USA	Isidoro-Ayza et al. 2017
KY679258 ◁	17272-015 clone #6	NAG01 PPC	2001	*R. sylvatica*	Augusta	Virginia, USA	Isidoro-Ayza et al. 2017
KY679259 ◁	17272-015 clone #7	NAG01 PPC	2001	*R. sylvatica*	Augusta	Virginia, USA	Isidoro-Ayza et al. 2017
KY679260 ◁	17272-015 clone #9	NAG01 PPC	2001	*R. sylvatica*	Augusta	Virginia, USA	Isidoro-Ayza et al. 2017
KY679261 ◁	17272-015 clone #10	NAG01 PPC	2001	*R. sylvatica*	Augusta	Virginia, USA	Isidoro-Ayza et al. 2017
KY679262 ◁	18587-005 clone #1	NAG01 PPC	2003	*R. sphenocephala*	Harrison	Mississippi, USA	Isidoro-Ayza et al. 2017
KY679263 ◁	18587-005 clone #2	NAG01 PPC	2003	*R. sphenocephala*	Harrison	Mississippi, USA	Isidoro-Ayza et al. 2017
KY679264 ◁	18587-005 clone #3	NAG01 PPC	2003	*R. sphenocephala*	Harrison	Mississippi, USA	Isidoro-Ayza et al. 2017
KY679265 ◁	18587-005 clone #4	NAG01 PPC	2003	*R. sphenocephala*	Harrison	Mississippi, USA	Isidoro-Ayza et al. 2017
KY679266	18587-005 clone #5	NAG01 PPC	2003	*R. sphenocephala*	Harrison	Mississippi, USA	Isidoro-Ayza et al. 2017
KY679267 ◁	18587-005 clone #6	NAG01 PPC	2003	*R. sphenocephala*	Harrison	Mississippi, USA	Isidoro-Ayza et al. 2017
KY679268 ◁	18587-005 clone #7	NAG01 PPC	2003	*R. sphenocephala*	Harrison	Mississippi, USA	Isidoro-Ayza et al. 2017

KY679269 ◁	18587-005 clone #8	NAG01 PPC	2003	*R. sphenocephala*	Harrison	Mississippi, USA	Isidoro-Ayza et al. 2017
KY679270 ◁	18709-002 clone #14	NAG01 PPC	2003	*R. sphenocephala*	Prince George's	Maryland, USA	Isidoro-Ayza et al. 2017
KY679271 ◁	18709-002 clone #15	NAG01 PPC	2003	*R. sphenocephala*	Prince George's	Maryland, USA	Isidoro-Ayza et al. 2017
KY679272 ◁	18709-002 clone #17	NAG01 PPC	2003	*R. sphenocephala*	Prince George's	Maryland, USA	Isidoro-Ayza et al. 2017
KY679273 ◁	18709-002 clone #19	NAG01 PPC	2003	*R. sphenocephala*	Prince George's	Maryland, USA	Isidoro-Ayza et al. 2017
KY679274 ◁	18709-002 clone #20	NAG01 PPC	2003	*R. sphenocephala*	Prince George's	Maryland, USA	Isidoro-Ayza et al. 2017
KY679275 ◁	18709-002 clone #29	NAG01 PPC	2003	*R. sphenocephala*	Prince George's	Maryland, USA	Isidoro-Ayza et al. 2017
KY679276 ◁	18709-002 clone #30	NAG01 PPC	2003	*R. sphenocephala*	Prince George's	Maryland, USA	Isidoro-Ayza et al. 2017
KY679277 ◁	18709-002 clone #31	NAG01 PPC	2003	*R. sphenocephala*	Prince George's	Maryland, USA	Isidoro-Ayza et al. 2017
KY679278 ◁	18761-005 clone #1	NAG01 PPC	2003	*R. sphenocephala*	Prince George's	Maryland, USA	Isidoro-Ayza et al. 2017
KY679279 ◁	18761-005 clone #2	NAG01 PPC	2003	*R. sphenocephala*	Prince George's	Maryland, USA	Isidoro-Ayza et al. 2017
KY679280 ◁	18761-005 clone #3	NAG01 PPC	2003	*R. sphenocephala*	Prince George's	Maryland, USA	Isidoro-Ayza et al. 2017
KY679281 ◁	18761-005 clone #4	NAG01 PPC	2003	*R. sphenocephala*	Prince George's	Maryland, USA	Isidoro-Ayza et al. 2017
KY679282 ◁	18761-005 clone #6	NAG01 PPC	2003	*R. sphenocephala*	Prince George's	Maryland, USA	Isidoro-Ayza et al. 2017
KY679283 ◁	18761-005 clone #7	NAG01 PPC	2003	*R. sphenocephala*	Prince George's	Maryland, USA	Isidoro-Ayza et al. 2017
KY679284 ◁	18761-005 clone #8	NAG01 PPC	2003	*R. sphenocephala*	Prince George's	Maryland, USA	Isidoro-Ayza et al. 2017
KY679285 ◁	18761-005 clone #9	NAG01 PPC	2003	*R. sphenocephala*	Prince George's	Maryland, USA	Isidoro-Ayza et al. 2017
KY679286 ◁	22445-004 clone #1	NAG01 PPC	2007	*R. sphenocephala*	Suffolk	New York, USA	Isidoro-Ayza et al. 2017
KY679287 ◁	22445-004 clone #3	NAG01 PPC	2007	*R. sphenocephala*	Suffolk	New York, USA	Isidoro-Ayza et al. 2017
KY679288 ◁	22445-004 clone #4	NAG01 PPC	2007	*R. sphenocephala*	Suffolk	New York, USA	Isidoro-Ayza et al. 2017
KY679289 ◁	22445-004 clone #7	NAG01 PPC	2007	*R. sphenocephala*	Suffolk	New York, USA	Isidoro-Ayza et al. 2017
KY679290 ◁	22445-004 clone #8	NAG01 PPC	2007	*R. sphenocephala*	Suffolk	New York, USA	Isidoro-Ayza et al. 2017
KY679291 ◁	22445-004 clone #9	NAG01 PPC	2007	*R. sphenocephala*	Suffolk	New York, USA	Isidoro-Ayza et al. 2017
KY679292 ◁	22445-004 clone #12	NAG01 PPC	2007	*R. sphenocephala*	Suffolk	New York, USA	Isidoro-Ayza et al. 2017
KY679293 ◁	22445-004 clone #13	NAG01 PPC	2007	*R. sphenocephala*	Suffolk	New York, USA	Isidoro-Ayza et al. 2017
KY679294 ◁	24988-002 clone #2B	NAG01 PPC	2014	*R. sevosa*	Harrison	Mississippi, USA	Isidoro-Ayza et al. 2017
KY679295 ◁	24988-002 clone #9B	NAG01 PPC	2014	*R. sevosa*	Harrison	Mississippi, USA	Isidoro-Ayza et al. 2017
KY679296 ◁	24988-002 clone #10B	NAG01 PPC	2014	*R. sevosa*	Harrison	Mississippi, USA	Isidoro-Ayza et al. 2017
KY679297	24988-002 clone #13B	NAG01 PPC	2014	*R. sevosa*	Harrison	Mississippi, USA	Isidoro-Ayza et al. 2017
KY679298	24988-002 clone #14B	NAG01 PPC	2014	*R. sevosa*	Harrison	Mississippi, USA	Isidoro-Ayza et al. 2017

KY679299 ◁	24988-002 clone #24	NAG01 PPC	2014	*R. sevosa*	Harrison	Mississippi, USA	Isidoro-Ayza et al. 2017
KY679300	24988-002 clone #27	NAG01 PPC	2014	*R. sevosa*	Harrison	Mississippi, USA	Isidoro-Ayza et al. 2017
KY679301 ◁	24988-002 clone #30	NAG01 PPC	2014	*R. sevosa*	Harrison	Mississippi, USA	Isidoro-Ayza et al. 2017
KP122566	85.1	NAG01 PPC	2003	*R. sphenocephala*	Athens	Georgia, USA	Chambouvet et al. 2015
KP122567	85.3	NAG01 PPC	2003	*R. sphenocephala*	Athens	Georgia, USA	Chambouvet et al. 2015
KP122568	85.4	NAG01 PPC	2003	*R. sphenocephala*	Athens	Georgia, USA	Chambouvet et al. 2015
KP122569	85.5	NAG01 PPC	2003	*R. sphenocephala*	Athens	Georgia, USA	Chambouvet et al. 2015
EF675616	MJY-2007	NAG01 PPC	2003	*R. sphenocephala*	Athens	Georgia, USA	Davis et al. 2007
MF103770 ◁		NAG01 PPC		*R. sevosa*		Florida, USA	AE Savage, unpublished
MF103771 ◁		NAG01 PPC		*R. sevosa*		Florida, USA	AE Savage, unpublished
KP122571	T3.6.1	NAG01 Clade C	2010	*Hypsiboas geographicus*		French Guiana	Chambouvet et al. 2015
KP122591	SL10.A1	NAG01 Clade B	2013	*R. temporaria*	London	UK	Chambouvet et al. 2015
KP122637	A21.1	NAG01 Clade A	1998	*Afrana angolensis*		Tanzania	Chambouvet et al. 2015
KP122697	A11.2	NAG01 Clade A	2009	*Leptopelis vermiculatus*		Cameroon	Chambouvet et al. 2015
KP122738	CZ1.2_A2	NAG01 Clade A	2011	*Phrynobatrachus dispar*		Sao Tome	Chambouvet et al. 2015
AY919735	LG15-08	NAG01 alveolate		Lake George	Lake George	New York, USA	Richards et al. 2005
DQ244038	PAB5AU2004	NAG01 alveolate		Lake Pavin		France	Lefevre et al. 2007
EF196787	B91	NAG01 alveolate		lake water, Alpes		France	Lepere et al. 2008
EU162626	PAC11SP2005	NAG01 alveolate	2005	Lake Pavin		France	Lefevre et al. 2008
EU162629	PAA8SP2005	NAG01 alveolate	2005	Lake Pavin		France	Lefevre et al. 2008
AF530536	AT4-98	marine alveolate		Mid Atlantic Ridge			Lopez-Garcia et al. 2003
AF102171		*Perkinsus andrewsi*		non-amphibian			Coss et al. 2001
AF140295		*Perkinsus atlanticus*		non-amphibian			Robledo et al. 2000
AF497479		*Perkinsus marinus*		non-amphibian			Robledo et al. 1999
AY486139		*Perkinsus mediterraneus*		non-amphibian			Casas et al. 2004

Table S4.4. The top hit from the NCBI BLASTn MegaBLAST search of Panama tadpole 16S rDNA sequences in the nr database (accessed 18 June 2020).

Sample ID	Length	Query Cover (%)	E value	Identity (%)	Accession Number	Description
PA_T091	644	87	0	99.47	FJ784394	*Leptodactylus pentadactylus* voucher field number KRL 0838
PA_T092	631	89	0	99.47	FJ784394	*Leptodactylus pentadactylus* voucher field number KRL 0838
PA_T093	624	96	0	91.04	KY002923	*Hypsiboas lundii* voucher MCNAM 19591
PA_T094	622	96	0	90.89	KY002923	*Hypsiboas lundii* voucher MCNAM 19591
PA_T095	638	94	0	90.89	KY002923	*Hypsiboas lundii* voucher MCNAM 19591
PA_T096	652	92	0	90.61	MN921762	*Boana rosenbergi* isolate QCAZA23186
PA_T097	640	93	0	90.45	MN921762	*Boana rosenbergi* isolate QCAZA23186
PA_T098	627	96	0	90.61	MN921762	*Boana rosenbergi* isolate QCAZA23186
PA_T099	663	90	0	90.3	MN921762	*Boana rosenbergi* isolate QCAZA23186
PA_T105	655	85	0	99.47	FJ784435	*Engystomops pustulosus* voucher field number KRL 0916
PA_T106	650	86	0	99.65	KR863227	*Engystomops pustulosus* voucher AJC 1775
PA_T107	628	89	0	99.47	FJ784435	*Engystomops pustulosus* voucher field number KRL 0916
PA_T109	649	93	0	97.71	HQ290957	*Silverstoneia flotator*
PA_T115	634	92	0	97.96	AY843624	*Dendropsophus ebraccatus*
PA_T116	637	91	0	90.17	AY843597	*Dendropsophus anceps*
PA_T117	633	92	0	90.85	AY843597	*Dendropsophus anceps*
PA_T119	642	91	0	90.68	AY843597	*Dendropsophus anceps*
PA_T120	631	92	0	90.51	AY843597	*Dendropsophus anceps*
PA_T121	627	93	0	98.64	GQ366223	*Agalychnis callidryas* voucher RDS795
PA_T122	689	85	0	98.82	DQ502166	*Allobates talamancae* isolate 1147
PA_T123	629	89	0	99.82	KP149422	*Rhinella marina* voucher AJC 3852
PA_T124	665	86	0	93.57	EF566944	*Agalychnis callidryas* isolate DCC2134
PA_T126	629	93	0	98.14	AB612056	*Agalychnis callidryas*
PA_T128	642	88	0	99.65	KP149422	*Rhinella marina* voucher AJC 3852

PA_T129	650	87	0	99.82	KP149422	*Rhinella marina* voucher AJC 3852
PA_T131	599	96	0	97.96	DQ502166	*Allobates talamancae* isolate 1147
PA_T132	618	93	0	97.44	DQ502166	*Allobates talamancae* isolate 1147
PA_T133	639	91	0	99.15	DQ502166	*Allobates talamancae* isolate 1147
PA_T134	661	89	0	98.48	DQ502166	*Allobates talamancae* isolate 1147
PA_T135	624	92	0	92.13	DQ502166	*Allobates talamancae* isolate 1147
PA_T136	630	92	0	99.15	DQ502166	*Allobates talamancae* isolate 1147
PA_T138	630	92	0	99.15	DQ502166	*Allobates talamancae* isolate 1147
PA_T139	627	92	0	98.98	DQ502166	*Allobates talamancae* isolate 1147
PA_T140	630	92	0	99.15	DQ502166	*Allobates talamancae* isolate 1147
PA_T141	639	88	0	99.82	KP149422	*Rhinella marina* voucher AJC 3852
PA_T142	677	83	0	99.65	FJ784320	*Smilisca sila*
PA_T143	619	97	0	90.61	MN921762	*Boana rosenbergi* isolate QCAZA23186
PA_T144	631	88	0	96.12	KP149422	*Rhinella marina* voucher AJC 3852
PA_T147	628	89	0	99.47	KP149422	*Rhinella marina* voucher AJC 3852
PA_T148	629	89	0	99.65	KP149422	*Rhinella marina* voucher AJC 3852
PA_T149	631	89	0	95.13	KP149422	*Rhinella marina* voucher AJC 3852
PA_T150	635	89	0	99.29	KP149422	*Rhinella marina* voucher AJC 3852
PA_T151	631	89	0	99.65	FJ784320	*Smilisca sila*
PA_T153	619	91	0	99.65	FJ784320	*Smilisca sila*
PA_T155	630	89	0	99.47	FJ784320	*Smilisca sila*
PA_T156	622	89	0	94.18	FJ784320	*Smilisca sila*
PA_T157	636	87	0	91.3	FJ784320	*Smilisca sila*
PA_T158	663	85	0	99.65	FJ784320	*Smilisca sila*
PA_T159	630	89	0	99.12	FJ784320	*Smilisca sila*
PA_T160	615	91	0	99.12	FJ784320	*Smilisca sila*
PA_T161	623	96	0	90.45	MN921762	*Boana rosenbergi* isolate QCAZA23186
PA_T162	677	81	0	98.92	KR012611	*Rhinella alata* voucher CH:9192
PA_T163	693	79	0	98.92	KR012611	*Rhinella alata* voucher CH:9192
PA_T164	657	84	0	99.1	KR012611	*Rhinella alata* voucher CH:9192

PA_T165	697	79	0	99.1	KR012611	*Rhinella alata* voucher CH:9192
PA_T167	627	88	0	99.1	KR012611	*Rhinella alata* voucher CH:9192
PA_T168	698	79	0	99.1	KR012611	*Rhinella alata* voucher CH:9192
PA_T169	636	87	0	99.28	KR012611	*Rhinella alata* voucher CH:9192
PA_T170	658	84	0	99.1	KR012611	*Rhinella alata* voucher CH:9192
PA_T171	683	81	0	99.1	KR012611	*Rhinella alata* voucher CH:9192

Table S4.5. Details of published amphibian 16S rDNA sequences used as references in phylogenetic analysis presented in Figure 4.2.

Accession Number	Sample ID/voucher	Order	Sub-order	Super Family	Family	Species	Country	Reference
DQ502166	SIUC 7667	Anura	Neobatrachia	Dendrobatoidea	Aromobatidae	*Allobates talamancae*	Panama	Grant et al. (2006)
AY364562	QCAZ15562	Anura	Neobatrachia	Dendrobatoidea	Aromobatidae	*Colostethus talamancae*	Ecuador	Santos et al. (2003)
KP149439	AJC 3900	Anura	Neobatrachia	Dendrobatoidea	Aromobatidae	*Allobates niputide*	Colombia	Guarnizo et al. (2015)
DQ502211	OMNH 34474	Anura	Neobatrachia	Dendrobatoidea	Aromobatidae	*Allobates brunneus*	Brazil	Grant et al. (2006)
HQ290957	TNHCFS4804	Anura	Neobatrachia	Dendrobatoidea	Dendrobatidae	*Silverstoneia flotator*	Panama	Santos & Cannatella (2011)
DQ502104	MHNUC 321	Anura	Neobatrachia	Dendrobatoidea	Dendrobatidae	*Silverstoneia nubicola*	Colombia	Grant et al. (2006)
MK881437	QCAZ:42251	Anura	Neobatrachia	Dendrobatoidea	Dendrobatidae	*Epipedobates boulengeri*	Ecuador	Paez & Santiago (2019)
FJ784394	KRL 0838	Anura	Neobatrachia	Hyloidea	Leptodactylidae	*Leptodactylus pentadactylus*	Panama	Crawford et al. (2010)
MN921762	QCAZA23186	Anura	Neobatrachia	Hyloidea	Hylidae	*Boana rosenbergi*	Ecuador	Caminer & Ron (2020)
KY002923	MCNAM 19591	Anura	Neobatrachia	Hyloidea	Hylidae	*Hypsiboas lundii*	Brazil	Santiago et al. unpublished
KY002932	MCNAM 20163	Anura	Neobatrachia	Hyloidea	Hylidae	*Hypsiboas polytaenius*	Brazil	Santiago et al. unpublished
MH259792	ZUFRJ 15429	Anura	Neobatrachia	Hyloidea	Hylidae	*Brachychephalus sp.*	Brazil	Folly et al. unpublished
FJ784320		Anura	Neobatrachia	Hyloidea	Hylidae	*Smilisca sila*	Panama	Crawford et al. (2010)
AY843764	RdS 787	Anura	Neobatrachia	Hyloidea	Hylidae	*Smilisca phaeota*	MD, USA (captive)	Faivovich et al. (2005)
DQ830814	MZFC 17046	Anura	Neobatrachia	Hyloidea	Hylidae	*Triprion petasatus*	Mexico	Smith et al. unpublished
AY843601		Anura	Neobatrachia	Hyloidea	Hylidae	*Hyla arborea*	Germany (captive)	Faivovich et al. (2005)

DQ830810	LSUMZ 48181	Anura	Neobatrachia	Hyloidea	Hylidae	*Hyla cinerea*	LA, USA	Smith et al. unpublished
KR863227	AJC 1775	Anura	Neobatrachia	Hyloidea	Leptodactylidae	*Engystomops pustulosus*	Panama	Paz et al. (2015)
AY843624	RdS 790	Anura	Neobatrachia	Hyloidea	Hylidae	*Dendropsophus ebraccatus*	Belize	Faivovich et al. (2005)
AY843597	CFBH 5797	Anura	Neobatrachia	Hyloidea	Hylidae	*Dendropsophus anceps*	Brazil	Faivovich et al. (2005)
KR012611	CH:9192	Anura	Neobatrachia	Hyloidea	Bufonidae	*Rhinella alata*	Panama	dos Santos et al. (2015)
DQ158471	QCAZ 13896	Anura	Neobatrachia	Hyloidea	Bufonidae	*Rhinella margaritifera*		Pramuk (2006)
KP149422	AJC 3852	Anura	Neobatrachia	Hyloidea	Bufonidae	*Rhinella marina*	Colombia	Guarnizo et al. (2015)
AB612056	No. Hy01	Anura	Neobatrachia	Hyloidea	Phyllomedusidae	*Agalychnis callidryas*		Kurabayashi et al. (2011)
KC589394	MHUA_A_7316	Anura	Neobatrachia	Hyloidea	Phyllomedusidae	*Agalychnis terranova*	Colombia	Rivera-Correa et al. (2013
EF107170	0907AmbMex	Urodela		Salamandroidea	Ambystomatidae	*Ambystoma mexicanum*	Mexico	Roelants et al. (2007)
DQ283407	AMNH A164658	Urodela		Salamandroidea	Ambystomatidae	*Ambystoma tigrinum*	AZ, USA	Frost et al. (2006)
DQ283445	AMNH A168418	Urodela		Salamandroidea	Salamandridae	*Pleurodeles waltl*	(captive)	Frost et al. (2006)
DQ092266	Anc12	Urodela		Salamandroidea	Salamandridae	*Pleurodeles nebulosus*	Algeria	Carranza & Amat (2005)
AY581644	MHNG 2644.53	Anura	Mesobatrachia	Pipoidea	Pipidae	*Xenopus laevis*	Zambia	Evans et al. (2004)

Chapter 5. Discussion

Table S5.1. Specimen data for tadpoles from which gut tissue was harvested for profiling intestinal eukaryotic microbes. Samples highlighted in grey are positive for PCR detection of PPC (using total DNA extracted from liver tissue). PA_T128, HA_1, and HA_2 were confirmed using TA-cloning and Sanger sequencing. RSRB99 and RSRC73-74 were confirmed using a PPC-specific qPCR assay. Samples with a "×" in the "Used for library prep" column did not yield a PCR amplicon from total DNA extracted from gut tissue and were therefore excluded from further analysis.

Sample ID	Location	Site	Colletion date	Species	Family	Health	Used for library prep
PA_T128	PA	EVA3	22/11/2018	*Rhinella marina*	Bufonidae	normal	×
PA_T129	PA	EVA3	22/11/2018	*Rhinella marina*	Bufonidae	normal	×
PA_T130	PA	EVA3	22/11/2018	NA	NA	normal	×
PA_T131	PA	EVA4	22/11/2018	*Allobates talamancae*	Bufonidae	normal	×
PA_T132	PA	EVA4	22/11/2018	*Engystomops pustulosus*	Leptodactylidae	normal	×
PA_T133	PA	EVA4	22/11/2018	*Smilisca sila*	Hylidae	normal	×
PA_T134	PA	EVA4	22/11/2018	*Allobates talamancae*	Aromobatidae	normal	×
PA_T137	PA	EVA4	22/11/2018	NA	NA	normal	×
PA_T138	PA	EVA4	22/11/2018	*Allobates talamancae*	Aromobatidae	normal	×
PA_T151	PA	SNP7	24/11/2018	*Smilisca sila*	Hylidae	normal	×
PA_T152	PA	SNP7	24/11/2018	NA	NA	normal	×
PA_T153	PA	SNP7	24/11/2018	*Smilisca sila*	Hylidae	normal	×
PA_T154	PA	SNP7	24/11/2018	NA	NA	normal	×
PA_T155	PA	SNP7	24/11/2018	*Smilisca sila*	Hylidae	normal	×
PA_T156	PA	SNP7	24/11/2018	*Smilisca sila*	Hylidae	normal	×
PA_T162	PA	SNP8	24/11/2018	*Rhinella marina*	Bufonidae	normal	×

PA_T163	PA	SNP8	24/11/2018	*Rhinella marina*	Bufonidae	normal	×
PA_T164	PA	SNP8	24/11/2018	*Rhinella marina*	Bufonidae	normal	×
PA_T165	PA	SNP8	24/11/2018	*Rhinella marina*	Bufonidae	normal	×
PA_T166	PA	SNP8	24/11/2018	NA	NA	normal	×
PA_T167	PA	SNP8	24/11/2018	*Rhinella marina*	Bufonidae	normal	×
ACF4-45	FL, USA	ACF4	08/03/2019	*Lithobates sphenocephalus*	Ranidae	normal	×
ACF4-46	FL, USA	ACF4	08/03/2019	*Lithobates sphenocephalus*	Ranidae	normal	×
FFCC060	FL, USA	FFC3	05/03/2019	*Lithobates sphenocephalus*	Ranidae	normal	✓
FFCC061	FL, USA	FFC3	05/03/2019	*Lithobates sphenocephalus*	Ranidae	normal	✓
FFCC062	FL, USA	FFC3	05/03/2019	*Lithobates sphenocephalus*	Ranidae	normal	✓
FFCC063	FL, USA	FFC3	05/03/2019	*Lithobates sphenocephalus*	Ranidae	normal	✓
FFCC064	FL, USA	FFC3	05/03/2019	*Lithobates sphenocephalus*	Ranidae	normal	✓
FFRB020	FL, USA	FFR	05/03/2019	*Lithobates sphenocephalus*	Ranidae	normal	×
FFRB021	FL, USA	FFR	05/03/2019	*Lithobates sphenocephalus*	Ranidae	normal	×
FFRB022	FL, USA	FFR	05/03/2019	*Lithobates sphenocephalus*	Ranidae	normal	×
FFRB023	FL, USA	FFR	05/03/2019	*Lithobates sphenocephalus*	Ranidae	normal	✓
FFRB024	FL, USA	FFR	05/03/2019	*Lithobates sphenocephalus*	Ranidae	normal	×
NOX3-6	FL, USA	NOX3	09/03/2019	*Lithobates sphenocephalus*	Ranidae	normal	✓
NOX3-7	FL, USA	NOX3	09/03/2019	*Lithobates sphenocephalus*	Ranidae	normal	✓
NOX3-8	FL, USA	NOX3	09/03/2019	*Lithobates sphenocephalus*	Ranidae	normal	✓
PL503	FL, USA	PL	04/03/2019	*Lithobates sphenocephalus*	Ranidae	normal	×
PL504	FL, USA	PL	04/03/2019	*Lithobates sphenocephalus*	Ranidae	normal	×
PL505	FL, USA	PL	04/03/2019	*Lithobates sphenocephalus*	Ranidae	normal	✓
PL506	FL, USA	PL	04/03/2019	*Lithobates sphenocephalus*	Ranidae	normal	✓
PL507	FL, USA	PL	04/03/2019	*Lithobates sphenocephalus*	Ranidae	normal	✓
RSRB99	FL, USA	RSRP2	06/03/2019	*Lithobates sphenocephalus*	Ranidae	normal	✓
RSRC73	FL, USA	RSRP3	06/03/2019	*Lithobates sphenocephalus*	Ranidae	normal	✓
RSRC74	FL, USA	RSRP3	06/03/2019	*Lithobates sphenocephalus*	Ranidae	normal	✓
HA07	UK	Surrey	Jul-19	*Hyla arborea*	Hylidae	symptomatic	✓
HA08	UK	Surrey	Jul-19	*Hyla arborea*	Hylidae	symptomatic	✓

HA_1	UK	Surrey	Oct-19	*Hyla arborea*	Hylidae	symptomatic	✓
HA_2	UK	Surrey	Oct-19	*Hyla arborea*	Hylidae	symptomatic	✓

BIBLIOGRAPHY

Alacid E, Reñé A, Garcés E (2015) New insights into the parasitoid *Parvilucifera sinerae* life cycle: the development and kinetics of infection of a bloom-forming dinoflagellate host. *Protist* 166: 677-699

Andino F, Chen G, Li Z, Grayfer L, Robert J (2012) Susceptibility of *Xenopus laevis* tadpoles to infection by the ranavirus Frog virus 3 correlates with a reduced and delayed innate immune response in comparison with adult frogs. *Virology* 432: 435-443

Austin Jr RM (2000) Cutaneous microbial flora and antibiosis in *Plethodon ventralis*. In: Bruce RC, Jaeger RG, Houck LD (Eds), *The biology of plethodontid salamanders* (127-136). Kluwer Academic Plenum Publishers, New York

Avery OT, MacLeod CM, McCarty M (1944) Studies of the chemical nature of the substance inducing transformation of pneumococcal types. Induction of transformation by a deoxyribonucleic acid fraction isolated from *Pneumococcus* Type III. *J Exp Med* 79: 137-158

Balmer O & Tanner M (2011) Prevalence and implications of multiple-strain infections. *Lancet Infect Dis* 11: 868-878

Becker CG, Fonseca CR, Haddad CFB, Batista RF, Prado PI (2007) Habitat split and the global decline of amphibians. *Science* 318: 1775-1777

Berbee ML (2001) The phylogeny of plant and animal pathogens in the Ascomycota. *Physiol Mol Plant Pathol* 59: 165-187

Berdoy M, Webster JP, Macdonald DW (2000) Fatal attraction in rats infected with *Toxopasma gondii*. *P Roy Soc Lond B-Biol Sci* 267(1452): 1591-94

Berger L, Speare R, Daszak P, Green DE, Cunningham, AA, Goggin CL, Slocombe R, Ragan MA, Hyatt AD, McDonald KR, Hines HB, Lips KR, Marantelli G, Parkes H (1998) Chytridiomycosis causes amphibian mortality associated with population declines in the rain forest of Australia and Central America. *Proc Natl Acad Sci USA* 95: 9031-9036

Bickford D, Iskandar D, Barlian A (2008) A lungless frog discovered on Borneo *Curr Biol* 18: R374-R375

Black EM, Lowings JP, Smith J, Heaton PR, McElhinney LM (2002) A rapid RT-PCR method to differentiate six established genotypes of rabies and rabies-related viruses using TaqMan technology. *J Virol Methods* 105: 25-35

Blanchong JA, Robinson SJ, Samuel MD, Foster JT (2016) Application of genetics and genomics to wildlife epidemiology. *J Wildl Manage* 80: 593-608

Blaustein AR, Hoffman PD, Hokit DG, Kiesecker JM, Walls SC, Hays JB (1994) UV repair and resistance to solar UV-B in amphibian eggs: a link to population declines? *Proc Natl Acad Sci USA* 91:1791-1795

Blaxter ML, De Ley P, Garey JR, Liu LX, Scheldeman P, Vierstraete A, Vanfleteren JR, Mackey LY, Dorris M, Frisse LM, Vida JT, Thomas WK (1998) A molecular evolutionary framework for the phylum Nematoda. *Nature* 392: 71-75

Blooi M, Pasmans F, Longcore JE, Spitzen-van der Sluijs A, Vercammen F, Martel A (2013) Duplex real-time PCR for rapid simultaneous detection of Batrachochytrium dendrobatidis and Batrachochytrium salamandrivorans in amphibian samples. *J Clin Microbiol* 51: 4173-4177

Blouin NA, Lane CE (2012) Red algal parasites: models for a life history evolution that leaves photosynthesis behind again and again. *BioEssays* 34: 226-235

Borkin LJ, Belimov GT, Sedalishchev VT (1984) New data on distribution of amphibians and reptiles in Yakutia. *Proc Zool Inst USSR Acad Sci*, Leningrad 124: 89-101

Bower SM, Carnegie RB Goh B, Jones SR, Lowe GJ, Mak MW (2004) Preferential PCR amplification of parasitic protistan small subunit rDNA from metazoan tissues. *J Eukaryot Microbiol* 51: 325-332

Brunner JL, Schock DM, Collins JP (2007) Transmission dynamics of the amphibian ranavirus Ambystoma tigrinum virus. *Dis Aquat Org* 77: 87-95

Bull CM, Godfrey SS, Gordon DM (2012) Social networks and the spread of Salmonella in a sleepy lizard population. *Mol Ecol* 21: 4386-4392

Burdon JJ, Jarosz AM (1988) The ecological genetics of plant-pathogen interactions in natural communities. *Phil Trans R Soc Ser B* 321: 349-363

Bustin SA, Benes V, Garson JA, Hellemans J, Huggett J, Kubista M, Mueller R, Nolan T, Pfaffl MW, Shipley GL, Vandesompele J, Wittwer CT (2009) The MIQE

guidelines: minimum information for publication of quantitative real-time PCR experiments. *Clin Chem* 55: 611-622

Callahan BJ, McMurdie PJ, Rosen MJ, Han AW, Johnson AJA, Holmes SP (2016) DADA2: High-resolution sample inference from Illumina amplicon data. *Nat Methods* 13(7): 581-3

Caminer MA, Ron SR (2020) Systematics of the *Boana semilineata* species group (Anura: Hylidae), with a description of two new species from Amazonian Ecuador. *Zool J Linn Soc* DOI:10.1093/zoolinnean/zlaa002

del Campo J, Heger TF, Rodriguez-Martinez R, Worden AZ, Richards TA, Massana R, Keeling PJ (2019) Assessing the Diversity and Distribution of Apicomplexans in Host and Free-Living Environments Using High-Throughput Amplicon Data and a Phylogenetically Informed Reference Framework. *Front Microbiol* 10: 2373

Carey C, Bryant CJ (1995) Possible interrelations among environmental toxicants, amphibian development, and decline of amphibian populations. *Environ Health Perspect* 103(4): 13-17

Carey C, Cohen N, Rollins-Smith L (1999) Amphibian declines: an immunological perspective. *Dev Comp Immunol* 23: 459-472

Carranza S, Amat F (2005) Taxonomy, biogeography and evolution of *Euproctus* (Amphibia: Salamandridae), with the resurrection of the genus *Calotriton* and the description of a new endemic species from the Iberian Peninsula. *Zool J Linn Soc* 145(4): 555-582

Casas SM, et al. (2004) *Perkinsus mediterraneus* n. sp., a protistan parasite of the European flat oyster *Ostrea edulis* from the Balearic Islands, Mediterranean Sea. *Dis Aquat Organ* 58: 231-244

Cavalier-Smith T (2004) Only six kingdoms of life. *Proc R Soc Lond B* 271: 1251-1262

Cavalier-Smith T, Chao EE (2004) Protalveolate phylogeny and systematics and the origins of Sporozoa and dinoflagellates (phylum Myzozoa nom. Nov.) *Eur J Protistol* 40(3): 185-212

Chambouvet A, Morin P, Marie D, Guillou L (2008) Control of toxic marine dinoflagellate blooms by serial parasitic killers. *Science* 322(5905): 1254-1257

Chambouvet A, Gower DJ, Jirků M, Yabsley MJ, Davis AK, Leonard G, Maguire F, Doherty-Bone TM, Bittencourt-Silva GB, Wilkinson M, Richards TA (2015) Cryptic infection of a broad taxonomic and geographic diversity of tadpoles by Perkinsea protists. *Proc Natl Acad Sci USA* 112(34): E4743-E4751

Chambouvet A, Valigurová A, Pinheiro LM, Richards TA, Jirků M (2016) *Nematopsis temporariae* (Gregarinasina, Apicomplexa, Alveolata) is an intracellular infectious agent of tadpole livers. *Environ Microbiol Rep* 8: 675-679

Chambouvet A, Smilansky V, Jirků M, Isidoro-Ayza M, Itoı¨z S, Derelle E, et al. (2020) Diverse alveolate infections of tadpoles, a new threat to frogs? PLoS Pathog 16(2): e1008107

Chanson J, Hoffman M, Cox NA, Stuart S (2008) The State of the World's Amphibians. In: Stuart *et al.* (Eds) *Threatened Amphibians of the World* (33-52) Barcelona/Gland/Arlington: Lynx Edicions/IUCN/Conservation International

Chivian E (2013) Global environmental threats: why they are hard to see and how a medical model may contribute to their understanding. *Cardiovasc Diagn Ther* 3(2): 93-104

Chu FLE, Hale RC (1994) Relationship between pollution and susceptibility to infectious disease in the eastern oyster, *Crassostrea virginica*. *Mar Environ Res* 38(4): 243-256

Clarke B (1997) The natural history of amphibian skin secretions, their normal functioning and potential medical appliciations. *Biol Rev* 72(3): 365-379

Collins JP, Cheek JE (1983) Effect of food and density on development of typical and cannibalistic salamander larvae in Ambystoma tigrinum nebulosum. *Am Zool* 23: 77-84

Collins JP, Storfer A (2003) Global amphibian declines: sorting the hypotheses. *Divers Distributions* 9: 89-98

Cook JO (2008) Transmission and occurrence of *Dermomycoides* sp. in *Rana sevosa* and other ranids in the North Central Gulf of Mexico States (Thesis, University of Southern Mississippi)

Cook JO (2009) An alveolate agent in southeastern amphibians. Southeastern Partners in Amphibian and Reptile Conservation, Disease, Pathogens and

Parasites Task Team, Information Sheet 5 <www.separc.org/products/diseases-and-parasites-of-herpetofauna>. Accessed 11 January 2018

Coss CA, Robledo JAF, Ruiz GM, Vasta GR (2001) Description of *Perkinsus andrewsi* n. sp. isolated from the baltic clam (Macoma balthica) by characterization of the ribosomal RNA locus and development of a species-specific PCR-based diagnostic assay. *J Euk Microbiol* 48(52-61)

de Coster W, D'Hert S, Schultz DT, Cruts M, Van Broeckhoven C (2018) NanoPack: visualizing and processing long-read sequencing data. *Bioinformatics* 34(15): 2666-2669

Cox FEG (2002) History of Human Parasitology. *Clin Microbiol Rev* 15(4): 595-612

Crawford AJ, Lips KR, Bermingham E (2010) Epidemic disease decimates amphibian abundance, species diversity, and evolutionary history in the highlands of central Panama. *Proc Natl Acad Sci USA* 107: 13777-13782

Crompton T, Peitsch MC, MacDonald HR, Tschopp J (1992) Propidium iodide staining correlates with the extent of DNA degradation in isolated nuclei. *Biochem Biophys Res Commun* 183: 532-537

Crump ML (1983) Opportunistic cannibalism by amphibian larvae in temporary aquatic environments. *Am Nat* 121: 281-289

Crump ML (2009) Amphibian diversity and life history. In: Dodd Jr CK (Ed), *Amphibian Ecology and Conservation* (3-17) Oxford University Press, New York

Cullingham CI, CJ Kyle CJ, Pond BA, Rees EE, White BN (2009) Differential permeability of rivers to raccoon gene flow corresponds to rabies incidence in Ontario, Canada. *Mol Ecol* 18: 43-53

Curtis VA (2014) Infection-avoidance behaviour in humans and other animals. *Trends Immunol* 35: 457-464

Daszak P, Berger L, Cunningham AA, Hyatt AD, Green DE, Speare R (1999) Emerging infectious diseases and amphibian population declines. *Emerg Infect Dis* 5: 735-748

Daszak P, Strieby A, Cunningham AA, Longcore JE, Brown CC, Porter D (2004) Experimental evidence that the bullfrog (*Rana catesbeiana*) is a potential carrier of chytridiomycosis, an emerging fungal disease of amphibians. *Herpetol J* 14: 201-207

Davidson EW, Parris M, Collins JP, Longcore JE, Pessier AP, Brunner J (2003) Pathogenicity and transmission of chytridiomycosis in tiger salamanders (*Ambystoma tigrinum*) *Copeia* 2003: 601-607

Davis AK, Yabsley MJ, Keel MK, Maerz JC (2007) Discovery of a novel alveolate pathogen affecting Southern Leopard frogs in Georgia: description of the disease and host effects. *EcoHealth* 4: 310-317

Davis NM, Proctor DM, Holmes SP, Relman DA, Callahan BJ (2018) Simple statistical identification and removal of contaminant sequences in marker-gene and metagenomics data. *Microbiome* 6: 226

Day KP, Hayward RE, Dyer M (1998) The biology of *Plasmodium falciparum* transmission stages. *Parasitology* 116S: S95-S109

Debode F, Marien A, Janssen E, Bragard C, Berben G (2017) The influence of amplicon length on real-time PCR results. *Biotechnol Agron Soc Environ* 21: 3-11

Decelle J, Suzuki N, Mahe F, de Vargas C, Not F (2012) Molecular phylogeny and morphological evolution of the acantharia (radiolaria). *Protist* 163: 435-450

Densmore CL, Green DE (2007) Diseases of amphibians. *ILAR J* 48: 235-254

Devanga Ragupathi NK, Muthuirulandi Sethuvel DP, Inbanathan FY, Veeraraghavan B (2017) Accurate differentiation of *Escherichia coli* and *Shigella serogroups*: challenges and strategies. *New Microbes New Infect* 21: 58-62

Dickman M (1968) The effect of grazing by tadpoles on the structure of a periphyton community. *Ecology* 49(6): 1188-1190

Dixo M, Metzger JP, Morgante JS, Zamudio KR (2009) Habitat fragmentation reduces genetic diversity and connectivity among toad populations in the Brazilian Atlantic Coastal Forest. *Biol Conserv* 142: 1560-1569

Dong J, Olano JP, McBride JW, Walker DH (2008) Emerging pathogens: challenges and successes of molecular diagnostics. *J Mol Diagn* 10: 185-197

Duellman WE, Marion AB, Hedges SB (2016) Phylogenetics, classification, and biogeography of tree frogs (Amphibia: Anura: Arboranae). *Zootaxa* 4104(1): 001-109

Dungan CF, Reece KS, Hamilton RM, Stokes NA, Burreson EM (2007) Experimental cross-infection by *Perkinsus marinus* and *P. chesapeaki* in three sympatric species of Chesapeake Bay oysters and clams. *Dis Aquat Org* 76: 67-75

Echaubard P, Leduc J, Pauli B, Chinchar VG, Robert J, Lesbarreres D (2014) Environmental dependency of amphibian-ranavirus genotypic interactions: evolutionary perspectives on infectious diseases. *Evol Appl* 7: 723-733

Elgar MA, Crespi BJ (1992) Cannibalism: ecology and evolution among diverse taxa. Oxford University Press, Oxford

Ellison AR, Tunstall T, DiRenzo GV, Hughey MC, Rebollar EA, Belden LK, Harris RN, Ibáñez R, Lips KR, Zamudio KR (2015) More than skin deep: functional genomic basis for resistance to amphibian chytridiomycosis. *Genome Biol Evol* 7(1): 286-298

Elwood HJ, Olsen GJ, Sogin ML (1985) The small-subunit ribosomal RNA gene sequences from the hypotrichous ciliates *Oxytricha nova* and *Stylonychia pustulata*. *Mol Biol Evol* 12: 399-410

Evans BJ, Kelley DB, Tinsley RC, Melnick DJ, Cannatella DC (2004) A mitochondrial DNA phylogeny of African clawed frogs: phylogeography and implications for polyploid evolution. *Mol Phylogenet Evol* 33: 197-213

Evans KM, Wortley AH, Mann DG (2007) An assessment of potential diatom “barcode” genes (cox1, rbcL, SSU and ITS rDNA) and their effectiveness in determining relationships in Sellaphora (Bacillariophyta). *Protist* 158: 349-364

Ewald PW, Mims CA, Lachmann PJ, Hughes AL, Gillett JD, Parker CE (1994) Evolution of Mutation Rate and Virulence among Human Retroviruses. *Philos Trans R Soc Lond B Biol Sci* 346: 333-343

Faivovich J, Haddad CFB, Garcia PCA, Frost DR, Campbell JA, Wheeler WC (2005) Systematic review of the frog family Hylidae, with special reference to hylinae: phylogenetic analysis and taxonomic revision. *Bull Am Mus Nat Hist* 294: 6-228

Faivovich J, Haddad CFB, Baeta D, Jungfer KH, Alvares GFR, Brandao RA, Sheil C, Barrientos LS, Barrio-Amoros CL, Cruz CAG, Wheeler WC (2010) The phylogenetic relationships of the charismatic poster frogs, Phyllomedusinae (Anura, Hylidae). *Cladistics* 26: 227-261

Fast NM, Xue L, Bingham S, Keeling PJ (2002) Re-examining alveolate evolution using multiple protein molecular phylogenies. *J Eukaryot Microbiol* 49: 30-37

Feder ME, Burggren WW (1985) Skin breathing in vertebrates. *Sci Am* 253: 126-142

Fites JS, Ramsey JP, Holden WM, Collier SP, Sutherland DM, Reinert, LK, Gayek AS, Dermody TS, Aune TM, Oswald-Richter K, Rollins-Smith LA (2013) The invasive chytrid fungus of amphibians paralyzes lymphocyte responses. *Science 342*(6156): 366-369

Folly M, Amaral LC, Pombal JP Jr, Carvalho-e-Silva, SP. Underestimated biodiversity near the metropolitan region of Rio de Janeiro state, Brazil: a new pumpkin toadlet *Brachycephalus* (Brachycephalidae: Brachycephaloidea). Submitted (26-APR-2018) Zoology, National Museum, Federal University of Rio de Janeiro, Brazil

Fossiner W, Hawksworth David, eds. (2009) Protist Diversity and Geographical Distribution. *Topics in Biodiversity and Conservation*. Springer Netherlands. p. 111

Fredericks DN, Relman DA (1996) Sequence-based identification of microbial pathogens: a reconsideration of Koch's postulates. *Clin Microbiol Rev* 9(1): 18-33

Frost DR, Grant T, Faivovich J, Bain RH, Haas A, Haddad CFB, De Sa RO, Channing A, Wilkinson M, Donnellan SC, Raxworthy CJ, Campbell JA, Blotto BL, Moler P, Drewes RC, Nussbaum RA, Lynch JD, Green DM, Wheeler WC (2006) The amphibian tree of life. *Bull Am Mus Natl Hist* 297: 8-370

Gallant A, Klaver R, Casper G, Lannoo M (2007) Global rates of habitat loss and implications for amphibian conservation. *Copeia* 4: 967-979

Galli L, Pereira A, Marquez A, Mazzoni R (2006) Ranavirus detection by PCR in cultured tadpoles (*Rana catesbeiana* Shaw, 1802) from South America. *Aquaculture* 257: 78-82

Gardner RS, Wahba AJ, Basilio C, Miller RS, Lengyel P, Speyer JF (1962) Synthetic polynucleotides and the amino acid code, VII. *Proc Natl Acad Sci USA* 48: 2087-2094

Gascuel O (2017) BIONJ: an improved version of the NJ algorithm based on a simple model of sequence data. *Mol Biol Evol* 14: 685-695

Gauthier JD, Vasta GR (1995) *In vitro* culture of the eastern oyster parasite *Perkinsus marinus*: optimization of the methodology. *J Invertebr Pathol* 66: 156-168

Gentekaki E, Lynn DH (2009) High-level genetic diversity but no population structure inferred from nuclear and mitochondrial markers of the peritrichous ciliate *Carchesium polypinum* in the Grand River basin (North America). *Appl Environ Microbiol* 75: 3187-3195

Gile GH, Stern RF, James ER, Keeling PJ (2010) DNA barcoding of Chlorarachniophytes using nucleomorph ITS sequences. *J Phycol* 46: 743-750

Gleason FH, Chambouvet A, Sullivan BK, Lilje O, Rowley JJL (2014) Multiple zoosporic parasites pose a significant threat to amphibian populations. *Fungal Ecol* 11: 181-192

Goggin CL, Sewell KB, Lester RJG (1989) Cross-infection experiments with Australian *Perkinsus* species. *Dis Aquat Org* 7: 55-59

Gómez F (2012) A checklist and classification of living dinoflagellates (Dinoflagellata Alveolata). *CICIMAR Oceánides* 27: 65-140

Gong J, Dong J, Liu X, Massana R. (2013) Extremely high copy numbers and polymorphisms of the rDNA operon estimated from single cell analysis of oligotrich and peritrich ciliates. *Protist* 164: 369-379

Gortázar C, Diez-Delgado I, Barasona JA, Vicente J, De la Fuente J, Boadella M (2014) The wild side of disease control at the wildlife-livestock-human interface: a review. *Front Vet Sci* 1:1-12

Gosner KL (1960) A simplified table for staging anuran embryos and larvae with notes on identification. *Herpetologica* 16: 183-190

Gouy M, Guindon S, Gascuel O (2010) SeaView version 4: a multiplatform graphical user interface for sequence alignment and phylogenetic tree building. *Mol Biol Evol* 27(2): 221-224

Granoff A, Came PE, Rafferty KA (1965) The isolation and properties of viruses from *Rana pipiens*: their possible relationship to the renal adenocarcinoma of the leopard frog. *Ann NY Acad Sci* 126: 237-255

Grant T, Frost DR, Caldwell JP, Gagliardo R, Haddad CFB, Kok PJR, Means DB, Noonan BP, Schargel WE, Wheeler WC (2006) Phylogenetic systematics of dart-poison frogs and their relatives (Anura: Athesphatanura: Dendrobatidae). *Bull Amer Mus Nat Hist* 299: 1-262

Gratwicke B, Evans MJ, Jenkins PT, Kusrini MD, Moore RD, Sevin J, Wildt DE (2010) Is the international frog legs trade a potential vector for deadly amphibian pathogens? *Front Ecol Environ* 8: 438-442

Gray MJ, Miller DL, Hoverman JT (2009) Ecology and pathology of amphibian ranaviruses. *Dis Aquat Org* 87: 243-266

Grear DA, Samuel MD, Scribner KT, Weckworth BV, Langenberg JA (2010) Influence of genetic relatedness and spatial proximity on chronic wasting disease infection among female white-tailed deer. *J Appl Ecol* 47: 532-540

Green DE, Converse KA, Schrader AK (2002) Epizootiology of sixty-four amphibian morbidity and mortality events in the USA, 1996-2001. *Ann NY Acad Sci* 969: 323-339

Green DE, Feldman SH, Wimsatt J (2003) Emergence of a *Perkinsus*-like agent in anuran liver during die-offs of local populations: PCR detection and phylogenetic characterization. *Proc Am Assoc Zoo Vet* 2003:120-121

Gribble KE, Anderson DM (2007) High intraindividual, intraspecific, and interspecific variability in large-subunit ribosomal DNA in the heterotrophic dinoflagellates Protoperidinium, Diplosalis, and Preperidinium (Dinophyceae). *Phycologia* 46: 315-324

Griffiths RA, Pavajeau L (2008) Captive breeding, reintroduction, and the conservation of amphibians. *Conserv Biol* 22(4): 852-861

Guarnizo CE, Paz A, Muñoz-Ortiz A, Flechas SV, Méndez-Narvaéz J, Crawford AJ (2015) DNA barcoding survey of anurans across the Eastern Cordillera of Colombia and the impact of the Andes on cryptic diversity. *PloS One* 10(5): e0127312

Guerra V, Jardim L, Llusia D, Márquez R, Bastos RP (2020) Knowledge status and trends in description of amphibian species in Brazil. *Ecol Indic* 118: 106754

Hayes T, Haston K, Tsui M, Hoang A, Haeffele C, Vonk A (2002) Herbicides: feminization of male frogs in the wild. *Nature* 419: 895-896

Hebert PDN, Cywinska A, Ball SL, DeWaard JR (2003) Biological identifications through DNA barcodes. *Proc Royal Soc B* 270: 313-321

Hedrick PW, Kim TJ, Parker KM (2001) Parasite resistance and genetic variation in the endangered Gila topminnow. *Anim Conserv* 4: 103-109

Hershey AD, Chase MM (1952) Independent functions of viral protein and nucleic acid in growth of bacteriophage. *J Gen Physiol* 36: 39-56

Hossack BR, Pilliod DS (2011) Amphibian Responses to Wildfire in the Western United States: Emerging Patterns from Short-Term Studies. *Fire Ecol* 7: 129-144

Hoverman JT, Gray MJ, Miller DL (2010) Anuran susceptibilities to ranaviruses: role of species identity, exposure route, and a novel virus isolate. *Dis Aquat Org* 89: 97-107

Hoverman JT, Gray MJ, Haislip NA, Miller DL (2011) Phylogeny, life history, and ecology contribute to differences in amphibian susceptibility to ranaviruses. *Ecohealth* 8: 301-319

Isidoro-Ayza M, Lorch JM, Grear DA, Winzeler M, Calhoun DL, Barichivich WJ (2017) Pathogenic lineage of Perkinsea associated with mass mortality of frogs across the United States. *Sci Rep* 7(1): 10288

Isidoro-Ayza M, Grear DA, Chambouvet A (2018) Pathology and Case Definition of Severe Perkinsea Infection of Frogs. *Vet Pathol* 56(1): 133-142

IUCN, Conservation International, and NatureServe (2008) An analysis of amphibians on the 2008 IUCN Red List <www.iucnredlist.org/amphibians>. Downloaded on 2 January 2018

Jacob F, Monod J (1961) Genetic regulatory mechanisms in the synthesis of proteins. *J Mol Biol* 8: 318-356

Jancovich JK, Mao J, Chinchar VG, Wyatt C, Case ST, Kumar S, Valente G, Subramanian S, Davidson EW, Collins JP, Jacobs BL (2003) Genomic sequence of a ranavirus (family Iridoviridae) associated with salamander mortalities in North America. *Virology* 316 (1): 90-103

Jetz W, Pyron RA (2018) The interplay of past diversification and evolutionary isolation with present imperilment across the amphibian tree of life. *Nat Ecol Evol* 2**:** 850-858

Jones MEB, Armién AG, Rothermel BB, Pessier AP (2012) Granulomatous myositis associated with a novel alveolate pathogen in an adult southern leopard frog (*Lithobates sphenocephalus*). *Dis Aquat Org* 102: 163-167

Joneson S, Stajich JE, Shiu SH, Rosenblum EB (2011) Genomic transition to pathogenicity in chytrid fungi. *PLoS Pathog* 7(11): e1002338

Kalyaanamoorthy S, Minh BQ, Wong TKF, von Haeseler A, Jermiin LS (2017) ModelFinder: Fast model selection for accurate phylogenetic estimates. *Nat Methods* 14: 587-5

Karwacki EE, Atkinson MS, Ossiboff RJ, Savage AE (2018) Novel quantitative PCR assay specific for the emerging Perkinsea amphibian pathogen reveals seasonal infection dynamics. *Dis Aquat Org* 129: 85-98

Kats L, Ferrer R (2003) Alien predators and amphibian declines: review of two decades of science and the transition to conservation. *Divers Distributions 9*(2): 99-110

Kiesecker JM, Blaustein AR (1995) Synergism between UV-B radiation and a pathogen magnifies amphibian embryo mortality in nature. *Proc Natl Acad Sci USA* 92: 11049-11052

Kiesecker JM, Blaustein AR, Miller CL (2001) Potential mechanisms underlying the displacement of native red-legged frogs by introduced bullfrogs. *Ecology* 82: 1964-1970

Kiesecker JM (2002) Synergism between trematode infection and pesticide exposure: a link to amphibian deformities in nature? *Proc Natl Acad Sci USA* 99: 9900-9904

Kiesecker JM, Belden LK, Shea K, Rubbo MJ (2004) Amphibian decline and emerging diseases. *Am Sci* 92: 138-147

Knowles SC, Wood MJ, Alves R, Wilkin TA, Bensch S, Sheldon BC (2011) Molecular epidemiology of malaria prevalence and parasitaemia in a wild bird population. *Mol Ecol* 20: 1062-1076

Knutie SA, Wilkinson CL, Kohl KD, Rohr JR (2017) Early-life disruption of amphibian microbiota decreases later-life resistance to parasites. *Nat Commun* 8: 86

Koch R (1884a) The Etiology of Tuberculosis. *The Germ Theory of Disease* 2: 1-88

Koch R (1884b) An address on cholera and its bacillus. *Br Med J* 2(1236): 453-459

Koella JC, Sorensen TL, Anderson RA (1998) The malaria parasite *Plasmodium falciparum* increases the frequency of multiple feeding of its mosquito vector, *Anopheles gambiae*. *Proc R Soc Lond Ser B* 265: 763-768

Koren S, Walenz BP, Berlin K, Miller JR, Phillippy AM (2017) Canu: scalable and accurate long-read assembly via adaptive k-mer weighting and repeat separation. *Genome Res* 27(5): 722-736

Kosakyan A, Heger TJ, Leander BS, Todorov M, Mitchell EA, et al. (2012) COI barcoding of nebelid testate amoebae (Amoebozoa: Arcellinida): extensive cryptic diversity and redefinition of the hyalospheniidae schultze. *Protist* 163: 415-434

Kriger KM, Hines HB, Hyatt AD, Boyle DG, Hero JM (2006) Techniques for detecting chytridiomycosis in wild frogs: comparing histology with real-time TaqMan PCR. *Dis Aquat Org* 71: 141-148

Krueger F (2015) Trim Galore! http://www.bioinformatics.babraham.ac.uk/projects/trim_galore/

Kueneman JG, Parfrey LW, Woodhams DC, Archer HM, Knight R, McKenzie VJ (2014) The amphibian skin-associated microbiome across species, space and life history stages. *Mol Ecol* 23: 1238-1250

Kupferberg S (1997) Facilitation of periphyton production by tadpole grazing: functional differences between species. *Freshw Biol* 37: 427-439

Kunz W (2002) When is a parasite species a species? *Trends Parasitol* 18: 121-124

Kurabayashi A, Matsui M, Belabut DM, Yong H-S, Ahmad N, Sudin A, Kuramoto M, Hamidy A & Sumida M(2011) From Antarctica or Asia? New colonization scenario for Australian-New Guinean narrow mouth toads suggested from the findings on a mysterious genus *Gastrophrynoides*. *BMC Evol Biol* 11: 175

Kuris AM (1974) Trophic interactions: similarity of parasitic castrators to parasitoids. *Q Rev Biol* 49: 129-148

La Marca E, Lips KR, Lotters S, Puschendorf R, Ibanez R, Rueda-Almonacid JV, Schulte R, Marty C, Castro F, Manzanilla-Puppo J, Garcia-Perez JE, Bolanos F, Chaves G, Pounds JA, Toral E, Young BE (2005) Catastrophic population declines and extinctions in neotropical harlequin frogs (Bufonidae: Atelopus). *Biotropica* 37: 190-201

Lafferty KD (1999) The evolution of trophic transmission. *Parasitol Today* 15: 111-115

Landsberg JH, Kiryu Y, Tabuchi M, Waltzek TB, Enge KM, Reintjes-Tolen S, Preston A, Pessier AP (2013) Co-infection by alveolate parasites and frog virus 3-like ranavirus during an amphibian larval mortality in Florida, USA. *Dis Aquat Organ* 105: 89-99

Lara E, Mitchell EA, Moreira D, Lopez-Garcia P (2011) Highly diverse and seasonally dynamic protest community in a pristine peat bog. *Protist* 162(1) 14-32

Laurance WF, McDonald KR, Speare R (1996) Epidemic disease and the catastrophic decline of Australian rain forest frogs. *Conserv Biol* 10: 406-413

Lawler SP, Dritz D, Strange T, Holyoak M (1999) Effects of introduced mosquitofish and bullfrogs on the threatened California red-legged frog. *Conserv Biol* 13: 613-622

Leander BS, Keeling PJ (2004) Early evolutionary history of dinoflagellates and apicomplexans (Alveolata) inferred from HSP90 and actin phylogenies. *J Phycol* 40: 341-250

Lee JS, Bevins SN, Serieys LEK, Vickers W, Logan KA, Aldredge M, Boydston EE, Lyren LM, McBride R, Roelke-Parker M, Pecon-Slattery J, Troyer JL, Riley SP, Boyce WM, Crooks KR, VandeWoude S (2014) Evolution of puma lentivirus in bobcats (*Lynx rufus*) and mountain lions (*Puma concolor*) in North America. *J Virol* 88: 7727-7737

Lefèvre E, Bardot C, Noël C, Carrias JF, Viscogliosi E, Amblard C, Sime-Ngando T (2007) Unveiling fungal zooflagellates as members of freshwater picoeukaryotes:

Evidence from a molecular diversity study in a deep meromictic lake. *Environ Microbiol* 9(1): 61-71

Lefèvre E, Roussel B, Amblard C, Sime-Ngando T (2008) The molecular diversity of freshwater picoeukaryotes reveals high occurrence of putative parasitoids in the plankton. *PLoS One* 3(6): e2324

Lemmon EM, Lemmon AR, Cannatella DC. Geological and climatic forces driving speciation in the continentally distributed trilling chorus frogs (Pseudacris) Submitted (19-APR-2007) Integrative Biology, University of Texas, USA

Lepère C, Domaizon I, Dèbroas D (2008) Unexpected importance of potential parasites in the composition of the freshwater small-eukaryote community. *Appl Env Microbiol* 74(10): 2940-2949

Levine ND (1978) *Perkinsus* gen. n. and other new taxa in the protozoan phylum Apicomplexa. *J Parasitol* 64: 549

Levine ND (1988) Progress in taxonomy of the Apicomplexan protozoa. *J. Protozool.* 35 (4): 518-520

Lewis CH, Richards-Zawacki CL, Ibáñez R, Luedtke J, Voyles J, Houser P, Gratwicke B (2019) Conserving Panamanian harlequin frogs by integrating captive-breeding and research programs. *Biol Conserv* 236: 180-187

Lim L, McFadden GI (2010) The evolution, metabolism and functions of the apicoplast. *Philos Trans R Soc Lond B Biol Sci* 365(1541): 749-763

Lips KR, Brem F, Brenes R, Reeve JD, Alford RA, Voyles J, Carey C, Livo L, Pessier AP, Collins JP (2006) Emerging infectious disease and the loss of biodiversity in a neotropical amphibian community. *Proc Natl Acad Sci USA* 103: 3165-3170

Liu H, Probert I, Uitz J, Claustre H, Aris-Brosou S, et al. (2009) Extreme diversity in noncalcifying haptophytes explains a major pigment paradox in open oceans. *Proc Natl Acad Sci USA* 106: 12803-12808

Longcore JE, Pessier AP, Nichols DK (1999) *Batrachochytrium dendrobatidis* gen. et sp. nov., a chytrid pathogenic to amphibians. *Mycologia* 91: 219-222

Lopez-Garcia P, Philippe H, Gail F, Moreira D (2003) Autochthonous eukaryotic diversity in hydrothermal sediment and experimental micrcolonizers at the Mid-Atlantic Ridge. *Proc Natl Acad Sci USA* 100: 697-702

Lorch JM, Meteyer CU, Behr MJ, Boyles JG, Cryan PM, Hicks AC, Ballmann AE, Coleman AE, Coleman HT, Redell DN, Reeder DM, Blehert DS (2011) Experimental infection of bats with *Geomyces destructans* causes white-nose syndrome. *Nature* 480(7377): 376-378

Majji S, LaPatra S, Long SM, Sample R, Bryan L, Sinning A, Chinchar VG (2006) Rana catesbeiana virus Z (RCV-Z): a novel pathogenic ranavirus. *Dis Aquat Organ* 73: 1-11

Marande W, López-García P, Moreira D (2009) Eukaryotic diversity and phylogeny using small- and large-subunit ribosomal RNA genes from environmental samples. *Environ Microbiol* 11: 3179-3188

Martel A, Spitzen-van der Sluijs A, Blooi M, Bert W, Ducatelle R, Fisher MC, Woeltjes A, Bosman W, Chiers K, Bossuyt F, Pasmans F (2013) *Batrachochytrium salamandrivorans* sp. nov. causes lethal chytridiomycosis in amphibians. *Proc Natl Acad Sci USA* 110(38): 15325-15329

Martin M (2011) Cutadapt removes adapter sequences from high-throughput sequencing reads. EMBnet.journal 17

Martof B, Humphries RL (1959) Geographic variation in the wood frog Rana sylvatica. *Am Midl Nat* 61: 350-389

Marx V (2015) PCR heads into the field. *Nat Methods* 12: 393-397

Mazzoni R, Cunningham AA, Daszak P, Apolo A, Perdomo E, Speranza G (2003) Emerging pathogen of wild amphibians in frogs (*Rana catesbeiana*) farmed for international trade. *Emerg Infect Dis* 9: 995-998

McCutchan TF, de la Cruz VF, Lal AA, Gunderson JH, Elwood HJ, Sogin ML (1988) Primary sequences of two small subunit ribosomal RNA genes from Plasmodium falciparum. *Mol Biochem Parasitol* 28: 63-68

McKenzie VJ, Peterson AC (2012) Pathogen pollution and the emergence of a deadly amphibian pathogen. *Mol Ecol* 21: 5151-5154

de Meeûs T, Michalakis Y, Renaud F (1998) Santa Rosalia revisited: or why are there so many kinds of parasites in ‘The Garden of Earthly Delights’? *Parasitol Today* 14: 10-13

Mihaljevic JR, Hoverman JT, Johnson PTJ (2018) Co-exposure to multiple ranavirus types enhances viral infectivity and replication in a larval amphibian system. *Dis Aquat Org 132*: 23-35

Miller DM, Gray M, Storfer A (2011) Ecopathology of ranaviruses infecting amphibians. *Viruses* 3: 2351-2373

Moreira D, Von Der Heyden S, Bass D, Lopez-Garcia P, Chao E, Cavalier-Smith T (2007) Global eukaryote phylogeny: combined small- and large-subunit ribosomal DNA trees support monophyly of *Rhizaria*, *Retaria* and *Excavata*. *Mol Phylogenet Evol* 44: 255-266

Nassonova E, Smirnov A, Fahrni J, Pawlowski J (2010) Barcoding amoebae: comparison of SSU, ITS and COI genes as tools for molecular identification of naked lobose amoebae. *Protist* 161: 102-115

Naylor R, Williams SL, Strong DR (2001) Aquaculture—a gateway for exotic species. *Science* 294: 1655-1656

Nguyen L-T, Schmidt HA, von Haeseler A, and Bui Quang Minh (2015) IQ-TREE: A fast and effective stochastic algorithm for estimating maximum likelihood phylogenies. *Mol Biol Evol* 32: 268-274

Nirenberg MW, Matthaei JH (1961) The dependence of cell-free protein synthesis in E. coli upon naturally occurring or synthetic polyribonucleotides. *Proc Natl Acad Sci USA* 47: 1588-1602

Nirenberg M, Leder P, Bernfield M, Brimacombe R, Trupin J, Rottman F, O'Neal C (1965) RNA codewords and protein synthesis, VII. On the general nature of the RNA code. *Proc Natl Acad Sci USA 53*(5): 1161-1168

Nishimoto Y, Arisue N, Kawai S, Escalante AA, Horii T et al. (2008) Evolution and phylogeny of the heterogeneous cytosolic SSU rRNA genes in the genus Plasmodium. *Mol Phylogenet Evol* 47: 45-53

Norén F, Moestrup Ø, Rehnstam-Holm AS (1999) *Parvilucifera infectans* Norén et Moestrup gen. et sp. nov. (Perkinsozoa phylum nov.): a parasitic flagellate capable of killing toxic microalgae. *Eur J Protistol* 35: 233-254

O'Hanlon SJ et al. (2018) Recent Asian origin of chytrid fungi causing global amphibian declines. *Science* 360 (6389): 621-627

Ordás MC, Figueras A (1998) *In vitro* culture of *Perkinsus atlanticus*, a parasite of the carpet shell clam Ruditapes decussatus. *Dis Aquat Org* 33:129-136

Pace NR (2009) Mapping the tree of life: progress and prospects. *Microbiol Mol Biol R* 73(4): 565-576

Páez NB, Santiago RR (2019) Systematics of *Huicundomantis*, a new subgenus of *Pristimantis* (Anura, Strabomantidae) with extraordinary cryptic diversity and eleven new species. *Zookeys* 868: 1-112

Pallister J, Gould A, Harrison D, Hyatt A, Jancovich J, Heine H (2007) Development of real-time PCR assays for the detection and differentiation of Australian and European ranaviruses. *J Fish Dis* 30: 427-438

Palumbi SR, Martin AP, Romano SL, McMillan WO, Stice L, Grabowski G (1991) The Simple Fool's Guide to PCR. Dept. of Zoology, University of Hawaii, Honolulu

Pasquier LD, Schwager J, Flajnik MF (1989) The immune system of *Xenopus*. *Annu Rev* Immunol 7: 251-275

Pawlowski J, Audic S, Adl S, Bass D, Belbahri L, Berney C, et al. (2010) CBOL Protist Working Group: barcoding eukaryotic richness beyond the animal, plant, and fungal kingdoms. *PLoS Biol* 10(11): e1001419

Paz A, Ibáñez R, Lips KR, Crawford AJ (2015) Testing the role of ecology and life history in structuring genetic variation across a landscape: A comparative ecophylogeographic approach. *Mol Ecol* 24(14): 3723-3737

Pearman PB, Garner TWJ (2005) Susceptibility of Italian agile frog populations to an emerging strain of Ranavirus parallels population genetic diversity. *Ecol Lett* 8: 401-408

Peeler EJ, Oidtmann BC, Midtlyng PJ, Miossec L, Gozlan RE (2011) Non-native aquatic animals introductions have driven disease emergence in Europe. *Biol Invasions* 13: 1291-1303

Perkins, FO (1966) Life history studies of *Democystidium marinum*, an oyster pathogen. Dissertation. Florida State University. 273 p.

Perkins, FO (1988) Structure of protistan parasites found in bivalve molluscs. *Am Fish Soc Spec Pub* 18: 93-111

Pessier AP, Nichols DK, Longcore JE, Fuller MS (1999) Cutaneous chytridiomycosis in poison dart frogs (*Dendrobates* spp.) and White's tree frogs (*Litoria caerulea*). *J Vet Diagn Investig* 11:194-199

Pfenning DW, Ho SG, Hoffman EA (1998) Pathogen transmission as a selective force against cannibalism. *Anim Behav* 55: 1255-1261

Picco AM, Brunner JL, Collins JP (2007) Susceptibility of the endangered California tiger salamander, Ambystoma californiense, to ranavirus infection. *J Wildl Dis* 43: 286-290

Picco AM, Collins JP (2008) Amphibian commerce as a likely source of pathogen pollution. *Conserv Biol* 22(6): 1582-1589

Pilliod DS, Bury RB, Hyde EJ, Pearl CA, Corn PS (2003) Fire and amphibians in North America. *For Ecol Manag* 178: 163-181

Pizzatto L, Shine R (2011) You Are What You Eat: Parasite Transfer in Cannibalistic Cane Toads. Herpetologica: 67(2): 118-123

Poulin R (2013) Explaining variability in parasite aggregation levels among host samples. *Parasitology* 140: 541–546

Poulin R, Randhawa HS (2015) Evolution of parasitism along convergent lines: from ecology to genomics. *Parasitology* 142(Suppl 1): S6-S15

Pramuk JB (2006) Phylogeny of South American *Bufo* (Anura: Bufonidae) inferred from combined evidence. *Zool J Linn Soc* 146: 407-452

Pramuk JB, Robertson T, Sites JW, Noonan BP (2008) Around the world in 10 million years: biogeography of the nearly cosmopolitan true toads (Anura: Bufonidae). *Glob Ecol Biogeogr* 17: 72-83

Rachowicz LJ, Hero JM, Alford RA, Taylor JW, Morgan JAT, Vredenburg VT, Collins JP, Briggs CJ (2005) The novel and endemic pathogen hypotheses: competing explanations for the origin of emerging infectious diseases of wildlife. *Conserv Biol* 19: 1441-1448

Rahel FJ, Olden JD (2008) Assessing the effects of climate change on aquatic invasive species. *Conserv Biol* 22: 521-533

Rambaut A (2018) FigTree v1.4.4. Available at: http://tree.bio.ed.ac.uk/software/figtree/ (accessed April 2020)

Reed DH, Frankham R (2003) Correlation between fitness and genetic diversity. *Conserv Biol* 17: 230-237

Retallick RWR, Miera V, Richards KL, Field KJ, Collins JP (2006) A non-lethal technique for detecting the chytrid fungus *Batrachochytrium dendrobatidis* on tadpoles. *Dis Aquat Org* 72: 77-85

Richards TA, Vepritskiy AA, Gouliamova DE, Nierzwicki-Bauer SA (2005) The molecular diversity of freshwater picoeukaryotes from an oligotrophic lake

reveals diverse, distinctive and globally dispersed lineages. *Environ Microbiol* 7(9): 1413-1425

Richgels KLD, Russell RE, Adams MJ, White CL, Grant EHC (2016) Spatial variation in risk and consequence of *Batrachochytrium salamandrivorans* introduction in the USA. *R Soc Open Sci* 3: 150616

Rivera-Correa M, Duarte-Cubides F, Rueda-Almonacid JV, Daza JM (2013) A new red-eyed treefrog of *Agalychnis* (Anura: Hylidae: Phyllomedusinae) from middle Magdalena River valley of Colombia with comments on its phylogenetic position. *Zootaxa* 3636: 85-100

Rivers TM (1937) Viruses and Koch's postulates. *J Bacteriol* 33: 1-12

Robideau GP, De Cock AW, Coffey MD, Voglmayr H, Brouwer H, et al. (2011) DNA barcoding of oomycetes with cytochrome c oxidase subunit I and internal transcribed spacer. *Mol Ecol Resour* 11: 1002-1011

Robledo JA, Wright AC, Marsh AG, Vasta GR (1999) Nucleotide sequence variability in the nontranscribed spacer of the rRNA locus in the oyster parasite *Perkinsus marinus*. *J Parasitol* 85(4): 650-656

Robledo JA, Coss CA, Vasta GR (2000) Characterization of the ribosomal RNA locus of *Perkinsus atlanticus* and development of polymerase chain reaction-based diagnostic assay. *J Parasitol* 86(5): 972-978

Roelants K, Gower DJ, Wilkinson M, Loader SP, Biju SD, Guillaume K, Moriau L, Bossuyt F (2007) Global patterns of diversification in the history of modern amphibians. *Proc Natl Acad Sci USA* 104(4): 887-892

Rohr JR, Schotthoefer AM, Raffel TR, Carrick HJ, Halstead N, Hoverman JT, Johnson CM, Johnson LB, Lieske C, Piwoni MD, Schoff PK, Beasley VR (2008) Agrochemicals increase trematode infections in a declining amphibian species. *Nature* 455: 1235-1239

Rollins-Smith LA (1998) Metamorphosis and the amphibian immune system. *Immunol Rev* 166: 221-230

Rollins-Smith LA, Ramsey JP, Pask JD, Reinert LK, Woodhams DC (2011) Amphibian immune defences against chytridiomycosis: impacts of changing environments. *Integr Comp Biol* 51(4): 552-562

Rollins-Smith LA, Woodhams DC (2012) Amphibian immunity: staying in tune with the environment. In: Demas GE, Nelson RJ (Eds), *Ecoimmunology* (92-143). Oxford University Press, New York

Roug A, Geoghegan C, Wellington E, Miller WA, Travis E, Porter D, Cooper D, Clifford DL, Mazet JAK, Parsons S (2014) Utility of a fecal real-time PCR protocol for detection of *Mycobacterium bovis* infection in African buffalo (*Syncerus caffer*). *J Wildl Dis* 50: 140-142

Rowley JJL, Alford RA (2007) Behaviour of Australian rainforest stream frogs may affect the transmission of chytridiomycosis. *Dis Aquat Org* 77: 1-9

Rowley JJL, Gleason FH, Andreou D, Marshall WL, Lilje O, Gozlan R (2013) Impacts of mesomycetozoean parasites on amphibian and freshwater fish populations. *Fungal Biol Rev* 27: 100-111

Santiago PC, Silva GF, Nascimento LB, Pezzuti TL, Carvalho DC Jr. Morphological and molecular analyses are enough for anuran larvae identification at a Biosphere Reserve in Southeastern Brazil? Submitted (14-OCT-2016) Graduate Program in Biology of Vertebrates, Pontifical Catholic University of Minas Gerais, Brazil

Santos J, Coloma LA, Cannatella DC (2003) Multiple, recurring origins of aposematism and diet specialization in poison frogs. Proc Nat Acad Sci USA 100: 12792-12797

Santos JC, Cannatella DC (2011) Phenotypic integration emerges from aposematism and scale in poison frogs. *Proc Natl Acad Sci USA* 108: 6175-6180

dos Santos SP, Ibáñez R, Ron SR (2015) Systematics of the *Rhinella margaritifera* complex (Anura, Bufonidae) from western Ecuador and Panama with insights in the biogeography of *Rhinella alata*. *ZooKeys* 501: 109-14

Scheele BC, et al. (2019) Amphibian fungal panzootic causes catastrophic and ongoing loss of biodiversity. *Science* 363: 1459-1463

Schoch CL, Seifert KA, Huhndorf S, Robert V, Spouge JL, et al. (2012) Nuclear ribosomal internal transcribed spacer (ITS) region as a universal DNA barcode marker for Fungi. *Proc Natl Acad Sci USA* 109: 6241-6246

Skerratt LF, Berger L, Speare R, Cashins S, McDonald K, Phillott A, Hines H, Kenyon N (2007) The spread of chytridiomycosis has caused the rapid global decline and extinction of frogs. *EcoHealth* 4: 125-134

Smith SA, Arif S, Montes de Oca AN, Wiens JJ. A phylogenetic hotspot for evolutionary novelty and change in cranial morphology of Middle American treefrogs. Submitted (28-JUN-2006) Ecology and Evolution, Stony Brook University, Stony Brook, NY, USA

Spielman D, Brook BW, Briscoe DA, Frankham R (2004) Does inbreeding and loss of genetic diversity decrease disease resistance? *Conserv Genet* 5: 439-448

Standish I, Leis E, Schmitz N, Credico J, Erickson S, Bailey J, Kerby J, Phillips K, Lewis T (2018) Optimizing, validating, and field testing a multiplex qPCR for the detection of amphibian pathogens. *Dis Aquat Org* 129: 1-13

Stern RF, Horak A, Andrew RL, Coffroth M-A, Andersen RA, et al. (2010) Environmental barcoding reveals massive dinoflagellate diversity in marine environments. *PLoS One* 5: e13991

Stern RF, Andersen RA, Jameson I, Küpper FC, Coffroth M-A, Vaulot D, et al. (2012) Evaluating the ribosomal internal transcribed spacer (ITS) as a candidate dinoflagellate barcode marker. *PLoS One* 7(8): e42780

Stoecker DK (1999) Mixotrophy among dinoflagellates. *J Eukaryot Microbiol* 46: 397-401

Stuart SN, Chanson JS, Cox NA, Young BE, Rodrigues ASL, Fischman DL, Waller RW (2004) Status and trends of amphibian declines and extinctions worldwide. Science 306: 1783-1786

Sun G, Yang Z, Kosch TA, Summers K, Huang J (2011) Horizontal gene transfer may explain the evolution of extreme virulence in the devastating amphibian chytrid fungus. *BMC Evol Biol* 11:195

Tan WGH, Barkman TJ, Chinchar VG, Essani K (2004) Comparative genomic analysis of frog virus 3, type species of the genus *Ranavirus* (family Iridoviridae). *Virology* 323: 70-84

Taylor FJR (ed) (1987) The Biology of Dinoflagellates. *Bot Monogr* 21: i-xii, 1-785

Taylor FJR, Hoppenrath M, Saldarriaga JF (2008) Dinoflagellate diversity and distribution. *Biodivers Conserv* 17: 407-418

Taylor S, Wakem M, Dijkman G, Alsarraj M, Nguyen M (2010) A practical approach to RT-qPCR—publishing data that conform to the MIQE guidelines. Methods 50: S1-S5

Thomas CD, Cameron A, Green RE et al. (16 more authors) (2004) Extinction risk from climate change. Nature 427(6970): 145-148

Turner AK, Begon M, Jackson JA, Bradley JE, Paterson S (2011) Genetic diversity in cytokines associated with immune variation and resistance to multiple pathogens in a natural rodent population. *PLoS Genet* 7(10): e1002343

Villalba A, Reece KS, Ordas MC, Casas SM, Figueras A (2004) Perkinsosis in molluscs: a review. *Aquat Liv Resour* 17: 411-32

Vonesh JR, De La Cruz O (2002) Complex life cycles and density dependence: assessing the contribution of egg mortality to amphibian decline. *Oecol* 133: 325-333

Voyles J, Young S, Berger L, Campbell C, Voyles WF, Dinudom A, Cook D, Webb R, Alford RA, Skerratt LF, Speare R (2009) Pathogenesis of chytridiomycosis, a cause of catastrophic amphibian declines. *Science* 326: 582-585

Vredenburg VT, Knapp RA, Tunstall TS, Briggs CJ (2010) Dynamics of an emerging disease drive large-scale amphibian population extinctions. *Proc Natl Acad Sci USA* 107: 9689-9694

Wahba AJ, Gardner RS, Basilio C, Miller RS, Speyer JF, Lengyel P (1963) Synthetic polynucleotides and the amino acid code, VIII. *Proc Natl Acad Sci USA.* 49: 116-122

Wake DB, Vredenburg VT (2008) Are we in the midst of the sixth mass extinction? A view from the world of amphibians. *Proc Natl Acad Sci USA* 105: 11466-11473

Wake MH, Donnelly MA (2010) A new lungless caecilian (Amphibia: Gymnophiona) from Guyana. *Proc R Soc B* 227(1683): 915-922

Walker SF, Bosch J, James TY, Litvintseva AP, Valls JAO, Piña S, García G, Rosa GA, Cunningham AA, Hole S, Griffiths R, Fisher MC (2008) Invasive pathogens threaten species recovery programs. *Curr Biol* 8: R853-R854

Warne RW, LaBumbard B, LaGrange S, Vredenburg VT, Catenazzi A (2016) Co-infection by chytrid fungus and *Ranaviruses* in wild and harvested frogs in the Tropical Andes. PLoS ONE 11(1): e0145864

Watson JD, Crick FHC (1953) Molecular structure of nucleic acids: A structure for deoxyribose nucleic acid. *Nature* 171: 737-738

Weinstein SB, Kuris AM (2016) Independent origins of parasitism in Animalia. *Biol Lett* 12(7): 20160324

Weldon C, du Preez LH, Hyatt AD, Muller R, Speare R (2004) Origin of the amphibian chytrid fungus. *Emerg Infect Dis* 10(12): 2100-2105

Westwood JH, Yoder JI, Timko MP, dePamphilis CW (2010) The evolution of parasitism in plants. *Trends Plant Sci* 15: 227-235

Whitfield SM, Geerdes E, Chacon I, Ballestero RE, Jimenez RR, Donnelly MA, Kerby JL (2013) Infection and co-infection by the amphibian chytrid fungus and ranavirus in wild Costa Rican frogs. *Dis Aquat Org* 104: 173-178

Wickham H (2016) *ggplot2: Elegant Graphics for Data Analysis*. Springer-Verlag New York. ISBN 978-3-319-24277-4, https://ggplot2.tidyverse.org

Wittwer CT, Herrmann MG, Gundry CN, Elenitoba-Johnson KS (2001) Real-time multiplex PCR assays. *Methods* 200125: 430-42

Wobeser G (2002) Disease management strategies for wildlife. *Rev Sci Tech* 21: 159-178

Woese CR, Fox GE (1977) Phylogenetic structure of the prokaryotic domain: the primary kingdoms. *Proc Natl Acad Sci USA* 74(11): 5088-5090

Woese CR (1987) Bacterial evolution. *Microbiol Rev* 51**:** 221-271

Woese CR, Kandler O, Wheelis ML (1990) Towards a natural system of organisms: proposal for the domains Archaea, Bacteria, and Eucarya. *Proc Natl Acad Sci USA* 87: 4576-4579

Woodhams DC, Bletz M, Kueneman J, McKenzie V (2016) Managing amphibian disease with skin microbiota. *Trends Microbiol* 24: 161-164

Yarza P, Yilmaz P, Glöckner FO, Reich M (2017) A phylogenetic framework for the kingdom Fungi based on 18S rRNA gene sequences. *Mar Genomics* 36: 33-39

Zukal J, Bandouchova H, Brichta J, et al. (2016) White-nose syndrome without borders: *Pseudogymnoascus destructans* infection tolerated in Europe and Palearctic Asia but not in North America. *Sci Rep* 6: 19829

Zuker M (2003) Mfold web server for nucleic acid folding and hybridization prediction. *Nucleic Acids Res.* 31(13): 3406-3415